Universidade do Minho
Escola de Engenharia

Ana Margarida Martins de Sousa

Stimulus Responsive Smart Supports and Scaffold/Cell Constructs for Bone Tissue Engineering

Julho de 2009

Stimulus Responsive Smart Supports and Scaffold/Cell Constructs for Bone Tissue Engineering
Ana Margarida Martins de Sousa
UMinho | 2009



Universidade do Minho
Escola de Engenharia

Ana Margarida Martins de Sousa

Stimulus Responsive Smart Supports and Scaffold/Cell Constructs for Bone Tissue Engineering

Tese de Doutoramento em Engenharia Biomédica

Trabalho efectuado sob a orientação do
Professor Rui L. Reis
e co-orientação da
Doutora Catarina M. Alves

Colaboração internacional:
Professor Antonios G. Mikos

Julho de 2009

É AUTORIZADA A REPRODUÇÃO INTEGRAL DESTA TESE/TRABALHO APENAS PARA EFEITOS DE INVESTIGAÇÃO, MEDIANTE AUTORIZAÇÃO ESCRITA DO INTERESSADO, QUE A TAL SE COMPROMETE.

Universidade do Minho, ____/____/____

_____

To my parents

“Serás capaz
de responder a tudo o que pergunto?”

Alexandre O’Neill

“Be happy for this moment
This moment is your life”

In *Rubayat* of Omar Khayyam

ACKNOWLEDGEMENTS

A thesis like this is never the product of a single mind. I have drawn inspiration and ideas from many people through the years. I would like to acknowledge individually to each person, but unfortunately, a few pages would not be enough.

I would like to acknowledge my advisor, Professor Rui Reis, for all the opportunities that he gave me. Looking back, after all these years, I can say that he was my best professor. It is because of his classes I chose his lab to do my internship. His enthusiasm, motivation, dynamism, youth, and strategy influenced my decision to join the 3B´s Research Group a few years ago. He always believed in me more than I did. I also thank his support and the opportunity to spend almost one year and half abroad without an FCT grant. He also gave me the opportunity to present my work and participate in the best conferences of the field and always gave me the necessary freedom to guide my research and to explore my ideas.

During my visits to Rice University, USA, Professor Mikos accepted to supervise my work and always made all the efforts to make my life there pleasant. I would like to express my sincere thanks for his help and crucial guidance. The thoughtful discussions and meetings will be never forgotten. These several visits had a remarkable input in my research work and allowed me to grow as a scientist. I deeply enjoyed working in Mikos lab. The courteousness and friendly environment of the Mikos lab was extremely appreciated. The time that I spent at Rice University was the happiest days of my professional life. And I really loved the extremely warm weather of Houston.

I want also to thank Kurt Kasper who helped me in the preparation of protocols and the *in vivo* surgeries. His pertinent suggestions, availability and support revising the manuscripts significantly increase their quality.

To my colleagues and friends at Mikos lab who helped me to feel at home and taught me so many things that I needed to know. My several periods abroad were great and successful mainly because of you. I want to deeply acknowledge all their attention and friendship, but also for holding me up through difficulties mainly when I felt sick and during the Ike hurricane that I was without power energy at home for 3 weeks. I will never forget what you did for me in the more adverse times.

To my co-advisor and friend Catarina who taught me so much. Your contribution in my life is beyond words. I learned how to plan everything in detail and to be organized. Our fruitful discussions and scientific plans have been memorable. I am tremendously grateful for your belief in me even when I had so many doubts. You are an example of strength and courage. I deeply acknowledge your optimism and confidence. You will never know how important you were in certain moments of my life. I cannot quantify how many hours we spent together (when we were

both in Portugal) or on the phone. We never had a schedule. You always had time!!! I will never forget our endless discussions, “blood sessions”, washing hands with EtOH (always!!!), and how good Technovit is!!!

Ana M. Martins acknowledges the PhD scholarship from European NoE EXPERTISSUES (NMP3-CT-2004-500283) and the funding from the European STREP HIPPOCRATES (NMP3-CT-2003-505758).

I owe a special debt to who helped me with corrections and thesis formatting.

To my friends that I met in 3B’s but already left. You were so important during the first years in the group that I can never describe how grateful I am because of what you have made for me. A special thank to Gabi for the wonderful week that we spent together in Philly and NY. That week made me feel reborn.

To the GO TEAM, a closest and small group of people that joined together to prepare a huge and unforgettable surprise for each member in one of the best days of our lives. Through the years I build up a strong relationship with each of you. Thank you for all the wonderful meetings, days, dinners, and happy hours.

I need to thank all my closest friends, you know who you are! I must say that I have many special people around me. But a special word is addressed to Ana Rita and Rui Pereira. My dearest Ana Rita needs to read how important she has been in my life. They have been through these years’ unimaginable friends. We have been together in the wonderful and bad times. They have been very special friends and they share with me the same values. Thank you for your patience (in this last months I almost did not have social life), true opinion, and loyalty. Our friendship is a proof that the distance means nothing. Thank you so much my *compagnons de route.*

To my twin brother, my mother, and my father, this thesis is dedicated to you. I am everything I am because I have you. You always have been supporting my dreams, choices, and decisions. This thesis would not exist without you. To my dearest nephews, Francisco and Afonso, for the asleep company during the writing of this thesis. I was always awake for your each 2 hours meal.

Stimulus Responsive Smart Supports and Scaffold/Cell Constructs for Bone Tissue Engineering

ABSTRACT

Tissue engineering (TE) has emerged as a new interdisciplinary science for the repair of various tissues, restoring their functions by means of using biomaterials, cells, and/or bioactive factors. Three main general strategies have been adopted for the creation of new bone tissue: i) direct *in vivo* implantation of isolated cells; ii) direct *in vivo* implantation of scaffolds; and iii) cells placed on or within scaffolds. In the bone tissue engineering approach, a temporary scaffold is required to serve as an adhesive substrate for the implanted cells and a physical support to guide the formation of the new tissue. In the second and third approaches, a porous material acts as a scaffold, serving in the later case as transplant vehicle for cultured cells and template to guide tissue regeneration, playing an important role in transforming the cell seeded scaffolds in to a new tissue.

The present thesis is divided in two main groups of studies: in the first one we describe the TE strategy of using scaffold and seeded cells with osteogenic media supplemented with several enzymes (Chapter III and IV). The second part describes the development of acellular scaffolds with *in situ* pore forming ability *in vitro*, improvement of their properties (namely degradation and osteoconductivity) and finally the validation of *in situ* pore forming concept *in vivo* (Chapters V, VI, VII and VIII).

Previously, it was demonstrated that starch/poly(ε-caprolactone) fiber mesh scaffolds have induced osteogenic differentiation of rat bone marrow stromal cells (MSCs) when cultured in flow perfusion bioreactors. The studies described in Chapters III and IV aimed to investigate the effect of complete osteogenic media supplemented with different enzymes in physiological concentrations similar to those found in human serum. The influence of these enzymes on the degradation of SPCL fiber meshes and on the osteogenic differentiation of MSCs seeded onto scaffolds was assessed. These studies were performed in static cultures and in flow perfusion bioreactors. After degradation studies in static and dynamic conditions in the presence of enzymes showed that SPCL did not lose its structural integrity. α-amylase had a remarkable effect on the degradation, increasing porosity and pore size of SPCL in both static and dynamic conditions. It was demonstrated that supplementation of culture media with lipase enhances the osteoblastic differentiation of the seeded MSCs and promotes matrix mineralization in static cultures. When flow perfusion bioreactors were used, the flow enhanced the infiltration of cells and facilitated better distribution of extracellular matrix throughout the scaffolds in the presence/absence of enzymes. The presence of flow and lipase improved the osteogenic differentiation of MSCs as compared with the other groups, enhanced mineralization and promoted uniform matrix distribution.

The second part of this thesis (Chapters V, VI, VII and VIII) described the development of almost non-porous chitosan and chitosan/starch scaffolds, with the ability of forming a porous structure *in situ* due to the attack by specific enzymes present in the human body (α-amylase and lysozyme). The results of the compressive tests showed that these scaffolds exhibit very good mechanical properties in both the dry and wet state. Degradation studies were performed using α-amylase and/or lysozyme at

concentrations similar to those found in human serum and showed that after enzymatic degradation there was the formation of a porous structure, indicating the potential of this methodology to obtain *in situ* forming scaffolds. Citotoxicity test revealed that the extracts of the materials were clearly non-toxic to L929 fibroblast cells. Analysis of cell adhesion and morphology of seeded osteoblastic-like cells in direct contact tests showed that the number of cells on chitosan/starch scaffolds was noticeably higher than that on chitosan scaffolds, which suggest that starch containing materials may promote cell adhesion and proliferation.

In order to improve the *in situ* pore forming scaffolds, a self-regulated degrading material with gradual *in situ* pore formation were developed. This approach is based on the incorporation of the lysozyme enzyme into biomimetic calcium phosphate (CaP) coatings. These coatings were prepared on the surface of chitosan scaffolds by means of a biomimetic coating technique, with the aim of controlling their degradation rate and preventing infection upon implantation. Two different environments were simulated: normal physiological conditions (pH 7.4) and inflammatory response (pH 5). At pH 7.4, the scaffolds remained more stable than those incubated at pH 5, which showed a rapid decrease in their initial weight and the formation of a highly porous structure.

Additional studies investigated the influence of a CaP biomimetic coating on osteogenic differentiation of rat marrow stromal cells (MSCs) and showed enhanced differentiation of rat MSCs seeded on the CaP coated chitosan-based scaffolds with lysozyme incorporated. At all culture times, CaP coated chitosan-based scaffolds with incorporated lysozyme enhanced osteoblastic differentiation of MSCs, bone matrix production, and mineralization. The ability of these CaP coated chitosan-based scaffolds with incorporated lysozyme to create an interconnected pore network *in situ* coupled with its positive effect on osteoblastic differentiation of MSCs and the production of mineralized matrix illustrate the strong potential of these scaffolds for application in bone tissue engineering strategies**.**

In order to validate the concept *in vivo,* a rat subcutaneous model was used to investigate the degradation of the scaffolds and the *in situ* pore formation. All scaffolds showed pronounced weight loss and pore formation as a function of time. All group conditions showed a significant increase in porosity after 12 weeks. After all time points no adverse tissue reaction was observed, and as degradation increased, histological analysis showed cells ingrowth throughout the implants. Using this innovative methodology, the ability of gradual *in situ* pore formation of these novel scaffolds was demonstrated *in vivo*.

As a concluding remark, it can be stated that the studies performed in this thesis proposed several successful strategies that might find application in a bone tissue engineering scenario.

Suportes Inteligentes com Capacidade de Responder a Estímulos e Novas Combinações Suportes/Células para Engenharia de Tecidos Ósseos

RESUMO

A Engenharia de Tecidos é uma ciência interdisciplinar recente que visa reparar diferentes tecidos, recuperando as suas funções usando biomateriais, células e/ou agentes bioactivos. As três estratégias que têm sido usadas para a criação de novo tecido ósseo incluem: i) implantação de células; ii) implantação de suportes tridimensionais; e iii) combinação das duas estratégias anteriores, usando células cultivadas nos suportes. Na engenharia de tecidos ósseos, os suportes são usados como substrato para células e também como suporte físico para as mesmas de forma a induzir a formação de novo tecido ósseo. Na segunda e terceira estratégias, descritas anteriormente, um material poroso funciona como suporte para cultura de células e para induzir a regeneração óssea, tendo um papel importante na diferenciação de células no tecido desejado.

Esta tese divide-se em dois estudos principais: o primeiro que descreve a estratégia de engenharia de tecidos utilizando um suporte poroso e células cultivadas no mesmo, usando meio osteogénico enriquecido com diferentes enzimas (Capítulos III e IV). A segunda parte desta tese descreve o desenvolvimento de suportes não porosos com a capacidade de formação de poros *in situ,* aperfeiçoamento das suas propriedades (nomeadamente no que respeita a degradação e osteoconductividade) e por último, a confirmação do conceito de formação de poros *in situ* nos suportes inteligentes quando implantados *in vivo* (Capítulos V, VI, VII e VIII).

Os estudos apresentados nos Capítulos IIII e IV tiveram como objectivo investigar o efeito do meio osteogénico enriquecido com diferentes enzimas em concentrações fisiológicas semelhantes às encontradas no soro humano. Estudou-se a influência destas enzimas na degradação de suportes porosos à base de amido e policaprolactona (SPCL) e na diferenciação osteogénica de células da medula óssea de rato. Estes estudos foram efectuados em condições estáticas e usando bioreactores de perfusão. Os estudos de degradação em condições estáticas e dinâmicas mostraram que na presença das enzimas, os suportes de SPCL não perderam a sua estrutura física. A α-amilase teve um efeito significativo na degradação dos suportes de SPCL, aumentando a sua porosidade e o tamanho de poros em condições estáticas e dinâmicas. Demonstrou-se também que a lipase no meio osteogénico melhorou a diferenciação osteogénica das células cultivadas nos suportes de SPCL e estimulou a mineralização da matriz extracelular em condições estáticas. Quando foram usados bioreactores de perfusão, verificou-se que o fluxo melhorou a infiltração das células e permitiu uma melhor distribuição de matriz extracelular no interior dos suportes. A combinação do fluxo (gerado pelos bioreactores) e a presença de lipase permitiram obter melhores resultados no que respeita a diferenciação osteogénica das células da medula óssea em todos os grupos estudados, induzindo mais mineralização e distribuição da matriz extracelular.

A segunda parte desta tese (Capítulos V, VI, VII and VIII) descreve o desenvolvimento de suportes não porosos à base de quitosano e combinação de quitosano com amido, com a capacidade de formarem uma estrutura porosa *in situ* devido à acção de enzimas específicas (α-amilase e lisozima – enzimas existentes no corpo humano). Os resultados dos estudos de compressão mostraram que

estes suportes têm propriedades mecânicas adequadas quando estudados nos estados seco e molhado.

Os estudos de degradação foram efectuados usando α-amilase e/ou lisozima em concentrações semelhantes às encontradas no soro humano e mostraram que induziram a formação de uma estrutura porosa, demonstrando o potencial destes suportes inteligentes com capacidade para responder a estímulos. Os testes de citotoxicidade com fibroblastos L929 mostraram a ausência de toxicidade dos extractos dos materiais. Os testes de contacto directo com uma linha celular de osteoblastos mostraram que o número de células nos suportes à base de quitosano e amido era maior do que nos suportes de quitosano, sugerindo que o amido pode promover a adesão e proliferação celular.

Desenvolveram-se suportes inteligentes com capacidade de responder a estímulos de forma a melhorar o comportamento dos suportes com capacidade de formação de poros *in situ*. Esta estratégia incluiu a incorporação de lisozima em revestimentos de fosfato de cálcio na superfície de suportes de quitosano usando a técnica de revestimentos biomiméticos com o objectivo de controlar a degradação dos suportes e prevenir infecções. Foram simuladas duas condições: condições fisiológicas normais (pH 7.4) e de resposta inflamatória (pH 5). A pH 7.4, os suportes mantiveram-se estáveis comparativamente aos estudados a pH 5, que mostraram um decréscimo de peso e a formação de estruturas porosas.

Estudos adicionais investigaram a influência dos revestimentos de fosfato de cálcio na diferenciação osteogénica de células da medula óssea e mostraram que estas diferenciaram-se na presença de lisozima. Em todos os tempos de cultura observou-se que os suportes de quitosano revestidos com fosfatos de cálcio e na presença de lisozima tiveram um melhor comportamento do que os restantes grupos estudados, nomeadamente na produção e mineralização da matriz extracelular. A capacidade destes suportes inteligentes em responder a estímulos e formar estruturas porosas, juntamente com o efeito positivo na diferenciação osteogénica de células da medula óssea, ilustram o potencial destes suportes para aplicações na área de engenharia de tecidos ósseos.

Por último, pretendeu-se confirmar o conceito de formação de poros *in vivo*. Diferentes tipos de suportes à base de quitosano e amido, revestidos ou não com fosfatos de cálcio e na presença/ausência de lisozima foram implantados em ratos usando um modelo subcutâneo. Os principais objectivos incluíram o estudo da degradação *in vivo* dos suportes e a formação de poros *in situ*. Todos os suportes apresentaram elevada perda de peso e formação de poros em função do tempo de implantação. Adicionalmente, todos os grupos mostram um aumento significativo na sua porosidade após 12 semanas. Em todos os tempos de implantação não foram detectadas reacções adversas e, conforme a degradação aumentou, as secções histológicas mostraram infiltração de células nos implantes. Esta metodologia inovadora mostrou a capacidade destes suportes inteligentes em responder a estímulos e deste modo serem capazes de induzir *per se* a formação de estruturas porosas.

As observações discutidas nesta tese propõem diferentes estratégias que poderão ser usadas com sucesso na área de engenharia de tecidos ósseos.

TABLE OF CONTENTS

Acknowledgements	i
Abstract	iii
Resumo	v
Table of contents	vii
List of abbreviations	xv
List of figures	xvii
List of tables	xxvii
Short *Curriculum vitae*	xxix
List of publications	xxxi
Introduction to the thesis format	xxxv
SECTION 1	**1**
CHAPTER I	**3**
INTRODUCTION	
PART I. Towards Osteogenic Differentiation of Marrow Stromal Cells and *In Vitro* Production of Mineralized Extracellular Matrix onto Natural Based Scaffolds	
Abstract	5
1. Introduction	6
2. Scaffolds of natural origin – polysaccharides	8
2.1. Chitosan	8
2.2. Starch	10
2.3. Alginate	11
3. CaP biomimetic coatings	12
3.1. Osteoconductivity	13
3.2. Osteoinductivity	13
3.3. Incorporation of biomolecules into CaP biomimetic coatings	14
4. Osteogenic differentiation of marrow stromal cells and mineralized ECM production *in vitro*	15
4.1. BMSCs versus MSCs	16
4.2. Osteogenic differentiation	17
4.3. Bone-specific matrix proteins	19
5. Summary	19
References	21

INTRODUCTION **35**

PART II. Naturally Derived Responsive and *In Situ*-Forming Scaffolds for Bone Tissue Engineering Applications: An Overview of the Last Decade

Abstract 35

1. Introduction 36

2. Scaffolds for bone tissue engineering 37

2.1. Mechanical properties 38

2.2. Mechanisms of polymer biodegradation 38

3. “Smart” and responsive scaffolds for bone tissue engineering 39

4. Chitosan scaffolds as a responsive biomaterial 40

5. Naturally derived *in situ* forming scaffolds 42

6. *In situ* pore-forming scaffolds 43

7. Conclusions 46

References 47

SECTION 2 **55**

CHAPTER II **57**

MATERIALS AND METHODS

1. Production of the materials 59

1.1. SPCL fiber mesh scaffolds 59

1.2. Chitosan-based scaffolds 59

1.3. Chitosan-based scaffolds coated with CaP coating and incorporated lysozyme 60

1.4. Reagents 60

2. Characterization of the developed scaffolds 60

2.1. Mechanical properties – compression tests 60

2.2. Degradation studies 61

2.2.1. Degradation studies with α-amylase or lipase in static and dynamic conditions 61

2.2.2. Degradation studies with α-amylase and lysozyme 61

2.2.3. Degradation studies at pH 7.4 and pH 5 61

2.2.4. Degradation studies with lysozyme 62

2.2.5. Water uptake and weight loss measurements 62

2.2.6. Scanning electron microscopy (SEM) 62

2.2.7. Thin-film X-Ray diffraction (TF-XRD) and Fourier Transformed infrared spectroscopy (FTIR) 62

2.2.8. Determination of lysozyme release and activity in solution 63

2.2.9. Micro-computed tomography (μ-CT) analysis 63

3. *In vitro* biological studies 64
3.1. Biocompatibility testing 64
3.1.1. Cell lines 64
3.1.2. Biocompatibility assays: extracts and cell adhesion studies 64
3.2. Culture of rat bone marrow stromal cells (MSCs) under static and flow perfusion conditions 65
3.2.1. Isolation, expansion and seeding of rat MSCs 65
3.2.2. Analysis of cultured scaffolds 66
3.2.2.1. Confocal and scanning electron microscopy (SEM) 66
3.2.2.2. DNA analysis 67
3.2.2.3. Alkaline phosphatase activity 67
3.2.2.4. Calcium deposition measurements 67
3.2.2.5. Fourier transformed infrared spectroscopy with attenuated total reflectance (FTIR-ATR) 68
3.2.2.6. Histology (H&E, von Kossa staining and tetracycline fluorescence) 68
4. *In vivo* studies 69
4.1. Implant preparation 69
4.2. Subcutaneous implantation 69
4.3. Preparation of specimens for weight loss measurements and μ-CT 70
4.4. Histological analysis 70
5. Statistics 71
References 72

SECTION 3 **75**
CHAPTER III **77**
The Role of Lipase and α-Amylase in the Degradation of Starch/Poly(ε-Caprolactone) Fiber Meshes and the Osteogenic Differentiation of Cultured Marrow Stromal Cells
Abstract 79
1. Introduction 80
2. Materials and methods 82
2.1. Scaffolds preparation and characterization 82
2.2. Degradation tests 82
2.3. Micro-Computed Tomography (μ-CT) 83
2.4. Isolation and expansion of rat bone marrow stromal cells 83
2.5. Cell seeding 84
2.6. DNA analysis 84

2.7. Alkaline phosphatase activity 85
2.8. Calcium deposition measurement 85
2.9. Microscopic analysis 85
2.10. Fourier transformed infrared spectroscopy with attenuated total reflectance (FTIR-ATR) 86
2.11. Statistics 86
3. Results and discussion 86
3.1. Degradation studies 86
3.2. Assays 93
3.3. Fourier transformed infrared spectroscopy with attenuated total reflectance (FTIR-ATR) 98
4. Conclusions 99
Acknowledgements 99
References 100

CHAPTER IV **103**

Combination of Enzymes and Flow Perfusion Conditions Improves Osteogenic Differentiation of Bone Marrow Stromal Cells Cultured upon Starch/Poly(ε-Caprolactone) Fiber Meshes

Abstract 105
1. Introduction 106
2. Materials and methods 107
2.1. Scaffold preparation 107
2.2. Isolation, expansion and seeding of rat bone marrow stromal cells 107
2.3. DNA analysis 108
2.4. Alkaline phosphatase activity 108
2.5. Calcium deposition measurement 109
2.6. Histological and microscopic analysis 109
2.7. Statistics 110
3. Results and discussion 110
3.1. DNA assay 110
3.2. Microscopic analysis 111
3.3. Alkaline phosphatase activity 113
3.4. Calcium deposition measurement 114
3.5. von Kossa staining and tetracycline fluorescence 116
4. Conclusions 118
Acknowledgements 119
References 119

SECTION 4 **121**

CHAPTER V **123**

Natural Origin Scaffolds with *In Situ* Pore Forming Capability for Bone Tissue Engineering Applications

Abstract 125

1. Introduction 126

2. Materials and methods 127

2.1. Materials 127

2.2. Scaffolds preparation 128

2.3. Degradation studies 128

2.4. Analysis of sample morphology by scanning electron microscopy (SEM) 128

2.5. Mechanical properties – compression tests 129

2.6. Cell lines used for biocompatibility testing 129

2.7. Biocompatibility evaluation: extracts and cell adhesion studies 129

3. Results and discussion 130

3.1. Characterization of the scaffolds morphology 130

3.2. Degradation behavior 130

3.3. Mechanical properties 135

3.4. Cytotoxic assessment of the extracts 135

3.5. Cell morphology evaluation 136

4. Conclusions 138

Acknowledgements 139

References 139

CHAPTER VI **143**

Chitosan Scaffolds Incorporating Lysozyme into CaP Coatings Produced by a Biomimetic Route: A Novel Concept for Tissue Engineering Combining a Self-Regulated Degradation System with *In Situ* Pore Formation

Abstract 145

1. Introduction 146

2. Materials and methods 147

2.1. Materials 147

2.2. Preparation of chitosan scaffolds 147

2.3. Preparation of CaP biomimetic coatings 147

2.4. Degradation studies 148

2.5. Determination of lysozyme activity in solution and released from the CaP Coatings 149

2.6. Statistics 149
3. Results and discussion 149
3.1. Development of CaP biomimetic coatings 149
3.2. Degradation studies 152
3.3. Lysozyme activity in solution and released from the coatings 156
4. Conclusions 157
Acknowledgements 157
References 158

CHAPTER VII 161

Natural Stimulus Responsive Scaffolds/Cells for Bone Tissue Engineering: Influence of Lysozyme upon Scaffold Degradation and Osteogenic Differentiation of Cultured Marrow Stromal Cells Induced by CaP Coatings

Abstract 163
1. Introduction 164
2. Materials and methods 166
2.1. Materials 166
2.2. Degradation studies 167
2.3. Micro-Computed Tomography (μ-CT) 167
2.4. MSCs isolation 168
2.5. Cell seeding 168
2.6. DNA analysis 169
2.7. Alkaline phosphatase activity measurements 169
2.8. Calcium deposition measurement 169
2.9. Microscopy analysis 170
2.10. Fourier transformed infrared spectroscopy with attenuated total reflectance (FTIR-ATR) 170
2.11. Statistics 170
3. Results and discussion 170
3.1. Degradation studies 170
3.2. Assays 174
3.3. Fourier transformed infrared spectroscopy with attenuated total reflectance (FTIR-ATR) 179
4. Conclusions 180
Acknowledgements 181
References 182

CHAPTER VIII **187**

***In Vivo* Responsive Self-Regulated Degradation System with *In Situ* Pore Formation Ability: A Novel Strategy for Bone Tissue Engineering**

Abstract 189

1. Introduction 190

2. Materials and methods 191

2.1. Materials 191

2.2. Implant preparation 192

2.3. Subcutaneous implantation 192

2.4. Preparation of samples for weight loss and μ-CT analysis 193

2.5. Weight loss measurements 194

2.6. Micro-computed tomography (μ-CT) analysis 194

2.7. Histology 195

2.8. Statistics 196

3. Results and discussion 197

3.1. Weight loss measurements 197

3.2. μ-CT analysis 198

3.3. Microscopic analysis 202

4. Conclusions 207

Acknowledgements 207

References 208

SECTION 5 **213**

CHAPTER IX **215**

GENERAL CONCLUSIONS AND FINAL REMARKS

LIST OF ABBREVIATIONS

A

ALP	alkaline phosphatase
ANOVA	analysis of variance
ATTC	american type culture collection
α-MEM	α-minimum essential medium

B

BMP	bone morphogenetic protein
BMP-2	bone morphogenetic protein-2
BMSC	bone marrow stromal cell
BMSSCs	Bone marrow stromal stem cells

C

C100	chitosan scaffolds
Ca^{2+}	calcium
$CaCl_2$	calcium chloride
CaP	calcium phosphate
CaPCH	calcium phosphate coated chitosan scaffolds
CaPCS	calcium phosphate coated chitosan/starch scaffolds
CaPCH	+ lysozyme calcium phosphate coated chitosan scaffolds with incorporated lysozyme
CaPCS	+ lysozyme calcium phosphate coated chitosan/starch scaffolds with incorporated lysozyme
CH	chitosan scaffolds
CO_2	carbone dioxide
CO_3^{2-}	carbonate
CS	chitosan/starch scaffolds
CS80-20	chitosan/starch scaffolds (80/20)
CS60-40	chitosan/starch scaffolds (60/40)

D

DD	degree of deacetylation
ddH_2O	double distilled water
DMEM	Dulbecco's Modified Eagle's medium
DNA	deoxyribonucleic acid
dsDNA	double stranded DNA

E

ECM	extracellular matrix

F

FBS	fetal bovine serum
FGF-1	fibroblat growth factor-1
FGF-2	fibroblat growth factor-2
FTIR	Fourier transform infrared spectroscopy
FTIR-ATR	Fourier transform infrared spectroscopy with attenuated total reflectance

H

HA	Hydroxyapatite
H&E	hematoxylin and eosin staining
HSD	honestly significantly different

I

IGF-2	insuline-like growth factor-2
ISO	International Organization for Standardization

K

KBr	potassium bromide

L

L929	mouse fibroblast cell line

M

µ-CT	micro-computed tomography
mg	micrograms
µL	microliters
MAPCs	multipotent adult progenitor cells
MPCs	mesodermal progenitor cells
mL	mililiters
MSC	mesenchymal stem cell
MTT	3-(4,5-dimethylthiazol-2-yl)-2,4-diphenyltetrazolium bromide

N

Na_2SO_4	sodium sulphate
NaOH	sodium hydroxide

O

OD	optical density

P

PBS	phosphate buffered saline
PCL	poly(ε-caprolactone)
pH	potential of hydrogen
PO_4^{3-}	Phosphate

R

RGD	arginine-glycine-aspartic acid
RT-PCR	reverse transcriptase polymerase chain reaction
rMSC	rat bone marrow stromal cell
rpm	rotations per minute

S

SaOS-2	human osteosarcoma cells
SD	standard deviation
SEM	scanning electron microscopy
SBF	simulated body fluid
1.0 SBF	simulated body fluid (normal concentration)
1.5 SBF	simulated body fluid (1.5x normal concentration)
SEM	scanning electron microscopy
SPCL	blend of starch and poly(ε-caprolactone)

T

3D	three dimensional
TF-XRD	thin-film X-ray diffraction
TGF-β	Transforming growth factor-β
TGF-β1	Transforming growth factor-β1
Tris-HCl	trisaminomethane hydrochloride

LIST OF FIGURES

SECTION 1
CHAPTER I
INTRODUCTION
PART II. Naturally Derived Responsive and *In Situ*-Forming Scaffolds for Bone Tissue Engineering Applications: An Overview of the Last Decade

Figure 1. Schematic representation of *in situ* pore forming concept. 44

Figure 2. Schematic representation of a self-regulated degrading material with gradual *in situ* pore formation ability. 46

SECTION 3
CHAPTER III
The Role of Lipase and α-Amylase in the Degradation of Starch/Poly(ε-Caprolactone) Fiber Meshes and the Osteogenic Differentiation of Cultured Marrow Stromal Cells

Figure 1. Weight loss profile (pH 7.4, 37ºC) of SPCL fiber mesh scaffolds using α-amylase (150 U/L) and lipase (110 U/L) under static and dynamic conditions up to 30 days. 88

Figure 2. SPCL fiber meshes images obtained by μ-CT before (A, G) and after degradation with α-amylase (150 U/L) under static (B-F) and dynamic (H-L) conditions up to 30 days. The scale bar is 2 mm and applies to all images. 89

Figure 3. SPCL fiber meshes images obtained by μ-CT before (A, G) and after degradation with lipase (110 U/L) under static (B-F) and dynamic (H-L) conditions up to 30 days. The scale bar is 2 mm and applies to all images. 90

Figure 4. Porosity (A) and pore interconnectivity (B) of SPCL fiber meshes after different degradation periods with lipase and α-amylase using static and dynamic conditions. Results are expressed as means ± standard deviation with n=3 for each bar. (+) indicates a significant difference ($p < 0.05$) between conditions as a function of time compared with control samples. (#) indicates a significant difference ($p < 0.05$) between static and dynamic conditions (using the same enzyme) at the same 92

time point. (*) indicates a significant difference ($p < 0.05$) between enzymes (lipase and α-amylase) using static conditions at the same time point, no significant differences were observed between dynamic conditions.

Figure 5. Pores size (A) and fibers thickness (B) of SPCL fiber meshes after degradation with lipase and α-amylase as a function of immersion time using static and dynamic conditions. Results are expressed as means ± standard deviation with n=3 for each bar. (+) indicates a significant difference ($p < 0.05$) between conditions as a function of time compared with control samples. (#) indicates a significant difference ($p < 0.05$) between static and dynamic conditions (using the same enzyme) at the same time point. (*) indicates a significant difference ($p < 0.05$) between enzymes (lipase and α-amylase) using static or dynamic conditions at the same time point. In Figure B (*) indicates that α-amylase has a significant difference at the same time point using static or dynamic conditions compared with lipase (except at day 21 using static conditions). 93

Figure 6. Cellularity of SPCL fiber meshes cultured *in vitro* with lipase, α-amylase and without enzymes for 8 and 16 days. Results are expressed as means ± standard deviation with n=3 for each bar. (*) indicates a significant difference ($p < 0.05$) between conditions at the same time point. (**) indicates a significant difference ($p < 0.05$) between 8 and 16 days for each condition. 94

Figure 7. SEM images of the surfaces of SPCL fiber mesh scaffolds cultured with lipase (A, D), α-amylase (B, E), and without enzymes (C, F) after day 8 (A, B, C) and day 16 (D, E, F). The scale bar is 500 μm and applies to all images. 94

Figure 8. Alkaline phosphatase activity of rat marrow stromal cells cultured *in vitro* upon SPCL fiber mesh scaffolds with lipase, α-amylase and without enzymes for up to 16 days. Results are expressed as means ± standard deviation with n=3 for each bar. (*) indicates a significant difference ($p < 0.05$) between conditions at the same time point. (**) indicates a significant difference ($p < 0.05$) between 8 and 16 days for each condition. 95

Figure 9. Calcium content of SPCL fiber mesh scaffolds cultured *in vitro* with lipase, α-amylase and without enzymes for 8 and 16 days expressed as total calcium per scaffold. Results are expressed as means ± standard deviation with *n*=3 for each bar. (*) indicates a significant difference ($p < 0.05$) between conditions after 16 days of culture. 96

Figure 10. Laser scanning confocal microscope images of rat marrow stromal cells stained with calcein-AM at the top surface of SPCL fiber meshes with lipase (A, D), α-amylase (B, E) and without enzymes (C, F) at 8 days (A, B, C) and 16 days (C, F). All images obtained using a 10X APO objective. The scale bar is 100 μm and applies to all images. 97

Figure 11. Laser scanning confocal microscopy images of SPCL fiber meshes cultured for 16 days with lipase (A), α-amylase (B) and without enzymes (C) obtained from depth projections. The scale bar is 100 μm and applies to all images. 97

Figure 12. FTIR-ATR spectra of SPCL fiber meshes before (A) and after 16 days of culture without enzymes (B), with α-amylase (C), and with lipase (D). 98

CHAPTER IV

Combination of Enzymes and Flow Perfusion Conditions Improves Osteogenic Differentiation of Bone Marrow Stromal Cells Cultured upon Starch/Poly(ε-Caprolactone) Fiber Meshes

Figure 1. Cellularity of SPCL fiber meshes cultured *in vitro* without enzymes, with α-amylase, lipase, α-amylase and lipase in static or flow perfusion conditions for 8 and 16 days. Results are expressed as means ± standard deviation with *n*=3 for each bar. (*) Indicates a significant difference ($p<0.05$) between 8 and 16 days; (**) indicates a significant difference ($p<0.05$) between groups (with and without enzymes) in static or flow conditions; and (#) indicates a significant difference ($p<0.05$) between flow and static conditions. 111

Figure 2. SEM images of the cross-sections of SPCL fiber mesh scaffolds cultured without enzymes (A), with α-amylase (B), with lipase (C) or with α-amylase and lipase in static conditions after 16 days. The scale bar is 400 μm and applies to all images. 112

Figure 3. SEM images of the cross-sections of SPCL fiber mesh scaffolds cultured without enzymes (A), with α-amylase (B), with lipase (C) or with α-amylase and lipase (D) in flow perfusion conditions after 16 days. The scale bar is 400 μm and applies to all images. 112

Figure 4. Representative histological cross-sections of SPCL fiber mesh scaffolds cultured for 16 days in flow perfusion conditions without enzymes (A), with α-amylase (B), with lipase (C) or with α-amylase and lipase (D). The flow direction was from the top of the image through the scaffold to the bottom. Sections have been stained with hematoxylin and eosin and shown at 4x magnification. The scale bar corresponds to 500 μm and applies to all images. 113

Figure 5. Alkaline phosphatase activity of rat bone marrow stromal cells cultured *in vitro* without enzymes, with α-amylase, with lipase, or with α-amylase and lipase upon SPCL fiber mesh scaffolds for up to 16 days in static and flow conditions. Results are expressed as means ± standard deviation with n=3 for each bar. (*) Indicates a significant difference (p<0.05) between 8 and 16 days; (**) indicates a significant difference (p<0.05) between groups (with and without enzymes) in static or flow conditions; and (#) indicates a significant difference (p<0.05) between flow and static conditions. 114

Figure 6. Calcium content of SPCL fiber mesh scaffolds cultured *in vitro* without enzymes, with α-amylase, with lipase, or with α-amylase and lipase in static and flow conditions for 8 and 16 days expressed as total calcium per scaffold. Results are expressed as means ± standard deviation with n=3 for each bar. (*) Indicates a significant difference (p<0.05) between 8 and 16 days; (**) indicates a significant difference (p<0.05) between groups (with and without enzymes) in static or flow conditions; and (#) indicates a significant difference (p<0.05) between flow and static conditions. 116

Figure 7. von Kossa stained histological sections of SPCL fiber mesh scaffolds cultured *in vitro* without enzymes, with α-amylase, with lipase, or with α-amylase and lipase for 16 days at different magnifications under flow perfusion conditions. 117

Figure 8. Sections of SPCL fiber meshes cultured without enzymes (A), with α-amylase (B), with lipase (C) or with α-amylase and lipase (D) for 16 days observed under fluorescent light, showing the tetracycline labelling of mineral in flow perfusion culture conditions. All images were obtained using a 4x APO objective. The scale bar is 500 μm and applies to all images. 118

SECTION 4

CHAPTER V

Natural Origin Scaffolds with *In Situ* Pore Forming Capability for Bone Tissue Engineering Applications

Figure 1. SEM micrographs of the developed scaffolds (transversal sections) before degradation: C100 (A), CS80-20 (B) and CS60-40 (C). The scale bar is 50 μm and applies to all images. 130

Figure 2. Water uptake of scaffolds as a function of immersion time in PBS (pH 7.4, T = 37º C). 131

Figure 3. SEM micrographs showing the morphology of chitosan-based scaffolds after 14 days in PBS with α-amylase solution (A-C100, C- CS80-20, D- CS60-40); after 30 days in same solution (B- C100); after 14 days in PBS with lysozyme solution (E- C100, F- CS80-20) and in the same period in PBS with α-amylase and lysozyme solution (G-C100, H-CS60-40). 133

Figure 4. Weight loss of chitosan/starch scaffolds as function of time in PBS with α-amylase (150 U/L) and lysozyme (13 mg/L) (pH 7.4, T = 37º C). 134

Figure 5. Results of the compression tests: modulus in dry and wet state. 135

Figure 6. Percentage of L929 viable cells determinated by the MTT in the presence of extracts derived from different formulations of the developed scaffolds. The percentage of viable cells was determined relating the optical density from the control, which is considered to have 100% viability. 136

Figure 7. SEM micrographs of the developed scaffolds surfaces, C100 (A and D), CS80-20 (B and E) and CS60-40 (C and F), before cell culture (A-C) and after 7 days of culture with L929 cells (D-F). 137

Figure 8. SEM micrographs of C100 (A, D), CS80-20 (B, E) and CS60-40 (C, F) scaffolds cultured with osteoblast-like cells after 3 (A-C) and 7 days (D-F) of culture. The scale bar is 200 μm and applies to all images. 138

CHAPTER VI

Chitosan Scaffolds Incorporating Lysozyme into CaP Coatings Produced by a Biomimetic Route: A Novel Concept for Tissue Engineering Combining a Self-Regulaed Degradation System with *In Situ* Pore Formation

Figure 1. SEM images of the surface of chitosan scaffolds: uncoated (A); coated with CaP layer at nucleation stage (B, B1) and after 7 days in the growth stage (D, D1); and coated with CaP layer with incorporated lysozyme at nucleation stage (C, C1) and after 7 days in the growth stage (E, E1). The scale bar is 50 μm for images A-E and 5 μm for images B1-E1. 150

Figure 2. FTIR spectra of CaP coatings, with and without incorporated lysozyme at nucleation stage (A) and TF-XRD spectra (B) of uncoated chitosan scaffolds (a); CaP coated chitosan scaffolds at nucleation stage (b) and after 7 days of growth (d); CaP coated chitosan with incorporated lysozyme at nucleation stage (c) and after 7 days of growth (e). 151

Figure 3. Weight loss profile of uncoated chitosan scaffolds, CaP coated chitosan scaffolds, CaP coated chitosan scaffolds with incorporated lysozyme as a function of immersion time at pH 7.4 (A) and pH 5 (B). (*) indicates a significant difference between time points for each condition. At pH 7.4 for each time point all difference between conditions is significant. (**) indicates a significant difference between conditions at the same time point. The weight loss at pH 5 for chitosan scaffolds is significantly different when compared with pH 7.4. 152

Figure 4. SEM images of chitosan scaffolds, CaP chitosan scaffolds and CaP chitosan scaffolds with incorporated lysozyme before and after degradation at pH 7.4 up to 30 days. Scale bar is 50 μm and applies to all images. 154

Figure 5. SEM images of chitosan scaffolds, CaP chitosan scaffolds and CaP chitosan scaffolds with incorporated lysozyme before and after degradation at pH 5 up to 14 days. The scale bar is 200 μm for all images except for images I1, L1, O1 (50 μm). 155

Figure 6. Lysozyme activity (measured as a decrease in the optical density of a *Micrococcus lysodeikticus* bacteria suspension) released from CaP coatings after immersion in buffer (pH 7.4) for 30 days (A) and lysozyme activity at pH 5 and 7.4 as a function of lysozyme concentration (B). 157

CHAPTER VII

Natural Stimulus Responsive Scaffolds/Cells for Bone Tissue Engineering: Influence of Lysozyme upon Scaffold Degradation and Osteogenic Differentiation of Cultured Marrow Stromal Cells Induced by CaP Coatings

Figure 1. Weight loss of chitosan (Ch) scaffolds after 21 days of immersion in PBS with lysozyme (1.5 g/L) solution. 171

Figure 2. Images of chitosan (Ch) scaffolds obtained by μ-CT: before degradation (A), after 3 days (B), 7 days (C), 14 days (D), and 21 days (E) of degradation with lysozyme (1.5 g/L). Lysozyme solution induced degradation and enhanced subsequent formation of pores in chitosan scaffolds as a function of immersion time. 172

Figure 3. Porosity (A) and interconnectivity (B) of chitosan scaffolds as a function of immersion time with lysozyme (1.5 g/L). Results are expressed as means ± standard deviation with $n = 3$ for each bar. (*) indicates a significant difference ($p < 0.05$) as a function of time compared with control samples. Immersion of chitosan scaffolds in lysozyme solution increased the porosity and pore interconnectivity of the scaffolds with time. 173

Figure 4. Pore size (A) and wall thickness (B) of chitosan scaffolds as a function of immersion time with lysozyme (1.5 g/L). Results are expressed as means ± standard deviation with $n = 3$ for each bar. (*) indicates a significant difference ($p < 0.05$) as a function of time compared with control samples. Immersion of chitosan scaffolds in lysozyme solution increased the mean pore size and decreased the mean wall thickness of the scaffolds with time. 173

Figure 5. Laser scanning confocal microscope images of cells stained with calcein-AM at the top surface of scaffolds after 8 days: (A) chitosan (Ch); (B) CaP coated chitosan scaffolds with incorporated lysozyme; (C) chitosan/starch (CS) and (D) CaP coated chitosan/starch scaffolds with incorporated lysozyme. All images obtained 45 minutes after incubation with calcein-AM using a 10X APO objective. The scale bar is 100 μm and applies to all images. Rat MSCs adhered to all scaffold formulations and maintained viability after 8 days of culture, with no differences observed among the groups. 174

Figure 6. Cellularity of chitosan-based scaffolds seeded with MSCs after 8, 16 and 21 days. Results are expressed as means ± standard deviation with n=3 for each bar. (*) indicates a significant difference ($p < 0.05$) between conditions at the same time point. (**) indicates a significant difference ($p < 0.05$) between different time periods for each condition. Ch, chitosan scaffolds; CaP/Ch+ lysozyme, CaP-coated chitosan scaffolds with incorporated lysozyme; CS, chitosan/ starch scaffolds; CaP/CS + lysozyme, CaP-coated chitosan/starch scaffolds with incorporated lysozyme. 175

Figure 7. (A) SEM images of the surfaces of cultured chitosan-based scaffolds after 8, 16 and 21 days. The scale bar is 500 μm and applies to all images. (B) SEM images of the surfaces of cultured chitosan-based scaffolds after 8, 16 and 21 days. The scale bar is 100 μm and applies to all images. 176

Figure 8. Alkaline phosphatase (ALP) activity of chitosan-based scaffolds seeded with MSCs after 8, 16 and 21 days. Results are expressed as means ± standard deviation with n=3 for each bar. (*) indicates a significant difference ($p < 0.05$) between conditions at the same time point. (**) indicates a significant difference ($p < 0.05$) between 8, 16 and 21 days for each condition. Ch, chitosan scaffolds; CaP/Ch+ lysozyme, CaP coated chitosan scaffolds with incorporated lysozyme; CS, chitosan/ starch scaffolds; CaP/CS + lysozyme, CaP coated chitosan/starch scaffolds with incorporated lysozyme. 177

Figure 9. Calcium content in chitosan-based scaffolds after day 16 and day 21 culture periods. Results are expressed as means ± standard deviation with *n*=3 for each bar. (*) indicates a significant difference ($p < 0.05$) between conditions at the same time point. (**) indicates a significant difference between day 16 and day 21 for each condition. Ch, chitosan scaffolds; CaP/Ch+ lysozyme, CaP coated chitosan scaffolds with incorporated lysozyme; CS, chitosan/ starch scaffolds; CaP/CS + lysozyme, CaP coated chitosan/starch scaffolds with incorporated lysozyme. 178

Figure 10. FTIR-ATR of chitosan (A), CaP/Ch + lysozyme (B), chitosan/starch (C) and CaP/CS + lysozyme scaffolds (D) before and after 16 and 21 days of culture with rat MSCs. Increases in amide, carbonate, and phosphate bands indicate increased deposition of mineralized ECM with time. 180

CHAPTER VIII

***In Vivo* Responsive Self-Regulated Degradation System with *In Situ* Pore Formation Ability: A Novel Strategy for Bone Tissue Engineering**

Figure 1. Aspect of the rat dorsum with 6 longitudinal incisions (A) immediately after subcutaneous implantation surgery and (B) after 5 days post-surgery. (C) Harvested scaffolds after 6 weeks with no signs of infection. 194

Figure 2. Weight loss profile of different groups after subcutaneous implantation for up to 12 weeks. Results are expressed as means ± standard deviation with *n* = 3 for each bar. (*) indicates a significant difference ($p < 0.05$) between groups at the same time point. (**) indicates a significant difference ($p < 0.05$) between the same condition at different time points. 198

Figure 3. Images of chitosan-based scaffolds obtained by μ-CT: before implantation (control) and after 3, 6 and 12 weeks of subcutaneous implantation. The scale bar is 1 mm and applies to all images. 200

Figure 4. Porosity (A) and interconnectivity (B) of chitosan-based scaffolds as a function of implantation time. Results are expressed as means ± standard deviation with *n* = 3 for each bar. (*) indicates a significant difference ($p < 0.05$) between groups at different time points compared with controls (0 days). (**) indicates a significant difference ($p < 0.05$) between different groups at the same time point. 201

Figure 5. Representative histological sections of scaffolds implanted subcutaneously stained with hematoxylin and eosin after 3, 6 and 12 weeks. The images are presented at 4x and 40x magnification. The scale bars represent 500 µm and apply to all images. Chitosan-based scaffolds (M) appear in red. Pores (P) appear filled by cells (Ce) in pink or blue. 203

Figure 6. Results of histological scoring of: (A) cellular growth within the implants and (B) degradation after 3, 6 and 12 weeks of subcutaneous implantation. Data are presented as means ± standard deviation for n = 4–5. (*) indicates a significant difference ($p < 0.05$) between group conditions at the same time point. (**) indicates a significant difference ($p < 0.05$) between the same condition at different time points. 204

Figure 7. Representative light microscope images of chitosan-based sections stained with von Kossa after 3, 6 and 12 weeks of subcutaneous implantation. The images are presented at 4x magnification. The scale bar is 500 µm and applies to all images. Chitosan-based scaffolds (M) are stained in gray. Pores (P) are filled with cells (Ce) and appear in pink. CaP coatings (CaP) appear in black. 206

LIST OF TABLES

SECTION 1

CHAPTER I

INTRODUCTION

PART II. Naturally Derived Responsive and *In Situ*-Forming Scaffolds for Bone Tissue Engineering Applications: An Overview of the Last Decade

Table 1. Mechanical properties of cancellous and cortical bone. 38

Table 2. Environmental stimuli that responsive, “smart”, “intelligent” or to which environmentally-sensitive polymers respond. 40

SECTION 2

CHAPTER II

MATERIALS AND METHODS

Table 1. Histological grading scale for degradation and cellular growth within the implants. 71

SECTION 4

CHAPTER VIII

***In Vivo* Responsive Self-Regulated Degradation System with *In Situ* Pore Formation Ability: A Novel Strategy for Bone Tissue Engineering**

Table 1. Histological grading scale for the degradation and cellular growth within the implants. 196

SHORT *CURRICULUM VITAE*

Ana M. Martins was born on May 21, 1979, in Braga, Portugal. She is currently a PhD candidate at the 3B's Research Group (Biomaterials, Biodegradables and Biomimetics), University of Minho, Portugal. Her doctoral work has been supervised by Prof. Rui L. Reis (also the Director of 3B's Research Group), Dr. Catarina Alves (Post-Doctoral Research Fellow at the 3B´s Research Group and Harvard University), and Prof. Antonios G. Mikos (Director of John W. Cox Laboratory of Biomedical Engineering and of the Center for Excellence in Tissue Engineering) from the Department of Bioengineering, Rice University, USA. She has just submitted her PhD thesis on Biomedical Engineering to the University of Minho, which was prepared in cooperation with Rice University, Houston, USA.

Ana Martins received her Bachelor of Science degree in Applied Biology from the University of Minho in 2004. As her senior research project she spent one year at the 3B´s Research Group under the supervision of Prof. Rui L. Reis, with her project graded with 19 (0-20 scale). In 2006, she also completed a Post-graduation Course on Processing and Characterization of Materials (first year of the Masters in Processing and Characterization of Materials), University of Minho, Portugal, with a final score of 15 (0-20 scale).

In April 2006, she formally started her PhD at the 3B's Research Group where she has been working on the development, characterization and modification with biomimetic coatings of novel scaffolds for bone tissue engineering. At the same time she received a scholarship for her doctoral research studies from the European Network of Excellence, EXPERTISSUES, which enabled her to perform her studies at Rice University, USA. During her PhD work she spent several periods in a total of almost one year and half at Rice University, under the supervision of Prof. Antonios G. Mikos. She was also mentor of an undergraduate student (Institute of Biosciences and Bioengineering) at Rice University. Additionally, at Rice University she learned and mastered procedures associated with the operation of a novel flow perfusion bioreactor system, she has acquired a firm foundation of knowledge and experience in the harvest and expansion of bone marrow stromal cells from rats and in the subcutaneous implantation of tissue engineering constructs in a rat animal model. Indeed, apart from knowledge and experience in progenitor cell biology, advanced cell culture techniques and animal models, Ana Martins has acquired training in natural based materials, enzymes and their biomedical applications through her research activities at the 3B's Research Group at the University of Minho in Portugal.

Ana M. Martins has been also involved in the writing and preparation of several grant proposals, both at National (Portuguese Foundation for Science and Technology) and European levels (Framework Programme VI).

As a result of her research she attended the most important international conferences in the field of Biomaterials, Tissue Engineering, and Regenerative Medicine. Presently, she is the first author of 7 papers in international refereed journals (2 published, 3 in press, and 3 submitted) and 1 book chapter (in press).

LIST OF PUBLICATIONS

The work performed during this PhD studies resulted in the following publications:

INTERNATIONAL JOURNAL WITH REFEREE

A.M. Martins, M.I. Santos, H.S. Azevedo, P.B. Malafaya, R.L. Reis. Natural origin scaffolds with *in situ* pore forming capability for bone tissue engineering applications. Acta Biomaterialia, 4, 1637-1645 (2008).

A.M. Martins, Q.P. Pham, P.B. Malafaya, R.A. Sousa, M.E. Gomes, R.M. Raphael, F.K. Kasper, R.L. Reis, A.G. Mikos. The Role of Lipase and α-Amylase in the Degradation of Starch/Poly(ε-Caprolactone) Fiber Meshes and the Osteogenic Differentiation of Cultured Marrow Stromal Cells. Tissue Engineering: Part A, 15, 295-305 (2009).

A.M. Martins, Q.P. Pham, P.B. Malafaya, R.M. Raphael, F.K. Kasper, R.L. Reis, A.G. Mikos. Natural Stimulus Responsive Scaffolds/Cells for Bone Tissue Engineering: Influence of Lysozyme upon Scaffold Degradation and Osteogenic Differentiation of Cultured Marrow Stromal Cells Induced by CaP Coatings. Tissue Engineering: Part A, in press, DOI: 10.1089=ten.tea.2008.0023 (2009).

A.M. Martins, R.C. Pereira, I.B. Leonor, H.S. Azevedo, R.L. Reis. Chitosan scaffolds incorporating lysozyme into CaP coatings produced by a biomimetic route: a novel concept for tissue engineering combining a self-regulated degradation system with *in situ* pore formation, Acta Biomaterialia, in press, doi:10.1016/j.actbio.2009.05.027 (2009).

A.M. Martins, A. Saraf, F. K. Kasper, A.G. Mikos, R.A. Sousa, C.M. Alves, R.L. Reis. Combination of enzymes and flow perfusion conditions improves osteogenic differentiation of bone marrow stromal cells cultured onto starch/poly(ε-caprolactone) fiber meshes, submitted.

A.M. Martins, F.K. Kasper, A.G. Mikos, J.D. Kretlow, A.R. Costa-Pinto, P.B. Malafaya, N.M. Neves, C.M. Alves, R.L. Reis. *In vivo* responsive self-regulated degradation system with *in situ* pore formation ability: a novel strategy for bone tissue engineering, submitted.

A.M. Martins, C.M. Alves, F. K. Kasper, A.G. Mikos, R.L. Reis. Naturally derived responsive and *in situ*-forming scaffolds for bone tissue engineering applications: an overview of the last decade, submitted.

BOOK CHAPTERS

A.M. Martins, C.M. Alves, R.L. Reis, A.G. Mikos, F.K. Kasper. Towards Osteogenic Differentiation of Marrow Stromal Cells and In Vitro Production of Mineralized Extracellular Matrix onto Natural Scaffolds in Biological Interactions on Materials Surfaces: Understanding and Controlling Protein, Cell and Tissue Responses, R. Bizios and D. Puleo, Eds., Springer, San Diego, in press, 2008 (DOI: 10.1007/978-0-387-98161-1_13).

INTERNATIONAL CONFERENCES

A.M. Martins , P.B. Malafaya, H.S. Azevedo, R.L. Reis, Chitosan/starch scaffolds with gradual in vivo pore forming ability, 18th European Conference on Biomaterials (ESB), Stuttgart, Germany, October 2003, poster presentation.

A.M. Martins , P.B. Malafaya, H.S. Azevedo, M.I. Santos , O.P. Coutinho, R.L. Reis, Natural origin scaffolds with in situ gradual pore forming capability: development and characterization, 7th World Biomaterials Congress, Sydney, Australia, May 2004, poster presentation.

A.M. Martins, M.I. Santos, H.S. Azevedo, P.B. Malafaya, O.P. Coutinho, R.L. Reis, Chitosan/starch scaffolds with *in situ* pore forming capability for tissue engineering applications, Meeting of the Tissue Engineering Society International and the European Tissue Engineering Society (TESI-ETES), Lausanne, Switzerland, October 2004, oral presentation.

A.M. Martins, H.S. Azevedo, I.B. Leonor, R.L. Reis, Chitosan Scaffolds Incorporating Degradative Enzymes Into Biomimetic Ca-P Coatings Able to Tailor the Degradation Rate, 30th Annual Meeting for the Society for Biomaterials (SFB), Memphis, United States of America, April 2005, oral presentation.

M.I. Santos, **A.M. Martins**, S. Fuchs, R.E. Unger, R.L. Reis, C.J. Kirkpatrick, Endothelialization of Chitosan/Starch Scaffolds with *in situ* Forming Ability as a New Approach for Bone Tissue Engineering Applications, 19th European Conference of Biomaterials (ESB), Sorrento, Italy, September 2005, oral presentation.

A.M. Martins, A.J. Salgado, H.S. Azevedo, I.B. Leonor, R.L. Reis, Lysozyme incorporation in biomimetic coated chitosan scaffolds: development and behaviour in contact with

osteoblastic-like cells, 8th Annual Meeting of Tissue Engineering Society International (TESI), Shanghai, China, October 2005, oral presentation.

A.M. Martins, R.C. Pereira, A.J. Salgado, H.S. Azevedo, I.B. Leonor, R.L. Reis, Chitosan Scaffolds Incorporating Lysozyme into Ca-P Biomimetic Coatings: Scaffolds for Tissue Regeneration Combining a Self-Regulating Degradation System With *In Situ* Pore Formation and Carrier Properties, 2006 Regenerate World Congress on Tissue Engineering and Regenerative Medicine (TERMIS), Pittsburgh, United States of America, April 2006, oral presentation.

A.M. Martins, R.C. Pereira, H.S. Azevedo, I.B. Leonor, R.L. Reis, Smart Chitosan Scaffolds Incorporating Lysozyme into Biomimetic Coatings Combining a Self-Regulating Degradation System with *In situ* Pore Formation: A Novel Concept for Tissue Engineering, InVENTS - 1st Marie Curie Cutting-edge Conference on New Developments on Polymers for Tissue Engineering: Replacement and Regeneration, Funchal, Madeira, Portugal, June 2006, poster presentation.

A.M. Martins, R.C. Pereira, H.S. Azevedo, I.B. Leonor, R.L. Reis, A Novel Concept for Tissue Engineering Based on Chitosan Smart Scaffolds and Biomimetic Coatings Containing Enzymes, Advances in Tissue Engineering 2007 – 15th Annual Short Course, Houston, USA, August 2006, poster presentation.

A.M. Martins, R.C. Pereira, H.S. Azevedo, I.B. Leonor, R.L. Reis, Chitosan/Biomimetic Ca-P Scaffolds Containing Enzymes as New Smart Material for Tissue Engineering, 3rd Marie Curie Cutting Edge InVENTS Conference, Funchal, Madeira, Portugal, June 2007, poster presentation.

A.M. Martins, Q.P. Pham, A.G. Mikos, Reis RL, Natural Stimulus Responsive Scaffolds/Cells for Bone Tissue Engineering: Influence of Ca-P Coatings and Lysozyme Incorporated into Scaffolds in Osteogenic Differentiation of Marrow Stromal Cells and theirs Degradation, 1st TERMIS Summer School, Funchal, Madeira, Portugal, June 2007, poster presentation.

A.M. Martins, Q.P. Pham, P.B. Malafaya, R.A. Sousa, M.E. Gomes, F.K. Kasper, A.G. Mikos, The role of lipase and alpha-amylase in both the degradation of starch/polycaprolactone fiber meshes and the osteogenic differentiation of rat marrow stromal cells, 8th World Biomaterials Congress, Amsterdam, The Netherlands, April 2008, poster presentation.

A.M. Martins, Q.P. Pham, P.B. Malafaya, R.M. Raphael, F.K. Kasper, R.L. Reis, A.G. Mikos, Smart and stimulus responsive chitosan-based scaffolds/cells for bone tissue engineering: influence of lysozyme upon scaffold degradation and osteogenic differentiation of cultured marrow stromal cells induced by CaP coatings, 2008 Annual TERMIS-EU Meeting, Porto, Portugal, June 2008, oral presentation.

A.M. Martins, A. Saraf, F.K. Kasper, C.M. Alves, R.L. Reis, A.G. Mikos, Lipase enhances osteogenic differentiation of cultured marrow stromal cells onto SPCL fiber meshes using flow perfusion bioreactors, TERMIS-NA, San Diego, USA, December 2008, poster presentation.

A.M. Martins, F.K. Kasper, J.D. Kretlow, A.R. Costa-Pinto, P.B. Malafaya,' N.M. Neves, C.M. Alves, R.L. Reis, A.G. Mikos, *In Vivo* Responsive Scaffolds with the Ability of In Situ Pore Formation: A Novel Strategy for Bone Tissue Engineering**,** 2nd TERMIS World Congress, Seoul, Republic of Korea, August 2009, accepted for poster presentation.

A.M. Martins, A. Saraf, R.A. Sousa, F.K. Kasper, C.M. Alves, R.L. Reis, A.G. Mikos, Towards Osteogenic Differentiation of Bone Marrow Stromal Cells Cultured onto Starch/ Poly(ε-caprolactone) Fiber Mesh Scaffolds: The Efficiency of Enzymes and Flow Perfusion Bioreactors, 2nd TERMIS World Congress, Seoul, Republic of Korea, August 2009, accepted for poster presentation.

INTRODUCTION TO THE THESIS FORMAT

This thesis is divided in five sections containing nine chapters, with six of them experimental. The contents of each section are summarized below.

SECTION 1 (Chapter I)

In the first part (**Part I**) it is discussed the preparation of naturally derived scaffolds of polysaccharide origin, the osteogenic differentiation of mesenchymal stem cells cultured on biomimetic calcium phosphate coatings, and the delivery of biomolecules associated with ECM mineralization. The second part (**Part II**) gives an overview of strategies that can modulate bone tissue regeneration by using naturally derived *in situ*-forming scaffolds.

SECTION 2 (Chapter II)

Chapter II contains the materials and experimental procedures used within the scope of this thesis, detailing what is included in the manuscripts that compose the results sections.

SECTION 3 (Chapter III and IV) consists of two chapters of experimental work.

Chapters III and IV describes the studies using starch/ poly(ε-caprolactone) fiber mesh scaffolds and osteogenic culture media supplemented with α-amylase and/or lipase in static cultures and flow perfusion bioreactors using rat bone marrow stromal cells. Degradation studies with α-amylase or lipase were also performed in static and dynamic conditions.

SECTION 4 (Chapters V, VI, VII and VIII) consists of four chapters of experimental work.

Chapter V describes the development of several scaffolds formulations based on chitosan and starch with the ability of forming a porous structure *in situ* due to the attack of specific enzymes present in the human body (α-amylase and lysozyme). Compressive analysis, degradation studies with α-amylase and/or lysozyme at concentrations similar to those found in human serum, extracts tests with L929 cells and direct contact tests with osteoblast-like cells were performed.

Chapter VI describes an innovative self-regulated degrading material with gradual *in situ* pore formation ability for bone tissue engineering applications. In this work, lysozyme was incorporated into calcium phosphate (CaP) coatings, on the surface of chitosan scaffolds using biomimetic coating technique, with the aim of controlling their degradation rate, subsequent formation of pores and to prevent infection upon implantation. To prove the concept of *in situ* pore formation, the coated scaffolds (with and without lysozyme) were incubated in two different solutions at different pHs to simulate normal physiological conditions (pH 7.4) and inflammatory response (pH 5).

Chapter VII reports the use of CaP coated chitosan-based scaffolds with incorporated lysozyme. This study was designed in order to assess the influence of lysozyme on the formation of pores in chitosan scaffolds, using a similar concentration to the one incorporated into CaP coatings. Additional studies investigated the influence of a CaP biomimetic coating and lysozyme on osteogenic differentiation of rat bone marrow stromal cells.

Chapter VIII presents the final experimental study performed for this thesis. This last study intends to validate the concept of *in situ* pore forming *in vivo using a rat* subcutaneous model. It was investigated the degradation of the scaffolds *in vivo* and the *in situ* formation of pores.

SECTION 5 (Chapter IX)

Chapter IX contains the general conclusions and final remarks regarding the overall work carried out under the scope of this thesis.

SECTION 1

CHAPTER I

INTRODUCTION

PART I.

Towards Osteogenic Differentiation of Marrow Stromal Cells and *In Vitro* Production of Mineralized Extracellular Matrix onto Natural Based Scaffolds

PART II.

Naturally Derived Responsive and *In Situ*-Forming Scaffolds for Bone Tissue Engineering Applications: An Overview of the Last Decade

CHAPTER I

INTRODUCTION

PART I. Towards Osteogenic Differentiation of Marrow Stromal Cells and *In Vitro* Production of Mineralized Extracellular Matrix onto Natural Based Scaffolds[1]

ABSTRACT

Tissue engineering has emerged as a new interdisciplinary field for the repair of various tissues, restoring their functions by using scaffolds, cells, and/or bioactive factors. A temporary scaffold acts as an extracellular matrix (ECM) analog to culture cells and guide the development of new tissue. In this chapter, we discuss the preparation of naturally derived scaffolds of polysaccharide origin, the osteogenic differentiation of mesenchymal stem cells (MSCs) cultured on biomimetic calcium phosphate (CaP) coatings, and the delivery of biomolecules associated with extracellular matrix mineralization.

[1] This chapter is based on the following publication:

A.M. Martins, C.M. Alves, R.L. Reis, A.G. Mikos, F.K. Kasper. Towards Osteogenic Differentiation of Marrow Stromal Cells and In Vitro Production of Mineralized Extracellular Matrix onto Natural Scaffolds in Biological Interactions on Materials Surfaces: Understanding and Controlling Protein, Cell and Tissue Responses, R. Bizios and D. Puleo, Eds., Springer, San Diego, in press, 2008 (DOI: 10.1007/978-0-387-98161-1_13).

1. INTRODUCTION

Bone is a dynamic, highly vascularized tissue with a unique capacity to heal and remodel without leaving a scar. It is the structural framework of the body and is composed of an inorganic mineral phase of hydroxyapatite and an organic phase of mainly type I collagen. Bone continuously resorbs and reforms in a remodeling process that is carried out by two types of bone cells: the bone-building osteoblasts and the bone-resorbing osteoclasts. Slowly and insidiously, bone deteriorates, losing minerals and structure. Bone injuries produced as a result of disease and/or trauma present a major health concern. A fracture, usually of the hip, wrist, or a vertebra, is often the first indication that osteoporosis has been weakening the bones of a patient for years (1). Treatment options include transplantation, surgical repair, prostheses, mechanical devices, and drug therapy (2). However, major damage to a tissue or organ can neither be repaired nor long-term recovery effected in a truly satisfactory way using these methods.

In this context, an emerging field of science termed “tissue engineering,” defined as an “interdisciplinary field that applies the principles of engineering and life sciences toward the development of biological substitutes that restore, maintain, or improve tissue function” (3) has been gaining significant recognition. Tissue engineering uses organ-specific cells for seeding a scaffold *ex vivo*, however it may also involve the implantation of an acellular construct for guided tissue regeneration (4). Indeed, a wide range of strategies exist for tissue engineering in general, and bone tissue engineering specifically.

Bone tissue engineering is a rapidly expanding field, full of innovative ideas for treating bone trauma and pathologies. Selection of the most appropriate material to produce a scaffold in bone related applications is a very important step toward the construction of a tissue engineered construct. There is an increasing interest in the production of novel scaffolds from renewable resources. Natural polymers are an attractive alternative to synthetic polymers for various clinical applications partly due to their biocompatibility and also because they are typically biodegraded by “normal” and/or enzymatic hydrolysis (carried out, in the majority of cases, by specific enzymes also present in the human body). Some of the advantages associated with naturally derived biomaterials are their cost effectiveness as well as the wide range of properties and structures attainable with these materials. A large number of different naturally derived biomaterials have been studied and proposed for bone tissue engineering applications, namely polysaccharides (chitosan, starch, alginate, hyaluronic acid, and cellulose, among others) and proteins (soy, collagen, fibrin). Polysaccharides, in particular, have some attractive properties, such as nontoxicity (pertinent monomer residues are not hazardous to health), high swelling ability and stability over a range of pH values.

For successful bone replacement, the ideal scaffold should be biocompatible (5-8) with the surrounding biological fluids and tissues to avoid any detrimental tissue response. The scaffolding material should degrade into nontoxic residues that can be easily removed from the body through normal excretion processes (5, 6, 8, 9). The scaffolds serve as temporary substrates for living cells as well as physical supports for tissue regeneration (10). Adequate surface area and appropriate surface energy are also needed to permit cell adhesion, promote cell proliferation, and allow retention of differentiated cell functions (5-8, 10). In addition, sufficient mechanical stability of the scaffold is necessary to maintain the desired shape and structure during cell culture *in vitro* and transplantation *in vivo*. Control of scaffold pore morphology is critical for controlling cell colonization rates and maintaining transport of oxygen, nutrients, and metabolic waste, as well as for supporting organization of the engineered tissue. Furthermore, angiogenesis, a requirement for survival and success of vascularized tissues, can be affected by the porosity of the scaffold. Pore morphology can also be expected to significantly affect scaffold degradation kinetics and the mechanical properties of the developing tissue (6, 11).

The scaffolds used for tissue engineering purposes mimic the extracellular matrix (ECM) of the regenerating bone environment. Thus, in addition to serving as a mechanical support, a tissue engineering scaffold may also be “informative” to the cells. An ideal three-dimensional construct for bone tissue engineering, above all discussed pertinent characteristics, should be simultaneously osteoinductive (capable of recruiting osteoprogenitor cells and stimulating their differentiation down the bone-forming cell lineage), osteoconductive (capable of supporting the formation of bone at the surface of the scaffold), and also resorbable and amenable to gradual replacement by newly formed bone (12). In the medical field, consideration of biodegradation is a priority on the list of safety standards when choosing polymers as potential biomaterials for tissue engineering applications. Naturally derived materials have recently gained interest, as they are structurally similar to the native extracellular matrix of many tissues; exhibit excellent biocompatibility; and induce minimal inflammatory response and tissue damage. Natural polymers may present a biologically active environment to the cells, since they usually contain domains that provide cues and can send important signals to guide cells at various stages of development (10).

A method to potentially increase the biological activity of a bone tissue engineering scaffold is to coat the surface of the scaffold with calcium phosphate. One of the main goals of calcium phosphate (CaP) coatings on bone tissue engineering scaffolds is to promote osteoconduction and by enhancing adhesion of osteogenic cells and ingrowth of bone into biomaterials (13). New technologies have been developed to promote osteogenic activity of

bone tissue engineering scaffolds. These approaches tend to integrate into the coatings osteoinductive or bioactive agents (e. g., enzymes and antibiotics), to immobilize constitutional elements of bone (e.g., growth factors including bone morphogenetic proteins [BMPs] and other members of the transforming growth factor [TGF]-β superfamily, adhesion proteins (e.g., collagen, fibronectin, laminin, and vitronectin) and peptides (e.g., the arginine-glycine-aspartic acid [RGD] sequences) on the surface of biomaterials. Immobilization and/or delivery of bioactive molecules at specific sites have been exploited to enhance cell adhesion, differentiation, and other cell functions as well as to promote mineralization of the ECM of the tissue engineered bone constructs.

2. SCAFFOLDS OF NATURAL ORIGIN – POLYSACCHARIDES

A large number of natural polymers, including polysaccharides, have been suggested as candidates for the production of scaffolds for bone tissue engineering purposes. Polysaccharides are relatively complex carbohydrates. They are high molecular weight polymers having one or more monosaccharide repeating units joined together by glycosidic bonds. Polysaccharides tend to be amorphous and insoluble in water. Some of the main advantages associated with this class of polymers are wide availability, cost effectiveness, good hemocompatibility (probably because of their similarities with heparin), nontoxicity, and a wide range of properties and structures suitable for biomedical applications. These polymers have been proposed as scaffolds for bone tissue engineering applications as well as carriers for cells and bioactive molecules (e.g., proteins, enzymes, and growth factors) for controlled release systems.

Chitosan, starch and alginate, three examples of polysaccharide materials, will be described in detail in the sections that follow.

2.1. Chitosan

Chitosan, a naturally derived polymer, is a partially deacetylated derivative of chitin, found in crustacea exoskeletons (e.g., shrimp, crab, and lobster), cell walls of fungi, and cuticles of insects (14, 15). Depending on the source and preparation procedure, the molecular weight of chitosan may range from 300 to more than 1,000 kDa (11). Chitosan is a suitable functional biomaterial because it is biocompatible, biodegradable, minimally immunogenic, nontoxic, and hydrophilic. Moreover, it has adsorption properties with remarkable affinity for proteins, and is not expensive (16-21). Some studies report that chitosan enhanced osteogenesis (22-24) and improved wound healing (25, 26). In addition, chitosan is a hemostatic agent (11, 16), with antithrombogenic properties (27). It has proved to be a useful excipient in various drug delivery systems due to its nontoxicity, high cohesive

and hydrophilic properties, and polycationic character resulting from primary amine groups, which provide a high charge density in acidic solutions (pH < 6.5) (18, 28). It is soluble in dilute or weak acids (such as acetic and formic acid), but it is normally insoluble in aqueous solutions above pH 6.5.

Chitosan is a binary polyheterosaccharide of *N*-acetylglucosamine and glucosamine with a β1→4 linkage. The superior tissue compatibility of chitosan can be partially attributed to its structural similarity to glycosaminoglycans, which are major components of the ECM of bone and cartilage (15, 29). Chitosan is easily hydrolyzed by various chitosanases (30), which are completely absent in mammals, and is biodegraded in the presence of lysozyme in aqueous medium *in vitro* (17, 31-35); this degradation process depends on the degree of deacetylation (31), which represents the proportion of *N*-acetyl-D-glucosamine units with respect to the total number of units (30). Chitosan degradation kinetics are inversely related to the degree of deacetylation (31, 32). *In vitro* and *in vivo*, chitosan is degraded by enzymatic hydrolysis; the primary agent of this process is lysozyme, which targets acetylated residues (36). Chitosan and glucosamine, its biodegradation product, are not toxic *in vivo* (37). Lysozyme, or muramidase, is an enzyme that catalyzes the hydrolysis of the peptidoglycan layer of bacterial cell walls (38). This enzyme is active over a broad pH range (from 3 to 8) and hydrolyzes its substrates both inside and outside cells. Lysozyme is widely distributed in the human body (39). It is found to occur in the nose the bronchus, bronchiole, middle ear, lacrimal gland, bone marrow and digestive tract (16), and in lymphocytes; lysozyme is also secreted by monocytes, macrophages, and granulocytes, which are the largest source of the enzyme (40, 41). Monocytes and macrophages are the primary contributors to the lysozyme content in human serum (41); the concentration in serum is in the range of 7 to 13 mg/L (39). The susceptibility of chitosan to degradation induced by lysozyme make the protein an attractive target for incorporation into this biodegradable material (29, 42-44).

Incorporation of active biomolecules, such as growth factors, has been used as a highly beneficial strategy for improving bone regeneration in tissue engineering applications. The biological activity of chitosan on bone regeneration has been confirmed in many studies (18, 45). Chitosan can be easily fabricated into bulk porous scaffolds, films, microparticles, sponges and beads. The feasibility of forming porous scaffolds permits wide application of this polymer in tissue engineering. This is mainly true for bone tissue engineering applications, because chitosan supports osteoblast proliferation and phenotypic expression (15). Chitosan fiber meshes with appropriate mechanical properties, developed by Tuzlakoglu *et al.* (46) exhibited bioactivity; this is very important aspect for biomaterials used as bone tissue engineering scaffolds. Martins *et al.* (35) proposed the development of

chitosan-based scaffolds with the capability of forming porous structures *in situ* following attack by specific enzymes (namely, α-amylase and lysozyme) present in the human body. In addition to the capability of forming pores *in situ,* other advantages these scaffolds have when compared with other conventional materials are their suitable mechanical properties and lack of toxicity. Coutinho *et al.* (47) studied the function of an osteoblastic-like cell line (SaOs-2) on chitosan blends with synthetic biodegradable polymers, and reported enhanced osteoblastic activity. Costa-Pinto *et al.* (48) formulated scaffolds based on blends of chitosan and synthetic polyesters, and provided evidence that these scaffolds are cytocompatible. Furthermore, chitosan-based scaffolds promoted the attachment and proliferation of mouse mesenchymal stem cells (MSCs) (48), which exhibited high levels of alkaline phosphatase activity and produced a mineralized ECM (48).

2.2. Starch

Starch is one of the most abundant naturally occurring polymers with properties that make it attractive for several biomedical applications. Starch is found as insoluble granules of α-amylose (20-30%) and amylopectin (70-80%) (49). Amylopectin polymers are highly branched structures containing (1→4)-α-D-glucose and (1→6)-α-D-glucose linkages, whereas amylose is much more linear with long stretches of (1→4)-α-D-glucose-linked monomer units. Starch is extremely difficult to process and is brittle when used without the addition of a plasticizer (49). Over the years, several other materials have been blended with starch to improve its processability, including several synthetic (50-54) and natural polymers, such as polysaccharides (35, 55) and proteins (56). Reis and co-workers (35, 57-70) have proposed use of starch-based scaffolds for biomedical applications. Starch exhibits low toxicity (35, 64), biodegradability (35, 70-72), and biocompatibility (73-75), which are excellent characteristics for bone tissue engineering applications. Compared with other biodegradable polymers, starch is inexpensive, and above all, reusable. Specific enzymes present in the human body, namely α-amylase in the blood plasma, can easily degrade starch. The main enzymes involved in starch degradation are α-amylases, β-amylases, α-glucosidases, and other debranching enzymes.

An important consideration of biodegradable materials of natural origin being considered for use in the biomedical field is the host response to the degradation products. Starch degradation products are oligosaccharides that can be metabolized to produce energy. Due to their degradation by α-amylases, this constitutes another strategy to control and tailor the degradation of starch-based scaffolds. Martins *et al.* (35) developed a novel biodegradable matrix based on chitosan and starch, with the ability of forming a porous structure *in situ* following attack by specific enzymes (namely, α-amylase and lysozyme) present in the human body. These researchers showed that pore size and distribution in the

chitosan matrix is controlled by the location of the ‘‘sacrificial’’ phase (i.e., native starch) that is enzymatically degradaded (35). This same study reported an interesting approach for the control of matrix degradation *in situ* and consequent pore formation, which could result in scaffolds with mechanical properties appropriate for the initial stage of implantation (35). Martins and co-workers (76) also studied the influence of α-amylase on the degradation of fiber mesh scaffolds based on a blend of starch and poly(ε-caprolactone) (SPCL) and demonstrated enhanced scaffold porosity and pore size and decreased average fiber diameter with time. Furthermore, culture of rat marrow stromal cells on SPCL fiber meshes (in medium supplemented with α-amylase) resulted in enhanced cell proliferation (76).

2.3. Alginate

Alginate (alginic acid or algin) is a linear polyuronate containing D-mannuronic acid and L-guluronic acid that is abundant in the cell walls of brown algae. Due to the biocompatibility and gelation of alginate with certain divalent cations, it is widely used for cell immobilization and encapsulation. Alginate is soluble in aqueous solutions at room temperature and forms stable gels in the presence of calcium, barium, and strontium without chemical crosslinking agents (77); for this reason, the viability and biological activity of entrapped cells and biochemical agents are maintained in alginate gels. As a biomaterial, alginate has a number of advantages including biocompatibility and nonimmunogenicity, which are related to its hydrophilicity (78, 79).

Several studies examined alginate sponges as scaffolds for tissue engineering applications (78) and reported that their structural and morphological properties are appropriate for cell culture and proliferation as well as for neovascularization (78). Other studies reported that alginate supports synthesis of pertinent ECM components by various cell types, and provides an amenable environment for cell encapsulation, drug delivery, and gene delivery (80). Alginate also permits the cotransplantation of multiple cell types and appropriate growth stimuli to promote, for example, the osteogenic phenotype (81). Encapsulated bone marrow stromal cells (BMSCs) were studied for the purpose of healing bone defects in orthopedics (82). Studies with gels containing MSCs and alginate beads loaded with vancomycin (a treatment for bone infections), reported that bone marrow-derived MSCs proliferated and expressed alkaline phosphatase, osteopontin, and type I collagen genes (83). Cai *et al.* (84) reported expression of bone specific ECM markers when they examined the ectopic bone forming ability of BMSc in combination with scaffolds made from alginate gel and implanted subcutaneously in nude mice for 8 weeks. Moreover, hydrogels such as alginate are effective cell substrates for both two dimensional (2D) (85) and 3D (78, 85) cell cultures, indicating the suitability of alginate for tissue engineering applications.

3. CaP BIOMIMETIC COATINGS

Ideally, tissue engineering scaffolds should mimic, to the greatest degree possible, the properties of the native target tissue in an effort to promote, direct, and control regeneration of a specific, desired type of tissue. The term “biomimetics” is used to describe a branch of science that seeks to produce such “bioinspired” materials for a variety of applications.

Compared with other biomaterals, CaPs have a unique characteristic for bone mimicry and substitution. Their composition resembles that of bone mineral; most importantly, they can induce a biological response similar to that generated during bone remodeling, which involves resorption and formation of new bone tissue (86). Osteoclasts are responsible for bone mineral degradation, resulting in bone resorption (86). During bone resorption, the degradation products of CaP (calcium and phosphate ions) are naturally metabolized but do not cause abnormally increased calcium and phosphate levels in urine, serum, or organs (87). It should be noted that osteoclasts degrade CaP in a similar fashion as they degrade natural bone (88-90).

In 1972 Hench *et al.* (91) showed that “Bioglass” (that is, glass in the Na_2O-CaO-SiO_2-P_2O_5 system), spontaneously bonded to living bone without formation of surrounding fibrous tissue. In the early 1990s, Kokubo and co-workers (92, 93) proposed that the essential requirement for a biomaterial to bond to living bone is the formation of bone-like apatite on the surface of the biomaterial when implanted *in vivo*. This *in vivo* apatite formation can be reproduced *in vitro* using a simulated body fluid (SBF), which is a solution containing inorganic ion concentrations similar to those of human extracellular fluids but without any cells or proteins (94). Under such *in vitro* conditions, the formed layer consists of carbonate apatite with small crystallites and low crystallinity (94). This apatite is referred to as “bone-like apatite” due to its similarity to apatite present in natural bone.

Biomimetic methodology for coating biomaterials with a bone-like apatite layer has been described in several publications (92, 95-98). This technique mimics the natural biomineralization processes, which involve controlled crystal phase nucleation and growth. The main advantage of the biomimetic methodology is the use of physiological conditions (pH 7.4 at 37ºC) simulating the conditions under which apatite is formed in bone. Moreover, this technique allows the incorporation of proteins and bioactive agents without compromising the activity of the agents (96, 98-101). In 1997, Reis *et al.* (95) adapted the methodology developed by Kokubo and used bioactive glass as a precursor of the nucleation and growth of CaP films on starch-based polymers. Briefly, for the preparation of the biomimetic CaP coatings based on the methodology previously developed by Abe *et al.* (92) and Kokubo (93) and adapted by Reis *et al.* (95), the materials under consideration were first impregnated with bioactive glass, and were then immersed in simulated body fluid (1.0 SBF)

solution for several days at 37ºC; this phase is known as the “nucleation stage” and allows formation of CaP nuclei. In order to accelerate apatite formation, the biomaterials were subsequently immersed at 37ºC in simulated body fluid solution (1.5 SBF) with an ionic concentration 1.5-fold greater than physiological; this condition enhances CaP nuclei growth. The CaP biomimetic coatings, which are thus formed, exhibit osteoconductive properties that will be discussed later in this chapter.

3.1. Osteoconductivity

Scaffolds for bone tissue engineering should be osteoconductive; that is, able to support the formation of bone within and/or upon the scaffold. Osteoconductivity has been observed when porous structures were implanted into or adjacent to bone. In such cases, osteoprogenitor cells migrated into pores and filled the porous structure with newly formed bone. This process is characterized by an initial ingrowth of fibrovascular tissue that invades the porous structure followed by later development of new bone directly within it (102). Hydroxyapatite-based materials are osteoconductive, provided that fully differentiated osteogenic cells are available at the site of implantation (12). Adsorption of growth factors from the local milieu and from the blood circulation contributes to the osteoconductivity of hydroxyapatite by creating suitable conditions for bone formation when implanted in an osseous environment *in vivo*. Many relatively insoluble CaP materials are osteoconductive, and, in some cases, may induce extraskeletal new bone formation (i.e., they are osteoinductive).

3.2. Osteoinductivity

Osteoinduction is the process by which stem and osteoprogenitor cells are recruited to the bone healing site and stimulated to undergo osteogenic differentiation (103). Osteoinductivity implies the ability of chemical compounds to induce osteogenic differentiation of uncommitted progenitor cells (12). It has been proposed that biomaterials do not have an osteoinductive character in the absence of appropriate osteoinductive agents, such as certain BMPs and other bioactive molecules (104). However, several studies have reported that some CaP biomaterials (105-107), namely CaP coatings (107, 108), may be osteoinductive. These CaP biomaterials may induce bone formation at extraskeletal sites without addition of osteogenic cells or bioactive agents. Hydroxyapatite is not osteoinductive because it cannot induce osteogenic differentiation of progenitor cells when implanted in a nonosseous environment, such as skin and muscle (12).

3.3. Incorporation of biomolecules into CaP biomimetic coatings

Numerous attempts have been made to improve the osteoconductivity of biomaterials. Coatings of CaP expedite osteoconduction and bone ingrowth at the surface of bone substitutes and, therefore, are useful strategies in tissue engineering endeavors for the regeneration of bone tissue. However, a methodology that enables regeneration of bone tissue should not only expedite osteoconduction, but also osteoinduction through biochemical pathways (109-112). It is known that BMPs can be incorporated into CaP implants (with adequate 3D geometry) to promote osteogenesis (112, 113); the surface of such implants, however, will be rapidly conditioned by several highly concentrated molecules (114). For this reason, other types of delivery-specific approaches have been investigated as alternatives that further functionalize and enhance the potential of CaP coatings. Specifically, the CaP biomimetic coatings have been used as a carrier of molecules including osteoinductive agents such as BMPs (115-117), other proteins (101, 118, 119, 120), enzymes (96, 98, 121), and antibiotics (122, 123).

Biomimetic CaP coatings, produced as described in early parts of this chapter, are deposited onto surfaces under physiological temperature and pH (110), enabling the coprecipitation and consequent incorporation of biologically active molecules (99). This approach circumvents difficulties common to plasma spraying techniques. By using low temperatures, biomimetic processes can be applied not only to highly resistant materials (e.g., metallic alloys) but also to polymeric and naturally derived implants (e.g., chitosan, starch, and collagen) for implantation (124).

The major objective of CaP coating is to provide appropriate biological composition and to improve the quality of the surfaces of various materials used for orthopedic applications. The conditions under which such a coating is prepared affects conformational stability of incorporated biomolecules, and thus the bioactivity and shelf-life of the final product. Such coatings, which are structurally and chemically comparable to the mineral component of bone, can possess favorable bioactive properties that may facilitate outcomes in cases of critical clinical need (122, 125).

This alternative coating technique may be used to produce systems with several advantages, such as reduction of burst release of incorporated molecules into the biological milieu. In this case, biomolecules incorporated in the inorganic phase are gradually released as the latticework undergoes degradation. The advent of the slow degradation of the coating modulates delivery of bioactive agents. Slow release of these chemical compounds may improve the osteoinductive capacity of the implant material (100, 126).

One of the potential applications of CaP coatings relates to the incorporation of bioactive agents and proteins. Azevedo *et al.* (121) used a biomimetic technique pertains to incorporate of bovine serum albumin and α-amylase into a CaP coating on the surface of a

starch-based polymer. In that study, the properties of resultant biomaterial were tailored by judicious choice of specific enzymes and their incorporation at different compositions and combinations into CaP coatings that retained their bioactivity (121). Efficient incorporation of active α-amylase into biomimetic coatings controlled the degradation rate of starch-based biomaterials. Similar results and applications were achieved with chitosan scaffolds after the incorporation of lysozyme (96, 98). Martins *et al.* (96, 98) incorporated lysozyme on the surface of chitosan scaffolds in order to control the degradation rate of chitosan and subsequent formation of pores. Furthermore, since lysozyme has antibacterial properties, these coatings may be used as a carrier for its sustained release, potentially mitigating infection at the implantation site. Several studies reported in the literature addressed incorporation of BMPs into biomimetic CaP layers (110, 116, 125, 127). These studies indicated that CaP coatings have the potential for sustained delivery of many other bioactive agents. Liu and co-workers (99) demonstrated that BMP-2 retained its osteoinductivity when delivered from biomimetic systems and that the osteoconductivity of implant material surfaces was affected by BMP-2 and its delivery mode (125).

In summary, the results discussed in this section support the strategy of adding osteoinductive signaling molecules into CaP biomimetic coatings for the purpose of inducing bone growth.

4. OSTEOGENIC DIFFERENTIATION OF MARROW STROMAL CELLS AND MINERALIZED ECM PRODUCTION *IN VITRO*

Biomaterials and scaffolds considered for bone tissue engineering are often evaluated *in vitro* for their ability to support adhesion, proliferation, and differentiation of progenitor cells along the osteogenic pathway prior to being evaluated *in vivo*. *In vitro* cell-scaffold interactions are determined using osteoblasts, osteosarcoma cell lines, and osteoprogenitor cells. The scaffolds used for this purpose mimic the ECM of bone and play a crucial role in supporting cell functions and differentiation, but may also be used to deliver biomolecules.

Osteoblastic differentiation of MSCs comprises cell proliferation, cell maturation, and matrix mineralization. During these phases, cells synthesize and secrete alkaline phosphatase, type I collagen, and other noncollagenous ECM proteins, such as osteocalcin, osteopontin, osteonectin, and bone sialoprotein. Mineralization occurs through accumulation of calcium and phosphorous in the ECM.

4.1. BMSCs versus MSCs

The osteoprogenitor cells used for bone tissue engineering purposes are derived from a various tissue sources. Bone marrow stroma consists of a heterogeneous population that provides structural and physiological support for hematopoietic cells (128). Bone marrow contains three main cell types: endothelial cells, hematopoietic cells, and stromal cells. Friedenstein *et al.* (129, 130) was the first to identify in bone marrow cell populations with strong osteogenic potential. When marrow cells are plated at low cell densities, bone marrow stromal cells (BMSCs) form colonies and are defined as “colony forming unit-fibroblasts” (CFU-Fs); this term indicates that each colony derives from a single proliferating progenitor (131). The term “BMSCs” is applied to isolated bone marrow cells with potential to form connective tissues (131).

Due to their high proliferation potential, BMSCs can be expanded in culture to obtain large numbers of cells starting from a small sample of bone marrow aspirate. The BMSC population contains precursor cells capable of extensive proliferation and differentiation into several phenotypes. Furthermore, BMSCs maintain their multipotential capacity during prolonged culture and multiple passages *in vitro*. Among these BMSCs there is a subpopulation of undifferentiated multipotent cells able to generate ‘‘mesenchyme’’, the mass of tissue that develops from the mesoderm of an embryo. This cell population is present in all postnatal tissues and is referred to as the “mesenchymal stem cell” (MSC) (132, 133). In the past, researchers working with cells from the bone marrow used different names to refer to the same cells. This practice leads to nomenclature confusion; for example, BMSCs have been reffered to as multipotent adult progenitor cells (MAPCs), MSCs, bone marrow stromal stem cells (BMSSCs), and mesodermal progenitor cells (MPCs) (134). What s presently known is that, if appropriately induced, these cells can also differentiate along multiple pathways to form various cells from a number of tissues, including bone, cartilage, and fat (135).

Stem cells are able to provide replacements for various differentiated cell types. The use of MSCs has several advantages, as they have unique biological properties, are capable of extensive replication in culture in an undifferentiated state, and can differentiate along multiple pathways to form various cells from a number of tissues, including bone, cartilage, and fat (4). Identification of stem cells using surface markers has not been definitive either, because similar markers are also present on nonstem cells, or because a particular marker may only be temporarily expressed on a stem cell at a certain stage or under specific conditions.

4.2. Osteogenic differentiation

In addition to being osteoconductive and osteoinductive, an ideal scaffold for bone tissue engineering application, should also be osteogenic (that is, containing living cells capable of differentiation into osteoblasts). Differentiation of MSCs along the osteoblastic lineage *in vitro* starts with a period of cell proliferation followed by synthesis and deposition of ECM components by the cells; accumulation of calcium finally leads to mineralization of the ECM. To induce osteogenic differentiation in MSCs, the culture medium is usually supplemented with osteogenic agents such as dexamethasone, β-glycerophosphate, and ascorbic acid.

Dexamethasone, a synthetic glucocorticoid, stimulates MSC proliferation and supports osteogenic lineage differentiation (136-138). Organic phosphates, such as β-glycerophosphate, also support osteogenesis by contributing to mineralization of the ECM and modulating osteoblast function (138-140). Free phosphates can also induce expression of osteogenic protein markers, such as osteopontin (138, 141). Other supplements, such as ascorbic acid, enhance collagen synthesis and upregulate alkaline phosphatase expression in bone cells. Ascorbic acid stimulates marrow stromal cells to differentiate along the osteoblast lineage (141-143). Furthermore, ascorbic acid promotes osteogenic induction evidenced by increased alkaline phosphatase activity and production of osteocalcin in osteogenic cultures (144).

Martins *et al.* (76) used marrow stromal cells cultured on blends of starch with poly(ε-caprolactone) scaffolds in static cultures and reported that the enzyme lipase enhanced osteogenic differentiation and promoted deposition of mineralized ECM. The BMP family of growth factors is frequently used for osteoinduction. BMP-2 increases calcium-containing nodule formation and the calcium content of osteogenic cultures *in vitro* (138). The TGF- β superfamily contains a large number of growth factors with different functions, many of which regulate cell proliferation and ECM production. Fibroblast growth factors (FGFs), namely FGF-1 and FGF-2 are produced by osteoblasts and are constituents of the bone matrix. Insulin-like growth factor (IGF) stimulates osteogenesis; IGF-2 is the most abundant growth factor found in bone matrix. Gomes *et al.* (145) demonstrated that an *in vitro* generated bone-like ECM produced by marrow stromal cells contains bioactive growth factors including TGF-β1, FGF-2, vascular endothelial growth factor (VEGF), and BMP-2. Pham *et al.* (146) reported that the gene expression profiles of various bone-related growth factors and ECM proteins in MSCs cultured in osteogenic media were upregulated; these chemical compounds are present in native bone tissue. Costa-Pinto *et al.* (48) studied the osteogenic differentiation of a mouse MSC line (BMC9) cultured on novel melt-based chitosan/polyester scaffolds and reported high levels of alkaline phosphatase activity and formation of a

calcified ECM; these results are evidence of differentiation of the cells along the osteogenic pathway.

Expression of osteoblastic phenotype markers in culture defines three different phases of bone-related activities: cell proliferation, ECM maturation, and ECM mineralization. During active cell proliferation, growth-related genes are expressed, and minimal levels of type I collagen are observed (147). Following this phase, a period of matrix maturation occurs when alkaline phosphatase is maximally expressed. Finally, the ECM becomes mineralized, the third period of the bone developmental sequence (147). There are two transition periods between the aforementioned developmental periods: the first occurs at the end of proliferative period and the second when expression of osteoblastic phenotype markers (such as osteocalcin and osteopontin), become significantly elevated with the onset of mineralization (147).

Alkaline phosphatase activity, an early marker of the osteoblastic phenotype, is upregulated at the onset of cell differentiation but subsequently decreases as cell differentiation progresses. Another marker of bone formation is calcium-containing mineral deposits in the ECM. To detect mineral deposition, tetracycline-HCl is added to the osteogenic culture media (148). Tetracycline acts as a fluorochrome-labeling agent for bone tissues (149). Tetracycline accumulates sites of bone formation and fluoresces brightly when activated with appropriate fluorescent light. Qualitative (or semiquantitative) analysis of calcium-containing mineral deposits in bone cell cultures uses von Kossa, alizarin red, and methylene blue/basic fuchsin staining methods (148, 150). An important artifact, which should be kept in mind when using these analyses, is that the ECM uptakes calcium independently from cell-mediated mineral deposition. For this reason, confirmation of the results obtained using the aforementioned staining methods should be complemented with data either diffraction or spectroscopy methods such as thin-film X-ray diffraction (TF-XRD) and Fourier transformed infrared spectroscopy (FTIR) (76, 150, 151).

Expression of osteopontin occurs during the mid- to late-stages of osteogenic differentiation of MSCs (152). Osteopontin is an extracellular protein secreted by differentiating osteoblasts that is upregulated both during cell proliferation and at the onset of ECM mineralization. Osteocalcin, another late-stage marker of osteoblastic differentiation, can be assessed using commercially available immunoassays. Immunohistochemistry using specific antibodies to detect the presence of growth factors, bone- and ECM-related proteins, and enzymes is well established and widely used. Reverse transcriptase polymerase chain reaction (RT-PCR) is used to determine expression of bone-related genes, such as osteoblast marker genes, growth factors, and ECM biomolecules, in MSCs (146).

4.3. Bone-specific matrix proteins

The bone matrix is not only composed of a mineralized phase, but also of an organic phase containing collagenous and other noncollagenous proteins, matrix metalloproteinases, proteoglycans, and glycoproteins. Bone formation involves regulated secretion, deposition, and removal of a complex array of these matrix proteins, which appear in a defined temporal and spatial sequence (12). Mineralization also dictates the spatial orientation of matrix deposition (12). Most proteins originally thought to be unique to the bone ECM were subsequently proven to be expressed in many other tissues of the body. Osteocalcin is the only protein still considered to be bone specific in bone mineralization (12).

As discussed previously, alkaline phosphatase is considered an early-stage marker of osteoblastic differentiation (147) and is expressed during the postcell proliferative period of ECM deposition. Type I collagen, the major ECM protein of bone, provides a template for subsequent mineralization (153). Alkaline phosphatase, collagen, and osteonectin are expressed at high levels near the end of cell proliferation and during the period of ECM deposition and maturation (141).

Osteopontin and bone sialoprotein, *N*-linked glycoproteins containing integrin-binding RGD motifs, are involved in cell-matrix interactions. Osteopontin is widely distributed in different tissues, whereas bone sialoprotein is highly enriched in bone and skeletal cartilage (154). Osteopontin, a phosphorylated glycoprotein associated with the early stages of osteogenesis that precede mineralization, is secreted by osteoblats into the mineralizing ECM during bone development (141, 155). In bone, bone sialoprotein is expressed by fully mature osteogenic cells capable of depositing mineralized matrix (154). Extracellular bone sialoprotein localizes to newly formed, mineralized bone matrix; its distribution coincides with that of mineral deposits (156). Bone sialoprotein, a protein expressed during early phases of bone deposition, controls both mineral formation and cell-matrix interactions (157). This protein is used as a marker of initial bone formation (157). The function of bone sialoprotein in bone, which is not been completely elucidated yet, may be related to the regulation of physiological mineralization of skeletal ECMs (156, 158). Osteocalcin is another marker of late-term osteogenic differentiation associated with osteoblast-mediated matrix deposition and mineralization (159, 160). Expression of osteopontin, osteocalcin, and bone sialoprotein occurs later during the third period of ECM mineralization.

5. SUMMARY

Surface modification of biomaterials uses methods that mimic biomineralization and enable the incorporation of bioactive molecules and agents; such treatments can improve both *in vitro* and *in vivo* osteogenic differentiation. The main objective of CaP coatings is

osteoconduction and enhanced adhesion of osteogenic cells onto biomaterial surfaces. Because CaP coatings have structures and chemical properties similar to those of native bone, they have great potential and promise to increase bone ingrowth in areas of clinical need.

Because they lack essential properties, such as bioactivity and osteoinductivity, most currently available polymers present limitations for bone-related biomedical application. In this respect then, the biomimetic coating technique discussed in the present chapter has the potential to impart these essential properties to biomaterials. Since CaP layers can be on 3D scaffolds the biomimetic coating approach has been receiving increased attention in the bone tissue engineering field.

Moreover, CaP coatings have been considered as a potential carrier for the delivery of various biomolecules, chosen for their physicochemical and biological properties, as well as for their osteoconductivity. Complementing the CaP biomimetic coating approach, incorporation of biomolecules provides osteoinductive properties to biomaterials. Since this method is carried out under physiological conditions, proteins, enzymes, and other bioactive agents can be incorporated into CaP layers without loss of their activity. A major advantage is the fact that the biomaterial-CaP coating-biomolecule can simultaneously exhibit osteoinductive and osteoconductive properties, because it can act as a carrier system for the controlled release of multiple biologically active proteins. Incorporation of enzymes into CaP layers coated on the surface of scaffolds (using the biomimetic coating technique) can be also used to control the degradation rate of the material substrate *in vivo*. An integrated approach combining a scaffold, CaP coatings, bioactive molecules and/or enzymes, and *in vitro* cultures may provide an optimal environment for cell adhesion and osteogenic differentiation as well as generate a mineralized ECM containing select bioactive molecules.

Incorporation of bioactive molecules into CaP coatings on scaffolds for bone tissue engineering applications has the potential to provide advanced tissue-specific constructs to promote improved alternative treatment of bone pathologies and trauma. The present chapter summarized the results of studies that used biomolecules important to elucidate important aspects such as details of the release profiles of entrapped bioactive molecules and retention of their bioactivity. Establishment and further development of nature-inspired techniques to design and formulate novel biomaterials could provide the next generation of effective scaffolds for bone tissue engineering.

REFERENCES

1. Marx J. Coming to grips with bone loss. Science. 2004 Sep 3;305(5689):1420-2.

2. Persidis A. Tissue engineering. Nature biotechnology. 1999 May;17(5):508-10.

3. Langer R, Vacanti JP. Tissue engineering. Science. 1993 May 14;260(5110):920-6.

4. Bianco P, Robey PG. Stem cells in tissue engineering. Nature. 2001 Nov 1;414(6859):118-21.

5. Hutmacher DW. Scaffolds in tissue engineering bone and cartilage. Biomaterials. 2000 Dec;21(24):2529-43.

6. Salgado AJ, Coutinho OP, Reis RL. Bone tissue engineering: state of the art and future trends. Macromolecular bioscience. 2004 Aug 9;4(8):743-65.

7. Atala A. Engineering tissues, organs and cells. Journal of tissue engineering and regenerative medicine. 2007 Mar-Apr;1(2):83-96.

8. Hutmacher DW, Schantz JT, Lam CX, Tan KC, Lim TC. State of the art and future directions of scaffold-based bone engineering from a biomaterials perspective. Journal of tissue engineering and regenerative medicine. 2007 Jul-Aug;1(4):245-60.

9. Langer R, Peppas NA. Advances in biomaterials, drug delivery, and bionanotechnology. AIChE Journal. 2003;49(12):2990-3006.

10. Langer R. Selected advances in drug delivery and tissue engineering. J Control Release. 1999 Nov 1;62(1-2):7-11.

11. Madihally SV, Matthew HW. Porous chitosan scaffolds for tissue engineering. Biomaterials. 1999 Jun;20(12):1133-42.

12. Riminucci M, Bianco P. Building bone tissue: matrices and scaffolds in physiology and biotechnology. Brazilian journal of medical and biological research = Revista brasileira de pesquisas medicas e biologicas / Sociedade Brasileira de Biofisica [et al. 2003 Aug;36(8):1027-36.

13. Daculsi G, Laboux O, Le Geros R. Outcome and perspectives in bioactive coatings: What's new, what's coming. ITBM-RBM. 2002;23:317-25.

14. Suh JK, Matthew HW. Application of chitosan-based polysaccharide biomaterials in cartilage tissue engineering: a review. Biomaterials. 2000 Dec;21(24):2589-98.

15. Lahiji A, Sohrabi A, Hungerford DS, Frondoza CG. Chitosan supports the expression of extracellular matrix proteins in human osteoblasts and chondrocytes. J Biomed Mater Res. 2000 Sep 15;51(4):586-95.

16. Muzzarelli RAA. Biochemical significance of exogenous chitins and chitosans in animals and patients. Carbohydrate Polymers. 1993;20(1):7-16.

17. Tomihata K, Ikada Y. In vitro and in vivo degradation of films of chitin and its deacetylated derivatives. Biomaterials. 1997 Apr;18(7):567-75.

18. Kumar MNVR. A review of chitin and chitosan applications. Reactive & Functional Polymers. 2000 Nov;46(1):1-27.

19. Benesch J, Tengvall P. Blood protein adsorption onto chitosan. Biomaterials. 2002 Jun;23(12):2561-8.

20. Krajewska B. Application of chitin- and chitosan-based materials for enzyme immobilizations: a review. Enzyme and Microbial Technology. 2004 Aug 5;35(2-3):126-39.

21. Kim IY, Seo SJ, Moon HS, Yoo MK, Park IY, Kim BC, et al. Chitosan and its derivatives for tissue engineering applications. Biotechnology advances. 2008 Jan-Feb;26(1):1-21.

22. Klokkevold PR, Vandemark L, Kenney EB, Bernard GW. Osteogenesis enhanced by chitosan (poly-N-acetyl glucosaminoglycan) in vitro. Journal of periodontology. 1996 Nov;67(11):1170-5.

23. Pound JC, Green DW, Chaudhuri JB, Mann S, Roach HI, Oreffo RO. Strategies to promote chondrogenesis and osteogenesis from human bone marrow cells and articular chondrocytes encapsulated in polysaccharide templates. Tissue engineering. 2006 Oct;12(10):2789-99.

24. Pound JC, Green DW, Roach HI, Mann S, Oreffo ROC. An ex vivo model for chondrogenesis and osteogenesis. Biomaterials. 2007;28(18):2839-49.

25. Ueno H, Yamada H, Tanaka I, Kaba N, Matsuura M, Okumura M, et al. Accelerating effects of chitosan for healing at early phase of experimental open wound in dogs. Biomaterials. 1999 Aug;20(15):1407-14.

26. Ueno H, Mori T, Fujinaga T. Topical formulations and wound healing applications of chitosan. Advanced drug delivery reviews. 2001 Nov 5;52(2):105-15.

27. Hoekstra A, Struszczyk H, Kivekas O. Percutaneous microcrystalline chitosan application for sealing arterial puncture sites. Biomaterials. 1998 Aug;19(16):1467-71.

28. Khor E. Chitin: a biomaterial in waiting. Current Opinion in Solid State & Materials Science. 2002 Aug;6(4):313-7.

29. Lee JY, Nam SH, Im SY, Park YJ, Lee YM, Seol YJ, et al. Enhanced bone formation by controlled growth factor delivery from chitosan-based biomaterials. J Control Release. 2002 Jan 17;78(1-3):187-97.

30. Chatelet C, Damour O, Domard A. Influence of the degree of acetylation on some biological properties of chitosan films. Biomaterials. 2001 Feb;22(3):261-8.

31. Pangburn SH, Trescony PV, Heller J. Lysozyme degradation of partially deacetylated chitin, its films and hydrogels. Biomaterials. 1982 Apr;3(2):105-8.

32. Sashiwa H, Saimoto H, Shigemasa Y, Ogawa R, Tokura S. Lysozyme susceptibility of partially deacetylated chitin. International journal of biological macromolecules. 1990 Oct;12(5):295-6.

33. Varum KM, Myhr MM, Hjerde RJ, Smidsrod O. In vitro degradation rates of partially N-acetylated chitosans in human serum. Carbohydrate research. 1997 Mar 26;299(1-2):99-101.

34. Martins AM, Pham QP, Malafaya PB, Raphael RM, Kasper FK, Reis RL, et al. "Smart" and stimulus responsive chitosan-based scaffolds/cells for bone tissue engineering: Influence of lysozyme upon scaffold degradation and osteogenic differentiation of cultured marrow stromal cells induced by cap coatings. Tissue Engineering Part A. 2008 May;14(5):795-.

35. Martins AM, Santos MI, Azevedo HS, Malafaya PB, Reis RL. Natural origin scaffolds with in situ pore forming capability for bone tissue engineering applications. Acta biomaterialia. 2008 Nov;4(6):1637-45.

36. Hirano S, Tsuchida H, Nagao N. N-acetylation in chitosan and the rate of its enzymic hydrolysis. Biomaterials. 1989 Oct;10(8):574-6.

37. Ma J, Wang H, He B, Chen J. A preliminary in vitro study on the fabrication and tissue engineering applications of a novel chitosan bilayer material as a scaffold of human neofetal dermal fibroblasts. Biomaterials. 2001 Feb;22(4):331-6.

38. Brouwer J, van Leeuwen-Herberts T, Otting-van de Ruit M. Determination of lysozyme in serum, urine, cerebrospinal fluid and feces by enzyme immunoassay. Clinica chimica acta; international journal of clinical chemistry. 1984 Sep 15;142(1):21-30.

39. Hankiewicz J, Swierczek E. Lysozyme in human body fluids. Clinica chimica acta; international journal of clinical chemistry. 1974 Dec 17;57(3):205-9.

40. Teijón C, Olmo R, Dolores Blanco M, Romero A, María Teijón J. Effects of lead administration at low doses by different routes on rat spleens. Study of response of splenic lymphocytes and tissue lysozyme. Toxicology. 2003;191(2-3):245-58.

41. Torsteinsdottir I, Hakansson L, Hallgren R, Gudbjornsson B, Arvidson NG, Venge P. Serum lysozyme: a potential marker of monocyte/macrophage activity in rheumatoid arthritis. Rheumatology (Oxford, England). 1999 Dec;38(12):1249-54.

42. Garcia Cruz DM, Escobar Ivirico JL, Gomes MM, Gomez Ribelles JL, Sanchez MS, Reis RL, et al. Chitosan microparticles as injectable scaffolds for tissue engineering. Journal of tissue engineering and regenerative medicine. 2008 Jul 10.

43. Abarrategi A, Civantos A, Ramos V, Sanz Casado JV, Lopez-Lacomba JL. Chitosan film as rhBMP2 carrier: delivery properties for bone tissue application. Biomacromolecules. 2008 Feb;9(2):711-8.

44. Park YJ, Lee YM, Park SN, Sheen SY, Chung CP, Lee SJ. Platelet derived growth factor releasing chitosan sponge for periodontal bone regeneration. Biomaterials. 2000 Jan;21(2):153-9.

45. Di Martino A, Sittinger M, Risbud MV. Chitosan: a versatile biopolymer for orthopaedic tissue-engineering. Biomaterials. 2005 Oct;26(30):5983-90.

46. Tuzlakoglu K, Alves CM, Mano JF, Reis RL. Production and characterization of chitosan fibers and 3-D fiber mesh scaffolds for tissue engineering applications. Macromolecular bioscience. 2004 Aug 9;4(8):811-9.

47. Coutinho DF, Pashkuleva IH, Alves CM, Marques AP, Neves NM, Reis RL. The effect of chitosan on the in vitro biological performance of chitosan-poly(butylene succinate) blends. Biomacromolecules. 2008 Apr;9(4):1139-45.

48. Costa-Pinto AR, Salgado AJ, Correlo VM, Sol P, Bhattacharya M, Charbord P, et al. Adhesion, Proliferation, and Osteogenic Differentiation of a Mouse Mesenchymal Stem Cell Line (BMC9) Seeded on Novel Melt-Based Chitosan/Polyester 3D Porous Scaffolds. Tissue Eng Part A. 2008 Jun 2008;14(6):1049-57.

49. Malafaya PB, Silva GA, Reis RL. Natural-origin polymers as carriers and scaffolds for biomolecules and cell delivery in tissue engineering applications. Advanced drug delivery reviews. 2007 May 30;59(4-5):207-33.

50. Trimnell D, Fanta GF. Formulations Prepared from Polyacrylamide and Starch. Journal of Polymer Materials. 1994 Dec;11(4):271-7.

51. Bastioli C, Cerutti A, Guanella I, Romano GC, Tosin M. Physical State and Biodegradation Behavior of Starch-Polycaprolactone Systems. Journal of Environmental Polymer Degradation. 1995 Apr;3(2):81-95.

52. Villar MA, Thomas EL, Armstrong RC. Rheological Properties of Thermoplastic Starch and Starch Poly(Ethylene-Co-Vinyl Alcohol) Blends. Polymer. 1995 Apr;36(9):1869-76.

53. Kotnis MA, Obrien GS, Willett JL. Processing and Mechanical-Properties of Biodegradable Poly(Hydroxybutyrate-Co-Valerate)-Starch Compositions. Journal of Environmental Polymer Degradation. 1995 Apr;3(2):97-105.

54. Mayer JM, Elion GR, Buchanan CM, Sullivan BK, Pratt SD, Kaplan DL. Biodegradable Blends of Cellulose-Acetate and Starch - Production and Properties. Journal of Macromolecular Science-Pure and Applied Chemistry. 1995;A32(4):775-85.

55. Nakamatsu J, Torres FG, Troncoso OP, Min-Lin Y, Boccaccini AR. Processing and characterization of porous structures from chitosan and starch for tissue engineering scaffolds. Biomacromolecules. 2006 Dec;7(12):3345-55.

56. Bajpai AK, Shrivastava J. alpha-Amylase induced enhanced enzymatic degradation of binary polymeric blends of crosslinked starch and gelatin. Journal of Macromolecular Science-Pure and Applied Chemistry. 2004 Jul;A41(8):949-69.

57. Gomes ME, Ribeiro AS, Malafaya PB, Reis RL, Cunha AM. A new approach based on injection moulding to produce biodegradable starch-based polymeric scaffolds: morphology, mechanical and degradation behaviour. Biomaterials. 2001 May;22(9):883-9.

58. Malafaya PB, Elvira C, Gallardo A, San Roman J, Reis RL. Porous starch-based drug delivery systems processed by a microwave route. Journal of biomaterials science. 2001;12(11):1227-41.

59. Elvira C, Mano JF, San Roman J, Reis RL. Starch-based biodegradable hydrogels with potential biomedical applications as drug delivery systems. Biomaterials. 2002 May;23(9):1955-66.

60. Espigares I, Elvira C, Mano JF, Vazquez B, San RJ, Reis RL. New partially degradable and bioactive acrylic bone cements based on starch blends and ceramic fillers. Biomaterials. 2002 Apr;23(8):1883-95.

61. Leonor IB, Sousa RA, Cunha AM, Reis RL, Zhong ZP, Greenspan D. Novel starch thermoplastic/Bioglass composites: mechanical properties, degradation behavior and in-vitro bioactivity. Journal of materials science. 2002 Oct;13(10):939-45.

62. Baran ET, Mano JF, Reis RL. Starch-chitosan hydrogels prepared by reductive alkylation cross-linking. Journal of materials science. 2004 Jul;15(7):759-65.

63. Boesel LF, Fernandes MH, Reis RL. The behavior of novel hydrophilic composite bone cements in simulated body fluids. J Biomed Mater Res B Appl Biomater. 2004 Aug 15;70(2):368-77.

64. Salgado AJ, Coutinho OP, Reis RL. Novel starch-based scaffolds for bone tissue engineering: cytotoxicity, cell culture, and protein expression. Tissue engineering. 2004 Mar-Apr;10(3-4):465-74.

65. Oliveira AL, Reis RL. Pre-mineralisation of starch/polycrapolactone bone tissue engineering scaffolds by a calcium-silicate-based process. Journal of materials science. 2004 Apr;15(4):533-40.

66. Pavlov MP, Mano JF, Neves NM, Reis RL. Fibers and 3D mesh scaffolds from biodegradable starch-based blends: production and characterization. Macromolecular bioscience. 2004 Aug 9;4(8):776-84.

67. Tuzlakoglu K, Bolgen N, Salgado AJ, Gomes ME, Piskin E, Reis RL. Nano- and micro-fiber combined scaffolds: a new architecture for bone tissue engineering. Journal of materials science. 2005 Dec;16(12):1099-104.

68. Malafaya PB, Stappers F, Reis RL. Starch-based microspheres produced by emulsion crosslinking with a potential media dependent responsive behavior to be used as drug delivery carriers. Journal of materials science. 2006 Apr;17(4):371-7.

69. Silva GA, Coutinho OP, Ducheyne P, Shapiro IM, Reis RL. Starch-based microparticles as vehicles for the delivery of active platelet-derived growth factor. Tissue engineering. 2007 Jun;13(6):1259-68.

70. Gomes ME, Azevedo HS, Moreira AR, Ella V, Kellomaki M, Reis RL. Starch-poly(epsilon-caprolactone) and starch-poly(lactic acid) fibre-mesh scaffolds for bone tissue engineering applications: structure, mechanical properties and degradation behaviour. Journal of tissue engineering and regenerative medicine. 2008 Jul;2(5):243-52.

71. Azevedo HS, Gama FM, Reis RL. In vitro assessment of the enzymatic degradation of several starch based biomaterials. Biomacromolecules. 2003 Nov-Dec;4(6):1703-12.

72. Balmayor ER, Tuzlakoglu K, Marques AP, Azevedo HS, Reis RL. A novel enzymatically-mediated drug delivery carrier for bone tissue engineering applications: combining biodegradable starch-based microparticles and differentiation agents. Journal of materials science. 2008 Apr;19(4):1617-23.

73. Mendes SC, Reis RL, Bovell YP, Cunha AM, van Blitterswijk CA, de Bruijn JD. Biocompatibility testing of novel starch-based materials with potential application in orthopaedic surgery: a preliminary study. Biomaterials. 2001 Jul;22(14):2057-64.

74. Marques AP, Reis RL, Hunt JA. The biocompatibility of novel starch-based polymers and composites: in vitro studies. Biomaterials. 2002 Mar;23(6):1471-8.

75. Salgado AJ, Coutinho OP, Reis RL, Davies JE. In vivo response to starch-based scaffolds designed for bone tissue engineering applications. Journal of biomedical materials research. 2007 Mar 15;80(4):983-9.

76. Martins AM, Pham QP, Malafaya PB, Sousa RA, Gomes ME, Raphael RM, et al. The role of lipase and α-amylase in both the degradation of starch/poly(ε-caprolactone) fiber meshes and the osteogenic differentiation of cultured marrow stromal cells. Tissue Eng Part A. 2008;in press.

77. Gu F, Amsden B, Neufeld R. Sustained delivery of vascular endothelial growth factor with alginate beads. J Control Release. 2004 May 18;96(3):463-72.

78. Shapiro L, Cohen S. Novel alginate sponges for cell culture and transplantation. Biomaterials. 1997 Apr;18(8):583-90.

79. Augst AD, Kong HJ, Mooney DJ. Alginate hydrogels as biomaterials. Macromolecular bioscience. 2006 Aug 7;6(8):623-33.

80. Orive G, Hernandez RM, Gascon AR, Calafiore R, Chang TM, De Vos P, et al. Cell encapsulation: promise and progress. Nature medicine. 2003 Jan;9(1):104-7.

81. Alsberg E, Anderson KW, Albeiruti A, Rowley JA, Mooney DJ. Engineering growing tissues. Proceedings of the National Academy of Sciences of the United States of America. 2002 Sep 17;99(19):12025-30.

82. Wong M. Alginates in tissue engineering. Methods in molecular biology (Clifton, NJ. 2004;238:77-86.

83. Hou T, Xu J, Li Q, Feng J, Zen L. In vitro evaluation of a fibrin gel antibiotic delivery system containing mesenchymal stem cells and vancomycin alginate beads for treating bone infections and facilitating bone formation. Tissue Eng Part A. 2008 Jul;14(7):1173-82.

84. Cai X, Lin Y, Ou G, Luo E, Man Y, Yuan Q, et al. Ectopic osteogenesis and chondrogenesis of bone marrow stromal stem cells in alginate system. Cell biology international. 2007 Aug;31(8):776-83.

85. Barralet JE, Wang L, Lawson M, Triffitt JT, Cooper PR, Shelton RM. Comparison of bone marrow cell growth on 2D and 3D alginate hydrogels. Journal of materials science. 2005 Jun;16(6):515-9.

86. Barrere F, van Blitterswijk CA, de Groot K. Bone regeneration: molecular and cellular interactions with calcium phosphate ceramics. International journal of nanomedicine. 2006;1(3):317-32.

87. den Hollander W, Patka P, Klein CP, Heidendal GA. Macroporous calcium phosphate ceramics for bone substitution: a tracer study on biodegradation with 45Ca tracer. Biomaterials. 1991 Aug;12(6):569-73.

88. Lu J, Descamps M, Dejou J, Koubi G, Hardouin P, Lemaitre J, et al. The biodegradation mechanism of calcium phosphate biomaterials in bone. J Biomed Mater Res. 2002;63(4):408-12.

89. Wenisch S, Stahl JP, Horas U, Heiss C, Kilian O, Trinkaus K, et al. In vivo mechanisms of hydroxyapatite ceramic degradation by osteoclasts: fine structural microscopy. Journal of biomedical materials research. 2003 Dec 1;67(3):713-8.

90. Zerbo IR, Bronckers AL, de Lange G, Burger EH. Localisation of osteogenic and osteoclastic cells in porous beta-tricalcium phosphate particles used for human maxillary sinus floor elevation. Biomaterials. 2005 Apr;26(12):1445-51.

91. Hench LL, Splinter RJ, Allen WC, Greenee TK. Bonding mechanisms at the inetrface of ceramics prosthetic materials. Journal of biomedical materials research. 1972;2:117-41.

92. Abe Y, Kokubo T, Yamamuro T. Apatite Coating on Ceramics, Metals and Polymers Utilizing a Biological Process. Journal of Materials Science-Materials in Medicine. 1990 Nov;1(4):233-8.

93. Kokubo T. Bioactive glass ceramics: properties and applications. Biomaterials. 1991 Mar;12(2):155-63.

94. Ohtsuki C, Kamitakahara M, Miyazaki T. Coating bone-like apatite onto organic substrates using solutions mimicking body fluid. Journal of tissue engineering and regenerative medicine. 2007 Jan-Feb;1(1):33-8.

95. Reis RL, Cunha AM, Fernandes MH, Correia RN. Treatments to induce the nucleation and growth of apatite-like layers on polymeric surfaces and foams. Journal of materials science. 1997 Dec;8(12):897-905.

96. Martins AM, Salgado AJ, Azevedo HS, Leonor IB, Reis RL. Lysozyme incorporation in biomimetic coated chitosan scaffolds: Development and behaviour in contact with osteoblastic-like cells. Tissue engineering. 2006 Apr;12(4):1018-9.

97. Tuzlakoglu K, Reis RL. Formation of bone-like apatite layer on chitosan fiber mesh scaffolds by a biomimetic spraying process. Journal of materials science. 2007 Jul;18(7):1279-86.

98. Martins AM, Pham QP, Malafaya PB, Raphael RM, Kasper FK, Reis RL, et al. Natural Stimulus Responsive Scaffolds/Cells for Bone Tissue Engineering: Influence of Lysozyme upon Scaffold Degradation and Osteogenic Differentiation of Cultured Marrow Stromal Cells Induced by CaP Coatings. Tissue Eng Part A.in press.

99. Liu Y, Hunziker EB, Layrolle P, De Bruijn JD, De Groot K. Bone morphogenetic protein 2 incorporated into biomimetic coatings retains its biological activity. Tissue engineering. 2004 Jan-Feb;10(1-2):101-8.

100. Liu Y, Hunziker EB, Randall NX, de Groot K, Layrolle P. Proteins incorporated into biomimetically prepared calcium phosphate coatings modulate their mechanical strength and dissolution rate. Biomaterials. 2003 Jan;24(1):65-70.

101. Azevedo HS, Leonor IB, Alves CM, Reis RL. Incorporation of proteins and enzymes at different stages of the preparation of calcium phosphate coatings on a degradable substrate by a biomimetic methodology. Materials Science & Engineering C-Biomimetic and Supramolecular Systems. 2005 Apr 28;25(2):169-79.

102. Cornell CN. OSTEOCONDUCTIVE MATERIALS AND THEIR ROLE AS SUBSTITUTES FOR AUTOGENOUS BONE GRAFTS. Orthopedic Clinics of North America. 1999;30(4):591-8.

103. Albrektsson T, Johansson C. Osteoinduction, osteoconduction and osseointegration. Eur Spine J. 2001 Oct;10 Suppl 2:S96-101.

104. Fujibayashi S, Neo M, Kim HM, Kokubo T, Nakamura T. Osteoinduction of porous bioactive titanium metal. Biomaterials. 2004 Feb;25(3):443-50.

105. Ripamonti U. Osteoinduction in porous hydroxyapatite implanted in heterotopic sites of different animal models. Biomaterials. 1996 Jan;17(1):31-5.

106. Yuan H, Li Y, de Bruijn JD, de Groot K, Zhang X. Tissue responses of calcium phosphate cement: a study in dogs. Biomaterials. 2000 Jun;21(12):1283-90.

107. Habibovic P, de Groot K. Osteoinductive biomaterials--properties and relevance in bone repair. Journal of tissue engineering and regenerative medicine. 2007 Jan-Feb;1(1):25-32.

108. Barrere F, van der Valk CM, Dalmeijer RA, Meijer G, van Blitterswijk CA, de Groot K, et al. Osteogenecity of octacalcium phosphate coatings applied on porous metal implants. Journal of biomedical materials research. 2003 Sep 15;66(4):779-88.

109. Liu Y, de Groot K, Hunziker EB. Osteoinductive implants: the mise-en-scene for drug-bearing biomimetic coatings. Ann Biomed Eng. 2004 Mar;32(3):398-406.

110. Liu Y, Li JP, Hunziker EB, de Groot K. Incorporation of growth factors into medical devices via biomimetic coatings. Philos Transact A Math Phys Eng Sci. 2006 Jan 15;364(1838):233-48.

111. El-Ghannam A. Bone reconstruction: from bioceramics to tissue engineering. Expert Review of Medical Devices. 2005;2(1 %R doi:10.1586/17434440.2.1.87):87-101.

112. Paul W, Sharma CP. Ceramic drug delivery: a perspective. J Biomater Appl. 2003 Apr;17(4):253-64.

113. LeGeros RZ. Properties of osteoconductive biomaterials: calcium phosphates. Clin Orthop Relat Res. 2002 Feb(395):81-98.

114. Vroman L, Adams AL. Rapid identification of proteins on flat surfaces, using antibody-coated metal oxide suspensions. J Immunol Methods. 1986 Nov 6;93(2):213-6.

115. Maus U, Andereya S, Gravius S, Ohnsorge JA, Niedhart C, Siebert CH. BMP-2 incorporated in a tricalcium phosphate bone substitute enhances bone remodeling in sheep. J Biomater Appl. 2008 May;22(6):559-76.

116. Liu Y, de Groot K, Hunziker EB. BMP-2 liberated from biomimetic implant coatings induces and sustains direct ossification in an ectopic rat model. Bone. 2005 May;36(5):745-57.

117. Ripamonti U, Yeates L, van den Heever B. Initiation of heterotopic osteogenesis in primates after chromatographic adsorption of osteogenin, a bone morphogenetic protein, onto porous hydroxyapatite. Biochem Biophys Res Commun. 1993 Jun 15;193(2):509-17.

118. Onuma K, Kanzaki N, Kobayashi N. Association of calcium phosphate and fibroblast growth factor-2: a dynamic light scattering study. Macromol Biosci. 2004 Jan 21;4(1):39-46.

119. Liu Y, Layrolle P, de Bruijn J, van Blitterswijk C, de Groot K. Biomimetic coprecipitation of calcium phosphate and bovine serum albumin on titanium alloy. J Biomed Mater Res. 2001 Dec 5;57(3):327-35.

120. Wen HB, de Wijn JR, van Blitterswijk CA, de Groot K. Incorporation of bovine serum albumin in calcium phosphate coating on titanium. J Biomed Mater Res. 1999 Aug;46(2):245-52.

121. Azevedo HS, Leonor IB, Alves CM, Reis RL. Incorporation of proteins and enzymes at different stages of the preparation of calcium phosphate coatings on a degradable substrate by a biomimetic methodology. Materials Science and Engineering: C. 2005;25(2):169.

122. Daculsi G, Laboux O, Le Geros R. Outcome and perspectives in bioactive coatings: What's new, what's coming. ITBM-RBM. 2002;23(6):317.

123. Radin S, Campbell JT, Ducheyne P, Cuckler JM. Calcium phosphate ceramic coatings as carriers of vancomycin. Biomaterials. 1997 Jun;18(11):777-82.

124. de Groot K, Geesink R, Klein CP, Serekian P. Plasma sprayed coatings of hydroxylapatite. J Biomed Mater Res. 1987 Dec;21(12):1375-81.

125. Liu Y, Enggist L, Kuffer AF, Buser D, Hunziker EB. The influence of BMP-2 and its mode of delivery on the osteoconductivity of implant surfaces during the early phase of osseointegration. Biomaterials. 2007 Jun;28(16):2677-86.

126. Klein CP, Patka P, Wolke JG, de Blieck-Hogervorst JM, de Groot K. Long-term in vivo study of plasma-sprayed coatings on titanium alloys of tetracalcium phosphate, hydroxyapatite and alpha-tricalcium phosphate. Biomaterials. 1994 Jan;15(2):146-50.

127. Liu Y, Huse RO, de Groot K, Buser D, Hunziker EB. Delivery mode and efficacy of BMP-2 in association with implants. J Dent Res. 2007 Jan;86(1):84-9.

128. Krebsbach PH, Kuznetsov SA, Bianco P, Robey PG. Bone marrow stromal cells: characterization and clinical application. Crit Rev Oral Biol Med. 1999;10(2):165-81.

129. Friedenstein AJ. Precursor cells of mechanocytes. Int Rev Cytol. 1976;47:327-59.

130. Friedenstein AJ. Marrow stromal fibroblasts. Calcified tissue international. 1995;56 Suppl 1:S17.

131. Owen M, Friedenstein AJ. Stromal stem cells: marrow-derived osteogenic precursors. Ciba Found Symp. 1988;136:42-60.

132. Caplan AI. Mesenchymal stem cells. J Orthop Res. 1991 Sep;9(5):641-50.

133. Caplan AI. Review: mesenchymal stem cells: cell-based reconstructive therapy in orthopedics. Tissue engineering. 2005 Jul-Aug;11(7-8):1198-211.

134. Derubeis AR, Cancedda R. Bone marrow stromal cells (BMSCs) in bone engineering: limitations and recent advances. Annals of biomedical engineering. 2004 Jan;32(1):160-5.

135. Bianco P, Riminucci M, Gronthos S, Robey PG. Bone marrow stromal stem cells: nature, biology, and potential applications. Stem Cells. 2001;19(3):180-92.

136. Bellows CG, Heersche JN, Aubin JE. Determination of the capacity for proliferation and differentiation of osteoprogenitor cells in the presence and absence of dexamethasone. Dev Biol. 1990 Jul;140(1):132-8.

137. Liu F, Aubin JE, Malaval L. Expression of leukemia inhibitory factor (LIF)/interleukin-6 family cytokines and receptors during in vitro osteogenesis: differential regulation by dexamethasone and LIF. Bone. 2002 Jul;31(1):212-9.

138. Tuan RS, Boland G, Tuli R. Adult mesenchymal stem cells and cell-based tissue engineering. Arthritis Res Ther. 2003;5(1):32-45.

139. Chung CH, Golub EE, Forbes E, Tokuoka T, Shapiro IM. Mechanism of action of beta-glycerophosphate on bone cell mineralization. Calcified tissue international. 1992 Oct;51(4):305-11.

140. Tenenbaum HC, Limeback H, McCulloch CA, Mamujee H, Sukhu B, Torontali M. Osteogenic phase-specific co-regulation of collagen synthesis and mineralization by beta-glycerophosphate in chick periosteal cultures. Bone. 1992;13(2):129-38.

141. Beck GR, Jr., Zerler B, Moran E. Phosphate is a specific signal for induction of osteopontin gene expression. Proceedings of the National Academy of Sciences of the United States of America. 2000 Jul 18;97(15):8352-7.

142. Quarles LD, Yohay DA, Lever LW, Caton R, Wenstrup RJ. Distinct Proliferative and Differentiated Stages of Murine Mc3t3-E1 Cells in Culture - an Invitro Model of Osteoblast Development. Journal of Bone and Mineral Research. 1992 Jun;7(6):683-92.

143. Franceschi RT, Iyer BS, Cui Y. Effects of ascorbic acid on collagen matrix formation and osteoblast differentiation in murine MC3T3-E1 cells. J Bone Miner Res. 1994 Jun;9(6):843-54.

144. Liu P, Oyajobi BO, Russell RG, Scutt A. Regulation of osteogenic differentiation of human bone marrow stromal cells: interaction between transforming growth factor-beta and 1,25(OH)(2) vitamin D(3) In vitro. Calcified tissue international. 1999 Aug;65(2):173-80.

145. Gomes ME, Bossano CM, Johnston CM, Reis RL, Mikos AG. In vitro localization of bone growth factors in constructs of biodegradable scaffolds seeded with marrow stromal cells and cultured in a flow perfusion bioreactor. Tissue engineering. 2006 Jan;12(1):177-88.

146. Pham QP, Kurtis Kasper F, Scott Baggett L, Raphael RM, Jansen JA, Mikos AG. The influence of an in vitro generated bone-like extracellular matrix on osteoblastic gene expression of marrow stromal cells. Biomaterials. 2008 Jun;29(18):2729-39.

147. Owen TA, Aronow M, Shalhoub V, Barone LM, Wilming L, Tassinari MS, et al. Progressive development of the rat osteoblast phenotype in vitro: reciprocal relationships in expression of genes associated with osteoblast proliferation and differentiation during formation of the bone extracellular matrix. J Cell Physiol. 1990 Jun;143(3):420-30.

148. Gomes ME, Sikavitsas VI, Behravesh E, Reis RL, Mikos AG. Effect of flow perfusion on the osteogenic differentiation of bone marrow stromal cells cultured on starch-based three-dimensional scaffolds. Journal of biomedical materials research. 2003 Oct 1;67(1):87-95.

149. Frost HM. Tetracycline-based histological analysis of bone remodeling. Calcif Tissue Res. 1969;3(3):211-37.

150. Boskey AL. Biomineralization: conflicts, challenges, and opportunities. J Cell Biochem Suppl. 1998;30-31:83-91.

151. Gomes ME, Holtorf HL, Reis RL, Mikos AG. Influence of the porosity of starch-based fiber mesh scaffolds on the proliferation and osteogenic differentiation of bone marrow stromal cells cultured in a flow perfusion bioreactor. Tissue engineering. 2006 Apr;12(4):801-9.

152. Holtorf HL, Jansen JA, Mikos AG. Flow perfusion culture induces the osteoblastic differentiation of marrow stroma cell-scaffold constructs in the absence of dexamethasone. Journal of biomedical materials research. 2005 Mar 1;72(3):326-34.

153. Hoshi K, Kemmotsu S, Takeuchi Y, Amizuka N, Ozawa H. The primary calcification in bones follows removal of decorin and fusion of collagen fibrils. J Bone Miner Res. 1999 Feb;14(2):273-80.

154. Bianco P, Fisher LW, Young MF, Termine JD, Robey PG. Expression of bone sialoprotein (BSP) in developing human tissues. Calcified tissue international. 1991 Dec;49(6):421-6.

155. Mark MP, Butler WT, Prince CW, Finkelman RD, Ruch JV. Developmental expression of 44-kDa bone phosphoprotein (osteopontin) and bone gamma-carboxyglutamic acid (Gla)-containing protein (osteocalcin) in calcifying tissues of rat. Differentiation. 1988;37(2):123-36.

156. Bianco P, Riminucci M, Silvestrini G, Bonucci E, Termine JD, Fisher LW, et al. Localization of bone sialoprotein (BSP) to Golgi and post-Golgi secretory structures in osteoblasts and to discrete sites in early bone matrix. J Histochem Cytochem. 1993 Feb;41(2):193-203.

157. Cancedda R, Castagnola P, Cancedda FD, Dozin B, Quarto R. Developmental control of chondrogenesis and osteogenesis. The International journal of developmental biology. 2000;44(6):707-14.

158. Hunter GK, Goldberg HA. Nucleation of hydroxyapatite by bone sialoprotein. Proceedings of the National Academy of Sciences of the United States of America. 1993 Sep 15;90(18):8562-5.

159. Lian JB, Stein GS. Concepts of osteoblast growth and differentiation: basis for modulation of bone cell development and tissue formation. Crit Rev Oral Biol Med. 1992;3(3):269-305.

160. Lian JB, Stein GS. The developmental stages of osteoblast growth and differentiation exhibit selective responses of genes to growth factors (TGF beta 1) and hormones (vitamin D and glucocorticoids). J Oral Implantol. 1993;19(2):95-105; discussion 36-7.

CHAPTER I

INTRODUCTION

PART II. Naturally Derived Responsive and *In Situ*-Forming Scaffolds for Bone Tissue Engineering Applications: An Overview of the Last Decade[2]

ABSTRACT

The use of bioabsorbable polymeric scaffolds is being investigated for use in bone tissue engineering applications, as their properties can be tailored to allow them to degrade and integrate at optimal rates as bone remodelling is completed. The main goal of this review is to highlight the "biomimetic" and "intelligent" properties exhibited by some specific natural scaffolds and their use in the bone tissue engineering field. To complement the fast evolution of the bone tissue engineering field, it is important to propose the use of responsive scaffolds and take advantage of bioinspired materials and their properties as emerging technologies. There is a growing interest and need for new biomaterials, such as "smart"/responsive materials with the capability to respond to changes in the *in vivo* environment have been devoted. This review will provide an overview of strategies that can modulate bone tissue regeneration by using *in situ*-forming scaffolds.

[2] This chapter is based on the following publication:

A.M. Martins, C.M. Alves, F.K. Kasper, A.G. Mikos, R.L. Reis. Naturally Derived Responsive and *In Situ*-Forming Scaffolds for Bone Tissue Engineering Applications: An Overview of the Last Decade, submitted.

1. INTRODUCTION

Bone is a highly vascular, living and dynamic tissue remarkable for its combination of mechanical properties and regenerative capacity. Bone possesses self-regeneration capacity. However, there is a limit to the size of bone fractures and defects that can be self-repaired. This limit is designated as the "critical size defect"[1-3] and will not heal during the lifetime of the patient. For large defects medical intervention is often necessary to repair the bone. A new field of research that proposes the regeneration of the tissue instead of its substitution is defined as tissue engineering: "an interdisciplinary field of research that applies the principles of engineering and the life sciences towards the development of biological substitutes that restore, maintain or improve tissue function"[4]. Tissue engineering strategies involving scaffolds include two general categories: (1) the use of acellular matrices (artificial scaffolds or decellularized tissues), which depend upon the natural ability of the body to regenerate for proper orientation and direction of new tissue growth, and (2) the use of scaffolds with cells[4, 5]. But the most classical paradigm of Tissue Engineering for tissue regeneration implies the use of a degradable support or scaffold material, bioactive factors and cells[4, 6, 7]. Several characteristics and properties have been described [8, 9] *as sine qua non* requirements for a suitable scaffold to be used in bone tissue engineering: biocompatibility, biodegradability into nontoxic products, and the ability to resorb at the adequate rate follow the repair of bone; adequate surface characteristics for cell adhesion and proliferation; an interconnected porous structure that enable tissue ingrowth, vascularisation, exchange of nutrients, oxygen and metabolites; and suitable mechanical properties matching those of the native tissue. The biomaterial must maintain its structural integrity during the first stages of the new bone formation. The main aim behind the different approaches of bone tissue engineering consists of developing a functionalized responsive and bioresorbable scaffold able to stimulate cell adhesion, proliferation and differentiation, with the objective that osteoblasts produce bone extracellular matrix (ECM).

Learning from Nature is a concept that implies mimicking Nature to develop novel functional biomaterials such as biomineralized, "smart" or bonelike composite materials[10-15]. "Smart" scaffolds and bioreactors are being developed to enable advanced procedures for delivery of bioactive molecules and mechanical stimuli to cultured cells in order to direct osteogenic differentiation[13, 14, 16-19]. It has been stimulated increased attention for responsive strategies *in vitro,* such as the use of flow perfusion bioreactors. The strategy includes the culture of bone marrow stromal cells onto scaffolds under flow conditions which allow a better distribution of nutrients and oxygen and the necessary mechanical stimuli for cellular differentiation along the osteogenic lineage[20-22]. This approach is an ideal system for the *ex vivo* production of bone constructs[23-25]. Notwithstanding the deeply discussed typical bone

tissue engineering strategy, which involves the use of a porous scaffold, cells and bioactive molecules, this review will focus on alternative approaches, such as the use of "smart"/responsive acellular scaffolds for bone tissue engineering applications.

The role of naturally derived materials and environmental stimuli in modulating bone regeneration will be discussed. While many excellent biomaterials have been developed in recent years, their translation into clinical practice has been slow. Chitosan was the selected natural polymer to be explored in this review mainly because of its pH responsive properties and biodegradability. The present review intends to provide an overview of the current state of the art of naturally derived responsive scaffolds and *in situ*-forming concepts for bone tissue engineering applications, their aims and limitations.

2. SCAFFOLDS FOR BONE TISSUE ENGINEERING

The simplest way to define a scaffold for tissue engineering is that it should provide mechanical support, shape, and cell-scale architecture for neo-tissue construction *in vitro* or *in vivo* as seeded cells expand and organize[26]. Scaffolds mimic the extracellular matrix and have a crucial role to play in supporting cell growth, differentiation and in delivering growth factors or other bioactive molecules. Extracellular matrix (ECM) is involved in bone formation, remodelling, and repair and its components include minerals, ions, proteins, and enzymes. The traditional scaffolds for bone tissue engineering should present standard parameters such as high porosity, large surface area, mechanical properties and pore sizes appropriate for the intended application, and a highly interconnected pore structure[4, 7, 27]. It has been reported that high porosity and pore sizes of 100-400 μm in the scaffold are necessary for bone ingrowth[7, 28]. In addition, biocompatibility and biodegradability are also required properties of scaffolds[13, 14]. In this review we will highlight some characteristics of acellular scaffolds, such as mechanical properties and biodegradability.

The degradation rate of the scaffolds must be tuned appropriately with the growth rate of the new tissue, by the time the injury site is totally regenerated the scaffold should be totally degraded[2, 13, 14]. If the degradation is faster than the tissue regeneration, the scaffolds will loose its support function for tissue growth. On the other hand, if the degradation is too slow compared to tissue formation, the scaffold will compromise the regeneration of the tissue. Mechanical properties of bulk materials represent an important group of characteristics to considerer in three-dimensional (3D) artificial ECM (scaffold) design[29]. Bulk materials are fundamental contributors to the mechanical integrity of the scaffold. This property is especially important for tissue engineering of structural tissues. Thus, the

scaffolds should have mechanical properties resembling those of healthy tissue during the period of tissue regeneration[7, 27]. Mechanical strength is needed for the creation of a 3D structure that will retain its structure after implantation, particularly in the reconstruction of hard and load-bearing bone tissues[28].

2.1. Mechanical properties

The mechanical properties of the implanted scaffold should ideally match those of living bone[7, 27, 30]. This demanding balance represents one limitation of scaffolds intended for bone regeneration and generally leads to mechanical biomaterial failure. Low mechanical strength of porous scaffolds may not be suitable for the repair of load-bearing tissues in some clinical applications[31]. Depending upon the application, mechanical properties should be studied keeping in mind the surrounding environment of the scaffold once placed in an *in vivo* system. The initial mechanical properties of the scaffold to be implanted are extremely important and ideally should be similar to those of the bone that is intended to be regenerated. Besides providing appropriate support in the early stages of healing, the long-term success of the biomaterial will depend on the efficacious graded load transfer needed in the later stages of the remodelling process[32]. The mechanical properties of the two types of bone, i.e., the cortical (compact) and cancellous (spongy) bone, are listed in Table 1. Highly porous structures with interconnected pores may fail their objective due to poor mechanical properties.

Table 1. Mechanical properties of cancellous and cortical bone (adapted from[7, 28, 33]).

	Compressive strength (MPa)	**Young's modulus (GPa)**
Cancellous bone	2-12	0.02-0.5
Cortical bone	100-230	2-30

2.2. Mechanisms of polymer biodegradation

Controlling the degradation of scaffolds to match the rate of bone growth, to create space for the new bone formation until full regeneration is reached, remains a major challenge in scaffold design. The ideal degradable material degrades during its intended

application or immediately after it. The process of polymer degradation describes the mechanisms through which polymer chains are cleaved to form oligomers and finally monomers[34]. The process of erosion designates the loss of material owing to monomers and oligomers leaving the polymer[34, 35]. All biodegradable polymers have hydrolysable bonds. Their most important degradation mechanism is enzymatic hydrolysis. The latter effect is designated as biodegradation meaning that the degradation is mediated by a biological process[34]. Several factors influence the kinetics of degradation: the type of chemical bonds, pH, polymer composition, crystallinity, molecular weight, porosity, water uptake and location of the implant[34]. Hydrophilic polymers absorb large quantities of water and increase degradation rates. Resorbable biomaterials have the ability to resorb over time. This behaviour is necessary to support the gradual ingrowth of cells and complete replacement of a regenerated matrix by normal tissue, and to avoid risk of complications that can be associated with the long-term presence of foreign material[36]. Scaffold evaluation also includes studying the appropriate degradation rate, which is important because as the scaffold degrades it is replaced by natural tissue. Biodegradation is generally required for a tissue engineering scaffold material, and the degradation rate also needs to match the neo tissue formation rate to ideally serve the template purpose[27, 28, 37]. Bone tissue engineering generally requires an artificial extracellular matrix (scaffold) to regenerate tissue at the site of implantation. This scaffold should disappear through absorption into the body as the new tissue is regenerated[37].

3. "SMART" AND RESPONSIVE SCAFFOLDS FOR BONE TISSUE ENGINEERING

Stimuli-responsive, "smart", "intelligent" or environmentally-sensitive polymers respond with large property changes to small chemical, physical or biochemical stimuli (Table 2). The concept of "smart" polymers derived from the development of biomaterials that show large conformational changes in response to small environmental stimuli such as temperature, ionic strength, pH, or light[26, 38]. The materials that respond to changes in their surrounding environment are very attractive because these changes, mainly *in vivo,* can be exploited to control parameters such as drug delivery, cell adhesion, mechanical properties, and permeability, among others[39]. The responses of the polymer may include precipitation or gelation, reversible adsorption on a surface, collapse of a hydrogel or surface graft, and alternation between hydrophilic and hydrophobic states[26, 40]. Natural polymers may present a more appropriate biological environment to the cells, since they usually contain domains that can send important signals to guide the cells at various stages of development[41]. Collagen and fibrin, natural ECM molecules, have been used as scaffolds for tissue engineering. They

have interesting biological properties for tissue engineering research[42-45]. However, their low mechanical properties, the risk of viral infection, antigenicity, instability and deterioration that follow long-term implantation limit the clinical applications of these natural biomaterials[37].

Table 2. Environmental stimuli that responsive, "smart", "intelligent" or to which environmentally-sensitive polymers respond (adapted from[40, 46]).

Physical	Chemical	Biochemical
Temperature		
Ionic strength	pH	Enzyme ligands
Solvents	Specific ions	Biochemical agents
Electrical and magnetic fields	Chemical agents	
Mechanical stress, strain		

4. CHITOSAN SCAFFOLDS AS A RESPONSIVE BIOMATERIAL

Polysaccharides are very attractive for tissue engineering applications mainly because of their biodegradability, biocompatibility and resemblance with the environment of the extracellular matrix[47, 48]. Examples of anionic naturally derived polymers are alginate, hyaluronic acid, chondroitin sulphate and carragenans[48]. However chitosan is the only cationic polysaccharide found in Nature. In the last decade, significant attention has been given to chitosan-based biomaterials[13, 49-55] in the field of bone tissue engineering. This review will focus on chitosan, a polycationic natural-origin polymer produced by the deacetylation of chitin, a natural component of crustacea exoskeletons (e.g. shrimp, crab, lobster, etc.), cell walls of fungi and cuticles of insects[54, 56]. Chitosan is a binary polyheterosaccharide of N-acetylglucosamine and glucosamine with a β1→4 linkage. The superior tissue compatibility of chitosan can be partially attributed to its structural similarity to glycosaminoglycans, which are major components of the ECM of bone and cartilage[54, 57]. Chitosan exhibits a pH-sensitive behavior due to the large quantities of amino groups on its chains. It is a biocompatible, pH-dependent cationic polymer, which is insoluble in aqueous solutions above pH 7[55]. However, in dilute or weak acids (pH<6), the protonated free amino groups of glucosamine facilitate solubility of the molecule[55]. Above pH 6.2 chitosan aqueous solutions lead to the formation of a hydrated gel-like precipitate[58, 59]. Temperature and pH have been extensively studied in the biomedical field because these two parameters can be easily controlled and applicable both *in vitro* and *in vivo*. Dias *et al.*[60] reported the use of

chitosan, a natural and pH-responsive polymer, grafted onto a biodegradable bioactive composite and investigated the effect of pH on the biomineralization process. The authors successfully developed “smart” biodegradable surfaces that respond to pH and that could be used to control the biomineralization process. They also found that the formation of biomimetic apatite was dependent on the conformational changes of chitosan across its critical pH and could be controlled by pH switching.

Chitosan hydrogels have been used in a number of gene and drug delivery applications and can deliver growth factors and pharmaceutical agents in a controlled fashion[61-63]. Due to its cationic nature and predictable degradation rate, chitosan-based materials bind growth factors and release them in a controlled manner[64].

Chitosan is degraded, depending on degree of deacetylation by enzymes such as lysozyme, N-acetyl-D-glucosaminidase and lipases[61]. *In vivo*, chitosan is degraded by enzymatic hydrolysis, primarily by lysozyme which appears to target acetylated residues[65, 66]. Degradation kinetics seem to be inversely related to the degree of deacetylation[65]. The degree of deacetylation represents the proportion of N-acetyl-D-glucosamine units with respect to the total number of units[67]. Lysozyme breaks down the chitosan polymer chain, diminishing its molecular weight until it becomes short enough to be processed by cells. Glucosamines, the final degradation products of chitosan, are nontoxic, nonimmunogenic, and noncarcinogenic[68]. *In vivo,* the final degradation products undergo normal metabolism pathways and may be incorporated into glycoproteins or excreted as carbon dioxide gas during respiration[69, 70]. Lysozyme or muramidase is an enzyme that catalyzes the hydrolysis of the peptidoglycan layer of bacterial cell walls[71]. This enzyme is active over a broad pH range from 3 to 8 and is suited to hydrolyze its substrates both inside and outside cells. Lysozyme is ubiquitous in the human body[72]. It is present in lymphocytes and also secreted by monocytes, macrophages, and granulocytes, which account for the largest source[73, 74]. Monocytes and macrophages are the dominating contributors to the lysozyme content in serum[73]. Human serum lysozyme is found in concentrations from 7 to 13 mg/L[72].

Chitosan possesses interesting characteristics, such as its ability to induce a minimal foreign body reaction, an intrinsic antibacterial nature[75, 76], and the ability to be molded in various shapes, namely porous structures, suitable for cell ingrowth and osteoconduction. The mechanical properties of chitosan scaffolds are dependent on the pore size and pore orientation[75].

5. NATURALLY DERIVED *IN SITU* FORMING SCAFFOLDS

The goal of the *in situ* generated implant strategy is used to engineer biomedical systems at their site of performance using minimally invasive surgeries[77]. Several approaches have been developed[78-80] namely synthetic *in situ* scaffolding materials that could deliver cells or provide a structure for tissue infiltration. Naturally occurring polymers that form thermoreversible gels include gelatine, carrageenan, cellulose derivatives, xyloglucan and chitosan with glycerophosphate[58]. Moreover, several natural biomaterials, including collagen, heparin, hyaluronate, and fibrin have been used for the preparation of injectable *in situ*-forming scaffolds[81-86]. Besides eliminating the need for *ex vivo* implant fabrication, the contact and adhesion between the biomaterial and native bone may be enhanced with a polymer formed directly in the bone defect (*in situ*)[87]. Current approaches for implanting medical devices often require complex surgeries. In the past few years, an increasing number of *in situ*-forming systems have been proposed for various biomedical applications, including drug delivery[88-90], cell encapsulation[58, 91], and tissue repair[83, 92, 93]. There are several possible mechanisms leading to *in situ* implant formation. It has become increasingly apparent that scaffolds for bone tissue engineering applications should provide more than temporary 3D structure for developing tissue construct. Due to the pH-sensitive character of chitosan, this polymer has great potential to be used in the fabrication of scaffold and gels that respond to localized conditions of pH in the human body. Hai Bang Lee *et al*.[94] stated that it is difficult to perform *ex vivo* fabrication of certain complex scaffold geometries. As an alternative, they reported the use of *in situ*–forming scaffolds as a promising approach for the fabrication of complicated scaffold geometries. The *in situ*–forming scaffold is based on the idea that if a biomaterial undergoes a simple liquid-to-gel phase transition under physiological conditions, it can be injected as a liquid, and then form the desired gel *in situ*[94-96]. As previously reported, Ruel-Gariepy *et al.*[58, 97] demonstrated that a mixture of chitosan and glycerol phosphate disodium salt (β-glycerophosphate) is capable of forming a gel scaffold *in situ.* These formulations possess a neutral pH, remain liquid at or below room temperature, and form monolithic gels at body temperature[58]. The stability of the solution at room temperature and the gelation time increases as the degree of deacetylation decreases[58, 97]. Hai Bang Lee *et al*.[94] described the development of *in situ*–forming chitosan gels, and their ability to offer a suitable scaffold for rat bone marrow stromal cells (rBMSCs) *in vitro* and *in vivo.* The *in situ*-forming scaffold provides numerous benefits, such as its being a noninvasive alternative for tissue engineering applications. These results showed that chitosan gel can serve as an *in situ*–forming gel scaffold for entrapped rBMSCs *in vivo*. Studies dealing with the role of stem/progenitor cells in osteogenesis show that chitosan has the ability to promote osteogenic progenitor cell recruitment and attachment, facilitating bone formation[98].

As cell and molecular biology converge with materials science and biomedical engineering, new applications will benefit from interactive biomaterials that serve to orchestrate cell attachment, growth and differentiation[26]. Recently, a considerable interest has been given to the development of "smart" materials with the ability to instruct the behaviour of cells by releasing bioactive molecules into the local environment[99, 100].

6. *IN SITU* PORE-FORMING SCAFFOLDS

One of the major challenges of bone tissue engineering is the development of scaffolds capable of promoting the differentiation of immature progenitor cells down an osteoblastic lineage (osteoinduction) encouraging the ingrowth of surrounding bone (osteoconduction) and integration into the surrounding tissue[101, 102]. The main goal of the *in situ* forming scaffolds strategy is to generate systems at their site of implantation using minimally invasive surgical procedures or eliminate some steps of the common strategies used in bone tissue engineering applications (i.e., cell seeding onto scaffolds *ex vivo*). Acellular scaffolds with properties capable to induce bone regeneration could be an interesting alternative.

One innovative approach was described by the group of by the group of Robert Langer[103] for the first time in 2003 proposing *in situ* pore formation in a polymer matrix by differential degradation. The common approaches have been developed to introduce porosity in a polymer matrix *ex vivo* and thus facilitate cell seeding either *in vitro* or *in vivo*. In that paper, the authors stated that controlling pore formation *in vivo* with specific tissue ingrowth could be beneficial for bone tissue engineering and presented a new paradigm for the formation of pores in a polymer matrix *in situ* [103]. For that, polymer microspheres were used as a pore-forming agent (porogen)[103].

It has been demonstrated that hydrophilic polymers such as chitosan, depending on the processing method and shape present suitable mechanical properties for bone tissue engineering applications[13].

The inclusion of enzymatically degradable phases in biomaterials seems to be a very promising approach to obtain scaffolds with adequate mechanical properties in the initial stage of implantation and with a gradual *in vivo* pore-forming ability. Martins *et al.*[13] described the development of a biodegradable matrix, based on chitosan and starch with the ability of forming a porous structure *in situ* due to the attack by specific enzymes present in the human body, taking advantage of the inflammatory response. One of the critical factors that can control bone tissue regeneration is the degradation rate of the scaffold, as previously

discussed. Tailoring the degradation rate of scaffolds can facilitate scaffold remodelling and replacement by cells *in situ*, enhancing bone tissue regeneration. Inflammation is often viewed as a negative event, but it is fundamental for tissue regeneration processes[104]. Consequently, modulating the response of implanted material by harnessing characteristics of the inflammatory response is a powerful tool for driving tissue regeneration *in situ*. In this section alternative strategies will be discussed, such as the potential of using responsive scaffolds to take advantage of the host inflammatory response and thus obtain a beneficial outcome for bone tissue engineering applications. When a material is implanted, an acute inflammation is initiated involving several cell types[105-107]. During inflammation neutrophils, monocytes and macrophages are present. These cells release lysosomal enzymes, such as lysozyme, into the surrounding tissue[108]. It has been suggested that macrophages and neutrophils produce superoxide, hydrogen peroxide and hydroxyl free radicals which contribute to the biodegradation of implanted materials[108]. The results of the compressive tests showed that these materials, based on chitosan and starch exhibited very interesting mechanical properties in the dry and even in the wet state[13]. The mechanical properties exhibited by the scaffolds in the wet state fall in the normal ranges of strength and modulus for trabecular bone[7, 28]. This approach seem to be a promising strategy to produce an *in vivo* responsive scaffold, the properties of which may be regulated by the bone regeneration process, with gradual formation of pores *in situ* and consequent resorption. Using this innovative methodology, the developed scaffolds can exhibit suitable mechanical properties at the initial stage of implantation due to the inexistence of macroporosity. The porosity will be formed *in situ* by enzymes present in the human body. In this work, authors aimed at developing a biodegradable matrix based on chitosan and native starch that forms a porous structure *in vivo* due to the incorporation of the “sacrifice” phase (native starch) that will be preferentially attacked by specific enzymes and other reactive species present in the human body during the inflammatory response (Figure 1).

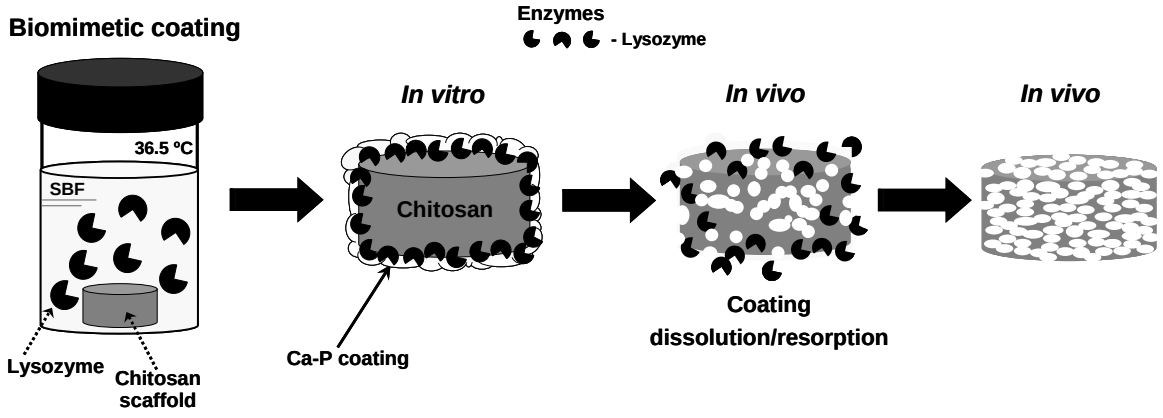


Figure 1. Schematic representation of *in situ* pore forming concept.

An alternative approach, involving the concept of bioactivity and osteoconduction, is to let degradation proceed along a coordinate of the healing process by making the material sensitive to the feedback provided by the cells involved in the healing response[109]. A biomimetic scaffold for bone tissue engineering can be any scaffolding material that mimics one or multiple characteristics of the natural ECM[110]. Functional materials such as calcium phosphate (CaP)[111] and hydroxyapatite[112] are often mixed with bulk materials to mimic bone ECM composition. CaP has a composition similar to bone mineral and can induce a biological response identical to that generated in bone remodelling[113]. The process of resorption of old bone mineral and formation of new bone is designated as bone remodelling[113]. The biomimetic technique for coating biomaterials with a bone-like apatite layer is well described[18, 114-116] and has been applied for the first time to biodegradable substrates and then to scaffolds by Reis *et al.*[18, 51, 61, 115, 117, 118]. Biomimetic CaP coating involves immersion of polymers in simulated body fluid (SBF), a solution with ion concentration identical to human plasma. CaP coatings have shown high efficiency in expediting bone osteoconduction[119]. However, for the regeneration of bone, osteoconduction is also important[100]. The incorporation of proteins and enzymes[18, 120-127] into CaP coatings is well documented. Further studies proposed an innovative self-regulated degrading material with gradual *in situ* pore formation ability for bone tissue engineering applications. In this study[127] one of the main aims was to improve the osteoconductive properties of chitosan scaffolds. For that, lysozyme was incorporated into CaP coatings, prepared on the surface of chitosan scaffolds using a biomimetic coating technique, with the aim of controlling their degradation rate and subsequent formation of pores. Furthermore, since lysozyme has antibacterial properties, these coatings may act as carriers for its sustained release, preventing infection upon implantation. Moreover, CaP coatings will enhance the osteoconductive properties of the chitosan scaffolds. Mineral deposition has been shown to slow scaffold degradation, probably by creating a barrier between the scaffold surface and surrounding environment[128]. In order to avoid this, one possible solution was the incorporation of the enzyme lysozyme to enhance degradation of chitosan scaffolds and subsequent formation of pores *in situ* (Figure 2).

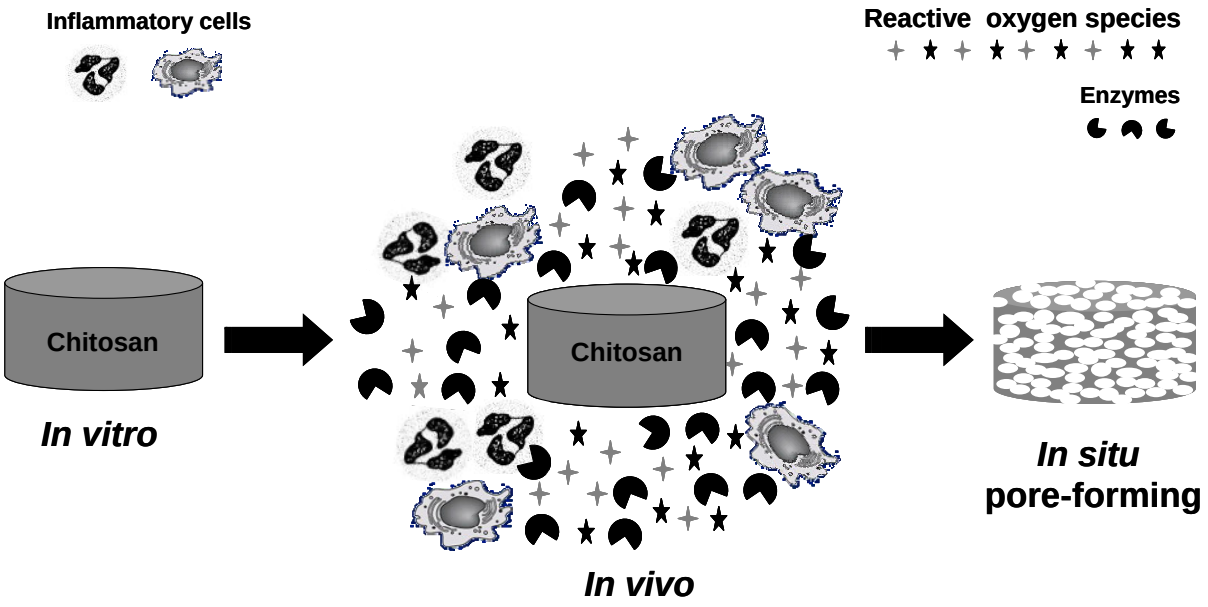


Figure 2. Schematic representation of a self-regulated degrading material with gradual *in situ* pore formation ability.

Responsive scaffolds for bone tissue engineering do not need to show the stimulus-dependent change in a reversible fashion. For example, after the cells or bioactive molecules are delivered, the scaffolds do not need to reverse the process. As it was discussed above, biodegradability and lack of cytotoxicity are required characteristics of bone tissue engineering scaffolds.

"Smart"/responsive polymers may offer promise for revolutionary improvements in tissue engineering scaffolds. Beyond the physical properties of polymers, a major goal is to improve the mechanical properties at the initial stage of implantation and if possible to avoid one of the most critical steps of the tissue engineering approach, that is the pre-seeding of the scaffolds with cells. Creating scaffolds with specific properties that *per se* could recruit cells to the site of implantation is in our opinion one of the main current challenges in the field.

7. CONCLUSIONS

Therapies for the treatment of lost tissue include tissue transplantation, surgical reconstruction, drug therapy, synthetic prostheses and medical devices or associations of those. The efforts to address their limitations have elicited the development of different

biomaterials and therapies. In this review we aimed at presenting as alternative approaches the engineering of responsive and in situ-forming scaffolds for bone regeneration.

Chitosan is one of the most promising natural polymers for bone tissue engineering due, in part, to its particular ability to form various shapes and structures. The predictable degradation rate and the ability of forming a porous structures and scaffolds *in situ* makes chitosan interesting alternative biomaterial for orthopaedic applications.

In the first part of this review, biodegradation and mechanical properties were highlighted as necessary requirements for the implantation of acellular scaffolds. In the second part, we presented developments and examples of naturally derived responsive scaffolds for bone tissue engineering. Finally, we described a new strategy for bone tissue engineering: the *in situ* pore-forming concept. Despite the recent advances, future research focusing on the development of novel scaffolds that *per se* could recruit the desirable cells, regenerate the site of implantation and reabsorb as a function of degradation time still comprises one of the most demanding and challenging strategies in the field of bone tissue engineering.

REFERENCES

1. J. P. Schmitz and J. O. Hollinger, *Clin Orthop Relat Res*, 1986, 299-308.

2. M. C. Kruyt, W. J. Dhert, H. Yuan, C. E. Wilson, C. A. van Blitterswijk, A. J. Verbout and J. D. de Bruijn, *J Orthop Res*, 2004, **22**, 544-551.

3. Z. S. Patel, S. Young, Y. Tabata, J. A. Jansen, M. E. Wong and A. G. Mikos, *Bone*, 2008, **43**, 931-940.

4. R. Langer and J. P. Vacanti, *Science*, 1993, **260**, 920-926.

5. A. Atala, *J Tissue Eng Regen Med*, 2007, **1**, 83-96.

6. R. Cancedda, B. Dozin, P. Giannoni and R. Quarto, *Matrix Biol*, 2003, **22**, 81-91.

7. D. W. Hutmacher, J. T. Schantz, C. X. Lam, K. C. Tan and T. C. Lim, *J Tissue Eng Regen Med*, 2007, **1**, 245-260.

8. D. W. Hutmacher, *Biomaterials*, 2000, **21**, 2529-2543.

9. D. W. Hutmacher, *J Biomater Sci Polym Ed*, 2001, **12**, 107-124.

10. P. B. Malafaya, M. E. Gomes, A. J. Salgado and R. L. Reis, *Adv Exp Med Biol*, 2003, **534**, 201-233.

11. G. A. Silva, F. J. Costa, O. P. Coutinho, S. Radin, P. Ducheyne and R. L. Reis, *J Biomed Mater Res A*, 2004, **70**, 442-449.

12. R. M. da Silva, J. F. Mano and R. L. Reis, *Trends Biotechnol*, 2007, **25**, 577-583.

13. A. M. Martins, M. I. Santos, H. S. Azevedo, P. B. Malafaya and R. L. Reis, *Acta Biomater*, 2008, **4**, 1637-1645.

14. A. M. Martins, Q. P. Pham, P. B. Malafaya, R. M. Raphael, F. K. Kasper, R. L. Reis and A. G. Mikos, *Tissue Eng Part A*, 2009.

15. L. J. Fan Xia, *Advanced Materials*, 2008, **20**, 2842-2858.

16. D. L. Kaplan, R. T. Moon and G. Vunjak-Novakovic, *Nat Biotechnol*, 2005, **23**, 1237-1239.

17. H. L. Holtorf, J. A. Jansen and A. G. Mikos, *Adv Exp Med Biol*, 2006, **585**, 225-241.

18. A. M. Martins, Q. P. Pham, P. B. Malafaya, R. M. Raphael, F. K. Kasper, R. L. Reis and A. G. Mikos, *Tissue Engineering Part A*, 2008, **14**, 795-795.

19. A. M. Martins, Q. P. Pham, P. B. Malafaya, R. A. Sousa, M. E. Gomes, R. M. Raphael, F. K. Kasper, R. L. Reis and A. G. Mikos, *Tissue Engineering Part A*, 2009, **15**, 295-305.

20. M. E. Gomes, C. M. Bossano, C. M. Johnston, R. L. Reis and A. G. Mikos, *Tissue Eng*, 2006, **12**, 177-188.

21. M. E. Gomes, H. L. Holtorf, R. L. Reis and A. G. Mikos, *Tissue Eng*, 2006, **12**, 801-809.

22. M. E. Gomes, V. I. Sikavitsas, E. Behravesh, R. L. Reis and A. G. Mikos, *J Biomed Mater Res A*, 2003, **67**, 87-95.

23. N. Datta, Q. P. Pham, U. Sharma, V. I. Sikavitsas, J. A. Jansen and A. G. Mikos, *Proc Natl Acad Sci U S A*, 2006, **103**, 2488-2493.

24. Q. P. Pham, F. K. Kasper, L. Scott Baggett, R. M. Raphael, J. A. Jansen and A. G. Mikos, *Biomaterials*, 2008, **29**, 2729-2739.

25. C. Aulin, F. Foroughi, R. Brown and J. Hilborn, *J Tissue Eng Regen Med*, 2009, **3**, 188-195.

26. M. E. Furth, A. Atala and M. E. Van Dyke, *Biomaterials*, 2007, **28**, 5068-5073.

27. A. J. Salgado, O. P. Coutinho and R. L. Reis, *Macromol Biosci*, 2004, **4**, 743-765.

28. S. Yang, K. F. Leong, Z. Du and C. K. Chua, *Tissue Eng*, 2001, **7**, 679-689.

29. J. Lee, M. J. Cuddihy and N. A. Kotov, *Tissue Eng Part B Rev*, 2008, **14**, 61-86.

30. K. F. Leong, C. M. Cheah and C. K. Chua, *Biomaterials*, 2003, **24**, 2363-2378.

31. S. J. Hollister, *Nat Mater*, 2005, **4**, 518-524.

32. J. S. Temenoff and A. G. Mikos, *Biomaterials*, 2000, **21**, 431-440.

33. J. Wilson, A. E. Clark, M. Hall and L. L. Hench, *J Oral Implantol*, 1993, **19**, 295-302.

34. A. Gopferich, *Biomaterials*, 1996, **17**, 103-114.

35. J. A. Tamada and R. Langer, *Proc Natl Acad Sci U S A*, 1993, **90**, 552-556.

36. J. A. Hubbell, *Biotechnology (N Y)*, 1995, **13**, 565-576.

37. F. Rosso, G. Marino, A. Giordano, M. Barbarisi, D. Parmeggiani and A. Barbarisi, *J Cell Physiol*, 2005, **203**, 465-470.

38. I. Y. Galaev and B. Mattiasson, *Trends Biotechnol*, 1999, **17**, 335-340.

39. B. D. Ratner and S. J. Bryant, *Annu Rev Biomed Eng*, 2004, **6**, 41-75.

40. A. S. Hoffman, P. S. Stayton, V. Bulmus, G. Chen, J. Chen, C. Cheung, A. Chilkoti, Z. Ding, L. Dong, R. Fong, C. A. Lackey, C. J. Long, M. Miura, J. E. Morris, N. Murthy, Y. Nabeshima, T. G. Park, O. W. Press, T. Shimoboji, S. Shoemaker, H. J. Yang, N. Monji, R. C. Nowinski, C. A. Cole, J. H. Priest, J. M. Harris, K. Nakamae, T. Nishino and T. Miyata, *J Biomed Mater Res*, 2000, **52**, 577-586.

41. R. Langer, *J Control Release*, 1999, **62**, 7-11.

42. E. Gentleman, A. N. Lay, D. A. Dickerson, E. A. Nauman, G. A. Livesay and K. C. Dee, *Biomaterials*, 2003, **24**, 3805-3813.

43. X. B. Yang, R. S. Bhatnagar, S. Li and R. O. Oreffo, *Tissue Eng*, 2004, **10**, 1148-1159.

44. C. Perka, O. Schultz, R. S. Spitzer, K. Lindenhayn, G. R. Burmester and M. Sittinger, *Biomaterials*, 2000, **21**, 1145-1153.

45. T. Osathanon, M. L. Linnes, R. M. Rajachar, B. D. Ratner, M. J. Somerman and C. M. Giachelli, *Biomaterials*, 2008, **29**, 4091-4099.

46. A. S. Hoffman, *Artif Organs*, 1988, **12**, 504-505.

47. J. F. Mano, G. A. Silva, H. S. Azevedo, P. B. Malafaya, R. A. Sousa, S. S. Silva, L. F. Boesel, J. M. Oliveira, T. C. Santos, A. P. Marques, N. M. Neves and R. L. Reis, *J R Soc Interface*, 2007, **4**, 999-1030.

48. J. F. Mano, *Advanced Engineering Materials*, 2008, **10**, 515-527.

49. A. R. Costa-Pinto, A. J. Salgado, V. M. Correlo, P. Sol, M. Bhattacharya, P. Charbord, R. L. Reis and N. M. Neves, *Tissue Eng Part A*, 2008, **14**, 1049-1057.

50. P. B. Malafaya, T. C. Santos, M. van Griensven and R. L. Reis, *Biomaterials*, 2008, **29**, 3914-3926.

51. A. M. Martins, R. C. Pereira, I. B. Leonor, H. S. Azevedo and R. L. Reis, *Acta Biomater*, 2009.

52. J. M. Oliveira, M. T. Rodrigues, S. S. Silva, P. B. Malafaya, M. E. Gomes, C. A. Viegas, I. R. Dias, J. T. Azevedo, J. F. Mano and R. L. Reis, *Biomaterials*, 2006, **27**, 6123-6137.

53. J. T. Oliveira, V. M. Correlo, P. C. Sol, A. R. Costa-Pinto, P. B. Malafaya, A. J. Salgado, M. Bhattacharya, P. Charbord, N. M. Neves and R. L. Reis, *Tissue Eng Part A*, 2008, **14**, 1651-1661.

54. A. Lahiji, A. Sohrabi, D. S. Hungerford and C. G. Frondoza, *J Biomed Mater Res*, 2000, **51**, 586-595.

55. S. V. Madihally and H. W. Matthew, *Biomaterials*, 1999, **20**, 1133-1142.

56. J. K. Suh and H. W. Matthew, *Biomaterials*, 2000, **21**, 2589-2598.

57. J. Y. Lee, S. H. Nam, S. Y. Im, Y. J. Park, Y. M. Lee, Y. J. Seol, C. P. Chung and S. J. Lee, *J Control Release*, 2002, **78**, 187-197.

58. E. Ruel-Gariepy and J. C. Leroux, *Eur J Pharm Biopharm*, 2004, **58**, 409-426.

59. A. Di Martino, M. Sittinger and M. V. Risbud, *Biomaterials*, 2005, **26**, 5983-5990.

60. C. I. Dias, J. F. Mano and N. M. Alves, *Journal of Materials Chemistry*, 2008, **18**, 2493-2499.

61. R. A. A. Muzzarelli, *Carbohydrate Polymers*, 2009, **76**, 167-182.

62. M. Prabaharan, *J Biomater Appl*, 2008, **23**, 5-36.

63. M. Prabaharan, J. J. Grailer, D. A. Steeber and S. Gong, *Macromol Biosci*, 2008, **8**, 843-851.

64. R. A. Muzzarelli, M. Mattioli-Belmonte, C. Tietz, R. Biagini, G. Ferioli, M. A. Brunelli, M. Fini, R. Giardino, P. Ilari and G. Biagini, *Biomaterials*, 1994, **15**, 1075-1081.

65. K. Tomihata and Y. Ikada, *Biomaterials*, 1997, **18**, 567-575.

66. S. Hirano, H. Tsuchida and N. Nagao, *Biomaterials*, 1989, **10**, 574-576.

67. C. Chatelet, O. Damour and A. Domard, *Biomaterials*, 2001, **22**, 261-268.

68. R. A. Muzzarelli, *Cell Mol Life Sci*, 1997, **53**, 131-140.

69. A. Abarrategi, A. Civantos, V. Ramos, J. V. Sanz Casado and J. L. Lopez-Lacomba, *Biomacromolecules*, 2008, **9**, 711-718.

70. J. Ma, H. Wang, B. He and J. Chen, *Biomaterials*, 2001, **22**, 331-336.

71. J. Brouwer, T. van Leeuwen-Herberts and M. Otting-van de Ruit, *Clin Chim Acta*, 1984, **142**, 21-30.

72. J. Hankiewicz and E. Swierczek, *Clin Chim Acta*, 1974, **57**, 205-209.

73. I. Torsteinsdottir, L. Hakansson, R. Hallgren, B. Gudbjornsson, N. G. Arvidson and P. Venge, *Rheumatology (Oxford)*, 1999, **38**, 1249-1254.

74. C. Teijon, R. Olmo, M. Dolores Blanco, A. Romero and J. Maria Teijon, *Toxicology*, 2003, **191**, 245-258.

75. I. Y. Kim, S. J. Seo, H. S. Moon, M. K. Yoo, I. Y. Park, B. C. Kim and C. S. Cho, *Biotechnol Adv*, 2008, **26**, 1-21.

76. C. Aimin, H. Chunlin, B. Juliang, Z. Tinyin and D. Zhichao, *Clin Orthop Relat Res*, 1999, 239-247.

77. D. Cohn, A. Sosnik and S. Garty, *Biomacromolecules*, 2005, **6**, 1168-1175.

78. R. Marchand and S. Woerly, *Neuroscience*, 1990, **36**, 45-60.

79. B. Balakrishnan and A. Jayakrishnan, *Biomaterials*, 2005, **26**, 3941-3951.

80. A. C. Wan, E. Khor and G. W. Hastings, *J Biomed Mater Res*, 1998, **41**, 541-548.

81. Y. D. Park, N. Tirelli and J. A. Hubbell, *Biomaterials*, 2003, **24**, 893-900.

82. H. Park, J. S. Temenoff, Y. Tabata, A. I. Caplan and A. G. Mikos, *Biomaterials*, 2007, **28**, 3217-3227.

83. D. W. Lim, D. L. Nettles, L. A. Setton and A. Chilkoti, *Biomacromolecules*, 2008, **9**, 222-230.

84. D. L. Nettles, K. Kitaoka, N. A. Hanson, C. M. Flahiff, B. A. Mata, E. W. Hsu, A. Chilkoti and L. A. Setton, *Tissue Eng Part A*, 2008, **14**, 1133-1140.

85. G. Tae, Y. J. Kim, W. I. Choi, M. Kim, P. S. Stayton and A. S. Hoffman, *Biomacromolecules*, 2007, **8**, 1979-1986.

86. K. A. B. C. W. P. J. C. E. S. Jennie Baier Leach, *Biotechnology and Bioengineering*, 2003, **82**, 578-589.

87. J. A. Burdick, R. F. Padera, J. V. Huang and K. S. Anseth, *J Biomed Mater Res*, 2002, **63**, 484-491.

88. A. Hatefi and B. Amsden, *J Control Release*, 2002, **80**, 9-28.

89. G. Chandrashekar and N. Udupa, *J Pharm Pharmacol*, 1996, **48**, 669-674.

90. S. Kumar, B. O. Haglund and K. J. Himmelstein, *J Ocul Pharmacol*, 1994, **10**, 47-56.

91. L. Klouda, M. C. Hacker, J. D. Kretlow and A. G. Mikos, *Biomaterials*, 2009.

92. J. Kirkham, A. Firth, D. Vernals, N. Boden, C. Robinson, R. C. Shore, S. J. Brookes and A. Aggeli, *J Dent Res*, 2007, **86**, 426-430.

93. Y. Zhang, H. H. Xu, S. Takagi and L. C. Chow, *J Mater Sci Mater Med*, 2006, **17**, 437-445.

94. M. H. Cho, K. S. Kim, H. H. Ahn, M. S. Kim, S. H. Kim, G. Khang, B. Lee and H. B. Lee, *Tissue Eng Part A*, 2008.

95. V. Crescenzi, L. Cornelio, C. Di Meo, S. Nardecchia and R. Lamanna, *Biomacromolecules*, 2007, **8**, 1844-1850.

96. M. S. Kim, S. K. Kim, S. H. Kim, H. Hyun, G. Khang and H. B. Lee, *Tissue Eng*, 2006, **12**, 2863-2873.

97. E. Ruel-Gariepy, A. Chenite, C. Chaput, S. Guirguis and J. Leroux, *Int J Pharm*, 2000, **203**, 89-98.

98. I. S. Kim, J. W. Park, I. C. Kwon, B. S. Baik and B. C. Cho, *Plast Reconstr Surg*, 2002, **109**, 1966-1977.

99. J. K. Leach and D. J. Mooney, *Expert Opin Biol Ther*, 2004, **4**, 1015-1027.

100. P. Habibovic and K. de Groot, *J Tissue Eng Regen Med*, 2007, **1**, 25-32.

101. T. Albrektsson and C. Johansson, *Eur Spine J*, 2001, **10 Suppl 2**, S96-101.

102. J. D. Kretlow and A. G. Mikos, *Tissue Eng*, 2007, **13**, 927-938.

103. V. P. Shastri, P. Hildgen and R. Langer, *Biomaterials*, 2003, **24**, 3133-3137.

104. G. Chan and D. J. Mooney, *Trends Biotechnol*, 2008, **26**, 382-392.

105. A. P. Marques, R. L. Reis and J. A. Hunt, *J Mater Sci Mater Med*, 2003, **14**, 167-173.

106. A. P. Marques, R. L. Reis and J. A. Hunt, *J Mater Sci Mater Med*, 2005, **16**, 1029-1043.

107. A. P. Marques, R. L. Reis and J. A. Hunt, *Macromol Biosci*, 2005, **5**, 775-785.

108. D. F. Williams and S. P. Zhong, *International biodeterioration & biodegradation* 1994, **34**, 95-130.

109. J. A. Hubbell, *Curr Opin Biotechnol*, 1999, **10**, 123-129.

110. P. X. Ma, *Adv Drug Deliv Rev*, 2008, **60**, 184-198.

111. M. J. Mondrinos, R. Dembzynski, L. Lu, V. K. Byrapogu, D. M. Wootton, P. I. Lelkes and J. Zhou, *Biomaterials*, 2006, **27**, 4399-4408.

112. D. A. Wahl, E. Sachlos, C. Liu and J. T. Czernuszka, *J Mater Sci Mater Med*, 2007, **18**, 201-209.

113. F. Barrere, C. A. van Blitterswijk and K. de Groot, *Int J Nanomedicine*, 2006, **1**, 317-332.

114. Y. Abe, T. Kokubo and T. Yamamuro, *Journal of Materials Science: Materials in Medicine*, 1990, **1**, 233-238.

115. R. L. Reis, A. M. Cunha, M. H. Fernandes and R. N. Correia, *Journal of Materials Science: Materials in Medicine*, 1997, **8**, 897-905.

116. K. Tuzlakoglu and R. L. Reis, *J Mater Sci Mater Med*, 2007, **18**, 1279-1286.

117. I. B. Leonor and R. L. Reis, *J Mater Sci Mater Med*, 2003, **14**, 435-441.

118. A. L. Oliveira, P. B. Malafaya and R. L. Reis, *Biomaterials*, 2003, **24**, 2575-2584.

119. C. N. Cornell, *Orthop Clin North Am*, 1999, **30**, 591-598.

120. H. S. Azevedo, I. B. Leonor, C. M. Alves and R. L. Reis, *Materials science & engineering C. Biomimetic and supramolecular systems* 2005, **25**, 169-179

121. I. B. Leonor, C. M. Alves, H. S. Azevedo and R. L. Reis, *Materials Science and Engineering: C*, 2009, **29**, 913-918

122. Y. Liu, K. de Groot and E. B. Hunziker, *Bone*, 2005, **36**, 745-757.

123. Y. Liu, E. B. Hunziker, P. Layrolle, J. D. De Bruijn and K. De Groot, *Tissue Eng*, 2004, **10**, 101-108.

124. Y. Liu, E. B. Hunziker, N. X. Randall, K. de Groot and P. Layrolle, *Biomaterials*, 2003, **24**, 65-70.

125. Y. Liu, P. Layrolle, J. de Bruijn, C. van Blitterswijk and K. de Groot, *J Biomed Mater Res*, 2001, **57**, 327-335.

126. Y. Liu, J. P. Li, E. B. Hunziker and K. de Groot, *Philos Transact A Math Phys Eng Sci*, 2006, **364**, 233-248.

127. A. M. Martins, R. L. Pereira, I. B. Leonor, H. S. Azevedo and R. L. Reis, *Acta Biomaterialia*, 2009, **doi:10.1016/j.actbio.2009.05.027**.

128. S. Maeno, Y. Niki, H. Matsumoto, H. Morioka, T. Yatabe, A. Funayama, Y. Toyama, T. Taguchi and J. Tanaka, *Biomaterials*, 2005, **26**, 4847-4855.

SECTION 2

CHAPTER II

MATERIALS AND METHODS

CHAPTER II

MATERIALS AND METHODS

1. PRODUCTION OF THE MATERIALS

1.1. SPCL fiber mesh scaffolds

Porous scaffolds used in the Chapters III and IV were based on a blend of corn starch and poly(ε-caprolactone) (SPCL, 30/70%) prepared using a fiber bonding technique [1]. SPCL fiber mesh scaffolds were cylinders with 8-mm diameter and thickness of 1.6 ± 0.1mm [2]. Previous studies have demonstrated that these scaffolds were able to induce ostegenic differentiation of rat marrow stromal cells when flow perfusion bioreactors were used, as well as, to express *in vitro,* several bone growth factors that are usually associated with bone formation *in vivo* [1, 3, 4].

1.2. Chitosan-based scaffolds

Finely ground chitosan (DD of 95%) powder was dissolved in acetic acid 1% (v/v) to obtain a 5% (w/v) clear solution (CH) without any particulate material. Because of the relatively high concentration, these solutions are quite viscous and consequently can be stirred only slightly. However, flow is still observed and it is still possible to inject such viscous solutions to fill out the moulds. Then, using the same procedure, other formulations were prepared using native corn starch with the following ratios: 80/20 chitosan/starch scaffolds (CS80-20) and 60/40 chitosan/starch scaffolds (CS60-40). The solutions were casted into moulds and frozen (-18 ºC) overnight.

To produce chitosan and chitosan/starch scaffolds, the solutions were immersed in a precipitation solution with containing 25% NaOH 1M and 75% of Na_2SO_4 0.5M (Panreac, Barcelona, Spain) adapted from Tuzlakoglu *et al.* [5]. After precipitation, the samples were washed repeatedly with distilled water to remove excess of salts, dried at 37 ºC and followed by successive washings for 5 days until no pH changes were detected. These scaffolds were used in the studies presented in Chapters V, VI, VII and VIII.

1.3. Chitosan-based scaffolds coated with CaP coating and incorporated lysozyme

The method to prepare the biomimetic CaP coatings was based on the methodology previously developed by Abe and Kokubo *et al.* [6] and adapted by Reis *et al.* [7, 8] consisting in an impregnation of the materials with bioactive glass (Bioglass®45S5, NovaMin Technology Inc or NOVABONE, Alachua, Florida, USA) followed by immersion in a simulated body fluid (SBF, 37 ºC, pH 7.4), presenting ionic concentrations similar to human blood plasma. Prior to the coating process, chitosan scaffolds (CH) and chitosan/starch scaffolds (CS) were sterilized by ethylene oxide. Bioglass® 45S5 was sterilized by immersion in ethanol solution (70% v/v) and then dried inside the hood. All the subsequent work was performed under sterile conditions in a hood. Briefly, CH and CS scaffolds were rolled in a wet bed of Bioglass® for the studies described in Chapter VI or in a rotator for 6 hours (Chapters VII and VIII). After that, the scaffolds where immersed in simulated body fluid (1.0 SBF) solution with and without lysozyme from chichen egg white (1 g/L) for 7 days at 37ºC (nucleation stage). This stage allows for the formation of CaP nuclei while lysozyme is incorporated. After the nucleation stage, all samples were washed with distilled water and immersed in a concentrated simulated body fluid solution (1.5 SBF) for 7 days at 37ºC in order to enhance CaP nuclei growth (growth stage). Four different samples were obtained using the biomimetic coating technique: CaP chitosan scaffolds (CaPCH), CaP chitosan/starch scaffolds (CaPCS), CaP chitosan scaffolds with incorporated lysozyme (CaPCH + lysozyme) and CaP chitosan/starch scaffolds with incorporated lysozyme (CaPCS + lysozyme). All the solutions were sterilized by filtration prior use.

1.4. Reagents

All chemical reagents used in the experimental results were purchased from Sigma (St. Louis, MO, USA) unless otherwise specified.

2. CHARACTERIZATION OF THE DEVELOPED SCAFFOLDS

2.1. Mechanical properties – compression tests

The mechanical properties of the materials described in Chapter V were evaluated on compression tests carried out in the dry and wet state in an Instron 4505 universal mechanical testing machine at a controlled environment (23 ºC and 55% RH). The crosshead speed was 2 mm min^{-1} 1% strain.

2.2. Degradation studies

Several degradation studies were carried out with and without enzymes in Chapters III, V, VI, and VII.

2.2.1. Degradation studies with α-amylase or lipase in static and dynamic conditions

Degradation studies were carried out by incubating samples in phosphate buffered saline (PBS) solution (0.1 M, pH 7.4) containing α-amylase (150 U/L) [9, 10] from *Bacillus sp.* or lipase (110 U/L) [10] from *Aspergillus niger*, both concentrations similar to those found in human serum, and sodium azide (0.2%), to avoid contamination, at 37 ºC up to 30 days under static and dynamic conditions (shaker at 70 rpm).The studies were performed in triplicate. The enzymatic degradation solutions were changed every 7 days to restore the original level of enzymatic activity. At the and of the degradation period, the samples were removed, washed thoroughly with distilled water, and dried in graded series of ethanol for later calculation of weight loss. These results are described in Chapter III.

2.2.2. Degradation studies with α-amylase and lysozyme

Degradation studies were carried out by incubating the scaffolds in phosphate buffered saline (PBS) solution (pH 7.4) containing α-amylase (150 U/L [9]) and/or lysozyme (13 mg/L [11, 12]) at concentrations similar to the ones found in human serum, at 37 ºC up to 90 days. A control was also performed by incubating the samples in buffer alone. Degradation solutions were also analyzed to measure the concentration of reducing sugars, released into the solution as a result of starch hydrolysis by α-amylase, using the dinitrosalicylic acid method. These studies are described in Chapter V.

2.2.3. Degradation studies at pH 7.4 and pH 5

In order to simulate *in vivo* conditions, degradation studies were carried out by incubating uncoated chitosan scaffolds, CaP coated chitosan scaffolds, with and without incorporated lysozyme, in two different buffer solutions: (i) Tris-HCl buffer (0.22 mM, pH 7.4) to simulate the normal pH found in human body and (ii) citrate buffer (1.0 mM, pH 5.0) to simulate the inflammatory response at 37 ºC for different periods of time. These studies are described in Chapter VI.

2.2.4. Degradation studies with lysozyme

Degradation studies presented in Chapter VII were performed by incubating the chitosan scaffolds (CH) in phosphate-buffered saline (PBS) solution (pH 7.4) with lysozyme (1.5 g/L), a concentration similar to the ones incorporated into CaP biomimetic coatings, at 37 ºC up to 21 days. Lysozyme solution was changed every 7 days.

2.2.5. Water uptake and weight loss measurements

At the end of each degradation period, the samples were removed and immediately weighed for determination of water uptake (Equation 1) (Chapter V), washed thoroughly with distilled water and dried for later calculation of weight loss (Equation 2) (Chapters III, V, VI, and VII):

$$\text{Water uptake (\%)} = [(w_w - w_i)/ w_i] \times 100 \qquad \text{(Equation 1)}$$

$$\text{Weight loss (\%)} = [w_i - w_f)/ w_i] \times 100 \qquad \text{(Equation 2)}$$

where w_i is the initial weight, w_w is the wet weight and w_f is the final weight of the sample.

2.2.6. Scanning electron microscopy (SEM)

The morphology of the samples described in Chapters V and VI and CaP coatings described in Chapter VI were mounted on aluminium stages, sputter with gold, and analysed by scanning electron microscopy (SEM, Leica Cambridge S-360, UK).

2.2.7. Thin-film X-Ray diffraction (TF-XRD) and Fourier Transformed infrared spectroscopy (FTIR)

In order to characterize the crystalline/amorphous nature of the CaP films described in Chapter VI, thin-film X-ray diffraction (TF-XRD, Philips X'Pert MPD, The Netherlands) was used. The data collection was performed by 2θ scan method with 1º as the incident beam angle using CuKα X-Ray line and a scan speed of 0.05º/min in 2θ. In addition, Infrared analysis (FTIR) of the coatings was performed in a Perkin- Elmer spectrometer (Perkin-Elmer 1600 series equipment, USA) to examine the chemical structure of the obtained CaP biomimetic coatings (Chapter VI). Coatings were scraped from the chitosan scaffolds, mixed with KBr (Riedel-de Haën, Germany) and then formed into a disc in a press. All spectra were obtained between 4400 and 450 cm^{-1} at a 2 cm^{-1} resolution.

2.2.8. Determination of lysozyme release and activity in solution

In order to evaluate the lysozyme activity and release from the CaP coating at pH 5 and pH 7.4 (Chapter VI), the *Micrococcus lysodeikticus* assay was used. This assay is based on the ability of lysozyme to hydrolyse the cell wall fragments of bacteria. For determining the activity of released lysozyme, coated scaffolds with incorporated lysozyme were immersed in buffer solution (pH 7.4) and incubated at 37 ºC for 30 days. The released lysozyme (150 µL) was added to a 100 µL of *Micrococcus lysodeikticus* suspension (2.3 mg/mL, pH 7.4) in a 96-well plate. The decrease in turbidity at 37 ºC was measured at 450 nm (Microplate Reader, Synergy^{TM} HT, BIO-TEK Instruments, Inc., USA) at 1 min intervals during 30 minutes. The same procedure was used to determine the enzyme activity at pH 5 and pH 7.4. For that, known enzyme concentrations were prepared in buffers at pH 5 and pH 7.4 and added to the bacteria suspension in the same buffer. The initial kinetic rate (OD slope at t = 0) was measured for each sample and a standard curve (lysozyme activity vs lysozyme concentration) was constructed. The activity of the lysozyme released after 30 days was determined from the standard curve.

2.2.9. Micro-computed tomography (µ-CT) analysis

The porosity, pore interconnectivity, pore size, and 3D structures of SPCL fiber meshes (Chapter III) and chitosan scaffolds (Chapter VII) were analyzed before and after *in vitro* degradation by microcomputed tomography (µ-CT). µ-CT was carried out with a high-resolution µ-CT Skyscan 1072 scanner (Skyscan, Kontich, Belgium). Data sets were reconstructed using standardized cone-beam reconstruction software (NRecon v1.4.3, SkyScan). Representative data sets were segmented with a dynamic threshold of 40-255 (grey values) and were used for morphometric analysis (CT Analyser, v1.5.1.5, SkyScan) and to build 3D models (ANT 3D creator, v2.4, SkyScan). The morphometric analysis included porosity, pore interconnectivity, mean pore size and mean fiber thickness. 3D virtual models of representative regions in the bulk of the scaffolds were created and registered using both image processing software (CT Analyser and ANT 3D creator). Further details can be found in Chapters III and VII.

3. *IN VITRO* BIOLOGICAL STUDIES

3.1. Biocompatibility testing

3.1.1. Cell lines

For biocompatibility assessment of the scaffolds studied in Chapter V, two different cell types were used: L929 (ECACC, European Collection of Cell Cultures), a mouse fibroblast cell line commonly used in cytotoxicity screenings, and SaOs-2 (ATCC, American Type Culture Collection), a cell line derived from human osteosarcoma. L929 and osteoblast-like SaOs-2 cell lines were selected because they are a model of a relevant cell type for the medical application of the implant. Both cell lines were cultured in Dulbecco's Modified Eagle's Medium (DMEM), supplemented with 10% fetal bovine serum (Biochrome) and 1% antibiotic/antimicotic solution. In all the experiments cells were kept in an incubator at constant temperature (37 ºC) and CO_2 concentration (5%).

3.1.2. Biocompatibility assays: extracts and cell adhesion studies

Biocompatibility screening was performed according to ISO guidelines. Two categories of *in vitro* cytotoxicity assays were performed to evaluate scaffolds developed in Chapter V: extract and direct contact tests. The scaffolds, previously sterilized by ethylene oxide, were immersed in complete culture medium for 24 h at constant temperature (37 ºC) and agitation (60 rpm). L929 cells were seeded in 96-well cell culture plates (10,000 cells cm^{-2}), in order to reach 80% confluence in 24 h. The extracts were filtered and placed in contact with the monolayer of L929 cells for 72 h. A control, with cells grown in the presence of complete culture medium, was included. Afterwards, the viability test MTT was performed. Briefly, the culture medium was replaced by a solution of MTT and the cells were incubated for 4 h. The viable cells, those with functional mitochondrial dehydrogenase, were able to reduce the yellow MTT into a purple formazan product. The end product was quantified by spectroscopy and the results expressed as percentage of cell viability. In the direct contact test, scaffolds were seeded with L929 cells (8×10^4/50 µl) and with osteoblast-like SaOs-2 cells (5×10^5 cells/ml) for 3 and 7 days. Prior to cell seeding, the chitosan/starch scaffolds were immersed in DMEM culture medium overnight. This step is intended to reduce culture medium uptake by the highly hydrophilic materials.

3.2. Culture of rat bone marrow stromal cells (MSCs) under static and flow perfusion conditions

3.2.1. Isolation, expansion and seeding of rat MSCs

Rat marrow stromal cells (MSCs) were harvested from the tibiae and femora of 41-44 days old (151-175 g) male Wistar rats (Charles River Laboratories, USA) using previously established methods [13]. Briefly, rats were euthanized using 4% isofluorane in CO_2. The leg bones were excised, the soft tissue was removed and the leg bones were placed in Dulbecco's Modified Eagle's Medium (DMEM) supplemented with 200 μg/ml of penicillin streptomycin fungizone antibiotic cocktail (PSF). This concentration of antibiotics is 4 times greater than the normal concentration used in cell culture to avoid contamination during the harvest process. The proximal end of each femur and distal end of each tibia were clipped. An 18-gauge needle was inserted into the hole in the knee joint in each bone, and the bone was flushed with 5 ml of complete osteogenic medium [α-MEM supplemented with 10% fetal bovine serum (FBS) from Cambrex/BioWhittaker (Walkersville, MD, USA), 50 μg/ml gentamicin, 100 μg/ml ampicilin, 10 mM fungizone, 50 μg/ml L-ascorbic acid, 0.01 M β-glycerophosphate, and 10^{-8} M dexamethasone]. The resulting marrow pellet was broken up by trituration, and cell suspensions from all bones were combined in a centrifuge tube. The cells were plated in 75 cm^2 flasks and cultured for 6 days in complete osteogenic media at 37 ºC in a humidified atmosphere of 95% air, 5% CO_2 to allow the expansion of the cells. Medium was changed at 1 and 3 days to remove the non-adherent cell population. In the case of Chapters III and VII, after 6 days, the cells were trypsinized, centrifuged and resuspended in a known amount of medium with 10% dimethyl sulfoxide (DMSO) to obtain a final concentration of $3x10^6$ cells/ml. Cells were aliquoted into cryotubes for storage (~ 1 ml cell suspension/crytube). Each cryotube of cells was stored at -80ºC overnight and then stored in liquid nitrogen. A known amount of cells were thawed and plated in 75 cm^2 culture flasks and cultured until confluence. At the end of this primary culture period, cells were lifted with trypsin solution (0.25% trypsin/0.02% EDTA), centrifuged and resuspended in a known amount of medium. In the case of studies reported on Chapter IV, cells were not frozen. Scaffolds were immersed in complete osteogenic medium overnight and on the following day were press fit into 6 or 8 mm diameter cassettes [for chitosan-based scaffolds (Chapter VII) and SPCL fiber meshes (Chapters III and IV), respectively]. Cassettes were placed into 6-well plates. Then, chitosan-based scaffolds were seeded with 280,000 cells in 100 μl and SPCL fiber meshes were seeded with 500,000 cells in 300 μl of complete osteogenic medium. Cells were allowed to attach for 2-3 hours before adding 10 ml of osteogenic

medium to each well of a 6-well plate. After 24 hours of attachment, the scaffolds were placed in new 6-well plates:

i) for 7 and 15 days with 3 different media conditions: complete osteogenic media with (1) lipase (110 U/L) [14], (2) α-amylase (150 U/L) [9, 14], or (3) without enzymes to study the degradation of SPCL fiber meshes under conditions simulating those found *in vivo*. Media were changed every 3 days. Each group consisted of *n* = 6 samples. This description corresponds to static culture conditions in Chapter III.

ii) static culture condition or in a flow perfusion bioreactor for 7 and 15 days with four different media conditions in the presence of complete osteogenic media (1) without enzymes, with (2) α-amylase (150 U/L) [10], (3) lipase (110 U/L) [14], or (4) α-amylase and lipase in concentrations similar to those found in the human blood serum. Media were changed every 2-3 days. Each group consisted of *n* = 6 samples. These studies were performed with SPCL fiber meshes and are well described in Chapter IV.

iii) for 7, 15, and 20 days with complete osteogenic medium. Media were changed every 3 days. Each group consisted of *n* = 6 samples. Chitosan scaffolds uncoated and coated with CaP and with and without incorporated lysozyme were used in this study. The results of this study are described in Chapter VII.

At the end of each culture period, samples were removed from the cassettes and rinsed with PBS solution. Three samples from each group were stored at -20 ºC in ddH_2O until analyses were performed.

3.2.2. Analysis of cultured scaffolds

3.2.2.1. Confocal and scanning electron microscopy (SEM)

After each time period, SPCL fiber mesh scaffolds were removed from the cassettes, were washed twice in PBS and were immersed in PBS with calcein-AM (Molecular Probes, Invitrogen, USA) for 45min for observation under laser scanning confocal microscopy (Zeiss LSM 510 META, Carl Zeiss, Oberkochen, Germany). Once inside the cells, calcein-AM is hydrolized by endogenous esterase into the highly negatively charged green fluorescent calcein, which is retained inside the cytoplasm.
Other samples were fixed with 2.5% glutaraldehyde for 30 minutes. Then, the scaffolds were washed with PBS and dehydrated in graded series of ethanol, dried by

hexamethyldisilazane, mounted on aluminium stages, sputter with gold, and examined with an FEI Quanta 400 Environmental Scanning Electron Microscope (Hillsboro, OR, USA).

3.2.2.2. DNA analysis

The cells in the constructs were lysed by repeated freeze-thaw cycles in ddH_2O. The DNA content of the lysates was quantified by using a DNA quantification kit (Picogreen, Molecular Probes) and correlated to a known amount of rat marrow stromal cells. Frozen scaffolds were thawed at room temperature, sonicated for 10 minutes, and vortexed to allow cellular DNA into solution. Buffer provided with the kit was diluted with ddH_2O and placed in each well of a 96-well plate at 100 μl/well. DNA standard solutions in ddH_2O in concentrations from 0-6 μg/ml were prepared, and 50 μl of standards/samples were added to each well of the 96-well plate. Picogreen dye solutions were prepared according to the instructions of the manufacturer using reagents provided in the kit and added at 150 μl/well. All these procedures were performed in triplicate. After 10 minutes of incubation in a dark room, the fluorescence at 545 nm was read on a plate reader (FLx800, Bio-Tek Instruments Inc., Winooski, VT, USA) to determine DNA concentrations per scaffold. A conversion factor of 2.7 pg DNA/cell was used to calculate cell number based on MSC standards.

3.2.2.3. Alkaline phosphatase activity

Alkaline phosphatase activity assays were performed on cell lysates using an established protocol [15]. Briefly, all samples were prepared in triplicate and compared against p-nitrophenol standards. For the assay, 96-well plates were used. In each well 80 μl of sample or standard, 20 μl of buffer solution, and 100 μl of substrate solution were added, and the plate was incubated for 1 hour at 37ºC. Each sample and standard was prepared in triplicate. The reaction was stopped by adding 100 μl of stop solution (0.3 N NaOH). The standard curve was generated by preparing dilutions of p-nitrophenol (0-250 μM). Absorbance was read at 405 nm on a plate reader (PowerWave x340; Bio-Tek Inc., Winooski, VT, USA) to determine the alkaline phosphatase activity per scaffold.

3.2.2.4. Calcium deposition measurements

Calcium content in the scaffolds was measured by using a Calcium Kit (Diagnostic Chemical Limited). After the ALP and DNA assays, a volume of 1N acetic acid equal to the volume remaining in each well was added to each sample (final concentration of 0.5N), and the plate was placed on an orbital shaker overnight. A volume of 300 μl of calcium assay reagent was added to 20 μl of sample solution in triplicate in 96-well plates. To generate a standard curve, serial dilutions of calcium chloride ($CaCl_2$) were prepared (0-50 μg/ml).

Absorbance was read at 650 nm in a spectrophotometric plate reader (FLx800, Bio-Tek Instruments Inc., Winooski, VT, USA). The calcium deposition in each scaffold is reported as $\mu g\ Ca^{2+}$.

3.2.2.5. Fourier transformed infrared spectroscopy with attenuated total reflectance (FTIR-ATR)

The cell/scaffold constructs after 16 days of culture were analysed by FTIR-ATR. The scaffolds were fixed in 2.5% glutaraldehyde, dehydrated in a graded series of ethanol and dried at room temperature. All spectra were recorded using 64 scans and 4 cm^{-1} in a FTIR spectrophotometer (IR Prestige-21 Fourier transform infrared spectrometer, Shimadzu).

3.2.2.6. Histology (H&E, von Kossa staining and tetracycline fluorescence)

Light microscopy analysis was used to evaluate the morphological appearance and infiltration of the bone marrow stromal cells and deposited matrix. Cultured samples were rinsed with PBS, fixed in 10% formalin solution and embedded in HistoPrep freezing medium (Fisher Scientific, Pittsburgh, PA, USA). Frozen sections of ~10-15 μm thickness were obtained using a cryostat (HM500, Microm, Walldorf, Germany) operating at -23 ºC and mounted onto Superfrost Plus glass slides (Fisher Scientific, Pittsburgh, PA, USA) and stained with hematoxylin and eosin (H&E) for histological evaluation. For visualization of mineralized tissue, additional sections were exposed to 5% silver nitrate solution under UV for 25 min and counterstained with 0.5% safranin O solution. Von Kossa stained sections were observed using a light microscope (Eclipse E600; Nikon, Melville, NY) and attached video camera (3CCD Color Video Camera DXC-950P; Sony, Park Ridge, NJ). Mineral deposition was also visualized in unstained sections under fluorescent light after adding tetracycline-HCl to the culture media at final concentration of 10 μg/mL [1, 16]. All the histological sections, except von Kossa stained sections were visualized using Olympus BX61 Motorized System Microscope and attached video camera Olympus DP70 equipped with a fluorescence lamp.

4. *IN VIVO* STUDIES

4.1. Implant preparation

In Chapter VIII, scaffolds with 5 mm diameter and approximately 1.5 mm thick were used. All scaffolds were sterilized by ethylene oxide gas for 14 h prior to implantation. One day before subcutaneous implantation surgery, the implants were removed from sterile bags and prewetted in phosphate buffered saline (PBS) solution in 24-well plates overnight under sterile conditions. The different experimental conditions evaluated *in vivo* were: chitosan scaffolds (Ch), chitosan/starch scaffolds (CS), CaP chitosan scaffolds (CaPCH), CaP chitosan/starch scaffolds (CaPCS), CaP chitosan scaffolds with incorporated lysozyme (CaPCH + lysozyme) and CaP chitosan/starch scaffolds with incorporated lysozyme (CaPCS + lysozyme).

4.2. Subcutaneous implantation

All animal manipulations were approved by Rice University's Institutional Animal Care and Use Comitee. Twenty four male Wistar rats 41-44 days old (Charles River Laboratories, USA) were used for subcutaneous implantation of acellular scaffolds. Three implantation periods were used: 3, 6 and 12 weeks. Animals were anesthetized with a 4% isoflurane/oxygen mixture, which was reduced to 2% during surgical manipulation. The rats were monitored to ensure that an appropriate surgical plane of anesthesia was maintained. Previously, the dorsum of the rat was shaved. Then, the animals were placed in a ventral position, the backs clipped and disinfected with povidone-iodine and six small longitudinal incisions were made. A pocket was created on each incision using blunt dissection, and one scaffold was placed in each pocket. One implant from each experimental condition was implanted in twenty four rats (six implants per rat). Each rat received 6 implants, 1 from each experimental group. A total number of 8 scaffolds per experimental group per time point were implanted. Previous studies reported successfully implantation of 6 materials in rat dorsal subcutaneous pockets using Wistar rats with similar or lower size [17-20]. The incisions have been closed with Vicryl 5-0 sutures. Each animal received a subcutaneous injection of sterile saline to aid post-operative recovery (1 ml/100 g/hour of anesthesia). Each animal received also a subcutaneous injection of buprenorphine (0.025 mg/kg) 8-12 hours after surgery. On the following day, two additional doses of buprenorphine (0.025 mg/kg) have been injected for continued post-operative analgesia (i.e. at 20-24 and 32-36 hours post-op). Once animals become active they returned to their cages. Animals were placed one per cage with water and food ad libitum. At each time point, animals were anesthetized by isoflurane inhalation

and euthanized with carbon dioxide inhalation. The implants were retrieved after a bilateral thoracotomy has been performed to ensure death.

4.3. Preparation of specimens for weight loss measurements and µ-CT

After each implantation time, three scaffolds of each group condition were subjected to a decellularization process for weight loss measurement and micro-computed tomography analysis. Briefly, the scaffolds were immersed in ddH_2O and placed in 24-well plate at -20 ºC. After that, scaffolds underwent three freeze/thaw cycles in liquid nitrogen and in a 37 ºC water bath, respectively, to disrupt attached cells and remove cellular debris [15]. After this process scaffolds were air-dried in a laminar flow hood.

4.4. Histological analysis

After euthanasia, the implants were retrieved along with the surrounding tissue and histologically processed. Five specimens of each group condition per time point were fixed in 10% neutral buffered formalin until further processing. The specimens were dehydrated in graded series of ethanol, immersed in infiltration solutions, embedded in Technovit glycol methacrylate (kit 8100, Heraeus Kulzer, EBSciences, CO) and subsequently polymerized. Three specimens of each group condition per time period were cut to obtain longitudinal sections and two specimens were cut to obtain transverse sections of 7 µm thickness using a modified microtome equipped with a tungsten blade (Leica RM 2155).

Sections were stained with H&E to evaluate the *in vivo* degradation, formation of pores and infiltration of cells through the implants. For visualization of the CaP coating, additional sections were exposed to 5% silver nitrate solution under UV for 25 min and counterstained with 0.5% safranin O solution (von Kossa staining). All images were obtained using Olympus BX61 Motorized System Microscope and attached video camera Olympus DP70. Histological sections from all time points were scored by three observers (AMM, ARP and CMA) blinded for group conditions and implantation time, and reached consensus on the final score. The cellular ingrowth within the implants and the degradation of each sample was qualitatively scored based on dissolution, cracks, fragmentation on a scale modified from De Jong as shown in Table 1 [21].

Table 1. Histological grading scale for degradation and cellular growth within the implants. (Adapted from De Jong *et al.* [21])

Scoring category	Response	Score
Cellular growth within implant	Abundance presence of cells and fibrous tissue around all fragments	4
	Marked presence of cells and/or formation of fibrous tissue around most fragments	3
	Moderate presence of cells in cracks of implant and/or formation of fibrous tissue around fragments of implant	2
	Minimal presence of cells within cracks of the implant (some cells present with or without connective tissue formation)	1
Degradation	Abundant degradation of implant with (almost) complete fragmentation	4
	Marked degradation of implant with presence of several fragments	3
	Moderate degradation of implant with cracks in implant and/or some fragments	2
	Minimal degradation of implant, some minor dissolution on edges, cracks in implant and/or small fragment present	1

5. STATISTICS

Results of DNA, ALP, and calcium assay in Chapters III and VII and weight loss results in Chapter VI are expressed as mean ± standard deviation with $n = 3$ for each group. Statistical significance of differences was determined using Student's t-test multiple comparison procedure at a confidence interval of 95% ($p < 0.05$).

Results of DNA, ALP, and calcium assay in Chapter IV and results of weight loss and μ-CT analysis in Chapter VIII are expressed as mean ± standard deviation with $n = 3$ for each group. Also, results of histological scoring are expressed as means ± standard deviation with $n = 4$-5 for each group. Single factor analysis of variance (ANOVA) was used to determine statistical significance within a data set. If ANOVA detected a significant difference within the data set, Tukey's honestly significantly different (HSD) multiple comparison test was used to determine significant differences between groups and conditions. All tests were conducted with confidence interval of 95% ($p < 0.05$).

REFERENCES

1. Gomes ME, Sikavitsas VI, Behravesh E, Reis RL, Mikos AG. Effect of flow perfusion on the osteogenic differentiation of bone marrow stromal cells cultured on starch-based three-dimensional scaffolds. J Biomed Mater Res A 2003 Oct 1;67(1):87-95.

2. Martins AM, Pham QP, Malafaya PB, Sousa RA, Gomes ME, Raphael RM, et al. The Role of Lipase and alpha-Amylase in the Degradation of Starch/Poly(epsilon-Caprolactone) Fiber Meshes and the Osteogenic Differentiation of Cultured Marrow Stromal Cells. Tissue Eng Part A 2009 Aug 23;15(2):295-305

3. Gomes ME, Bossano CM, Johnston CM, Reis RL, Mikos AG. In vitro localization of bone growth factors in constructs of biodegradable scaffolds seeded with marrow stromal cells and cultured in a flow perfusion bioreactor. Tissue engineering 2006 Jan;12(1):177-188.

4. Gomes ME, Holtorf HL, Reis RL, Mikos AG. Influence of the porosity of starch-based fiber mesh scaffolds on the proliferation and osteogenic differentiation of bone marrow stromal cells cultured in a flow perfusion bioreactor. Tissue engineering 2006 Apr;12(4):801-809.

5. Tuzlakoglu K, Alves CM, Mano JF, Reis RL. Production and characterization of chitosan fibers and 3-D fiber mesh scaffolds for tissue engineering applications. Macromol Biosci 2004 Aug 9;4(8):811-819.

6. Abe Y, Kokubo T, Yamamuro T. Apatite Coating on Ceramics, Metals and Polymers Utilizing a Biological Process. J Mater Sci-Mater M 1990 NOV;1(4):233-238.

7. Reis RL, Cunha AM, Fernandes MH, Correia RN. Treatments to induce the nucleation and growth of apatite-like layers on polymeric surfaces and foams. J Mater Sci Mater Med 1997 Dec;8(12):897-905.

8. Oliveira AL, Elvira C, Reis RL, Vazquez B, San Roman J. Surface modification tailors the characteristics of biomimetic coatings nucleated on starch-based polymers. J Mater Sci Mater Med 1999 Dec;10(12):827-835.

9. Azevedo HS, Gama FM, Reis RL. In vitro assessment of the enzymatic degradation of several starch based biomaterials. Biomacromolecules 2003 Nov-Dec;4(6):1703-1712.

10. Chawla JS, Amiji MM. Biodegradable poly(epsilon -caprolactone) nanoparticles for tumor-targeted delivery of tamoxifen. Int J Pharm 2002 Dec 5;249(1-2):127-138.

11. Hankiewicz J, Swierczek E. Lysozyme in human body fluids. Clin Chim Acta 1974 Dec 17;57(3):205-209.

12. Nordtveit RJ, Varum KM, Smidsrod O. Degradation of partially N-acetylated chitosans with hen egg white and human lysozyme. Carbohydrate Polymers 1996 Feb;29(2):163-167.

13. Maniatopoulos C, Sodek J, Melcher AH. Bone formation in vitro by stromal cells obtained from bone marrow of young adult rats. Cell Tissue Res 1988 Nov;254(2):317-330.

14. Junge W, Troge B, Klein G, Poppe W, Gerber M. Evaluation of a new assay for pancreatic amylase: performance characteristics and estimation of reference intervals. Clin Biochem 1989 Apr;22(2):109-114.

15. Datta N, Holtorf HL, Sikavitsas VI, Jansen JA, Mikos AG. Effect of bone extracellular matrix synthesized in vitro on the osteoblastic differentiation of marrow stromal cells. Biomaterials 2005 Mar;26(9):971-977.

16. Sikavitsas VI, Bancroft GN, Mikos AG. Formation of three-dimensional cell/polymer constructs for bone tissue engineering in a spinner flask and a rotating wall vessel bioreactor. J Biomed Mater Res 2002 Oct;62(1):136-148.

17. Yoshikawa T, Ohgushi H, Akahane M, Tamai S, Ichijima K. Analysis of gene expression in osteogenic cultured marrow/hydroxyapatite construct implanted at ectopic sites: a comparison with the osteogenic ability of cancellous bone. J Biomed Mater Res 1998 Sep 15;41(4):568-573.

18. Nishikawa M, Myoui A, Ohgushi H, Ikeuchi M, Tamai N, Yoshikawa H. Bone tissue engineering using novel interconnected porous hydroxyapatite ceramics combined with marrow mesenchymal cells: quantitative and three-dimensional image analysis. Cell transplantation 2004;13(4):367-376.

19. Uemura T, Dong J, Wang Y, Kojima H, Saito T, Iejima D, et al. Transplantation of cultured bone cells using combinations of scaffolds and culture techniques. Biomaterials 2003 Jun;24(13):2277-2286.

20. Oliveira JM, Kotokuki N, Tadokoro M, Hirose M, Mano JF, Reis RL, et al. Ex Vivo Culturing of Rat Bone Marrow Stromal Cells with Dexamethasone-loaded Carboxymethylchitosan/Poly(amidoamine) Dendrimer Nanoparticles Enhances Ectopic Bone Formation on Tissue Engineered Constructs. submitted 2008.

21. De Jong WH, Eelco Bergsma J, Robinson JE, Bos RR. Tissue response to partially in vitro predegraded poly-L-lactide implants. Biomaterials 2005 May;26(14):1781-1791.

SECTION 3

CHAPTER III

The Role of Lipase and α-Amylase in the Degradation of Starch/Poly(ε-Caprolactone) Fiber Meshes and the Osteogenic Differentiation of Cultured Marrow Stromal Cells

CHAPTER III

The Role of Lipase and α-Amylase in the Degradation of Starch/Poly(ε-Caprolactone) Fiber Meshes and the Osteogenic Differentiation of Cultured Marrow Stromal Cells[1]

ABSTRACT

The present work studies the influence of hydrolytic enzymes (α-amylase or lipase) on both the degradation of fiber mesh scaffolds based on a blend of starch with poly(ε-caprolactone) (SPCL) and the osteogenic differentiation of rat marrow stromal cells (MSCs) and subsequent formation of extracellular matrix (ECM) on these scaffolds under static culture conditions. The biodegradation profile of SPCL fiber meshes was investigated using enzymes that are specifically responsible for the enzymatic hydrolysis of SPCL using concentrations similar to those found in human serum. These degradation studies were performed using both static and dynamic conditions. After several degradation periods (3, 7, 14, 21, and 30 days) weight loss measurements and micro-Computed Tomography (μ-CT) analysis (specifically porosity, interconnectivity, mean pore size and fiber thickness) were performed. The SPCL scaffolds were seeded with rat MSCs and cultured for 8 and 16 days using complete osteogenic media with and without enzymes (α-amylase or lipase). Results indicate that culture medium supplemented with enzymes enhanced cell proliferation after 16 days of culture as compared with samples cultured without enzymes. With respect to the calcium content of the constructs, no calcium was detected in scaffolds cultured with α-amylase or without enzymes after each time period. However, SPCL scaffolds cultured with lipase presented calcium deposition after the 8th day, showing a significant increase at the 16th day. Lipase appears to positively influence osteoblastic differentiation of rat MSCs and to enhance matrix mineralization. Furthermore, scanning electron microscopy images showed that the enzymes do not have a deleterious effect on the 3D structure of SPCL fiber meshes, meaning that the scaffolds after 16 days did not lose their structural integrity. Confocal micrographs have shown cells to be evenly distributed and infiltrated within the SPCL fiber meshes up to 410 μm from the surface. This study demonstrates that supplementation of

[1]This chapter is based on the following publication:

A.M. Martins, Q.P. Pham, P.B. Malafaya, R.A. Sousa, M.E. Gomes, R.M. Raphael, F.K. Kasper, R.L. Reis, and A.G. Mikos. The Role of Lipase and α-Amylase in the Degradation of Starch/Poly(ε-Caprolactone) Fiber Meshes and the Osteogenic Differentiation of Cultured Marrow Stromal Cells. Tissue Engineering: Part A, 15, 295-305 (2009).

culture media with lipase holds great potential for the generation of bone tissue engineering constructs from MSCs seeded onto SPCL fiber meshes, as lipase enhances the osteoblastic differentiation of the seeded MSCs and promotes matrix mineralization without deleteriously affecting the structural integrity of the meshes over 16 days of culture.

1. INTRODUCTION

Tissue engineering, as it was defined by Langer and Vacanti (1) in 1993, “is an interdisciplinary field of research that applies the principles of engineering and the life sciences towards the development of biological substitutes that restore, maintain or improve tissue function.” Specific tissue engineering applications, such as bone regeneration, often need a temporary scaffold with a three-dimensional architecture to support tissue growth. The ideal scaffold should be biodegradable and bioresorbable to support the growth of new bone. The scaffold degradation rate should complement the growth rate of the new bone in a manner that, by the time the defect/injury site is completely regenerated, the scaffold is totally degraded (1, 2). Biodegradable materials have the capacity to temporarily mimic the original structural function of the tissue and to degrade by controlled mechanisms into products easily eliminated by the body’s metabolic pathways (3). In this perspective, we used enzymes present in human serum that are responsible for the enzymatic degradation of starch and poly(ε-caprolactone) (SPCL) (α-amylase and lipase, respectively) in order to simulate conditions found *in vivo*. In this study, we used SPCL, a blend of starch with poly(ε-caprolactone). Starch itself is one of the most abundant naturally occurring polymers, presenting a combination of attractive properties that is increasingly advancing its use in a variety of applications. Starch-based biomaterials are biocompatible (4, 5) and biodegradable (6, 7). Studies with starch-based scaffolds showed that their degradation products do not have a negative effect on human osteosarcoma cells (SaOS-2 cell line) (8). Previous studies with SPCL fiber meshes have also shown that these scaffolds were able to support the attachment, proliferation and differentiation of bone marrow stromal cells (MSCs) (9, 10). Biomaterials based on starch degrade by α-amylase. In principle, the *in vivo* resorption rate of blends based on starch can be regulated by controlling the percentage of starch in the material, preferentially attacked by enzymatic hydrolysis.

PCL is a biodegradable aliphatic polyester currently used in an array of biomedical applications. Several studies have reported that PCL is degraded by lipase (11-14). Lipases are water-soluble enzymes that hydrolyze ester bonds of water soluble substrates such as triglycerides, phospholipids and cholesteryl esters (15, 16). The lipase gene family consists

of multiple lipases that share a similar sequence structure at the genetic and protein level thus indicating a common ancestral origin. However, these lipases have disparate and organ specific expression, indicating that they may have evolved relatively specific roles. The human lipases include the pre-duodenal lingual and gastric lipase and the extra-duodenal pancreatic, hepatic, lipoprotein (LPL) and endothelial lipase (17). The pancreatic, hepatic, lipoprotein and endothelial lipase are members of the lipase gene family (17). Lipoprotein lipase has been described as a marker of adipogenic differentiation (18-20). Serum lipase is mainly derived from pancreatic cells, while other sources in the human body are the digestive track, adipose tissue, lung, milk and leucocytes (3, 21). Several authors have described different enzymatic effects of lipase on PCL using species of lipase obtained from diverse sources (12, 13). The experimental results obtained with lipase seem to be influenced by enzyme characteristics such as source and specificity. Some studies have also reported that the biodegradation rate of PCL depends on the shape and inherent surface/volume ratio of the PCL substrate, with films being slowly degraded, while nano/microparticles are very quickly degraded (13).

Previous studies using static and dynamic (flow perfusion bioreactor) culture conditions for rat marrow stromal cells on SPCL fiber meshes have shown that flow perfusion conditions enhance differentiation of marrow stromal cells with subsequent formation of a bone-like extracellular matrix (9, 10). Holtorf *et al.* (22) showed that flow perfusion culture induced osteoblastic differentiation of rat marrow stromal cells seeded on scaffolds, even in the absence of dexamethasone (a glucocorticoid media supplement that promotes osteoblastic differentiation of bone marrow stromal cells in culture).

In this work we propose a novel approach, using static cultures and complete osteogenic media supplemented with enzymes to study simultaneously the influence of α-amylase and lipase on the degradation of SPCL fiber meshes as a function of immersion time and on the osteodifferentiation of rat marrow stromal cells.

This work intends to mimic *in vitro* the *in vivo* degradation of the SPCL fiber meshes using enzymes responsible for their degradation at the same concentrations as those found in human serum. Besides characterizing the susceptibility of SPCL fiber meshes to enzymatic degradation, this study aims also to investigate the osteogenic differentiation of rat marrow stromal cells (MSCs) and subsequent formation of extracellular matrix (ECM) under static conditions in the presence of hydrolytic enzymes (lipase or α-amylase). By seeding rat MSCs onto SPCL fiber meshes and culturing them under static conditions using osteogenic media supplemented with lipase and α-amylase enzymes, we aimed to answer the following

questions: 1) What is the role of lipase and α-amylase in the degradation of SPCL fiber mesh scaffolds? 2) Is the integrity of SPCL fiber mesh scaffolds rapidly compromised by enzymatic degradation, and if so, which enzyme is the most influential? 3) Is there any effect of α-amylase and lipase on the osteogenic differentiation of rat marrow stromal cells?

2. MATERIALS AND METHODS

2.1. Scaffolds preparation and characterization

Porous scaffolds used in this study were based on a blend of corn starch and poly (ε-caprolactone) (SPCL, 30/70 %) prepared by a fiber bonding technique (9). Scaffolds were cylinders with 8 mm diameters and heights of 1-1.5 mm. Prior to cell seeding, scaffolds were sterilized by ethylene oxide gas for 14 hours. All chemical reagents were purchased from Sigma (St. Louis, MO) unless otherwise specified.

2.2. Degradation tests

Serum α-amylase and serum lipase in healthy adults are in range of 46-244 U/L (3, 23) and 30-190 U/L (3, 24), respectively. Degradation studies were carried out by incubating samples in phosphate buffered saline (PBS) solution (0.1M, pH 7.4) containing α-amylase (150 U/L) (3, 23) from *Baccillus sp.* or lipase (110 U/L) (3, 24) from *Aspergillus niger*, both concentrations similar to those found in human serum, and sodium azide (0.2%), to avoid contaminations, at 37ºC up to 30 days under static and dynamic conditions (shaker at 70 rpm). The studies were performed in triplicate. The enzymatic degradation solutions were changed every 7 days to restore the original level of enzymatic activity. At the end of the degradation period, the samples were removed, washed thoroughly with distilled water and dried in a graded series of ethanol for later calculation of weight loss (1).

$$(1)\quad \text{Weight loss (\%)} = \frac{\text{Initial weight} - \text{Final weight}}{\text{Initial weight}}$$

2.3. Micro-Computed Tomography (μ-CT)

The scaffolds (*n*=3) were analysed using micro-Computed Tomography (μ-CT) before and after degradation with both enzymes (lipase or α-amylase) for the different periods of immersion (0, 3, 14 and 21 days) in both static and dynamic conditions. μ-CT was carried out with a high-resolution μ-CT Skyscan 1072 scanner (Skyscan, Kontich, Belgium) using a resolution of pixel size of 8.79 μm and integration time of 1.9 ms. The X-ray source was set at 40 keV of energy and 250 μA of current. Approximately 400 projections were acquired over a rotation range of 180° with a rotation step of 0.45°. Data sets were reconstructed using standardized cone-beam reconstruction software (NRecon v1.4.3, SkyScan). The output format for each sample was 300 serial 1024x1024 bitmap images. Representative data sets of 200 slices were segmented into binary images with a dynamic threshold of 40-255 (grey values) and were used for morphometric analysis (CT Analyser, v1.5.1.5, SkyScan) and to build 3D models (ANT 3D creator, v2.4, SkyScan). The morphometric analysis included porosity, pore interconnectivity, mean pore size and mean fiber thickness. 3D virtual models of representative regions in the bulk of the scaffolds were created, visualized and registered using both image processing softwares (CT Analyser and ANT 3D creator).

2.4. Isolation and expansion of rat bone marrow stromal cells

Rat marrow stromal cells (MSCs) were harvested from the tibiae and femora of 41-44 days old (151-175 g) male Wistar rats (Charles River Laboratories, USA) using established methods (25). Briefly, rats were euthanized using 4% isofluorane in CO_2. The leg bones were excised, the soft tissue was removed and the leg bones were placed in Dulbecco's Modified Eagle's Medium (DMEM) supplemented with 200 μg/ml of penicillin streptomycin fungizone antibiotic cocktail (PSF). This concentration of antibiotics is 4 times greater than the normal concentration used in cell culture to avoid contamination during the harvest process. The proximal end of each femur and distal end of each tibia were clipped. An 18-gauge needle was inserted into the hole in the knee joint in each bone, and the bone was flushed with 5 ml of complete osteogenic medium [α-MEM supplemented with 10% fetal bovine serum (FBS) from Cambrex/BioWhittaker (Walkersville, MD), 50 μg/ml gentamicin, 100 μg/ml ampicilin, 10 mM fungizone, 50 μg/ml L-ascorbic acid, 0.01 M β-glycerophosphate, and 10^{-8} M dexamethasone]. The resulting marrow pellet was broken up by trituration, and cell suspensions from all bones were combined in a centrifuge tube.

The cells were plated in 75 cm^2 flasks and cultured for 6 days in complete osteogenic media at 37 ºC in a humidified atmosphere of 95% air, 5% CO_2 to allow the expansion of the cells. Medium was changed at 1 and 3 days to remove the non-adherent cell population. After 6 days, the cells were trypsinized, centrifuged, resuspended in a known amount of medium and 10% dimethyl sulfoxide (DMSO) to obtain a final concentration of $3x10^6$ cells/ml. Cells were aliquoted into cryotubes for storage (~ 1 ml cell suspension/ crytube). Each cryotube of cells was stored at -80ºC overnight and then stored in liquid nitrogen.

2.5. Cell seeding

A known amount of cells were thawed and plated in 75 cm^2 culture flasks and cultured until confluence. At the end of this primary culture period, cells were lifted with trypsin solution (0.25% trypsin/0.02% EDTA), centrifuged and resuspended in a known amount of medium.

SPCL fiber mesh scaffolds were immersed in complete osteogenic medium overnight and were pressed fit into 8 mm diameter cassettes on the following day. Cassettes were placed into 6-well plates. Then, SPCL scaffolds were seeded with 500,000 cells in 300 μl of complete osteogenic medium. Cells were allowed to attach for 3 hours before adding 10 ml of osteogenic medium to each well of a 6-well plate. After 24 hours of attachment, the scaffolds were placed in new 6-well plates for 7 and 15 days with 3 different media conditions: complete osteogenic media with (1) lipase (110 U/L), (2) α-amylase (150 U/L), or (3) without enzymes to study the degradation of SPCL fiber meshes under conditions simulating those found *in vivo*. Media were changed every 3 days. Each group consisted of *n* = 6 samples.

2.6. DNA analysis

The cells in the cell/scaffold constructs were lysed by freeze-thaw in ddH_2O. The DNA content of the lysates was quantified by using a DNA quantification kit (Picogreen, Molecular Probes) and correlating to a known amount of rat marrow stromal cells. Frozen scaffolds were thawed at room temperature, sonicated for 10 minutes, and vortexed to allow cellular DNA into solution. Buffer provided with the kit was diluted with ddH_2O and placed in each well of a 96-well plate at 100 μl/well. DNA standard solutions in ddH_2O in concentrations from 0-6 μg/ml were prepared, and 50 μl of standards/samples were added to each well of the 96-well plate. Picogreen dye solutions were prepared according the instructions of the

manufacturer using reagents provided in the kit and added at 150 μl/well. All these procedures were performed in triplicate. After 10 minutes of incubation in a dark room, the fluorescence at 545 nm was read on a plate reader (FLx800, Bio-Tek Instruments Inc., Winooski, Vermont) to determine DNA concentrations per scaffold. A conversion factor of 2.7 pg DNA/cell was used to calculate cell number based on MSC standards.

2.7. Alkaline phosphatase activity

Alkaline phosphatase (ALP) activity was determined using an established protocol (26) by measuring the conversion of *p*-nitrophenylphosphate to *p*-nitrophenol. All reagents were purchased from Sigma (St. Louis, MO). For the assay, 96-well plates were used. In each well 80 μl of sample or standard, 20 μl of buffer solution, and 100 μl of substrate solution were added, and the plate was incubated for 1 hour at 37ºC. Each sample and standard was prepared in triplicate. The reaction was stopped by adding 100 μl of stop solution (0.3 N NaOH). The standard curve was generated by preparing dilutions of *p*-nitrophenol (0-250 μM). Absorbance was read at 405 nm on a plate reader to determine enzyme concentration per construct.

2.8. Calcium deposition measurement

Calcium content in the SPCL fiber mesh scaffolds was measured by using a Calcium Kit (Diagnostic Chemical Limited). After the ALP and DNA assays, a volume of 1N acetic acid equal to the volume remaining in each well was added to each well (final concentration of 0.5N), and the plate was placed on an orbital shaker overnight. A volume of 300 μl of calcium assay reagent was added to 20 μl of sample solution in triplicate in 96-well plates. To generate a standard curve, serial dilutions of $CaCl_2$ were prepared (0-50 μg/ml). Absorbance was read at 650 nm in a spectrophotometric plate reader. The calcium deposition in each scaffold is reported as μg Ca^{2+}.

2.9. Microscopic analysis

After each time period, SPCL fiber mesh scaffolds were removed from the cassettes, washed with PBS and stained with calcein-AM (Molecular Probes) according to the manufacturer's instructions. To visualize the distribution of cells within the scaffolds, after 45

minutes of immersion in PBS with calcein-AM, images were recorded using a laser scanning confocal microscope with a 10X APO objective (Zeiss LSM 510 Axiovert, Carl Zeiss, Germany). Depth projections of the surface (up to 410 μm) were obtained and the cells were colored as a function of their distance from the surface.

Scanning electron microscopy (SEM) was used to evaluate the morphological appearance of the rat bone marrow cells. Samples for SEM analysis were washed twice in PBS and fixed with 2.5% glutaraldehyde for 30 minutes. Then, the scaffolds were washed with PBS and dehydrated in a graded series of ethanol, and dried by hexamethyldisilazane.

2.10. Fourier transformed infrared spectroscopy with attenuated total reflectance (FTIR-ATR)

The cell/scaffold constructs after 16 days of culture were analysed by FTIR-ATR. The scaffolds were fixed in 2.5% glutaraldehyde, dehydrated in a graded series of ethanol and dried at room temperature. All spectra were recorded using 64 scans and 4 cm^{-1} in a FTIR spectrophotometer (IR Prestige-21 Fourier transform infrared spectrometer, Shimadzu).

2.11. Statistics

Results of DNA, ALP, and calcium assay are expressed as mean ± standard deviation with n=3 for each group. Statistical significance of differences was determined using Student's t-test multiple comparison procedure at a confidence interval of 95% ($p < 0.05$).

3. RESULTS AND DISCUSSION

3.1. Degradation studies

The main aims of the degradation studies were to simulate physiological conditions using enzymes present in human serum that would be responsible for enzymatic hydrolysis of SPCL fiber mesh scaffolds *in vivo*, to control and tailor the degradation rate of the SPCL scaffolds, and finally to evaluate the possibility of increasing their porosity and pore interconnectivity through degradation.

SPCL is a blend of starch with poly(ε-caprolactone). In this study, scaffolds based on SPCL were prepared by a fiber bonding process that uses heat to promote the bonding of the fibers previously obtained by melt-spinning (9).

When analysing weight loss profiles using α-amylase and lipase, few differences were observed between static and dynamic conditions for each enzyme (Figure 1). One of the enzymes responsible for starch hydrolysis is α-amylase. The scaffolds immersed in α-amylase presented the highest weight loss as compared with lipase. In presence of this enzyme it was observed after 3 days a weight loss of approximately 25%, which slightly increases to 30% weight loss upon 30 days of immersion (Figure 1). Nevertheless, immersion periods up to 30 days did not cause the scaffolds to lose their structural integrity. These observed results are in agreement with previous studies using α-amylase (3, 7).

Lipase is an enzyme responsible for hydrolysis of ester bonds in polyesters, and some studies have shown that lipase enhances PCL degradation (7, 27, 28). PCL is a hydrophobic crystalline polymer that degrades very slowly *in vitro* in the absence of enzymes and *in vivo* as well. The *in vitro* degradation can be enhanced in the presence of the enzyme lipase (28). The values of weight loss in the presence of lipase are not so pronounced compared with those obtained in presence of α-amylase but these values are in agreement with other studies (27). Weight loss remains constant up to 21 days, slightly increasing after afterward (Figure 1). The enzymatic degradation of PCL by lipase has been reported by several studies (11-14, 29). It is apparent from Figure 1 that the degradation of SPCL occurs in the presence of lipase, this enzyme being responsible for only 7.7 ± 1.6 % weight loss after 30 days of immersion under dynamic conditions. These results are in accordance with several published studies (12, 13). Hoshino *et al.* (12) showed the influence of different commercially available lipases on degradation of PCL. They presented the results of biodegradability of PCL films after 100 days incubation at 37º C and some commercial lipase species were able to degrade PCL completely, namely from *alcaligenes sp*., *Rhizopus niveus*, *Rhizopus oryzae*, *Chromobacterium viscosum* and *Candida rugosa*. However, they presented different results with other lipases that showed values of weight loss below 5%, as when using the same lipase employed in this study - *Aspergillus niger.* These results are in accordance with the weight loss after 30 days reported here. In contrast to its slow hydrolytic degradation, other studies with PCL showed high values of weight loss during enzymatic degradation when using *Pseudomonas cepacia* lipase, which has a specific activity on PCL segment degradation (14).

It is obvious that α-amylase and lipase contributed to different degrees to the degradation of the SPCL fiber mesh scaffolds and the studies presented here with α-amylase show that this enzyme is responsible for higher values of weight loss as compared to the ones obtained with lipase (Figure 1).

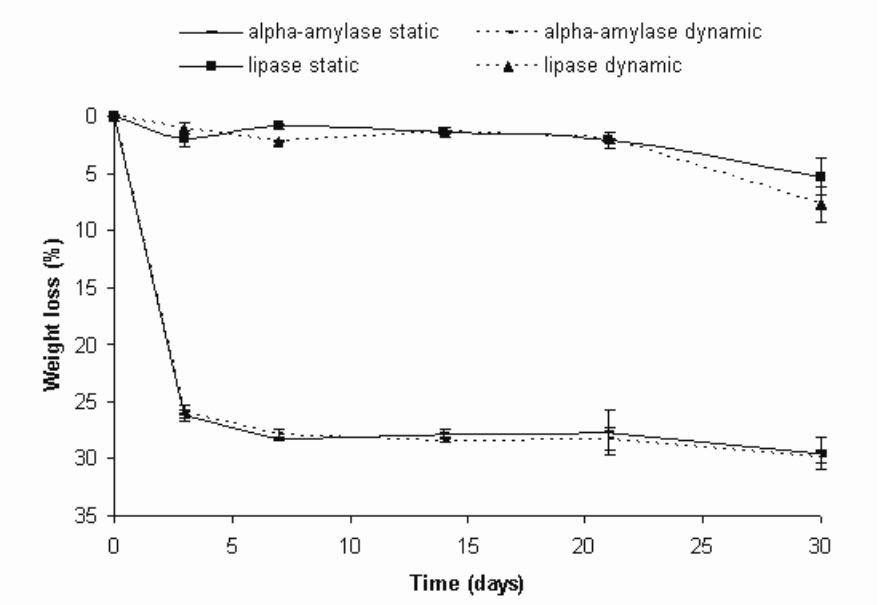


Figure 1. Weight loss profile (pH 7.4, 37ºC) of SPCL fiber mesh scaffolds using α-amylase (150 U/L) and lipase (110 U/L) under static and dynamic conditions up to 30 days.

The morphological changes induced by degradation with these enzymes can be further confirmed by virtual 3D models obtained by μ-CT, where it can be seen that SPCL fiber mesh scaffolds were affected by α-amylase and lipase (Figure 2). However, as confirmed by weight loss results, α-amylase had a great effect in SPCL fiber meshes mainly at day 21 (Figure 2K) and day 30 (Figure 2F and 2L). In Figure 3, it is possible to observe the 3D virtual models obtained by μ-CT as a function of immersion time in PBS using lipase solution. The effect of lipase is not so pronounced as compared with images obtained after degradation with α-amylase, nevertheless slight changes in SPCL fiber meshes were observed as a function of immersion time (Figure 3).

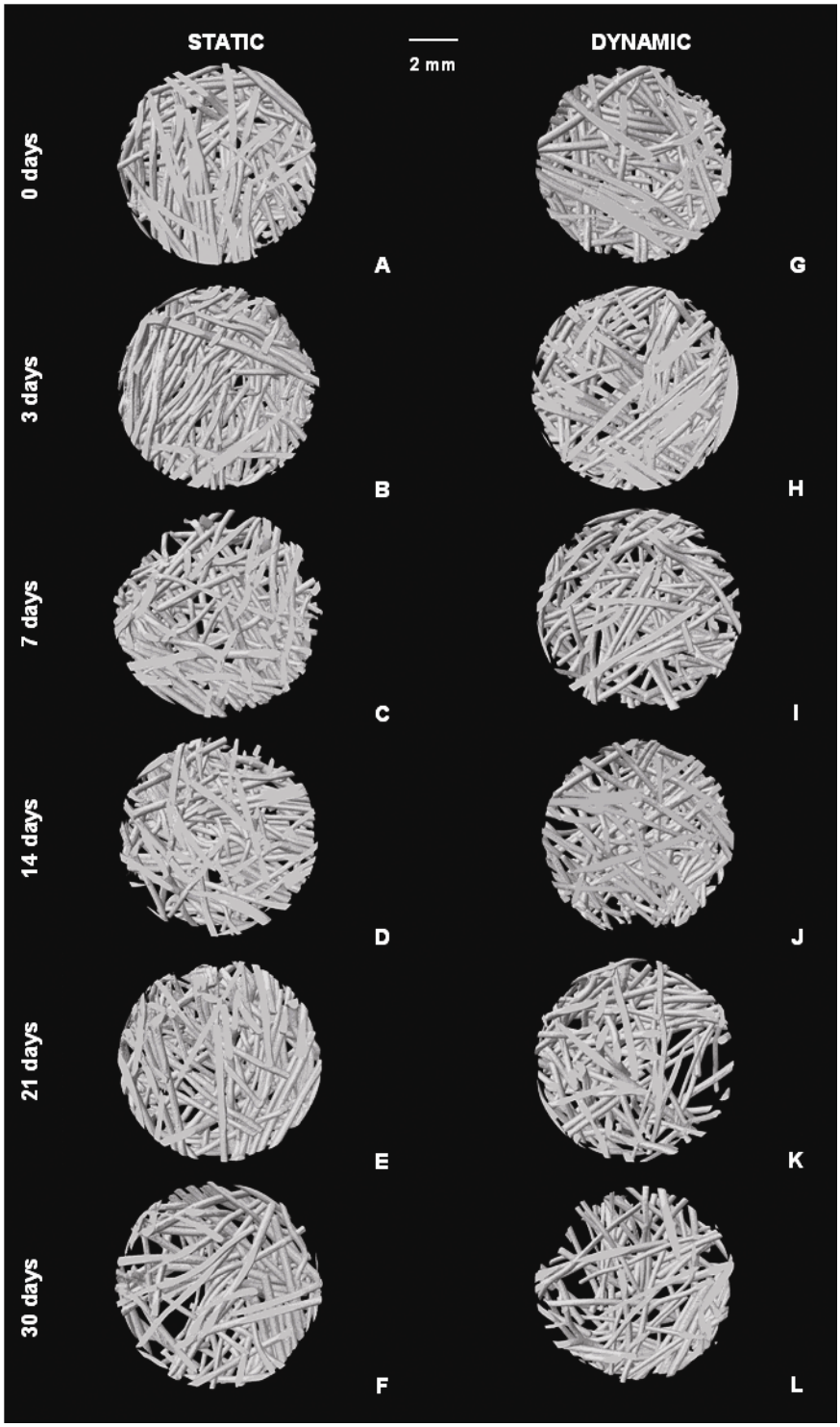


Figure 2. SPCL fiber meshes images obtained by μ-CT before (A, G) and after degradation with α-amylase (150 U/L) under static (B-F) and dynamic (H-L) conditions up to 30 days. The scale bar is 2 mm and applies to all images.

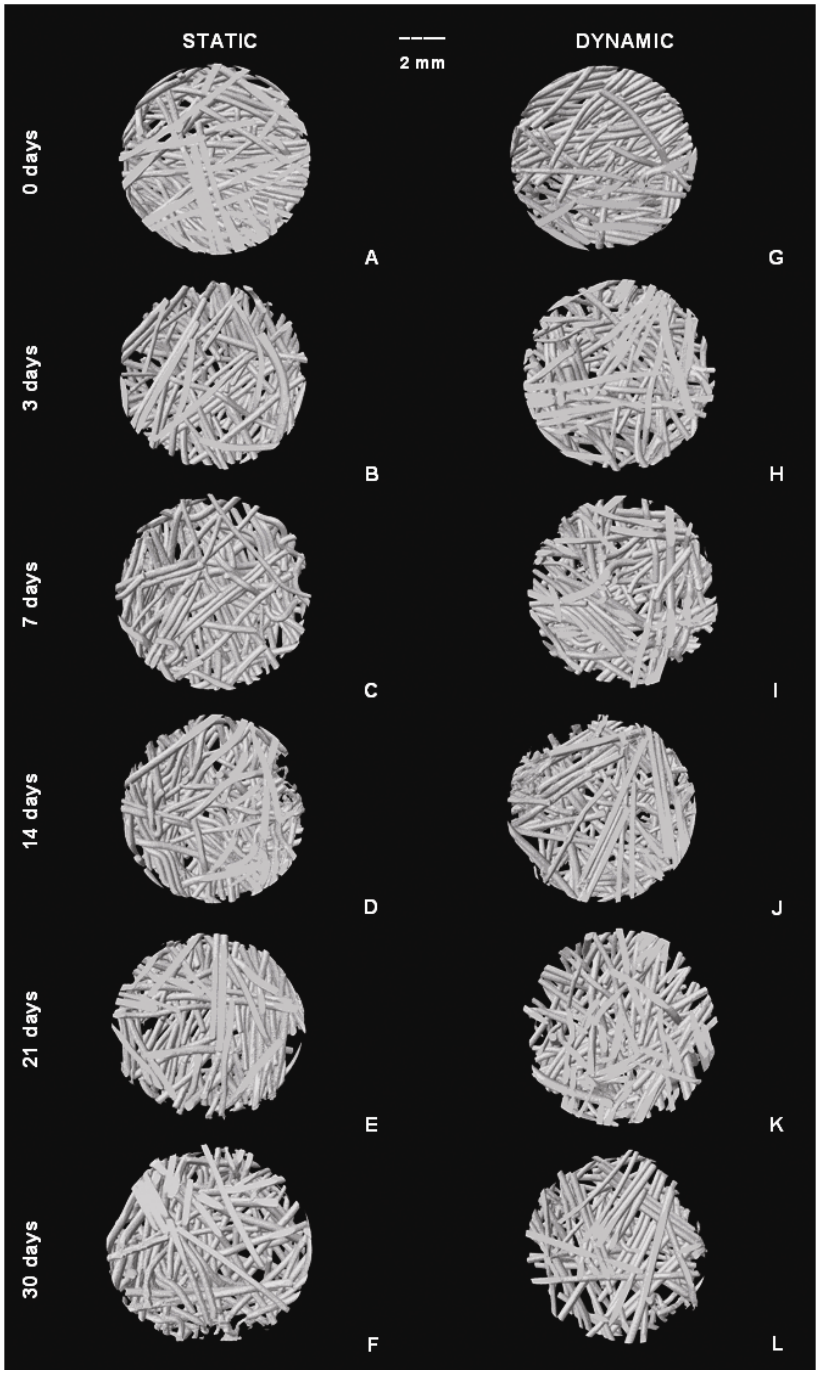


Figure 3. SPCL fiber meshes images obtained by μ-CT before (A, G) and after degradation with lipase (110 U/L) under static (B-F) and dynamic (H-L) conditions up to 30 days. The scale bar is 2 mm and applies to all images.

SPCL fiber mesh scaffolds before degradation presented an average porosity of 59.8 ± 2.6 % (Figure 4A), with approximately 97% pore interconnectivity (Figure 4B). According to Figure 4A, it is possible to see that both degradation conditions (lipase and α-amylase) enhance the porosity of the scaffolds. Porosity results (Figure 4A) show that both enzymes

(lipase and α-amylase) have a significant effect on SPCL degradation as a function of degradation time. When lipase was used a significant increase in porosity was observed as a function of immersion time using dynamic conditions compared with control samples. Furthermore, a significant difference in porosity was obtained using lipase and dynamic conditions compared to results obtained with the same enzyme using static conditions. Lipase seems to be influenced by agitation (dynamic conditions) as seen in Figure 4A, the porosity increases when compared with both control samples and static conditions. In addition, no effect of lipase upon SPCL porosity using static conditions was observed.

In contrast with results obtained with lipase, α-amylase has a significant effect on SPCL degradation using either static or dynamic conditions (Figure 4A). Moreover, results when α-amylase was used, show that all time periods (except day 30 using dynamic conditions) under static or dynamic conditions presented a significant increase in porosity when compared with control samples (Figure 4A). The effect of α-amylase on porosity seems to be independent of using static or dynamic conditions, being obvious when analysing Figure 4A. When comparing results obtained after degradation with lipase or α-amylase for the same period of time, a significant increase in porosity was observed only for the 3rd and 7th day using α-amylase in static conditions. Some differences can be observed between static and dynamic conditions for both enzymes: the positive effect of lipase on the porosity of the scaffolds is higher for dynamic conditions, while the effect of α-amylase on porosity appears to be less dependent on the circulation (static/dynamic) of the degrading media (Figure 4A).

The interconnectivity of SPCL scaffolds before degradation is very high (around 97%), and for all periods, the interconnectivity increases both under static and dynamic conditions with α-amylase (Figure 4B), although such differences are not easily perceptible through visual inspection due to the high range of interconnectivity. The same trend was observed for lipase (Figure 4B), and no significant differences were observed. However, the interconnectivity when α-amylase or lipase was used seems to be influenced by dynamic conditions.

The average pore size also increases upon degradation with lipase. According to porosity results (Figure 4A) the same trend is observed for pore size when lipase is used (Figure 5A). The pore size increase upon degradation with lipase is more pronounced for dynamic conditions (Figure 5A), being significantly different when compared with control samples or static conditions (Figure 5A). In this respect, dynamic conditions enhance the size of the pores (Figure 5A) relative to static conditions. As observed in Figure 4A, static

conditions seem to not interfere with the size of pores when lipase was used (Figure 5A). The pore size of the scaffolds increases upon degradation with α-amylase as compared with control samples, however this difference is only significant for the 7th and 14th day either using static or dynamic conditions. A significant increase in pore size is also observed when α-amylase was used in static conditions when compared with lipase (7th and 14th day).

The thickness of the fibers remains more or less constant using lipase (Figure 5B), which supports the low weight loss observed for lipase degradation media (Figure 1). No significant differences are observed between static or dynamic conditions. α-amylase decreases the thickness of the fibers both using static and dynamic conditions compared with control samples as a function of time. It is evident that fiber diameter decreases upon degradation with α-amylase, however differences between static and dynamic conditions are not significant, except for the 3rd day of degradation using dynamic conditions. Comparing the action of lipase and α-amylase on fiber thickness, it is possible to observe a significant decrease when lipase was used under either static or dynamic conditions.

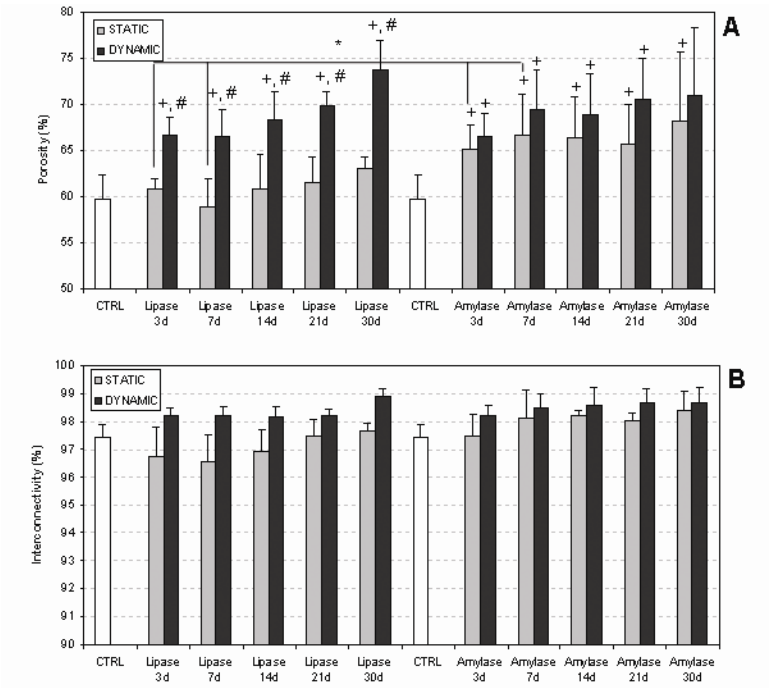


Figure 4. Porosity (A) and pore interconnectivity (B) of SPCL fiber meshes after different degradation periods with lipase and α-amylase using static and dynamic conditions. Results are expressed as means ± standard deviation with *n*=3 for each bar. (+) indicates a significant difference ($p < 0.05$) between conditions as a function of time compared with control samples. (#) indicates a significant difference ($p < 0.05$) between static and dynamic conditions (using the same enzyme) at the same time point. (*) indicates a significant difference ($p < 0.05$) between enzymes (lipase and α-amylase) using static conditions at the same time point, no significant differences were observed between dynamic conditions.

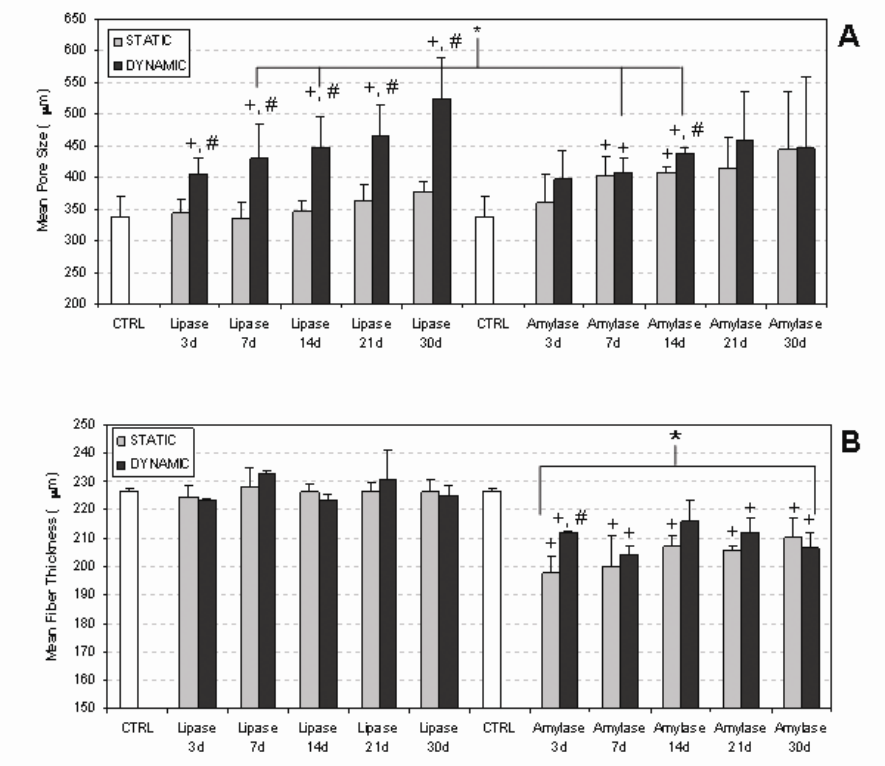


Figure 5. Pores size (A) and fibers thickness (B) of SPCL fiber meshes after degradation with lipase and α-amylase as a function of immersion time using static and dynamic conditions. Results are expressed as means ± standard deviation with *n*=3 for each bar. (+) indicates a significant difference ($p < 0.05$) between conditions as a function of time compared with control samples. (#) indicates a significant difference ($p < 0.05$) between static and dynamic conditions (using the same enzyme) at the same time point. (*) indicates a significant difference ($p < 0.05$) between enzymes (lipase and α-amylase) using static or dynamic conditions at the same time point. In Figure B (*) indicates that α-amylase has a significant difference at the same time point using static or dynamic conditions compared with lipase (except at day 21 using static conditions).

3.2. Assays

The results of scaffold cellularity are presented in Figure 6. The DNA assay showed a significant increase ($p<0.05$) in late cell proliferation for SPCL fiber meshes that were cultured with osteogenic medium with lipase or α-amylase. After 16 days the number of cells from scaffolds cultured with enzymes was much higher than the scaffolds cultured without enzymes, their cellularity increased 3-5 times between day 8 and day 16 of culture. In contrast, the DNA results showed a non-significant decrease in cell proliferation after 16 days for SPCL scaffolds cultured in static cultures without enzymes in agreement with previous experiments (9, 10). Scanning electron microscopy (SEM) images confirm these results. A

significant improvement of cell proliferation on the surface of SPCL fiber meshes cultured with enzymes is apparent (Figure 7).

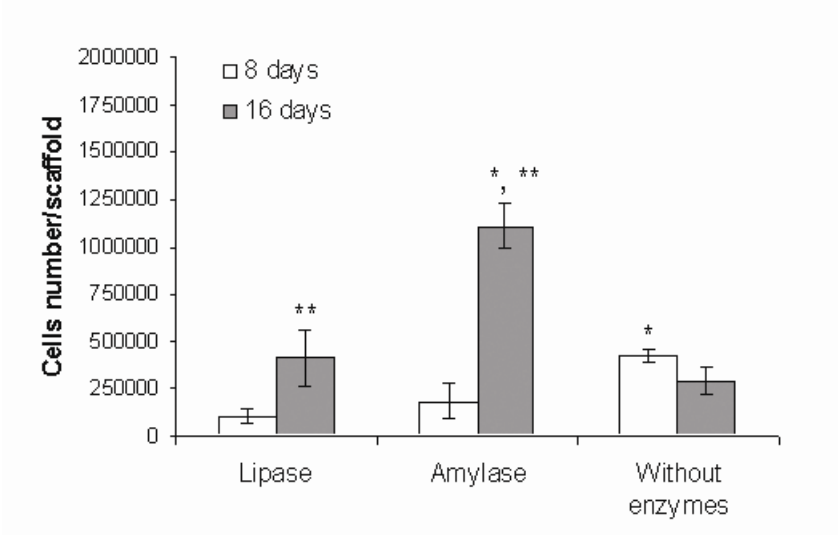


Figure 6. Cellularity of SPCL fiber meshes cultured *in vitro* with lipase, α-amylase and without enzymes for 8 and 16 days. Results are expressed as means ± standard deviation with *n*=3 for each bar. (*) indicates a significant difference ($p < 0.05$) between conditions at the same time point. (**) indicates a significant difference ($p < 0.05$) between 8 and 16 days for each condition.

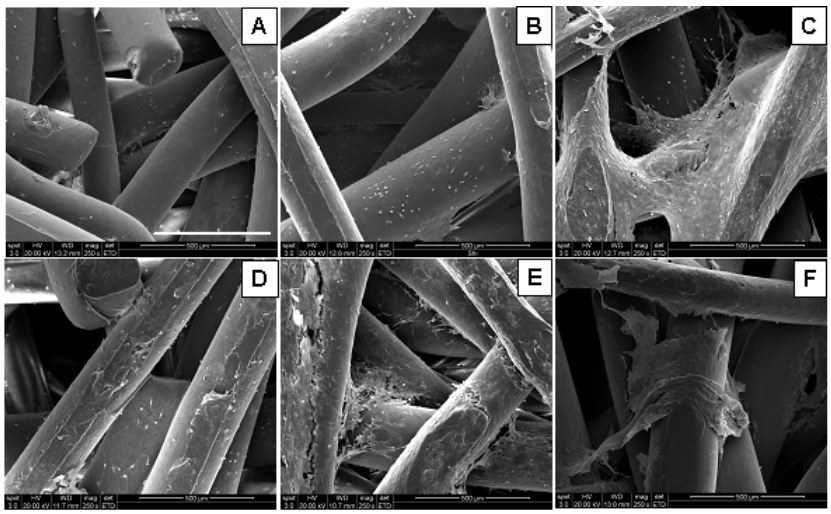


Figure 7. SEM images of the surfaces of SPCL fiber mesh scaffolds cultured with lipase (A, D), α-amylase (B, E), and without enzymes (C, F) after day 8 (A, B, C) and day 16 (D, E, F). The scale bar is 500 μm and applies to all images.

Alkaline phosphatase is an enzyme expressed by cells and is an early marker of osteoblastic differentiation. The alkaline phosphatase expression showed highest values at day 8 of culture for all conditions (Figure 8). According to Figure 8, ALP activity without enzymes (control) is significantly higher than in groups with enzymes. Usually a maximum value of ALP coincides with early osteoblastic differentiation of marrow stromal cells. There was a significant difference between the scaffolds cultured with and without enzymes for each time period. The presence of each enzyme decreased the ALP activity with respect to the control. All conditions presented a decrease of ALP at day 16, which was expected as after this period, ALP activity usually decreases and mineralization starts to take place (9).

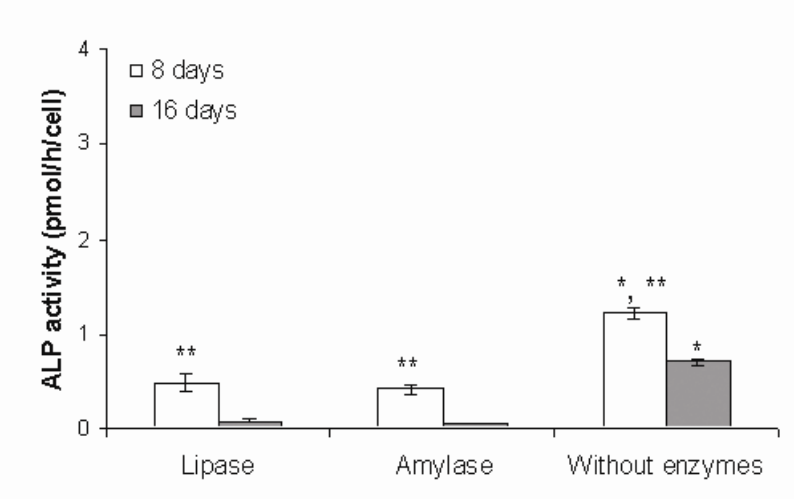


Figure 8. Alkaline phosphatase activity of rat marrow stromal cells cultured *in vitro* upon SPCL fiber mesh scaffolds with lipase, α-amylase and without enzymes for up to 16 days. Results are expressed as means ± standard deviation with n=3 for each bar. (*) indicates a significant difference ($p < 0.05$) between conditions at the same time point. (**) indicates a significant difference ($p < 0.05$) between 8 and 16 days for each condition.

The decrease of ALP expression when lipase was added to the culture medium (Figure 8) is related to an increase in calcium deposition (Figure 9). The production of a mineralized matrix is considered the endpoint in the osteoblastic differentiation of marrow stromal cells. Previous studies presented low levels of calcium deposition in static cultures (9, 10). After calcium deposition measurements, no calcium was detected in scaffolds cultured with α-amylase or without enzymes after both time periods. However, SPCL fiber mesh scaffolds cultured with lipase presented calcium deposition after day 8 with a

significant increase after 16 days (p<0.05). These values obtained for calcium deposition were similar (22, 30) or higher (31, 32) when compared with previous studies conducted in static cultures using different fiber meshes. Lipase seems to positively influence osteoblastic differentiation of rat marrow stromal cells and enhance matrix mineralization.

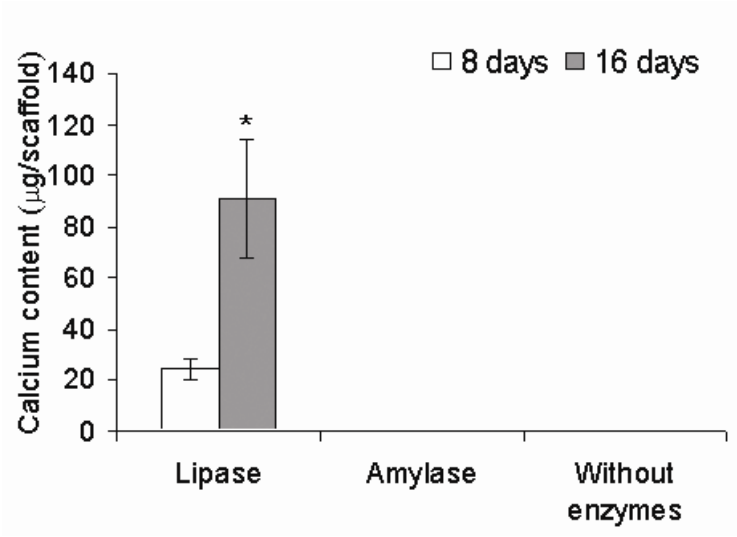


Figure 9. Calcium content of SPCL fiber mesh scaffolds cultured *in vitro* with lipase, α-amylase and without enzymes for 8 and 16 days expressed as total calcium per scaffold. Results are expressed as means ± standard deviation with n=3 for each bar. (*) indicates a significant difference (p < 0.05) between conditions after 16 days of culture.

Figure 10 presents different images obtained by laser scanning confocal microscopy showing that cells are viable, well spread and cover the entire surface of the fibers at day 8 and 16.

The images presented in Figure 11 were obtained from depth projections of SPCL fiber meshes after 16 days and show the infiltration of cells to a depth of 410 μm for all culture conditions and the presence of monolayers of cells covering the fibers.

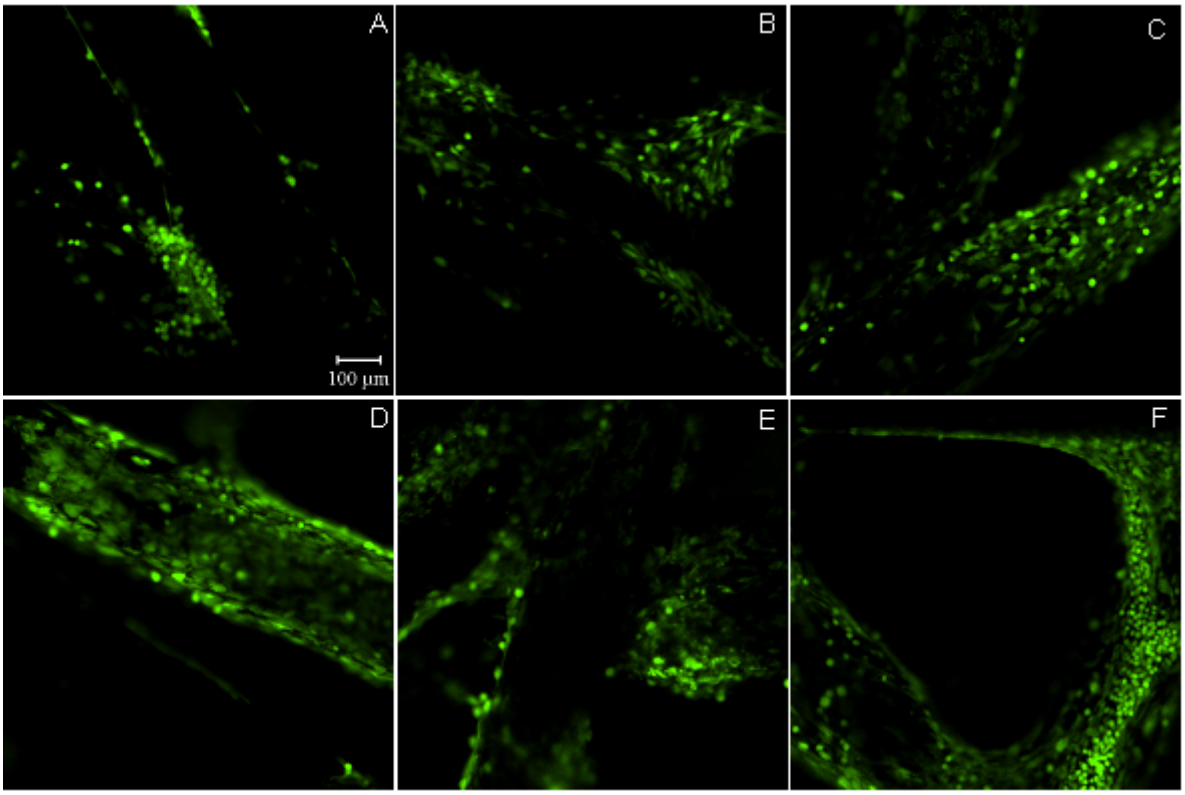


Figure 10. Laser scanning confocal microscope images of rat marrow stromal cells stained with calcein-AM at the top surface of SPCL fiber meshes with lipase (A, D), α-amylase (B, E) and without enzymes (C, F) at 8 days (A, B, C) and 16 days (C, F). All images obtained using a 10X APO objective. The scale bar is 100 µm and applies to all images.

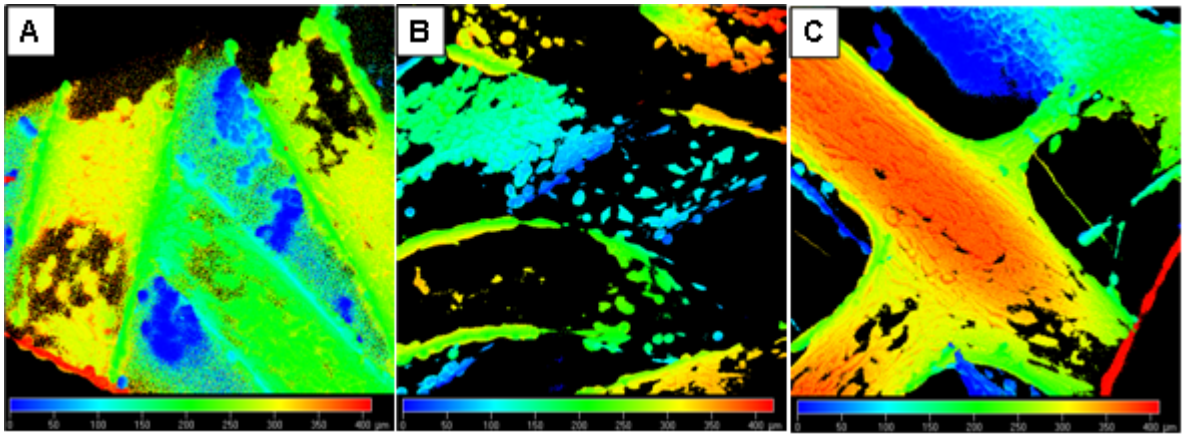


Figure 11. Laser scanning confocal microscopy images of SPCL fiber meshes cultured for 16 days with lipase (A), α-amylase (B) and without enzymes (C) obtained from depth projections. The scale bar is 100 µm and applies to all images.

3.3. Fourier transformed infrared spectroscopy with attenuated total reflectance (FTIR-ATR)

In this study, FTIR-ATR spectra were obtained from SPCL cultured for 16 days under static conditions with and without enzymes (α-amylase or lipase). This method was used as a complement to the calcium assay. When α-amylase or lipase were added to osteogenic media, it was possible to see bands centered at 1650 and 1542 cm^{-1} that can be attributed to amide I and amide II. The amide I band represents the stretching vibrations of C=O bonds in the backbone of the proteins (33). Furthermore, the amide II band arises from the combination of C-N stretching and N-H bending vibrations of the protein backbone (33). Analysing the spectra when enzymes were added to culture media, it is possible to detect amide I and amide II bands, which confirms that these enzymes were able to adsorb to the SPCL fiber mesh surfaces. In addition, these bands can be correlated to the protein matrix formation. Moreover, phosphate bands located at 1020 cm^{-1} similar to the ones found in carbonate apatite were observed in SPCL fiber meshes cultured with lipase, clearly suggesting the presence of mineralized extracellular matrix and corroborating the results obtained from the calcium assay.

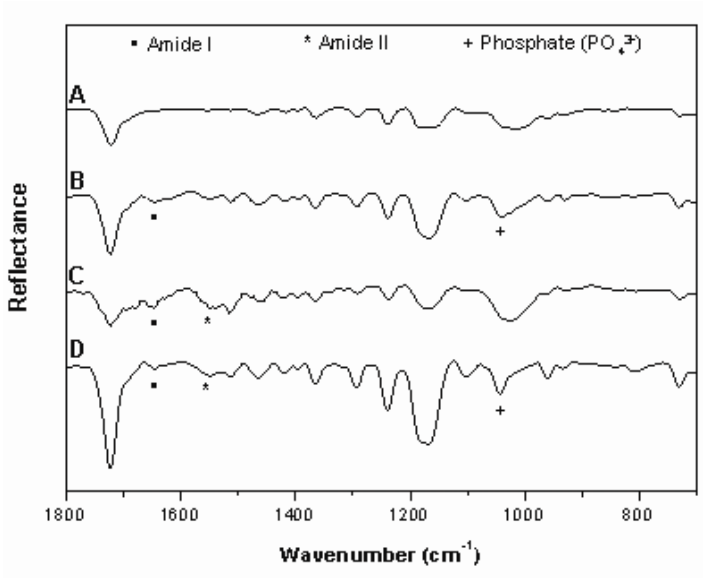


Figure 12. FTIR-ATR spectra of SPCL fiber meshes before (A) and after 16 days of culture without enzymes (B), with α-amylase (C), and with lipase (D).

4. CONCLUSIONS

This study demonstrates the effect of lipase and α-amylase on degradation of SPCL fiber mesh scaffolds, showing that after 30 days these enzymes did not have a negative effect on SPCL fiber integrity. The positive effect of lipase on the porosity and size of pores was clearly visible when dynamic conditions were used. Porosity, pore size and fiber thickness were also enhanced by α-amylase. However, no significant differences were observed under static and dynamic conditions, when α-amylase solution was used. SPCL fiber meshes cultured with media supplemented with α-amylase or lipase revealed that these enzymes promoted the proliferation of rat marrow stromal cells. Furthermore, this study confirms by calcium content measurement and FTIR analysis that lipase has a superior effect in osteodifferentiation of rat marrow stromal cells and promotes extracellular matrix mineralization when added to osteogenic culture medium as compared with results obtained without enzymes or with α-amylase. These results demonstrate that supplementation of culture media with lipase holds great potential for the generation of bone tissue engineering constructs from MSCs seeded onto SPCL fiber mesh scaffolds, as lipase enhances the osteoblastic differentiation of the seeded MSCs and promotes matrix mineralization without deleteriously affecting the structural integrity of the meshes over 16 days of culture.

ACKNOWLEDGEMENTS

The authors would like to acknowledge Dr. Helena Azevedo and Dr. Serena Danti. This work was supported by the European NoE EXPERTISSUES (NMP3-CT-2004-500283), the European STREP HIPPOCRATES (NMP3-CT-2003-505758), the Portuguese Foundation for Science and Technology (FCT) through POCTI and/or FEDER programmes. This work was also supported by a grant from the National Institute of Health (R01 DE15164) (AGM) and a Bioengineering Research Partnership with the Baylor College of Medicine through the National Institute of Biomedical Imaging and Bioengineering (NIH Grant No. 5 R01 EB005173-02). FKK is supported by a training fellowship from the Keck Center Nanobiology Training Program of the Gulf Coast Consortia (NIH Grant Nº 5 T90 DK070121-03).

REFERENCES

1. Langer, R., and Vacanti, J.P. Tissue engineering. Science 260, 920, 1993.

2. Hutmacher, D.W., Schantz, J.T., Lam, C.X.F., Tam, K.C., and Lim, T.C. State of the art and future directions of scaffold-based bone engineering from a biomaterials perspective. Journal of Tissue Engineering and Regenerative Medicine 1, 245, 2007.

3. Azevedo, H.S., and Reis, R.L. Understanding the enzymatic degradation of biodegradable polymers and strategies to control their degradation rate. In: Reis, R.L., and Roman, J.S., eds. Biodegradable systems in tissue engineering and regenerative medicine: CRC Press, 2005, pp. 177-201.

4. Mendes, S.C., Reis, R.L., Bovell, Y.P., Cunha, A.M., van Blitterswijk, C.A., and de Bruijn, J.D. Biocompatibility testing of novel starch-based materials with potential application in orthopaedic surgery: a preliminary study. Biomaterials 22, 2057, 2001.

5. Marques, A.P., Reis, R.L., and Hunt, J.A. The biocompatibility of novel starch-based polymers and composites: in vitro studies. Biomaterials 23, 1471, 2002.

6. Gomes, M.E., Ribeiro, A.S., Malafaya, P.B., Reis, R.L., and Cunha, A.M. A new approach based on injection moulding to produce biodegradable starch-based polymeric scaffolds: morphology, mechanical and degradation behaviour. Biomaterials 22, 883, 2001.

7. Azevedo, H.S., Gama, F.M., and Reis, R.L. In vitro assessment of the enzymatic degradation of several starch based biomaterials. Biomacromolecules 4, 1703, 2003.

8. Salgado, A.J., Coutinho, O.P., and Reis, R.L. Novel starch-based scaffolds for bone tissue engineering: cytotoxicity, cell culture, and protein expression. Tissue Eng 10, 465, 2004.

9. Gomes, M.E., Sikavitsas, V.I., Behravesh, E., Reis, R.L., and Mikos, A.G. Effect of flow perfusion on the osteogenic differentiation of bone marrow stromal cells cultured on starch-based three-dimensional scaffolds. J Biomed Mater Res A 67, 87, 2003.

10. Gomes, M.E., Holtorf, H.L., Reis, R.L., and Mikos, A.G. Influence of the porosity of starch-based fiber mesh scaffolds on the proliferation and osteogenic differentiation of bone marrow stromal cells cultured in a flow perfusion bioreactor. Tissue Eng 12, 801, 2006.

11. Mochizuki, M., Hirano, M., Kanmuri, Y., Kudo, K., and Tokiwa, Y. Hydrolysis of Polycaprolactone Fibers by Lipase - Effects of Draw Ratio on Enzymatic Degradation. J Appl Polym Sci 55, 289, 1995.

12. Hoshino, A., and Isono, Y. Degradation of aliphatic polyester films by commercially available lipases with special reference to rapid and complete degradation of poly(L-lactide) film by lipase PL derived from Alcaligenes sp. Biodegradation 13, 141, 2002.

13. Zeng, J., Chen, X., Liang, Q., Xu, X., and Jing, X. Enzymatic degradation of poly(L-lactide) and poly(epsilon-caprolactone) electrospun fibers. Macromol Biosci 4, 1118, 2004.

14. Miao, Z.M., Cheng, S.X., Zhang, X.Z., Wang, Q.R., and Zhuo, R.X. Degradation and drug release property of star poly(epsilon-caprolactone)s with dendritic cores. J Biomed Mater Res B Appl Biomater 81, 40, 2007.

15. Wong, H., and Schotz, M.C. The lipase gene family. Journal of lipid research 43, 993, 2002.

16. Hasham, S.N., and Pillarisetti, S. Vascular lipases, inflammation and atherosclerosis. Clin Chim Acta 372, 179, 2006.

17. Mukherjee, M. Human digestive and metabolic lipases - a brief review. J Mol Catal B-Enzym 22, 369, 2003.

18. Schoonjans, K., PeinadoOnsurbe, J., Lefebvre, A.M., Heyman, R.A., Briggs, M., Deeb, S., Staels, B., and Auwerx, J. PPAR alpha and PPAR gamma activators direct a distinct tissue-specific transcriptional response via a PPRE in the lipoprotein lipase gene. Embo Journal 15, 5336, 1996.

19. Palacios, V.G., Morita, I., and Murota, S. Expression of adipogenesis markers in a murine stromal cell line treated with 15-deoxy Delta(12,14)-prostaglandin J(2), interleukin-11,9-cis retinoic acid and vitamin K-2. Prostaglandins Leukotrienes and Essential Fatty Acids 65, 215, 2001.

20. De Coppi, P., Bartsch, G., Siddiqui, M.M., Xu, T., Santos, C.C., Perin, L., Mostoslavsky, G., Serre, A.C., Snyder, E.Y., Yoo, J.J., Furth, M.E., Soker, S., and Atala, A. Isolation of amniotic stem cell lines with potential for therapy. Nature Biotechnology 25, 100, 2007.

21. Tietz, N.W., and Shuey, D.F. Lipase in serum--the elusive enzyme: an overview. Clin Chem 39, 746, 1993.

22. Holtorf, H.L., Jansen, J.A., and Mikos, A.G. Flow perfusion culture induces the osteoblastic differentiation of marrow stroma cell-scaffold constructs in the absence of dexamethasone. J Biomed Mater Res A 72, 326, 2005.

23. Junge, W., Troge, B., Klein, G., Poppe, W., and Gerber, M. Evaluation of a new assay for pancreatic amylase: performance characteristics and estimation of reference intervals. Clin Biochem 22, 109, 1989.

24. Chawla, J.S., and Amiji, M.M. Biodegradable poly(epsilon-caprolactone) nanoparticles for tumor-targeted delivery of tamoxifen. International Journal of Pharmaceutics 249, 127, 2002.

25. Maniatopoulos, C., Sodek, J., and Melcher, A.H. Bone formation in vitro by stromal cells obtained from bone marrow of young adult rats. Cell Tissue Res 254, 317, 1988.

26. Datta, N., Holtorf, H.L., Sikavitsas, V.I., Jansen, J.A., and Mikos, A.G. Effect of bone extracellular matrix synthesized in vitro on the osteoblastic differentiation of marrow stromal cells. Biomaterials 26, 971, 2005.

27. Zeng, J., Chen, X.S., Liang, Q.Z., Xu, X.L., and Jing, X.B. Enzymatic degradation of poly(L-lactide) and poly (epsilon-caprolactone) electrospun fibers. Macromolecular Bioscience 4, 1118, 2004.

28. Chawla, J.S., and Amiji, M.M. Biodegradable poly(epsilon -caprolactone) nanoparticles for tumor-targeted delivery of tamoxifen. Int J Pharm 249, 127, 2002.

29. Pulkkinen, M., Malin, M., Tarvainen, T., Saarimaki, T., Seppala, J., and Jarvinen, K. Effects of block length on the enzymatic degradation and erosion of oxazoline linked poly-epsilon-caprolactone. Eur J Pharm Sci 31, 119, 2007.

30. Sikavitsas, V.I., Bancroft, G.N., Holtorf, H.L., Jansen, J.A., and Mikos, A.G. Mineralized matrix deposition by marrow stromal osteoblasts in 3D perfusion culture increases with increasing fluid shear forces. Proc Natl Acad Sci U S A 100, 14683, 2003.

31. Sikavitsas, V.I., Bancroft, G.N., Lemoine, J.J., Liebschner, M.A., Dauner, M., and Mikos, A.G. Flow perfusion enhances the calcified matrix deposition of marrow stromal cells in biodegradable nonwoven fiber mesh scaffolds. Ann Biomed Eng 33, 63, 2005.

32. Holtorf, H.L., Datta, N., Jansen, J.A., and Mikos, A.G. Scaffold mesh size affects the osteoblastic differentiation of seeded marrow stromal cells cultured in a flow perfusion bioreactor. J Biomed Mater Res A 74, 171, 2005.

33. Xie, J., Riley, C., Kumar, M., and Chittur, K. FTIR/ATR study of protein adsorption and brushite transformation to hydroxyapatite. Biomaterials 23, 3609, 2002.

CHAPTER IV

Combination of Enzymes and Flow Perfusion Conditions Improves Osteogenic Differentiation of Bone Marrow Stromal Cells Cultured upon Starch/Poly(ε-Caprolactone) Fiber Meshes

CHAPTER IV

Combination of Enzymes and Flow Perfusion Conditions Improves Osteogenic Differentiation of Bone Marrow Stromal Cells Cultured upon Starch/Poly(ε-Caprolactone) Fiber Meshes[1]

ABSTRACT

Previous studies have shown that α-amylase and lipase are capable of enhancing the degradation of fiber meshes of blends of starch and poly(ε-caprolactone) (SPCL) under dynamic conditions, and consequently to promote the proliferation and osteogenic differentiation of bone marrow stromal cells (MSCs). This study investigated the effect of flow perfusion bioreactor culture in combination with enzymes such as α-amylase and lipase on the osteogenic differentiation of rat MSCs. SPCL fiber meshes were seeded with rat MSCs and cultured with osteogenic medium supplemented with α-amylase, lipase or a combination of the two for 8 or 16 days using both static or fluid flow perfusion conditions. It was found that lipase and its combination with α-amylase enhanced cell proliferation after 16 days. In addition, the flow perfusion culture enhanced the infiltration of cells and facilitated greater distribution of extracellular matrix throughout the scaffolds in the presence/absence of enzymes. A significant amount of calcium was detected after 16 days in all groups cultured in flow perfusion conditions compared with static cultures. Nevertheless, when α-amylase and lipase were included in the flow perfusion cultures, the calcium content was 379 ± 30 μg/scaffold after as few as 8 days. The highest calcium content (1271 ± 32 μg/scaffold) was obtained for SPCL/cell constructs cultured for 16 days in the presence of lipase and flow. Furthermore, von Kossa staining and tetracycline fluorescence of histological sections demonstrated mineral deposition within the scaffolds for all groups cultured for 16 days under flow perfusion conditions. However, all the data corroborate that lipase coupled with flow perfusion conditions improve the osteogenic differentiation of MSCs and enhance extracellular matrix mineralization.

[1] This chapter is based on the following publication:

A.M. Martins, A. Saraf, F. K. Kasper, A.G. Mikos, R.A. Sousa, C.M. Alves, R.L. Reis. Combination of enzymes and flow perfusion conditions improves osteogenic differentiation of bone marrow stromal cells cultured onto starch/poly(ε-caprolactone) fiber meshes, submitted

1. INTRODUCTION

An ideal scaffold for bone tissue engineering should be biodegradable and bioresorbable while being able to support the growth of new bone. The scaffold degradation rate should complement the growth rate of the new bone such that the scaffold degrades in time for the new bone to occupy the site of defect or injury.[1] In the case of starch and poly(ε-caprolactone) (SPCL) scaffolds[2,3], α-amylase[4-8] and lipase[5,9,10] have been shown to facilitate the enzymatic hydrolysis of the starch and PCL components of the scaffold, respectively. Additionally, studies have also shown pronounced degradation of SPCL biomaterials when lipase and α-amylase were used together.[5,6] Since these enzymes are naturally present in humans, lipase and α-amylase were used in this study at human blood serum concentrations to simulate *in vivo* conditions. *In vitro*, these enzymes have previously induced the degradation of SPCL scaffolds under static as well as dynamic conditions, as is indicated by the enhanced porosity and pore size of the scaffolds. In addition, the presence of these enzymes in culture media has induced the proliferation of rat marrow stromal cells cultured on SPCL scaffolds.

In this study we were interested in examining the osteogenic potential of α-amylase and lipase when added to osteogenic culture media in flow perfusion culture of MSCs. The osteogenic differentiation of MSCs *in vitro* starts with a period of cellular proliferation, followed by extracellular matrix (ECM) deposition and maturation, and ultimately mineralization of the matrix.[11,12] To induce osteogenic differentiation of MSCs, the culture medium is typically supplemented with osteogenic agents such as ascorbic acid, β-glycerophosphate, and dexamethasone. To further facilitate osteogenesis, growth factors such as BMP-2 and BMP-4 have been added to culture media. However, most studies do not take into account the effect of physiological enzymes on cellular differentiation and scaffold degradation; two events that are integral to designing successful strategies for bone tissue engineering. For example, a previous study in our laboratory described that lipase positively influences osteoblastic differentiation of rat MSCs and enhances matrix mineralization under static conditions when added to osteogenic culture medium. Previous studies with SPCL fiber mesh scaffolds using flow perfusion bioreactors have shown that flow perfusion conditions enhanced osteoblastic differentiation of rat bone marrow stromal cells (MSCs)[2,3] due to the improved mass transport to the scaffold interior[13] and to the mechanical stimulation of cells caused by the fluid shear force within the scaffold.[14]

Due to previous promising results indicating the osteoblastic differentiation of MSCs in the presence of lipase under static conditions, it was hypothesized in the present study that the addition of mechanical stimulation of MSCs via fluid flow in the bioreactor would

enhance osteogenesis of MSCs in the presence of enzymes such as lipase and α-amylase at physiological concentrations. Specifically, this study was designed to investigate the following: (1) The efficacy of α-amylase and/or lipase enzymes as osteogenic supplements in culture media for osteogenic differentiation of rat bone marrow stromal cells and (2) the effect of lipase and α-amylase at physiological concentrations, in combination with flow perfusion conditions, on the osteogenic differentiation of rat bone marrow stromal cells.

2. MATERIALS AND METHODS

2.1. Scaffold preparation

Blends of corn starch and poly(ε-caprolactone) (SPCL, 30/70%) fiber mesh scaffolds were prepared by a fiber bonding technique with a porosity of 60 ± 3% and an average fiber diameter of 226 ± 1 μm. The porosity and fiber diameter were determined using micro-computed tomography (μ-CT) as previously described.[8] The average pore size was 339 ± 31 μm.[8] Scaffolds were die-punched into 8 mm diameter discs (thickness = 1-1.5 mm). Further details on the scaffolds can be found elsewhere.[2,3] Prior to cell seeding, scaffolds were sterilized by exposure to ethylene oxide gas for 14 hours. All chemical reagents were purchased from Sigma (St. Louis, MO, USA), unless otherwise specified.

2.2. Isolation, expansion and seeding of rat bone marrow stromal cells

Rat bone marrow stromal cells (MSCs) were obtained from femura and tibiae of 41-44 day-old male Wistar rats (Charles River Laboratories, USA) using the method described by Maniatoupoulos *et al.*[15] The harvested cells were cultured in a humidified atmosphere with 5% CO_2 at 37ºC until they were confluent. Medium was changed at 1 and 3 days to remove the non-adherent cell population.

SPCL fiber mesh scaffolds were immersed in complete osteogenic medium [α-MEM supplemented with 10% fetal bovine serum (FBS) from Cambrex/BioWhittaker (Walkersville, MD, USA), 50 μg/mL gentamicin, 100 μg/mL ampicilin, 10 mM fungizone, 50 μg/mL L-ascorbic acid, 0.01 M β-glycerophosphate, and 10^{-8} M dexamethasone] overnight and were press fit into 8 mm diameter cassettes on the following day. Cassettes were placed into 6-well plates. Each scaffold was seeded with 500,000 cells in 300 μl of complete osteogenic medium as described previously.[8] Cells were allowed to attach for 2 hours before adding 10 ml of osteogenic medium to each well of the 6-well plate. After 24 hours of attachment, the

scaffolds were placed in new 6-well plates (static culture condition) or in a flow perfusion bioreactor for 7 and 15 days with four different media conditions; specifically, complete osteogenic media (i) without enzymes, (ii) with α-amylase (150 U/L)[8,16], (iii) with lipase (110 U/L)[8,17], or (iv) with α-amylase and lipase in concentrations similar to those found in human blood serum.

Media were changed every 2-3 days. Each group consisted of *n* = 6 samples. At the end of each culture period, samples were removed from the cassettes and rinsed with phosphate buffered saline (PBS) solution. Three samples from each group were stored at -20ºC in ddH_2O for biochemical analysis. The remaining samples were fixed with 2.5% glutaraldehyde for scanning electron microscopy (SEM) analysis or with 10% formalin solution for histological evaluation.

2.3. DNA analysis

The cells in the constructs were lysed by repeated freeze-thaw cycles in ddH_2O. The DNA content of the lysates was quantified by using a DNA quantification kit (PicoGreen, Molecular Probes) and correlated to DNA from a known amount of rat marrow stromal cells. Frozen scaffolds were thawed at room temperature, sonicated for 10 minutes, and vortexed to allow cellular DNA into solution. Buffer provided with the kit was diluted with ddH_2O and placed in each well of a 96-well plate at 100 μl/well. DNA standard solutions in ddH_2O in concentrations from 0-6 μg/ml were prepared, and 50 μl of standards/samples were added to each well of the 96-well plate. PicoGreen dye solutions were prepared according to the instructions of the manufacturer using reagents provided in the kit and added at 150 μl/well. All these procedures were performed in triplicate. After 10 minutes of incubation in a dark room, the fluorescence at 545 nm was read on a plate reader (FLx800, Bio-Tek Instruments Inc., Winooski, VT, USA) to determine DNA concentrations per scaffold. A conversion factor of 2.7 pg DNA/cell was used to calculate cell number based on MSC standards.

2.4. Alkaline phosphatase activity

Alkaline phosphatase activity assays were performed on cell lysates using an established protocol.[18] All samples were prepared in triplicate and compared against *p*-nitrophenol standards. The reaction was stopped by adding 100 μl of 0.3 N NaOH. Absorbance was read at 405 nm on a plate reader (PowerWave x340; Bio-Tek Inc., Winooski, VT, USA) to determine the alkaline phosphatase activity per scaffold.

2.5. Calcium deposition measurement

Calcium content in the SPCL fiber mesh scaffolds was measured by using a Calcium Kit (Diagnostic Chemical Limited, Oxford, CT, USA). After the ALP and DNA assays, a volume of 1 N acetic acid equal to the volume remaining in each well was added to each sample (final concentration of 0.5 N), and the plate was placed on an orbital shaker overnight. A volume of 300 μl of calcium assay reagent was added to 20 μl of sample solution in triplicate in 96-well plates. To generate a standard curve, serial dilutions of $CaCl_2$ were prepared (0-50 μg/ml). Absorbance was read at 650 nm using a spectrophotometric plate reader (FLx800, Bio-Tek Instruments Inc., Winooski, VT, USA). The calcium deposition in each scaffold is reported as μg Ca^{2+}.

2.6. Histological and microscopic analysis

After each time period, SPCL fiber mesh scaffolds were removed from the cassettes, washed twice in PBS, and fixed with 2.5% glutaraldehyde for 30 minutes. Then, the scaffolds were washed with PBS and dehydrated in a graded series of ethanol, dried by hexamethyldisilazane, mounted on aluminium stages, sputter coated with gold, and examined with an FEI Quanta 400 Environmental Scanning Electron Microscope (Hillsboro, OR, USA). Scanning electron microscopy (SEM) and light microscopy were used to evaluate the morphological appearance and infiltration of the bone marrow stromal cells and deposited matrix. The samples for SEM observation were cut in half for analysis of both the top and bottom; additionally, cross-sections were cut. The samples were sputter-coated with gold, examined and photographed with an FEI Quanta 400 Environmental Scanning Electron Microscope (Hillsboro, OR, USA).

The remaining cultured samples were rinsed with PBS, fixed in 10% formalin solution and embedded in HistoPrep freezing medium (Fisher Scientific, Pittsburgh, PA, USA). Frozen sections of ~10-15 μm thickness were obtained using a cryostat (HM500, Microm, Walldorf, Germany) operating at -23 ºC and mounted onto Superfrost Plus glass slides (Fisher Scientific, Pittsburgh, PA, USA), then stained with hematoxylin and eosin for histological evaluation. For visualization of mineralized tissue, additional sections were exposed to 5% silver nitrate solution under UV for 25 min and counterstained with 0.5% safranin O solution. von Kossa stained sections were observed using a light microscope (Eclipse E600; Nikon, Melville, NY, USA) and attached video camera (3CCD Color Video Camera DXC-950P; Sony, Park Ridge, NJ, USA). Mineral deposition was also visualized in

unstained sections under fluorescent light after adding tetracycline-HCl to the culture media at a final concentration of 10 μg/mL.[2,14] All the histological sections, except von Kossa stained sections, were visualized using an Olympus BX61 Motorized System Microscope and attached video camera Olympus DP70 equipped with a fluorescence lamp.

2.7. Statistics

Results of DNA, ALP, and calcium assay are expressed as mean ± standard deviation with $n = 3$ for each group. Single factor analysis of variance (ANOVA) was used to determine statistical significance within a data set. If ANOVA detected a significant difference within the data set, Tukey's honestly significantly different (HSD) multiple comparison test was used to determine significant differences between groups and conditions. All tests were conducted with a confidence interval of 95% ($p < 0.05$).

3. RESULTS AND DISCUSSION

3.1. DNA assay

A significant improvement in cell number was generally observed in flow perfusion conditions when compared with static cultures (Figure 1). SEM images and H&E stained sections also confirm these results (Figures 2, 3 and 4). The SPCL/cell constructs cultured without enzymes or with α-amylase in flow perfusion conditions reached their peak cellularities at day 8, and after that point they demonstrated a significant decrease in the number of cells measured in each scaffold (Figure 1), in agreement with previous experiments.[2,3] In contrast, the DNA results showed an increase in cell numbers after 16 days for SPCL scaffolds cultured with lipase or with both enzymes. Scaffolds cultured in the presence of lipase or with both enzymes, under flow conditions after 16 days, had almost 3 and 2 times higher cellularity, respectively, when compared with SPCL/cell constructs cultured for 16 days under flow conditions without enzymes.

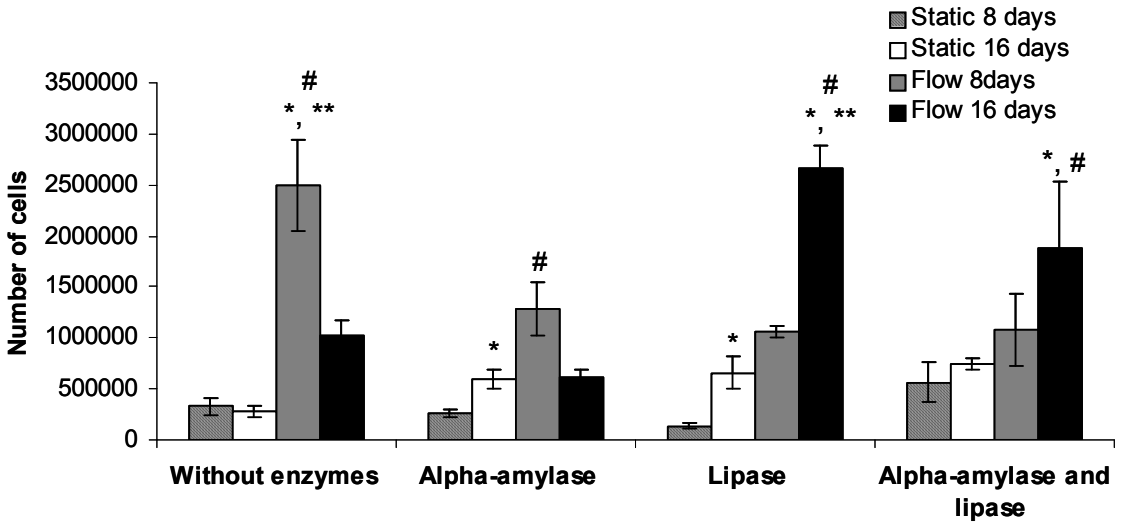


Figure 1. Cellularity of SPCL fiber meshes cultured *in vitro* without enzymes, with α-amylase, lipase, α-amylase and lipase in static or flow perfusion conditions for 8 and 16 days. Results are expressed as means ± standard deviation with n=3 for each bar. (*) Indicates a significant difference (p<0.05) between 8 and 16 days; (**) indicates a significant difference (p<0.05) between groups (with and without enzymes) in static or flow conditions; and (#) indicates a significant difference (p<0.05) between flow and static conditions.

3.2. Microscopic analysis

Cross-sections of all groups were visualized using SEM to evaluate cell morphology and infiltration and deposition of extracellular matrix. Culturing the constructs in a flow perfusion bioreactor enhanced the infiltration of MSCs for all groups (Figure 3). Previous studies have also demonstrated that flow perfusion culture increased the distribution and infiltration of cells as compared with static culture.[2,19-21] This was further confirmed by histological evaluation of the scaffolds (Figure 4). The cellular distribution observed in static as well as flow conditions was not influenced by the presence of the enzymes. Cross-sectional images of all groups cultured under flow perfusion conditions revealed infiltration of cells through the bottom of the scaffolds and the presence of matrix between fibers deeper within the scaffolds (Figure 3) as compared to constructs that were cultured statically (Figure 2). Furthermore, SEM images indicated that the enzymes did not have a deleterious effect on the structure of SPCL fiber meshes, meaning that the constructs did not loose their structural integrity after 16 days, even when flow perfusion conditions and enzymes were used (Figure 3). This was further confirmed with histological cross sections, which additionally showed that there were no observable differences between scaffolds cultured in flow conditions with respect to the distribution and infiltration of cells (Figure 4).

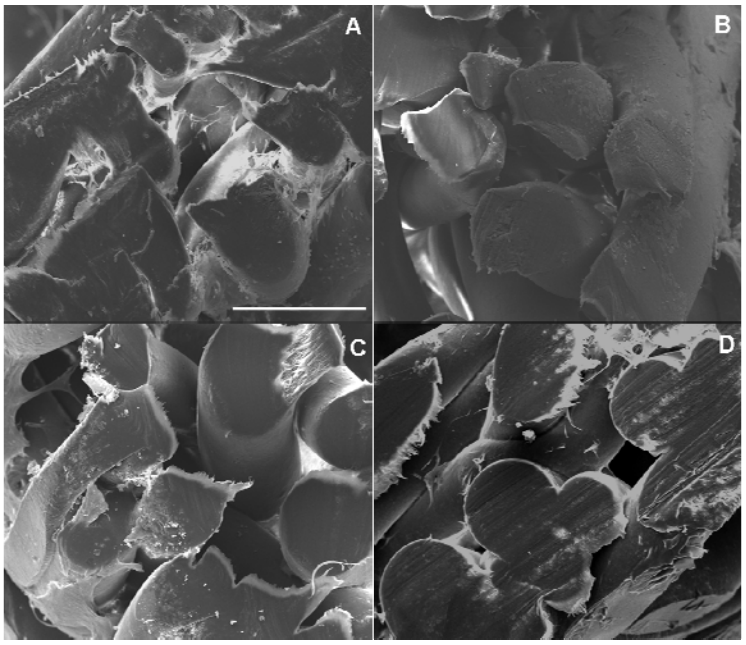


Figure 2. SEM images of the cross-sections of SPCL fiber mesh scaffolds cultured without enzymes (A), with α-amylase (B), with lipase (C) or with α-amylase and lipase in static conditions after 16 days. The scale bar is 400 μm and applies to all images.

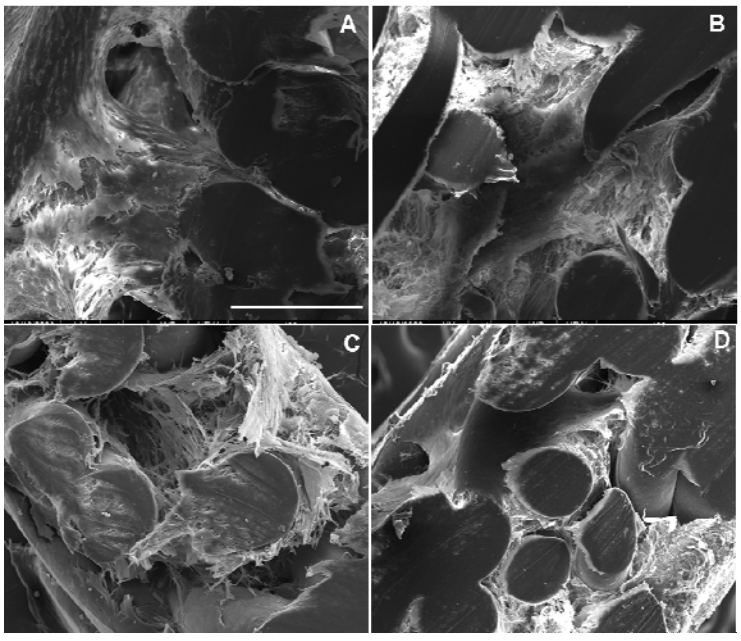


Figure 3. SEM images of the cross-sections of SPCL fiber mesh scaffolds cultured without enzymes (A), with α-amylase (B), with lipase (C) or with α-amylase and lipase (D) in flow perfusion conditions after 16 days. The scale bar is 400 μm and applies to all images.

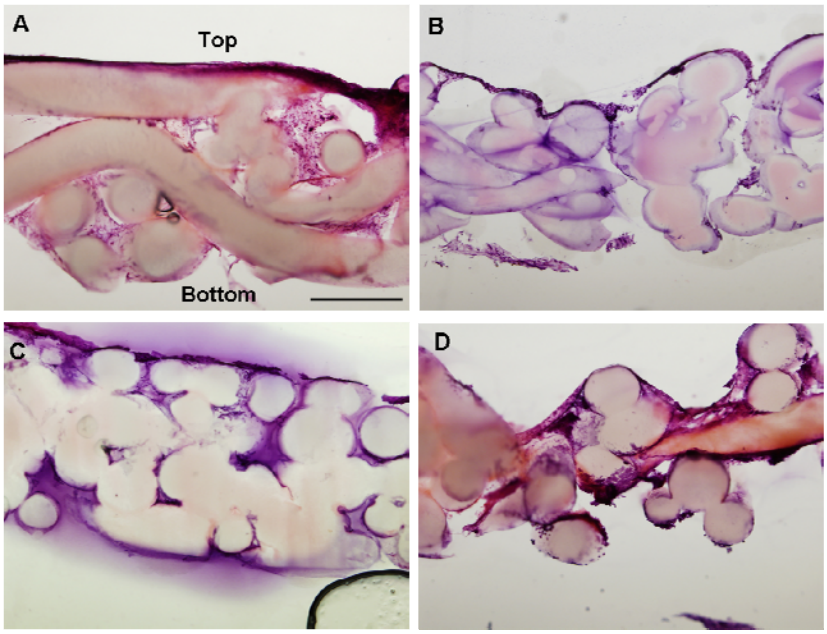


Figure 4. Representative histological cross-sections of SPCL fiber mesh scaffolds cultured for 16 days in flow perfusion conditions without enzymes (A), with α-amylase (B), with lipase (C) or with α-amylase and lipase (D). The flow direction was from the top of the image through the scaffold to the bottom. Sections have been stained with hematoxylin and eosin and shown at 4x magnification. The scale bar corresponds to 500 μm and applies to all images.

3.3. Alkaline phosphatase activity

ALP is considered to be an early stage marker of osteogenic differentiation.[12] Typically a rise and fall of ALP activity is characteristic of osteoblastic differentiation.[2,3] However, ALP can be expressed at high levels near the end of the proliferative period and during the period of extracellular matrix deposition and maturation.[12] Such a trend is observed in Figure 5, where all groups cultured under flow conditions, with the exception of SPCL/cell constructs supplemented with both enzymes, had a significant increase of ALP activity at day 16. The highest peak of ALP activity was observed for SPCL/cell constructs cultured without enzymes in flow perfusion conditions. The ALP activity was normalized to reflect the ALP activity per cell. Results show significant differences between flow perfusion and static cultures for complete osteogenic media without enzymes, with α-amylase and with lipase. Flow significantly enhanced the ALP activity for all groups, with the exception of SPCL/cell constructs cultured with α-amylase and lipase. There was no apparent positive effect of adding enzymes to culture media on ALP activity implying that the influence of enzymes predominantly affected the later osteoblastic differentiation, as characterized by

mineralization (Figure 5), more than the early osteoblastic differentiation, as characterized by ALP activity.

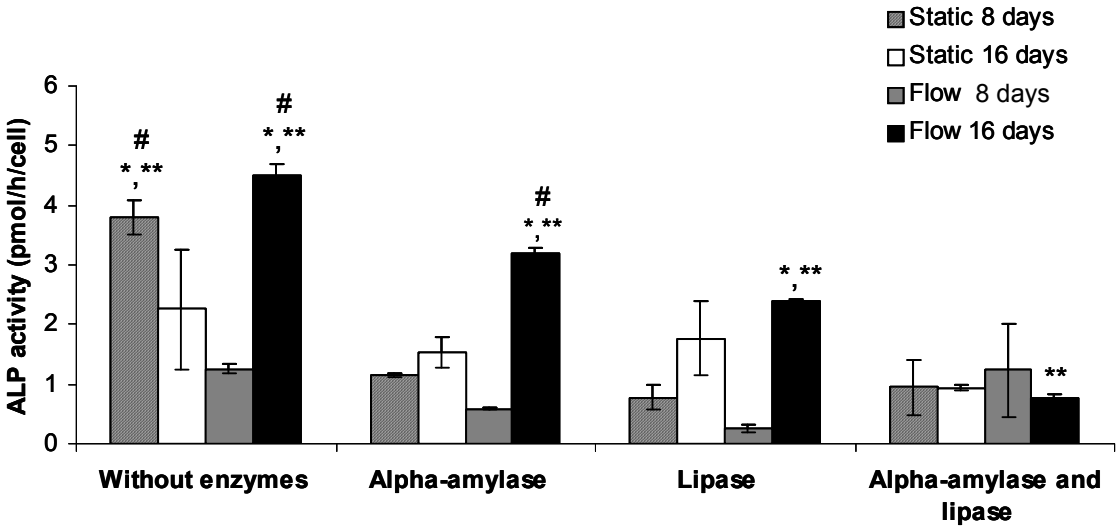


Figure 5. Alkaline phosphatase activity of rat bone marrow stromal cells cultured *in vitro* without enzymes, with α-amylase, with lipase, or with α-amylase and lipase upon SPCL fiber mesh scaffolds for up to 16 days in static and flow conditions. Results are expressed as means ± standard deviation with n=3 for each bar. (*) Indicates a significant difference (p<0.05) between 8 and 16 days; (**) indicates a significant difference (p<0.05) between groups (with and without enzymes) in static or flow conditions; and (#) indicates a significant difference (p<0.05) between flow and static conditions.

3.4. Calcium deposition measurement

The calcium content in scaffolds is an indication of the production of mineralized matrix and a marker of the late-stage osteoblastic differentiation of cells.[11,14] Even in static cultures, there was a significant increase in the mineralization of SPCL/cell constructs in the presence of either enzyme between day 8 and 16. It has been previously reported that lipase enhanced osteogenic differentiation of MSCs under static conditions.[8] A similar increase in calcium deposition under static conditions with α-amylase was observed in the present study as well, although a combination of the enzymes failed to produce a similar increase in calcium deposition. The calcium data were corroborated by SEM images where it is possible to see the cross-sections of the constructs and the enhanced distribution of MSCs and ECM throughout the constructs when flow perfusion bioreactors were used (Figure 3). In flow perfusion conditions, the mineralized matrix content of all groups (with or without enzyme supplementation) cultured for 16 days was greatly increased over those cultured in static conditions (Figure 6). SPCL/cell constructs cultured with lipase under flow perfusion conditions showed increased calcium content (1271 ± 32 μg/scaffold) when compared with

SPCL cultured without enzymes (907 ±124 μg/scaffold). In addition, SPCL/cell constructs cultured in flow perfusion bioreactors with both enzymes (α-amylase and lipase) showed significantly greater calcium deposition at 8 days when compared with other groups. The calcium data were further corroborated by SEM images, where cross-sections of the constructs showed deeper and more extensive distribution of mineralized ECM throughout the constructs when flow perfusion bioreactors were used (Figure 3).

One of the objectives of this study was to examine the efficacy of the enzymes in inducing osteogenic differentiation. The literature indicates that besides being responsible for poly(ε-caprolactone) degradation, lipase plays an important role in osteoblastic differentiation of rat bone marrow stromal cells when added to culture media.[8] Under flow perfusion conditions and in the presence of lipase, SPCL/cell constructs cultured for 16 days in the present study showed the highest amount of calcium (1271 ± 32 μg/scaffold). However, the calcium content of SPCL/cell constructs cultured under flow perfusion condition with culture medium supplemented with both enzymes (α-amylase and lipase) was 737 ± 25 μg/scaffold, only slightly higher than that obtained with culture medium supplemented with α-amylase. This indicates that the presence of α-amylase does not enhance the deposition of calcium and therefore the osteogenic differentiation of MSCs. Furthermore, α-amylase does not appear to improve the cellularity of MSCs on the SPCL constructs. Considering these results, it can be hypothesized that the lower calcium amount could be related to the lower cell number obtained with cellular scaffold constructs treated with α-amylase. The decrease in cell number observed with α-amylase could be attributed to the loss of surface area of SPCL fiber scaffolds, due to the dissolution of starch present within the scaffold in the presence of α-amylase. It has been previously shown that SPCL scaffolds, which are a blend of 30% starch and 70% PCL, undergo significant weight loss in the presence of α-amylase.[8] A weight loss of approximately 25% was observed between day 7 and 14 in α-amylase, which was significantly greater than the weight loss observed in the presence of lipase alone. This study indicated that the weight loss in the presence of α-amylase was mainly due to the partial degradation and release of starch present in the SPCL scaffolds. Moreover, when SPCL/cell constructs were cultured under flow and in the presence of α-amylase, the number of cells was lower when compared with the other groups. For this condition, the calcium data reflected a lower degree of mineralization. One possible explanation could be related to the degradation of starch by α-amylase after 16 days of culture under flow conditions. Previous degradation studies with α-amylase showed a pronounced weight loss of approximately 25% after 3 days which increased slightly to 30% after 30 days.[8] Since SPCL is a blend of 30% starch and 70% poly(ε-caprolactone), this weight loss might be related with the degradation of starch. Based on this hypothesis, α-amylase does not have a negative effect on

osteogenic differentiation of MSCs, but the differences observed in the data might be related to the degradation of the starch component of the fibers.

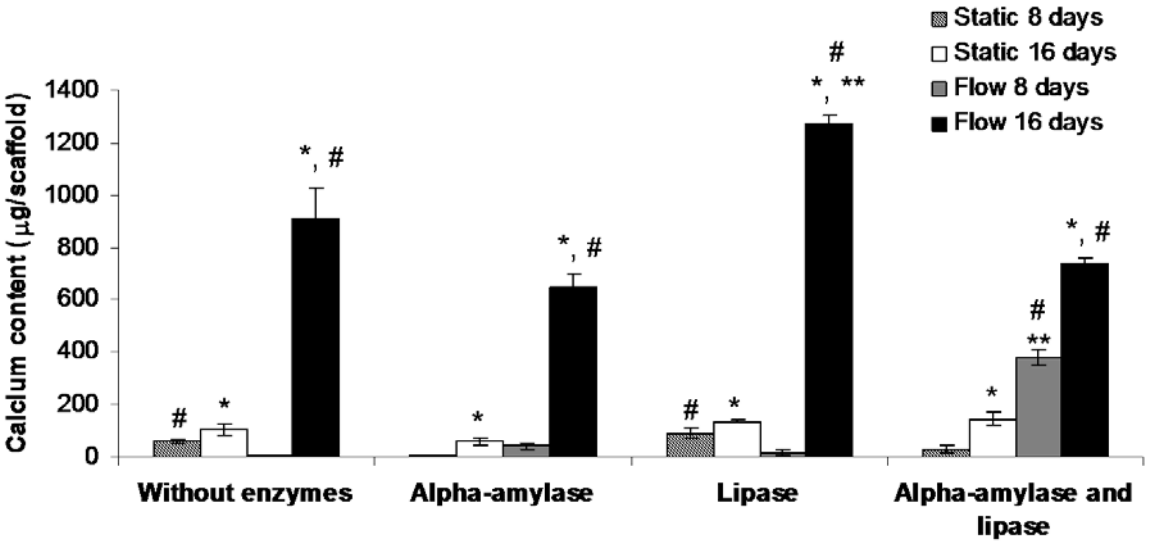


Figure 6. Calcium content of SPCL fiber mesh scaffolds cultured *in vitro* without enzymes, with α-amylase, with lipase, or with α-amylase and lipase in static and flow conditions for 8 and 16 days expressed as total calcium per scaffold. Results are expressed as means ± standard deviation with n=3 for each bar. (*) Indicates a significant difference (p<0.05) between 8 and 16 days; (**) indicates a significant difference (p<0.05) between groups (with and without enzymes) in static or flow conditions; and (#) indicates a significant difference (p<0.05) between flow and static conditions.

3.5. von Kossa staining and tetracycline fluorescence

Mineral deposition is considered to be a marker of full maturation of the osteoblast phenotype in differentiating bone marrow stromal cells. The von Kossa stained sections of all groups cultured for 16 days demonstrated that flow perfusion had a positive effect in the deposition of extracellular matrix, in agreement with the previous results.[2]

Tetracycline is a fluorochrome-labeling agent for bone tissues.[22] Tetracycline accumulates at bone forming sites and fluoresces brightly when activated with fluorescent light. Figure 8 indicates numerous regions in the interior of the scaffolds from all groups cultured under flow conditions where mineral deposition has occurred after 16 days in culture. In contrast, minimal tetracycline fluorescence appeared in scaffolds cultured under static conditions (data not shown). Furthermore, tetracycline fluorescence shows that mineral was more evenly distributed within the scaffold when the constructs were cultured in flow conditions, whereas constructs cultured statically had fluorescence limited to the outer edges of the scaffold. As noted previously, Figure 8A and Figure 8C show an enhanced distribution

and greater amount of mineral deposition throughout the SPCL/cell constructs cultured without enzymes or with lipase, when compared with SPCL/cell constructs cultured with α-amylase or both enzymes together.

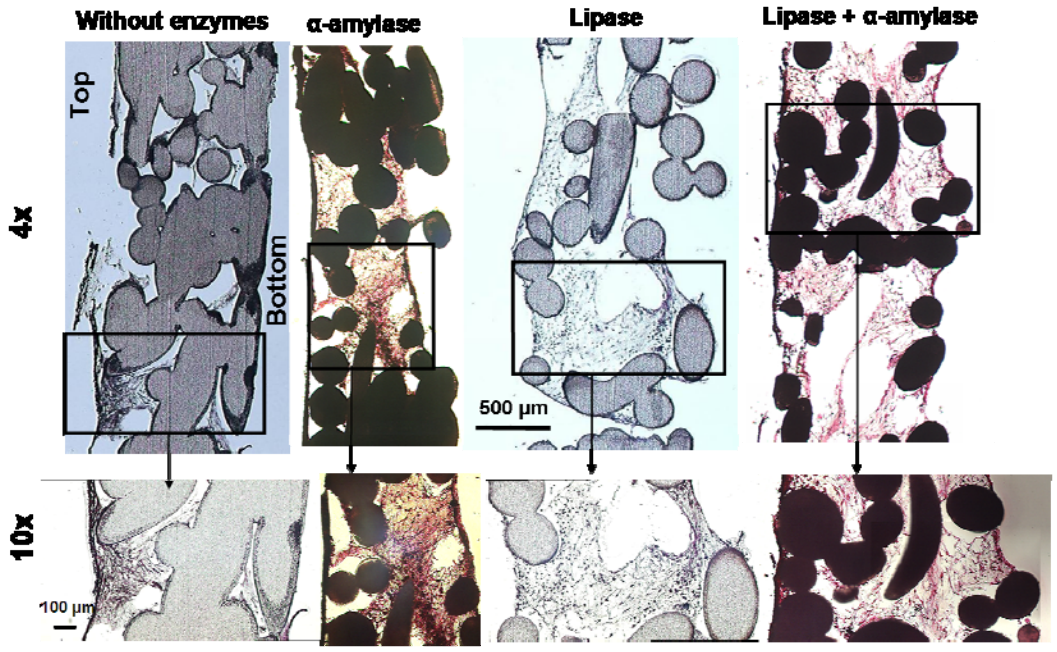


Figure 7. von Kossa stained histological sections of SPCL fiber mesh scaffolds cultured *in vitro* without enzymes, with α-amylase, with lipase, or with α-amylase and lipase for 16 days at different magnifications under flow perfusion conditions.

SEM imaging, von Kossa staining, and tetracycline images showed that the mesh pores of the flow perfusion samples were almost completely filled with matrix after 16 days when SPCL/cell constructs were cultured with osteogenic medium supplemented with lipase. These results were also corroborated by the calcium data, presented above, where the greatest content of calcium was measured when lipase was present. Osteogenic culture medium supplemented with lipase did not only stimulate enhancement of mineralized matrix deposition (Figure 6) but also generated mineralized extracellular matrix that was distributed throughout the porosity of the scaffolds (Figures 7C and 8C). Lipase is a molecule previously shown to be capable of directing osteoblastic differentiation of rat MSCs cultured statically.[8] This work corroborates these previous findings and further shows that lipase promotes the osteoblastic differentiation of rat MSCs, especially when coupled with flow perfusion culture.

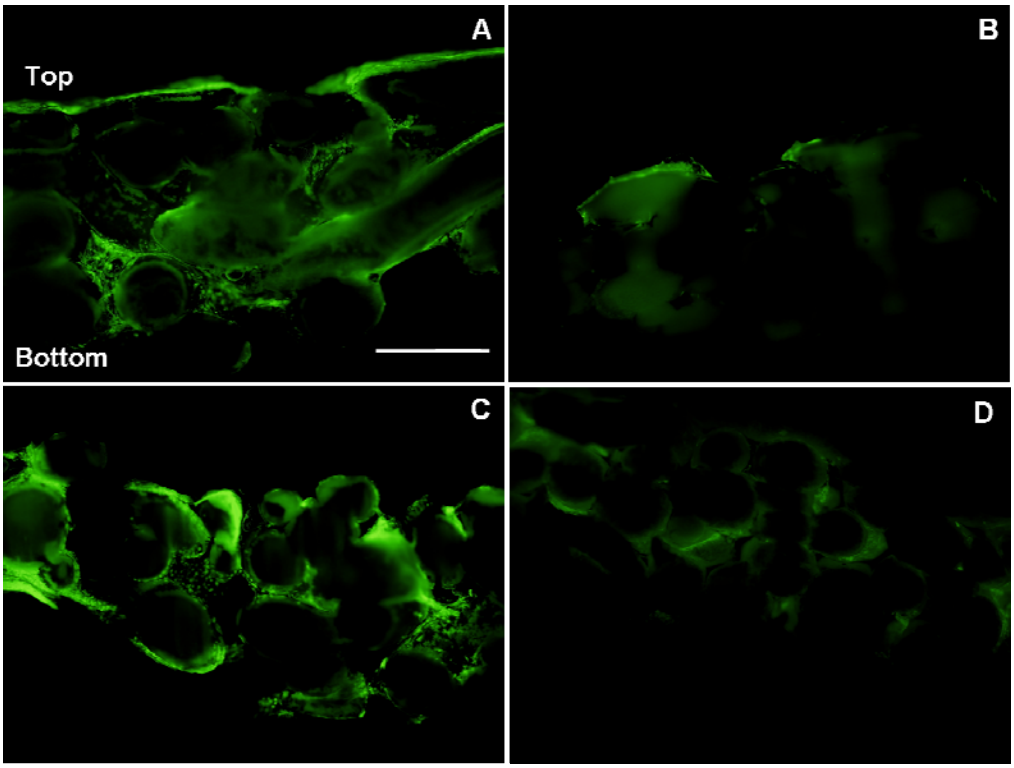


Figure 8. Sections of SPCL fiber meshes cultured without enzymes (A), with α-amylase (B), with lipase (C) or with α-amylase and lipase (D) for 16 days observed under fluorescent light, showing the tetracycline labelling of mineral in flow perfusion culture conditions. All images were obtained using a 4x APO objective. The scale bar is 500 μm and applies to all images.

4. CONCLUSIONS

This work demonstrates that osteogenic media supplemented with α-amylase, or with α-amylase and lipase together, and cultured in flow perfusion bioreactors did not enhance osteoblastic differentiation of rat marrow stromal cells compared with SPCL/cell constructs without enzymes. However, it was observed that SPCL fiber mesh scaffold/MSC constructs cultured with osteogenic medium supplemented with lipase under flow perfusion were more mineralized than the other groups examined, which indicates late-stage osteoblastic differentiation of MSCs. This study demonstrates that lipase and flow perfusion conditions act as effective osteogenic stimuli in the differentiation of rat marrow stromal cells, also promoting the production of mineralized extracellular matrix. This strategy of using scaffolds that are enzymatically degraded by enzymes naturally present in the human blood serum, together with demonstrated improvement of osteoblastic differentiation of MSCs by lipase under flow perfusion conditions shows promising results for bone tissue engineering applications.

ACKNOWLEDGEMENTS

The authors would like to acknowledge Ana R. Costa-Pinto for her help on discussion of the obtained data and to the Portuguese Foundation for Science and Technology (FCT) for the Postdoctoral Grant to Catarina M. Alves (SFRH/BPD/26763/2006). This work was supported by the European NoE EXPERTISSUES (NMP3-CT-2004-500283).

REFERENCES

1. Hutmacher DW, Schantz JT, Lam CXF, Tam KC, Lim TC. State of the art and future directions of scaffold-based bone engineering from a biomaterials perspective. Journal of Tissue Engineering and Regenerative Medicine 2007;1(4):245-260.
2. Gomes ME, Sikavitsas VI, Behravesh E, Reis RL, Mikos AG. Effect of flow perfusion on the osteogenic differentiation of bone marrow stromal cells cultured on starch-based three-dimensional scaffolds. J Biomed Mater Res A 2003;67(1):87-95.
3. Gomes ME, Holtorf HL, Reis RL, Mikos AG. Influence of the porosity of starch-based fiber mesh scaffolds on the proliferation and osteogenic differentiation of bone marrow stromal cells cultured in a flow perfusion bioreactor. Tissue Eng 2006;12(4):801-9.
4. Azevedo HS, Gama FM, Reis RL. In vitro assessment of the enzymatic degradation of several starch based biomaterials. Biomacromolecules 2003;4(6):1703-12.
5. Balmayor ER, Tuzlakoglu K, Marques AP, Azevedo HS, Reis RL. A novel enzymatically-mediated drug delivery carrier for bone tissue engineering applications: combining biodegradable starch-based microparticles and differentiation agents. J Mater Sci Mater Med 2008;19(4):1617-23.
6. Gomes ME, Azevedo HS, Moreira AR, Ella V, Kellomaki M, Reis RL. Starch-poly(epsilon-caprolactone) and starch-poly(lactic acid) fibre-mesh scaffolds for bone tissue engineering applications: structure, mechanical properties and degradation behaviour. J Tissue Eng Regen Med 2008;2(5):243-52.
7. Martins AM, Santos MI, Azevedo HS, Malafaya PB, Reis RL. Natural origin scaffolds with in situ pore forming capability for bone tissue engineering applications. Acta Biomater 2008;4(6):1637-45.
8. Martins AM, Pham QP, Malafaya PB, Sousa RA, Gomes ME, Raphael RM, Kasper FK, Reis RL, Mikos AG. The Role of Lipase and alpha-Amylase in the Degradation of Starch/Poly(epsilon-Caprolactone) Fiber Meshes and the Osteogenic Differentiation of Cultured Marrow Stromal Cells. Tissue Eng Part A 2009;15(2):295-305.
9. Mochizuki M, Hirano M, Kanmuri Y, Kudo K, Tokiwa Y. Hydrolysis of Polycaprolactone Fibers by Lipase - Effects of Draw Ratio on Enzymatic Degradation. Journal of Applied Polymer Science 1995;55(2):289-296.

10. Zeng J, Chen X, Liang Q, Xu X, Jing X. Enzymatic degradation of poly(L-lactide) and poly(epsilon-caprolactone) electrospun fibers. Macromol Biosci 2004;4(12):1118-25.
11. Owen TA, Aronow M, Shalhoub V, Barone LM, Wilming L, Tassinari MS, Kennedy MB, Pockwinse S, Lian JB, Stein GS. Progressive development of the rat osteoblast phenotype in vitro: reciprocal relationships in expression of genes associated with osteoblast proliferation and differentiation during formation of the bone extracellular matrix. J Cell Physiol 1990;143(3):420-30.
12. Beck GR, Jr., Zerler B, Moran E. Phosphate is a specific signal for induction of osteopontin gene expression. Proc Natl Acad Sci U S A 2000;97(15):8352-7.
13. Bancroft GN, Sikavitsas VI, van den Dolder J, Sheffield TL, Ambrose CG, Jansen JA, Mikos AG. Fluid flow increases mineralized matrix deposition in 3D perfusion culture of marrow stromal osteoblasts in a dose-dependent manner. Proc Natl Acad Sci U S A 2002;99(20):12600-5.
14. Sikavitsas VI, Bancroft GN, Holtorf HL, Jansen JA, Mikos AG. Mineralized matrix deposition by marrow stromal osteoblasts in 3D perfusion culture increases with increasing fluid shear forces. Proc Natl Acad Sci U S A 2003;100(25):14683-8.
15. Maniatopoulos C, Sodek J, Melcher AH. Bone formation in vitro by stromal cells obtained from bone marrow of young adult rats. Cell Tissue Res 1988;254(2):317-30.
16. Junge W, Troge B, Klein G, Poppe W, Gerber M. Evaluation of a new assay for pancreatic amylase: performance characteristics and estimation of reference intervals. Clin Biochem 1989;22(2):109-14.
17. Chawla JS, Amiji MM. Biodegradable poly(epsilon-caprolactone) nanoparticles for tumor-targeted delivery of tamoxifen. International Journal of Pharmaceutics 2002;249(1-2):127-138.
18. Datta N, Holtorf HL, Sikavitsas VI, Jansen JA, Mikos AG. Effect of bone extracellular matrix synthesized in vitro on the osteoblastic differentiation of marrow stromal cells. Biomaterials 2005;26(9):971-977.
19. Sikavitsas VI, Bancroft GN, Lemoine JJ, Liebschner MA, Dauner M, Mikos AG. Flow perfusion enhances the calcified matrix deposition of marrow stromal cells in biodegradable nonwoven fiber mesh scaffolds. Ann Biomed Eng 2005;33(1):63-70.
20. Pham QP, Sharma U, Mikos AG. Electrospun poly(epsilon-caprolactone) microfiber and multilayer nanofiber/microfiber scaffolds: characterization of scaffolds and measurement of cellular infiltration. Biomacromolecules 2006;7(10):2796-805.
21. Gomes ME, Bossano CM, Johnston CM, Reis RL, Mikos AG. In vitro localization of bone growth factors in constructs of biodegradable scaffolds seeded with marrow stromal cells and cultured in a flow perfusion bioreactor. Tissue Eng 2006;12(1):177-88.
22. Frost HM, Vilanueva AR, Jett S, Eyring E. Tetracycline-based analysis of bone remodelling in osteopetrosis. Clin Orthop Relat Res 1969;65:203-17.

SECTION 4

CHAPTER V

Natural Origin Scaffolds with *In Situ* Pore Forming Capability for Bone Tissue Engineering Applications

CHAPTER V

Natural Origin Scaffolds with *In Situ* Pore Forming Capability for Bone Tissue Engineering Applications[1]

ABSTRACT

This work describes the development of a biodegradable matrix, based on chitosan and starch, with the ability of forming a porous structure *in situ* due to the attack by specific enzymes present in the human body (α-amylase and lysozyme). Scaffolds with three different compositions were developed: chitosan (C100) and chitosan/starch (CS80-20, CS60-40). Compressive tests results showed that these materials exhibit very promising mechanical properties, namely a high modulus in dry and wet state. The compressive modulus in dry state for C100 was 580±33 MPa, CS80-20 (402±62 MPa) and CS60-40 (337±78 MPa). Degradation studies were performed using α-amylase and/or lysozyme at concentrations similar to those found in human serum, at 37 ºC up to 90 days. SEM micrographs showed that after enzymatic degradation there was the formation of a porous structure, indicating the potential of this methodology to obtain *in situ* forming scaffolds. In order to evaluate the biocompatibility of the scaffolds, extracts and direct contact tests were performed. Results with MTT test showed that the extracts of the materials were clearly non-toxic to L929 fibroblast cells. Analysis of cell adhesion and morphology of seeded osteoblastic-like cells in direct contact tests, at day 7, showed that the number of cells on CS80-20 and CS60-40 was noticeably higher than that on C100, which suggests that starch containing materials may promote cell adhesion and proliferation. This combination of properties seems to be a very promising approach to obtain scaffolds with gradual *in vivo* pore forming capability for bone tissue engineering applications.

[1] This chapter is based on the following publication:

A.M. Martins**,** M.I. Santos, H.S. Azevedo, P.B. Malafaya, R.L. Reis. Natural origin scaffolds with *in situ* pore forming capability for bone tissue engineering applications. Acta Biomaterialia, 4, 1637-1645 (2008).

1. INTRODUCTION

Tissue engineering has recently emerged as a new interdisciplinary science to repair injured body parts and restore their functions by using laboratory-grown tissues, materials and artificial implants. An ideal scaffold to be used for bone tissue engineering should possesses characteristics of excellent biocompatibility, adequate pore size, controllable biodegradability and suitable mechanical properties [1-3]. The choice of the appropriate fabrication technique is critical because it can significantly influence the properties of the implant and its degradation characteristics. There is, therefore, an increasing need to look for new materials and methodologies to produce scaffolds for bone tissue engineering. One interesting possibility is to develop an *in vivo* responsive scaffold which properties may be regulated by the bone regeneration process, with gradual formation of pores *in situ* and consequent resorption. This hypothesis seems to be very promising due the control of degradation *in situ* and consequent pore formation, which allows to have scaffold with the required mechanical properties in the initial stage of implantation.

One of the present trends in implantable applications requires materials that are derived from nature. Natural origin materials have been demonstrated to promote healing at a faster rate and are expected to exhibit greater compatibility with human tissues. The combination of chitosan with other materials appears to be a common theme in a various reports [4,5]. Chitosan is a linear copolymer of N-acetyl-D-glucosamine and D-glucosamine and it is a deacetylated derivative of chitin. The degree of deacetylation (DD) represents the proportion of D-glucosamine units with respect to the total number of units. DD is a structural parameter which influences physicochemical properties [6] such as solubility, crystallinity, swelling behavior and biological properties [6], namely the biodegradation by lysozyme [7,8], the wound healing properties [9] and the osteogenesis enhancement [10]. One of the interesting features of chitosan is its cationic nature, resulting from primary amine groups, thus forming water-insoluble ionic complexes with a variety of a polyanionic substances. It is normally insoluble in aqueous solution above pH 7. However, in diluted acids (pH < 6), the free amino groups are protonated and polymer becomes soluble. Chitosan has been applied to induce the extracellular matrix formation in tissue regenerative therapy [11]. The degradation of chitosan in the human body has been reported to be carried out by lysozyme [7,8]. The degradation kinetics appears to be inversely related to degree of deacetylation [8,12]. Lysozyme, or muramidase, is an enzyme that catalyzes the hydrolysis of the peptidoglycan layer of bacterial cell walls. Human lysozyme is found in various body fluids in concentrations from 7 to 13 mg/l[13-15] in serum and from 450 to 1230 mg/l in tears[13,14], saliva[13,14] and other fluids including those surrounding cartilage [16]. Following implantation of a biomaterial, neutrophils and monocyte-derived macrophages will be present around the foreign material

in both the acute and chronic phases of inflammation. A number of enzymes, such as lysozyme, and reactive species will be released from these cells.

Biodegradable starch-based polymeric biomaterials have been studied and proposed for a wide range of biomedical applications. Starch is one of the most abundant naturally occurring polymers, presenting a combination of properties that is steadily increasing its uses on several technologies. Starch is a natural polymer that presents excellent characteristics to be applied in the biomaterials field, which are mainly low toxicity[17,18], biodegradability[19], biocompability[20,21]. It is inexpensive and above all reusable. The main enzymes involved in starch degradation are α-, β-, amylase, glucosidase and other debranching enzymes. Starch is hydrolysed to glucose, maltose and dextrin. It is well known that salivary amylase is involved in the gastric and intestinal digestion of starch in food components. Amylase can also be found in human serum.

The aim of this work was to develop a biodegradable matrix, based in chitosan and native starch, that will form a porous structure *in vivo* by the preferential attack of the matrix by specific enzymes present in the human body (namely the α-amylase and lysozyme). The inclusion of an enzymatically degradable phase in biomaterials may constitute an interesting approach to obtain scaffolds with adequate mechanical properties and with a gradual *in situ* pore forming ability. Using this innovative methodology, the developed scaffolds can exhibit very promising mechanical properties, due the inexistence of macroporosity, at the initial stage of implantation. The porosity will be formed *in situ* by enzymes present in human body.

In this work, chitosan/starch scaffolds were developed by using a precipitation method. These systems were analyzed in terms of morphology, degradation behavior and mechanical properties. This study also addressed the effect of leachables from developed scaffolds on the viability of mouse fibroblasts and the influence of the constructs surface on the morphology, adhesion and spreading of fibroblast and human osteoblasts.

2. MATERIALS AND METHODS

2.1. Materials

Chitosan with DD of 92% (determinated by the titration method as described in [22]) and native corn starch were purchased from Sigma (St. Louis, USA). Sodium hydroxide (NaOH) and sodium sulphate (Na_2SO_4) were supplied from Panreac (Barcelona, Spain) α-amylase from *Bacillus amyloliquefaciens* was obtained by Genencor International, Inc. (Rochester,

NY, USA); egg white lysozyme and bovine serum albumin (BSA) were purchased from Sigma (St. Louis, USA).

2.2. Scaffolds preparation

Chitosan was dissolved in acetic acid 1% (v/v) to obtain a 5% (w/v) solution (C100). Then, using the same procedure other formulations were prepared with the following ratios: 80/20 chitosan/starch scaffolds (CS80-20) and 60/40 chitosan/starch scaffolds (CS60-40). The solutions were casted into moulds and frozen (-18ºC) overnight. They were then immersed in a precipitation solution (25% NaOH 1M and 75% Na_2SO_4 0.5M) overnight, adapted from Tuzlakoglu *et al*.[23]. After precipitation, the samples were washed repeatedly with distilled water to remove excess of salts, dried at 37ºC and followed by successive washings for 5 days until no pH changes were detected.

2.3. Degradation studies

Degradation studies were carried out by incubating the scaffolds in phosphate buffered saline (PBS) solution (pH 7.4) containing α-amylase (150 U/L[15,24]) and/or lysozyme 13 mg/L[13-15]), at concentrations similar to the ones found in human serum, at 37ºC up to 90 days. A control was also performed by incubating the samples in buffer alone. At the end of the degradation period, the samples were removed and immediately weighed for determination of water uptake, washed thoroughly with distilled water and dried for later calculation of weight loss. Degradation solutions were also analyzed to measure the concentration of reducing sugars, released into the solution as result of starch hydrolysis by α-amylase, using the dinitrosalicylic acid method.

2.4. Analysis of sample morphology by scanning electron microscopy (SEM)

The cross-sections morphology, before and after degradation, was observed by scanning electron microscopy (SEM) in a Leica Cambridge S360. All samples were previously coated with a gold layer (Fisons Instruments, Sputter Coater SC502, UK).

2.5. Mechanical properties – compression tests

The mechanical properties of the materials were evaluated on compression tests carried out in the dry and wet state in an Instron 4505 universal mechanical testing machine at a controlled environment (23ºC and 55% RH). The cross-head speed was 2 mm/min until 1% strain.

2.6. Cell lines used for biocompatibility testing

For biocompatibility assessment of the different formulations of the developed scaffolds two different cell types were used: L929 (ECACC, European Collection of Cell Cultures), a mouse fibroblast cell line and SaOs-2 (ATCC, American Type Culture Collection), a cell line derived from human osteosarcoma. L929 is a cell line commonly used in cytotoxicity testing and osteoblast-like SaOs-2 cells were chosen because they are a model of a relevant cell type for the medical application of the implant. Both cell lines were cultured in Dulbecco's Modified Eagle's Medium (DMEM, Sigma, St Louis, USA), supplemented with 10% Foetal Bovine Serum (FBS, Biochrome) and 1% antibiotic/antimicotic solution (Sigma, St. Louis, USA). In all the experiments cells were kept in an incubator at constant temperature (37ºC) and CO_2 concentration (5%).

2.7. Biocompatibility evaluation: extracts and cell adhesion studies

In the scope of biocompatibility assessment, and according to ISO norms, two categories of *in vitro* cytotoxicity assays were performed: extract and direct contact tests. The scaffolds, previously sterilized by ethylene oxide, were extracted in complete culture medium for 24h at constant temperature (37ºC) and agitation (60 rpm). L929 cells were seeded in 96 wells cell culture plates (10 000 cells/cm^2), in order to reach 80% confluence in 24h. The extracts were filtered and placed in contact with the monolayer of L929 cells for 72hrs. A control, with cells grown in the presence of complete culture medium, was included. Afterwards, the viability test MTT was performed. Briefly, the culture medium was replaced by a solution of MTT and the cells were incubated for 4 hrs. The viable cells, those with functional mitochondrial dehydrogenase, were able to reduce the yellow MTT into a purple formazan product. The end product was quantified by spectroscopy and the results expressed as percentage of cell viability.

In direct contact test, the developed scaffolds were seeded with L929 cells (8x 10^4/50 µL) and with osteoblast-like cells (5x10^5 cells/mL), for 3 and 7 days. Prior to cell seeding, the

chitosan/starch scaffolds were immersed in culture medium overnight. This step intends to reduce culture medium uptake by the highly hydrophilic materials. After each time point, the samples were fixed with glutaraldehyde, dehydrated, critical point dried and gold sputtered for SEM observation.

3. RESULTS AND DISCUSSION

3.1. Characterization of the scaffolds morphology

In this work, degradable scaffolds based on chitosan and native corn starch were developed aimed to be used in bone tissue engineering applications. Three different compositions were prepared and tested. Figure 1 shows the interior morphology of the obtained scaffolds. C100 material exhibits a smooth surface (Figure 1A), whereas in the micrographs of CS80-20 and CS60-40 scaffolds (Figure 1B and 1C) it is possible to observe that the starch granules are homogenously distributed along the chitosan matrix, as well its incorporation in the chitosan matrix. Starch granules have dimensions from 0.5 to 175 μm [25] that is main dependent from its origin. SEM micrographs (Figure 1B and 1C) shows that starch granules from native corn starch have dimensions from 5-10 μm. The proposed processing technique is based in a precipitation solution. This technique was used with the aim of promoting the ionic complexation. This precipitation method does not allow to obtain a macroporous structure (Figure 1). The macroporosity will be formed *in situ* by human enzymes present in human serum.

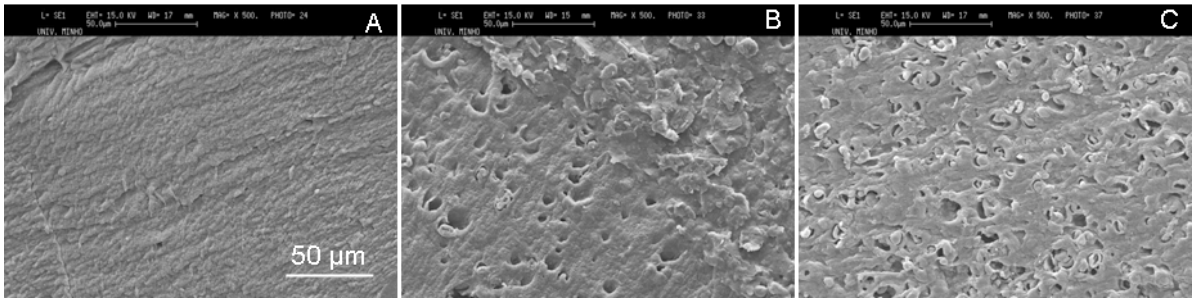


Figure 1. SEM micrographs of the developed scaffolds (transversal sections) before degradation: C100 (A), CS80-20 (B) and CS60-40 (C). The scale bar is 50 μm and applies to all images.

3.2. Degradation behavior

The main aim of these degradation studies, using α-amylase and lysozyme with similar concentrations to the ones found in human serum, is to simulate the physiological

conditions and subsequent pore formation. It is expected that this innovative methodology will induce the formation of pores. The pore size and its distribution in the scaffold can be controlled by the location of the 'sacrifice' phase (native starch) that will also control the water uptake behavior due to the different hydrophilic nature of the materials. The hypothesis of this work is related with the formation of pores due to the degradation induced by specific enzymes ubiquitous in the human body. After implantation it is expect that a porous structure will formed *in situ* allowing the penetration of the cells deep into these scaffolds.

Concerning the water uptake in PBS, the C100 scaffolds present the highest hydration degree, of about 140% (Figure 2). The ability of a material to keep water and its water permeability are important parameters to be studied, since it will influence the absorption of body fluids and the transfer of cell nutrients and metabolites through the materials. The diffusity of nutrients is a very important parameter since in an *in vivo* situation, a porous structure will be formed, induced by enzymes present in human body allowing the penetration of cells deep into the scaffolds. As expected, the water uptake of CS80-20 and CS60-40 is lower than C100, which is due to the presence of starch that is less hydrophilic than chitosan (Figure 2). The weight loss in PBS was not significant (data not shown). The highest weight loss was observed in CS60-40. This fact can be explained by the presence of starch granules that are physically distributed. These results suggest that different percentages of starch influence the degradation rate.

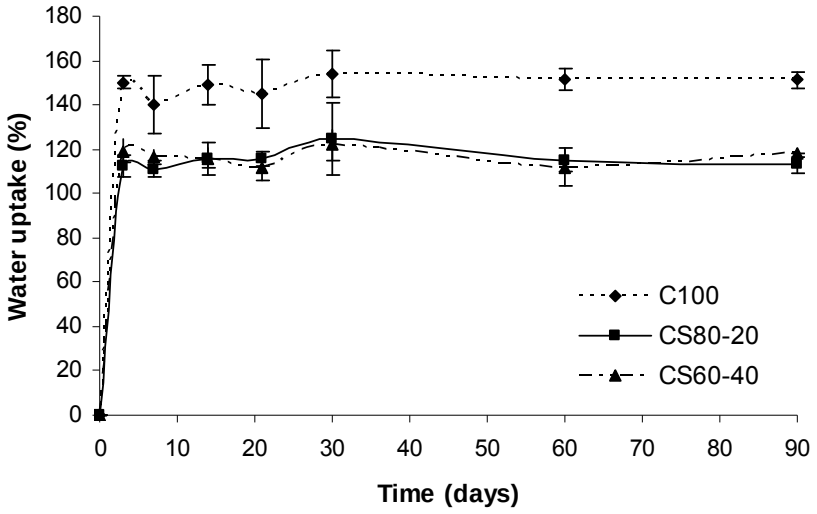


Figure 2. Water uptake of scaffolds as a function of immersion time in PBS (pH 7.4, T = 37º C).

All scaffolds were sectioned to observe the interior morphology and formation of pores induced by enzymes at similar concentrations to those found in human serum. By SEM observation it was detected, as expected, the attack of the native starch phase (CS80-20 and CS60-40) (Figures 3C and 3D) in the presence of α-amylase. It was also observed that α-amylase induced the formation of pores in C100 material (Figures 3A and 3B). It was also reported by Muzzarelli *et al.* [26] that α-amylase was able to attack the chitosan material.

In the presence of lysozyme, it was possible to detect the preferential attack of C100 (Figure 3E) since this enzyme is able to hydrolyse chitosan in some extend. It is expected that, when the scaffolds will be implanted in the body, the chitosan would be degraded gradually by lysozyme and then reabsorbed. Lysozyme is known to be ubiquitous in the body[13,27]. The main advantage of biodegradable over non-biodegradable materials is the disappearance of implanted foreign materials which might elicit foreign body reactions from the host's defence system during their long term contact with a living structure. Since lysozyme is present in cellular lysosomes and lysosomal rupture is associated with inflammation, it has been assumed that the source of the increased lysozyme activity is the release of enzyme from the lysossomes of phagocytic cells[28]. When any material is implanted an acute inflammatory response will occur, and it is known in this situation the pH values will decrease and high levels of lysozyme are secreted to the surround medium. Furthermore, it has been demonstrated that the initial degradation rate of chitosan at pH 4.5 is about five times higher than the rate at pH 7.0[14]. The results obtained in this work showed the attack of C100 by lysozyme and the consequent pore formation.

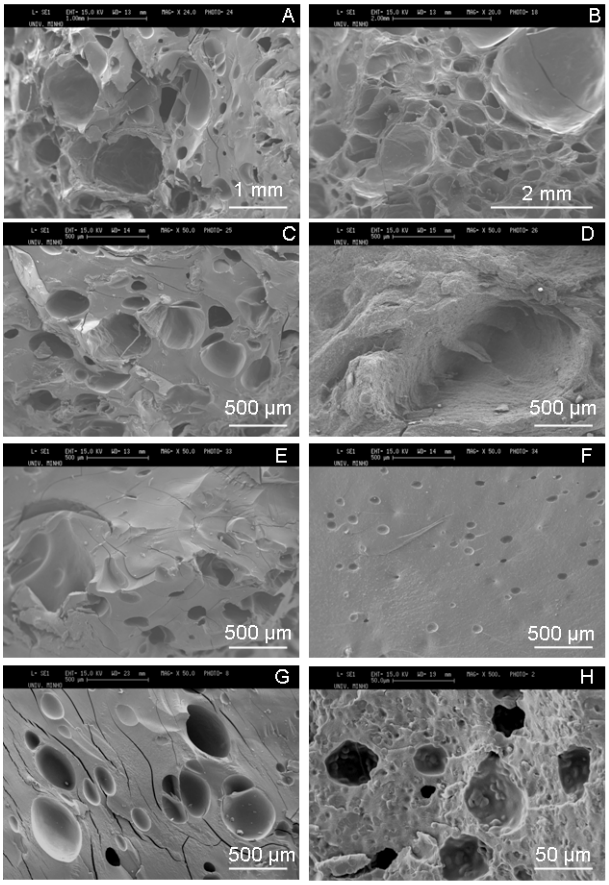


Figure 3. SEM micrographs showing the morphology of chitosan-based scaffolds after 14 days in PBS with α-amylase solution (A-C100, C- CS80-20, D- CS60-40); after 30 days in same solution (B- C100); after 14 days in PBS with lysozyme solution (E- C100, F- CS80-20) and in the same period in PBS with α-amylase and lysozyme solution (G-C100, H-CS60-40).

In order to investigate the effect of an enzyme cocktail, containing α-amylase and lysozyme together, on the overall degradation rate of the materials, as well as on the type of porosity obtained, the materials were also simultaneously incubated with these enzymes. Analysing the results presented in Figure 4 it is possible to observe that CS60-40 showed the highest weight loss, when compared with CS80-20 and C100. The higher susceptibility of CS60-40 to enzymatic degradation may be related with the presence of a higher surface area for preferential attack, due to the interface between the two components. SEM micrographs (Figures 3G and 3H) show that after enzymatic degradation there is the formation of a porous structure. Some studies showed that pore sizes less than 15-50 µm result in fibrovascular ingrowth, pore sizes of 50-150 µm encourage osteoid formation, and pore sizes greater than 150 µm encourage the ingrowth of mineralized bone[29].

Since the formation of pores in the presence of lysozyme was not so pronounced compared to those obtained with α-amylase or the two enzymes together (α-amylase and lysozyme) these studies must be improved. One possible alternative could be the incorporation of lysozyme in higher concentrations at the surface of these materials. It might be adequate to enhance the *in vivo* performance using a CaP coating since these materials itself are not osteoconductive/osteoconductive. Several papers report the incorporation of enzymes or bioactive agents into CaP coatings in order to promote their degradation and/or their osteoconductive/osteoinductive potential[30-32]. It is expected also that in an *in vivo* situation the pore formation will occur more rapidly, due the inflammatory response that decreases the pH and also because high levels of lysozyme will be released by several cells such as neutrophils, monocytes and macrophages.

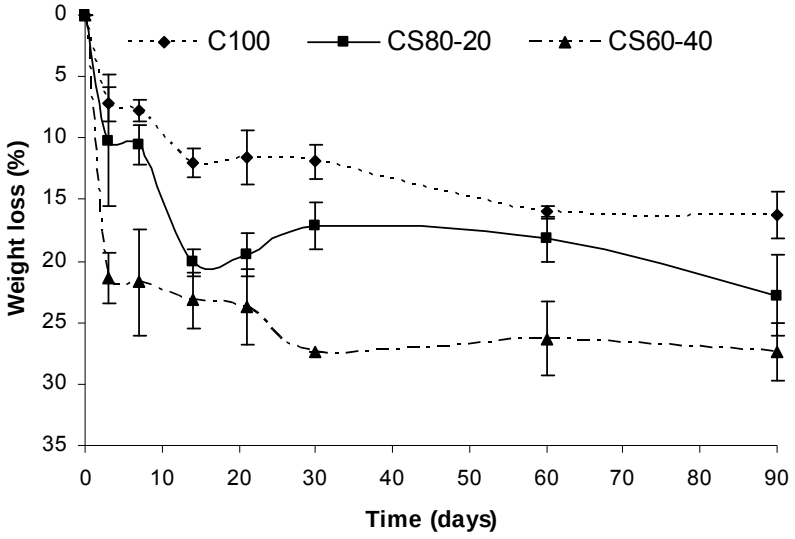


Figure 4. Weight loss of chitosan/starch scaffolds as function of time in PBS with α-amylase (150 U/L) and lysozyme (13 mg/L) (pH 7.4, T = 37º C).

After enzymatic degradation it was observed the formation of a porous structure, indicating the potential of this methodology to obtain "smart" *in vivo* forming scaffolds for bone tissue engineering applications.

The *in vitro* pore formation in the presence of enzymes at the similar concentration to those found in human plasma is clear. It is expected that in an *in vivo* situation the pore formation will occur more rapidly, due to the presence of other enzymes and cells.

3.3. Mechanical properties

A hard material, with a high initial mechanical strength and an adequate degradation rate, is normally required for bone tissue engineering applications. The results of the compressive tests showed that these materials exhibit very interesting mechanical properties in the dry and even in the wet state. The highest compressive modulus was observed for C100 (580±33 MPa) in the dry state. For CS80-20 and CS60-40, the compressive moduli in the dry state were 402±62 MPa and 337±78 MPa, respectively (Figure 5). The values found are higher than the typical values presented for chitosan-based materials. The modulus decreased with increasing amounts of starch present in the scaffolds. This can be due to the poor adhesion between the phases, since it is a physical mixture, i.e., the 'sacrifice' phase is acting as nucleation site for fracture propagation. In the wet state, it was observed the same tendency, but the values were lower, as it was expected (C100: 107±15 MPa, CS80-20: 53±3 MPa and CS60-40: 31±1 MPa) (Figure 5). The mechanical properties exhibited by the scaffolds in the wet state fall in the normal ranges of strength and modulus for trabecular bone which are about 0.02-0.5 GPa [1,3] for compressive modulus and 2-12 MPa [1,3] for strength.

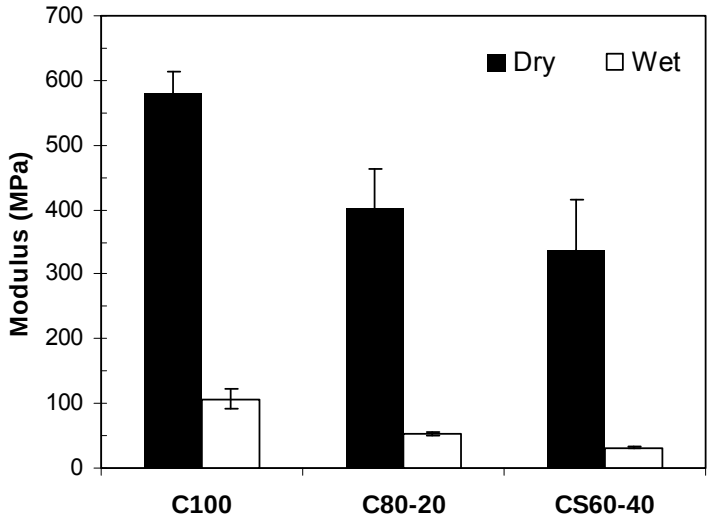


Figure 5. Results of the compression tests: modulus in dry and wet state.

3.4. Cytotoxic assessment of the extracts

In order to evaluate the cytotoxicity of the substances that leach out of the developed scaffolds the viability assay (MTT test) was performed. This test is based on mitochondria viability, where only functional mitochondria can oxidize an MTT solution, giving a typical blue-violet end product. Figure 6 shows that for CS80-20 and CS60-40 the percentage of

viable cells was around 100%, thus comparable to the control. On the other hand, the value of viable L929 cells in contact with C100 leachables was lower (75%). MTT assay suggested that the extracts from the developed scaffolds, produced by precipitation method, were non-toxic towards mouse fibroblasts.

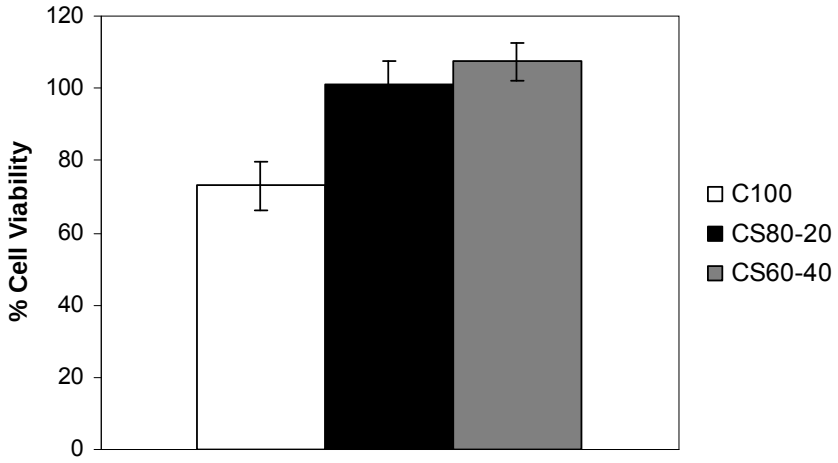


Figure 6. Percentage of L929 viable cells determinated by the MTT in the presence of extracts derived from different formulations of the developed scaffolds. The percentage of viable cells was determined relating the optical density from the control, which is considered to have 100% viability.

3.5. Cell morphology evaluation

The absence of cytotoxicity, however, does not confer knowledge about the biocompatibility of a biomaterial[33]. In order to verify if the developed scaffolds support the functions shared by many cell types such as membrane integrity, adhesion to surfaces and replication, adhesion studies with the cell line L929 were performed. At the end of 7 days, regardless of the scaffold formulation, all constructs were covered with a monolayer of cells (Figure 7). The fibroblasts had a typical spindle-shape morphology and exhibited cytoplasmatic projections strongly attached to the scaffolds. Only in CS80-20 there were some rounded cells denoting that they were in an earlier adhesion step (Figure 7B). L929 cells were able to adhere, spread filopodia and stretch over the surface of the developed scaffolds. The slight toxicity of C100 extracts detected in MTT assay did not have any negative effect on the ability of L929 cells to adhere and spread on the surface of the construct.

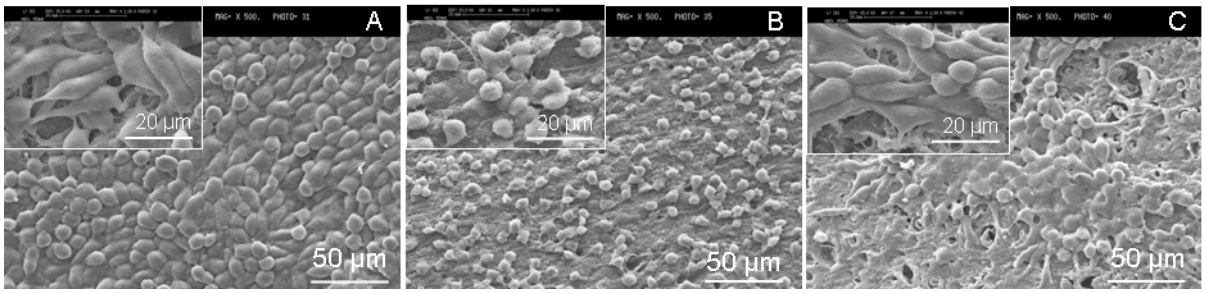


Figure 7. SEM micrographs of the developed scaffolds surfaces, C100 (A and D), CS80-20 (B and E) and CS60-40 (C and F), before cell culture (A-C) and after 7 days of culture with L929 cells (D-F).

Cellular attachment and migration of osteoblast cells over the bone substituting material surface are essential to obtain effective wound filling and bone tissue adaptation[34]. For that, osteoblast-like cells were seeded on C100, CS80-20 and CS60-40 and the adhesion profile, as well as cell morphology was documented by SEM. On day 3 of culture, SEM examination revealed osteoblasts aggregates sparsely distributed over the surface of C100 (Figure 8A). At the same time point, the amount of cells attached to the surface of CS80-20 was higher, although cells did not cover the entire surface of the scaffold (Figure 8B). Figure 8C shows the surface of CS60-40 covered by a compact monolayer of osteoblasts just after 3 days of culture. At this time point is quite notorious the differences between the chitosan scaffold (C100) and the chitosan/starch scaffolds (CS80-20 and CS60-40). The same trend was observed at the end of 7 days. On the C100 scaffold the growth was limited to some restricted areas and probably these areas were the result of the expansion of the cellular aggregates seen after 3 days (Figure 8D). On the other hand, in chitosan-starch scaffolds (CS80-20 and CS60-40) the surface was homogenously covered by a multilayer of osteoblast-like cells (Figures 8E and 8F).

Cell adhesion and spreading are influenced by the physicochemical characteristics of the underlaying solid surface[35]. CS80-20 and CS60-40 supported in the same extent the adhesion of fibroblasts and osteoblasts. However, SaOs-2 behaved in a different way on the surface of C100 scaffold. The poorer spreading on C100 maybe related with the higher chitosan content that renders the surface more hydrophilic. This impairs the adsorption of serum proteins and consequently cell adhesion[35]. Another explanation to the difference between the starch blended scaffolds and chitosan scaffold could be the topography. A higher level of roughness appears capable of enhancing osteoblast adhesion and subsequent proliferation and differentiation[36]. The starch granules present in CS80-20 and CS60-40 increase the roughness of the surface and therefore improve cell growth and attachment (Figures 8E and 8F).

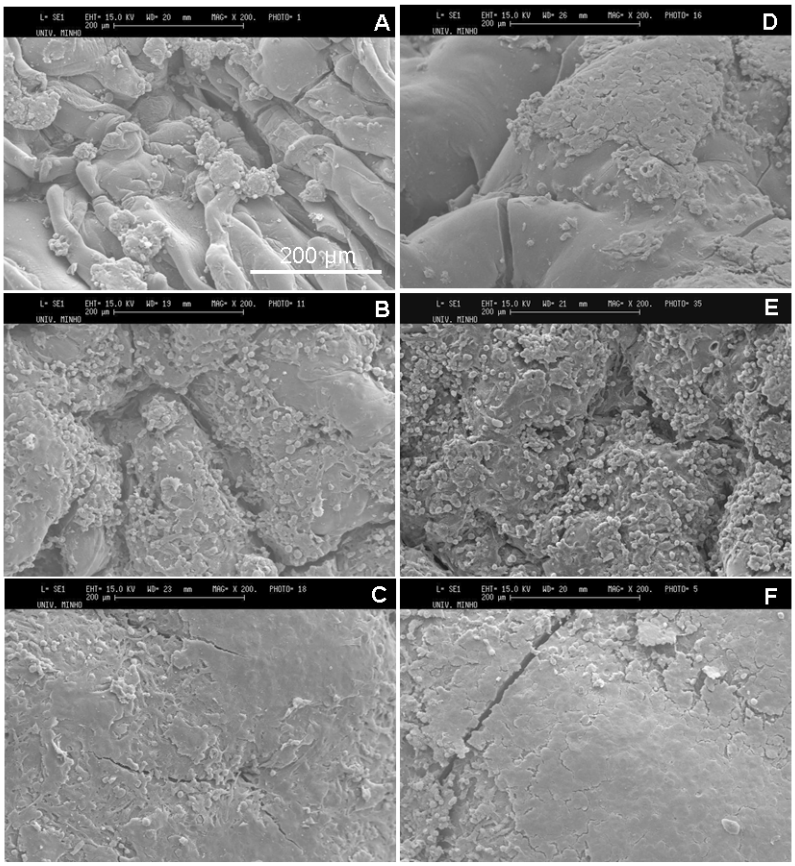


Figure 8. SEM micrographs of C100 (A, D), CS80-20 (B, E) and CS60-40 (C, F) scaffolds cultured with osteoblast-like cells after 3 (A-C) and 7 days (D-F) of culture. The scale bar is 200 μm and applies to all images.

4. CONCLUSIONS

Scaffolds based on chitosan and starch were developed and characterised to be used in bone tissue engineering applications. The results of the compressive tests showed that these materials exhibit very promising mechanical properties in dry and wet state. After enzymatic degradation there was the formation of a porous structure, indicating the potential of this methodology to obtain “smart” *in situ* forming scaffolds. These “smart” scaffolds, with *in situ* pore forming capability and interesting mechanical properties, seem to be advantageous when compared with other conventional materials. Regarding the biocompatibility studies, the extracts of the developed scaffolds were not toxic and concerning the osteoblast attachment, CS80-20 and CS60-40 showed to be a better substratum than C100. These results indicate that the incorporation of starch has a favourable affect in the interaction with osteoblasts.

This combination of properties seems to be a very promising approach to obtain scaffolds with gradual *in situ* pore formation ability for bone tissue engineering applications.

ACKNOWLEDGEMENTS

This work was supported by the European NoE EXPERTISSUES (NMP3-CT-2004-500283), the European STREP HIPPOCRATES (NMP3-CT-2003-505758), and the Portuguese Foundation for Science and Technology (FCT) through POCTI and/or FEDER programmes.

REFERENCES

1. Yang SF, Leong KF, Du ZH, Chua CK. The design of scaffolds for use in tissue engineering. Part 1. Traditional factors. Tissue Engineering 2001;7(6):679-689.

2. Salgado AJ, Coutinho OP, Reis RL. Bone tissue engineering: state of the art and future trends. Macromol Biosci 2004;4(8):743-65.

3. Hutmacher DW, Schantz JT, Lam CXF, Tan KC, Lim TC. State of the art and future directions of scaffold-based bone engineering from a biomaterials perspective. Journal of Tissue Engineering and Regenerative Medicine 2007;1(4):245-260.

4. Suh JK, Matthew HW. Application of chitosan-based polysaccharide biomaterials in cartilage tissue engineering: a review. Biomaterials 2000;21(24):2589-98.

5. Oliveira JM, Rodrigues MT, Silva SS, Malafaya PB, Gomes ME, Viegas CA, Dias IR, Azevedo JT, Mano JF, Reis RL. Novel hydroxyapatite/chitosan bilayered scaffold for osteochondral tissue-engineering applications: Scaffold design and its performance when seeded with goat bone marrow stromal cells. Biomaterials 2006;27(36):6123-37.

6. Chatelet C, Damour O, Domard A. Influence of the degree of acetylation on some biological properties of chitosan films. Biomaterials 2001;22(3):261-8.

7. Varum KM, Myhr MM, Hjerde RJ, Smidsrod O. In vitro degradation rates of partially N-acetylated chitosans in human serum. Carbohydr Res 1997;299(1-2):99-101.

8. Tomihata K, Ikada Y. In vitro and in vivo degradation of films of chitin and its deacetylated derivatives. Biomaterials 1997;18(7):567-575.

9. Ueno H, Mori T, Fujinaga T. Topical formulations and wound healing applications of chitosan. Adv Drug Deliv Rev 2001;52(2):105-15.

10. Klokkevold PR, Vandemark L, Kenney EB, Bernard GW. Osteogenesis enhanced by chitosan (poly-N-acetyl glucosaminoglycan) in vitro. Journal of Periodontology 1996;67(11):1170-1175.

11. Muzzarelli RA, Mattioli-Belmonte M, Tietz C, Biagini R, Ferioli G, Brunelli MA, Fini M, Giardino R, Ilari P, Biagini G. Stimulatory effect on bone formation exerted by a modified chitosan. Biomaterials 1994;15(13):1075-81.

12. Sashiwa H, Saimoto H, Shigemasa Y, Ogawa R, Tokura S. Lysozyme susceptibility of partially deacetylated chitin. Int J Biol Macromol 1990;12(5):295-6.

13. Hankiewicz J, Swierczek E. Lysozyme in human body fluids. Clin Chim Acta 1974;57(3):205-9.

14. Nordtveit RJ, Varum KM, Smidsrod O. Degradation of partially N-acetylated chitosans with hen egg white and human lysozyme. Carbohydrate Polymers 1996;29(2):163-167.

15. Azevedo HS, Reis RL. Understanding the enzymatic degradation of biodegradable polymers and strategies to control their degradation rate. In: Reis RL, San Roman J, editors. Biodegradable systems in tissue engineering and regenerative medicine: CRC Press; 2005. p 177-201.

16. Muzzarelli RAA. Biochemical significance of exogenous chitins and chitosans in animals and patients. Carbohydr Res 1993;20(7):16.

17. Gomes ME, Reis RL, Cunha AM, Blitterswijk CA, de Bruijn JD. Cytocompatibility and response of osteoblastic-like cells to starch-based polymers: effect of several additives and processing conditions. Biomaterials 2001;22(13):1911-7.

18. Salgado AJ, Coutinho OP, Reis RL. Novel starch-based scaffolds for bone tissue engineering: cytotoxicity, cell culture, and protein expression. Tissue Eng 2004;10(3-4):465-74.

19. Azevedo HS, Gama FM, Reis RL. In vitro assessment of the enzymatic degradation of several starch based biomaterials. Biomacromolecules 2003;4(6):1703-1712.

20. Marques AP, Reis RL, Hunt JA. The biocompatibility of novel starch-based polymers and composites: in vitro studies. Biomaterials 2002;23(6):1471-8.

21. Salgado AJ, Coutinho OP, Reis RL, Davies JE. In vivo response to starch-based scaffolds designed for bone tissue engineering applications. J Biomed Mater Res A 2007;80(4):983-9.

22. Tan SC, Khor E, Tan TK, Wong SM. The degree of deacetylation of chitosan: advocating the first derivative UV-spectrophotometry method of determination. Talanta 1998;45(4):713-719.

23. Tuzlakoglu K, Alves CM, Mano JF, Reis RL. Production and characterization of chitosan fibers and 3-D fiber mesh scaffolds for tissue engineering applications. Macromol Biosci 2004;4(8):811-9.

24. Junge W, Troge B, Klein G, Poppe W, Gerber M. Evaluation of a new assay for pancreatic amylase: performance characteristics and estimation of reference intervals. Clin Biochem 1989;22(2):109-14.

25. Reis RL, Cunha AM. Starch and starch based thermoplastics. In: Jurgen KH, Buschow, R., Cahn, W., Flemings, M. C., Ilschner, B., Kramer, E. J., Mahajan, S., editor. Encyclopedia of Materials Science and Technology. Amsterdam: Pergamon-Elsevier Science; 2001. p 8810-8816.

26. Muzzarelli RAA, Mattioli-Belmonte M, Miliani M, Muzzarelli C, Gabbanelli F, Biagini G. In vivo and in vitro biodegradation of oxychitin-chitosan and oxypullulan-chitosan complexes. Carbohydrate Polymers 2002;48(1):15-21.

27. Brouwer J, Vanleeuwenherberts T, Ottingvanderuit M. Determination of Lysozyme in Serum, Urine, Cerebrospinal-Fluid and Feces by Enzyme-Immunoassay. Clinica Chimica Acta 1984;142(1):21-30.

28. Greenwal.Ra, Tsang A, Diamond HS, Josephso.As. Human Cartilage Lysozyme. Journal of Clinical Investigation 1972;51(9):2264-&.

29. Petite H, Viateau V, Bensaid W, Meunier A, de Pollak C, Bourguignon M, Oudina K, Sedel L, Guillemin G. Tissue-engineered bone regeneration. Nature Biotechnology 2000;18(9):959-963.

30. Liu Y, Hunziker EB, Randall NX, de Groot K, Layrolle P. Proteins incorporated into biomimetically prepared calcium phosphate coatings modulate their mechanical strength and dissolution rate. Biomaterials 2003;24(1):65-70.

31. Liu Y, de Groot K, Hunziker EB. BMP-2 liberated from biomimetic implant coatings induces and sustains direct ossification in an ectopic rat model. Bone 2005;36(5):745-57.

32. Azevedo HS, Leonor IB, Alves CM, Reis RL. Incorporation of proteins and enzymes at different stages of the preparation of calcium phosphate coatings on a degradable substrate by a biomimetic methodology. Materials Science & Engineering C-Biomimetic and Supramolecular Systems 2005;25(2):169-179.

33. Van Kooten TG, Klein CL, Kohler H, Kirkpatrick CJ, Williams DF, Eloy R. From cytotoxicity to biocompatibility testing in vitro: cell adhesion molecule expression defines a new set of parameters. J Mater Sci Mater Med 1997;8(12):835-41.

34. Park YJ, Lee YM, Park SN, Sheen SY, Chung CP, Lee SJ. Platelet derived growth factor releasing chitosan sponge for periodontal bone regeneration. Biomaterials 2000;21(2):153-159.

35. Horbett TA, Ratner BD, Schakenraad JM, Schoen FL. Some Background Concepts. In: Ratner BD, Hoffman AS, Schoen FJ, Lemons JE, editors. Biomaterials Science - An Introduction to Materials in Medicine. San Diego, USA: Academic Press; 1996. p 133-164.

36. Montanaro L, Arciola CR, Campoccia D, Cervellati M. In vitro effects on MG63 osteoblast-like cells following contact with two roughness-differing fluorohydroxyapatite-coated titanium alloys. Biomaterials 2002;23(17):3651-9.

CHAPTER VI

Chitosan Scaffolds Incorporating Lysozyme into CaP Coatings Produced by a Biomimetic Route: A Novel Concept for Tissue Engineering Combining a Self-Regulated Degradation System with *In Situ* Pore Formation

CHAPTER VI

Chitosan Scaffolds Incorporating Lysozyme into CaP Coatings Produced by a Biomimetic Route: A Novel Concept for Tissue Engineering Combining a Self-Regulated Degradation System with *In Situ* Pore Formation[1]

ABSTRACT

This study describes an innovative self-regulated degrading material with gradual *in situ* pore formation ability for bone tissue engineering applications. This approach is based on the incorporation of the lysozyme enzyme into calcium phosphate (CaP) coatings, prepared on the surface of chitosan scaffolds by means of a biomimetic coating technique with the aim of controlling their degradation rate and subsequent formation of pores. However, because lysozyme has antibacterial properties, these coatings may act as a carrier for its sustained release, preventing infection upon implantation. In order to prove the concept of *in situ* pore formation, the coated scaffolds (with and without lysozyme) were incubated in two different solutions at different pH to simulate normal physiological conditions (pH 7.4) and inflammatory response (pH 5). The weight loss and morphology of the scaffolds was monitored over time. At pH 7.4, the scaffolds remained more stable than at pH 5. The scaffolds incubated at pH 5 showed a rapid decrease in their initial weight and scanning electron microscopy imaging revealed the formation of a highly porous structure. Furthermore, evaluation of the activity of the incorporated lysozyme revealed that the enzyme was able to hydrolyse the peptidoglycan of the bacteria cell walls (as detected by the decrease in optical density with time), indicating that the enzyme remained active after being incorporated into the CaP coating.

[1] This chapter is based on the following publication:

A.M. Martins, R.C. Pereira, I.B. Leonor, H.S. Azevedo, R.L. Reis. Chitosan scaffolds incorporating lysozyme into CaP coatings produced by a biomimetic route: a novel concept for tissue engineering combining a self-regulated degradation system with *in situ* pore formation, Acta Biomaterialia, in press, doi:10.1016/j.actbio.2009.05.027, (2009).

1. INTRODUCTION

A novel concept in tissue engineering which proposes *in situ* pore-forming scaffolds has been reported previously[1]. Chitosan has been considered a promising material for tissue engineering applications. It is a linear copolymer of *N*-acetyl-D-glucosamine and D-glucosamine, derived from chitin by a deacetylation reaction. The degree of deacetylation (DD) measures the percentage of glucosamine units in the polymer chain and influences its physicochemical properties such as solubility, crystallinity, and swelling behavior and biological properties[2], namely osteogenesis enhancement[3]. The degradation kinetics appear to be inversely related to the DD[4]. It has been demonstrated that chitosan is degraded *in vitro* and *in vivo* by lysozyme[4,5], an enzyme ubiquitous in the human body[6,7]. Lysozyme can attack cell wall polysaccharides of different bacterial species, especially Gram-positive bacteria, leading to rupture of the cell wall and killing of the micro-organism[8,9]. This study proposes the incorporation of the lysozyme enzyme into calcium phosphate (CaP) coatings, prepared on the surface of chitosan scaffolds by means of a biomimetic coating technique, with the aim of controlling their degradation rate and subsequent formation of pores. Furthermore, since lysozyme has antibacterial properties, these coatings may act as a carrier for its sustained release, preventing infection upon implantation. An improvement in the osteoconductivity of implants has been achieved by coating their surfaces with CaP layers[10-12]. The biomimetic methodology for coating biomaterials with a bone-like apatite layer has been described in several publications[13-17]. This technique mimics natural biomineralization processes, involving controlled crystal nucleation and growth control over the phase of the mineral deposited[18]. The main advantage of the biomimetic methodology is the use of physiological conditions (pH 7.4 at 37 ºC) simulating the manner in which apatite is formed in bone. Moreover, this technique allows the incorporation of proteins and bioactive agents into CaP coatings without compromising their activity[19-22]. An ideal material for the purpose of a temporary support for bone replacement should feature an adequate range of mechanical properties with convenient degradation kinetics, bone-bonding behavior and biocompatible performance[23].

In order to enhance the formation of pores *in situ*, chitosan scaffolds coated with CaP layers and lysozyme incorporated into the coatings were developed, presenting properties that promote degradation and osteoconductive potential. Lysozyme enzyme was incorporated into CaP coatings on the surface of chitosan scaffolds by means of a biomimetic route[13,14,22]. Moreover, CaP coatings enhance the osteoconductive properties of the chitosan scaffolds.

This study was designed to answer the following questions: Can a hydrolytic enzyme be incorporated at the surface of chitosan scaffolds without compromising its activity? Is it possible to develop a non-porous scaffold with in situ pore-forming ability? How many days does it takes to have a porous scaffold in situ fully interconnected simulating *in vivo* conditions?

2. MATERIALS AND METHODS

2.1. Materials

Chitosan with a DD of 92% and medium molecular weight was obtained from Sigma (St. Louis, USA). Bioglass® 45S5 with the following composition: 45 SiO_2, 24.5 CaO, 24.5 Na_2O and 6.0 P_2O_5 (in wt.%) was supplied by NovaMin Technology Inc. (Alachua, FL).

2.2. Preparation of chitosan scaffolds

Chitosan scaffolds were prepared as previously described by Martins *et al.*[1]. Briefly, chitosan was dissolved in acetic acid 1% (v/v) to obtain a 5% (w/v) solution. Then, the solution was casted into polyethylene moulds and frozen (-18ºC) overnight. After that, they were immersed in a precipitation solution (25% NaOH 1M and 75% Na_2SO_4 0.5M) overnight, adapted from the method developed by Tuzlakoglu *et al.*[24]. After precipitation, the samples were washed several times with distilled water and dried at 37 ºC.

2.3. Preparation of CaP biomimetic coatings

The method of preparing the CaP coatings was based on the methodology previously developed by Abe *et al.*[13] and adapted by Reis *et al.*[14,15] consisting in impregnation of the materials with bioactive glass called Bioglass® 45S5, followed by immersion in a simulated body fluid (SBF, 37 ºC, pH 7.4), presenting ionic concentrations similar to human blood plasma. Prior to the coating process, chitosan scaffolds were sterilized by ethylene oxide. Bioglass® 45S5 was sterilized by immersion in ethanol solution (70% v/v) and then dried inside the hood. All the subsequent work was performed under sterile conditions in a hood. Briefly, chitosan scaffolds were rolled in a wet bed of Bioglass® 45S5. After that, the scaffolds were immersed in a 1.0 SBF solution, without (control) and with lysozyme (1 g/L) from chicken egg white (Fluka, USA), for 7 days at 37 ºC, a period known as the nucleation stage,

which allows CaP nuclei formation. After the nucleation stage, all samples were washed with distilled water and immersed in a concentrated 1.5 SBF solution for 3, 7 and 14 days at 37ºC, in order to enhance CaP nuclei growth. All the solutions were sterilized by filtration prior to use. After each time period, chitosan scaffolds were washed with distilled water and dried until surface characterization was performed. The morphology of the CaP coatings obtained was analysed by scanning electron microscopy (SEM; Leica Cambridge S-360, UK). Prior to microstructure analysis, specimens were coated with gold using a Fisons Instruments Coater (Polaron SC 502, UK). In order to characterize the crystalline/amorphous nature of the films, thin-film X-ray diffraction (TF-XRD; Philips X'Pert MPD, The Netherlands) was used. Data collection was performed by 2θ scan method with 1º as the incident beam angle using Cu$K\alpha$ X-Ray line and a scan speed of 0.05º/min in 2θ. In addition, infrared analysis (FTIR) of the coatings was performed in a Perkin-Elmer spectrometer (Perkin-Elmer 1600 series equipment, USA) to examine the chemical structure of the CaP biomimetic coatings obtained. Coatings were scraped from the chitosan scaffolds, mixed with KBr (Riedel-de Haën, Germany) and then formed into a disc in a press. All spectra were obtained between 4400 and 450 cm^{-1} at a 2 cm^{-1} resolution.

2.4. Degradation studies

In order to simulate *in vivo* conditions, degradation studies were carried out by incubating uncoated chitosan scaffolds and CaP coated chitosan scaffolds, with and without incorporated lysozyme, in two different buffer solutions: (i) Tris-HCl buffer (0.22 mM, pH 7.4) to simulate the normal pH found in human body; and (ii) citrate buffer (1.0 mM, pH 5.0) to simulate the inflammatory response at 37 ºC for different periods of time. At the end of each degradation period, the samples were removed, washed with distilled water and dried for later calculation of weight loss (1). The morphology of the scaffolds after degradation was analysed by SEM.

$$(1)\quad \text{Weight loss (\%)} = \frac{\text{Initial weight} - \text{Final weight}}{\text{Initial weight}}$$

2.5. Determination of lysozyme activity in solution and released from the CaP coatings

In order to evaluate the lysozyme activity and that released from the CaP coating at pH 5 and pH 7.4, the *Micrococcus lysodeikticus* assay was used. This assay is based on the ability of lysozyme to hydrolyse the cell wall fragments of bacteria. For determining the activity of released lysozyme, coated scaffolds with incorporated lysozyme were immersed in buffer solution (pH 7.4) and incubated at 37 ºC for 30 days. The released lysozyme (150 µL) was added to a 100 µL of *Micrococcus lysodeikticus* suspension (2.3 mg/mL, pH 7.4) in a 96-well plate. The decrease in turbidity at 37 ºC was measured at 450 nm (Microplate Reader, Synergy^{TM} HT, BIO-TEK Instruments, Inc., USA) at 1 min intervals during 30 minutes. The same procedure was used to determine the enzyme activity at pH 5 and pH 7.4. For that, known enzyme concentrations were prepared in buffers at pH 5 and pH 7.4 and added to the bacteria suspension in the same buffer. The initial kinetic rate (OD slope at t = 0) was measured for each sample, and a standard curve (lysozyme activity vs lysozyme concentration) was constructed. The lysozyme activity released after 30 days was determined from the standard curve.

2.6. Statistics

Results of weight loss are expressed as means ± standard deviation with n=3 for each group. The statistical significance of differences was determined using Student's t-test multiple comparison procedure at a confidence interval of 95% ($p < 0.05$).

3. RESULTS AND DISCUSSION

3.1. Development of CaP biomimetic coatings

Figure 1 shows SEM images of the uncoated chitosan scaffold (Figure 1A) and CaP coated chitosan scaffolds after immersion in SBF solution in the presence (Figures 1C and 1E) and absence (Figures 1B and 1D) of lysozyme. At the nucleation stage, it is possible to observe for both conditions (with and without lysozyme) the formation of apatite nuclei (Figures 1B and 1C). Lysozyme incorporation in the nucleation stage did not significantly affect the morphology of the coatings (Figure 1C**)**. In the first 7 days of the growth stage for both conditions, it is possible to observe that the size of CaP nuclei increased, forming a dense and compact CaP film. This means that immersion in SBF solution promotes the growth of CaP layer over time. At higher magnifications, after 7 days of growth, the

morphology of the coatings is similar in the presence and absence of lysozyme, demonstrating the typical cauliflower morphology (Figures 1D1 and 1E1). Lysozyme incorporation into the coatings did not affect the morphology and growth of the coatings as a function of immersion time.

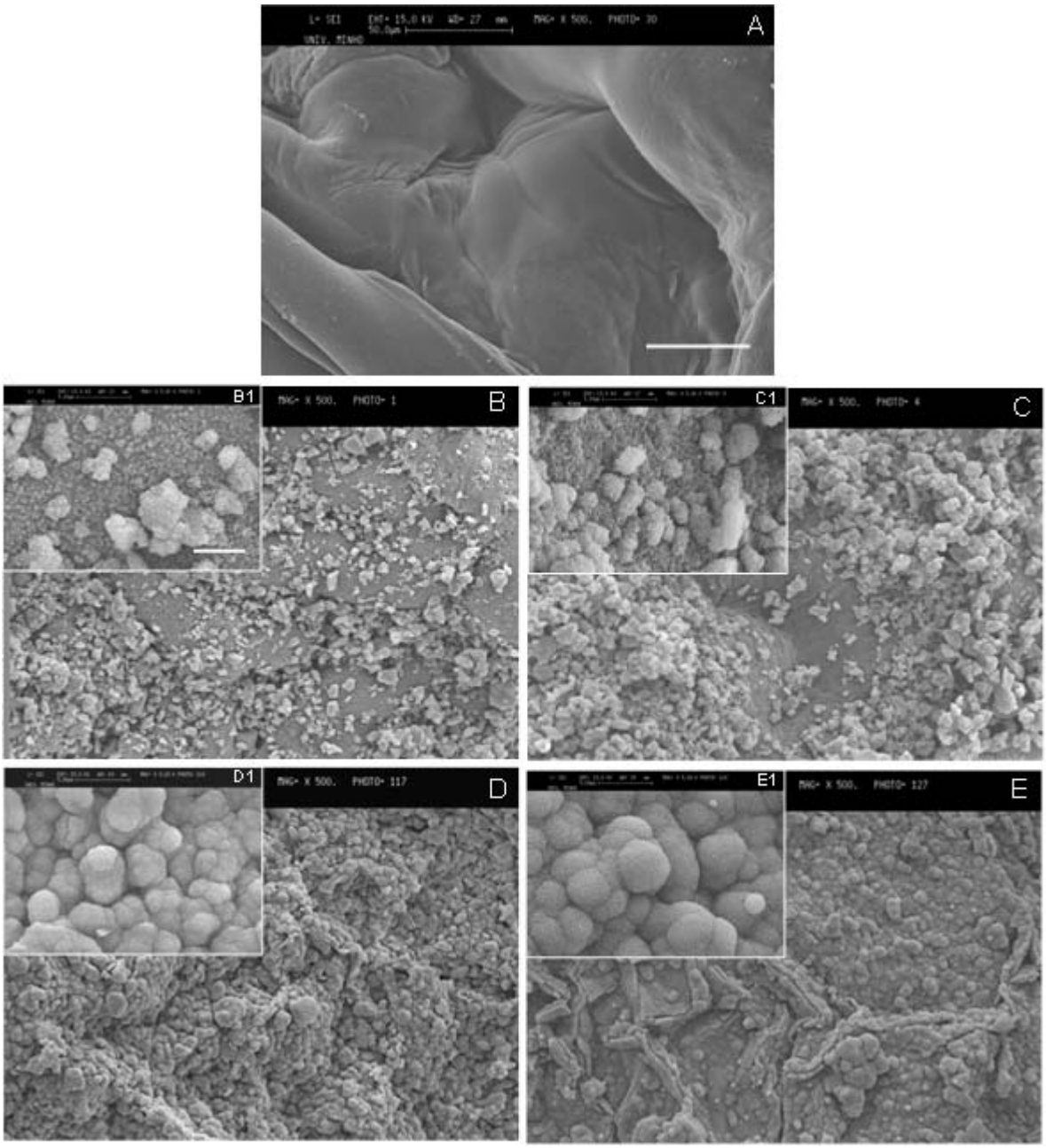


Figure 1. SEM images of the surface of chitosan scaffolds: uncoated (A); coated with CaP layer at nucleation stage (B, B1) and after 7 days in the growth stage (D, D1); and coated with CaP layer with incorporated lysozyme at nucleation stage (C, C1) and after 7 days in the growth stage (E, E1). The scale bar is 50 μm for images A-E and 5 μm for images B1-E1.

Figure 2A presents the infrared spectra of CaP coatings with and without lysozyme (control) at nucleation stage. Analysis of CaP coatings in absence of lysozyme shows the presence of phosphate (PO_4^{3-}) groups (bands at 1055, 602 and 556 cm^{-1}). Moreover, the presence of carbonate (CO_3^{2-}) bands (1492 cm^{-1} and 1441 cm^{-1}) was detected. When lysozyme was added at nucleation stage, the same phosphate and carbonate groups were also detected (Figure 2A). In the spectrum of CaP coating with lysozyme, the appearance of amide I band (1656 cm^{-1}) was observed indicating that lysozyme is incorporated in the coating. The amide I band represents the stretching vibrations of C=O bonds in the backbone of the proteins [22,25]. FTIR spectra of both CaP coatings, with and without lysozyme, confirmed an apatite layer formation on the surface of the scaffolds, with similar composition of the major mineral component of the bone[26].

TF-XRD analyses were performed to determine whether the CaP coatings were crystalline or amorphous. Figure 2B shows TF-XRD patterns of CaP coatings in the absence and presence of lysozyme. No crystalline peaks were detected for CaP coated chitosan scaffolds with or without incorporated lysozyme at nucleation stage (Figures 2Bb and 2Bc). After 7 days of growth, two characteristic peaks of hydroxyapatite are visible in the diffraction patterns of CaP coatings in the presence and absence of lysozyme, which are confirmed by comparison to an XRD pattern of standard hydroxyapatite (JCPDS 9-432) (Figures 2Bd and 2Be). These TF-XRD patterns confirm the formation of apatite layer owing to the presence of apatite peaks. However, the apatite formed appears to be mainly amorphous. These results together with FTIR spectra suggest that the mineral formed is a carbonate apatite mineral similar to the major mineral component of bone.

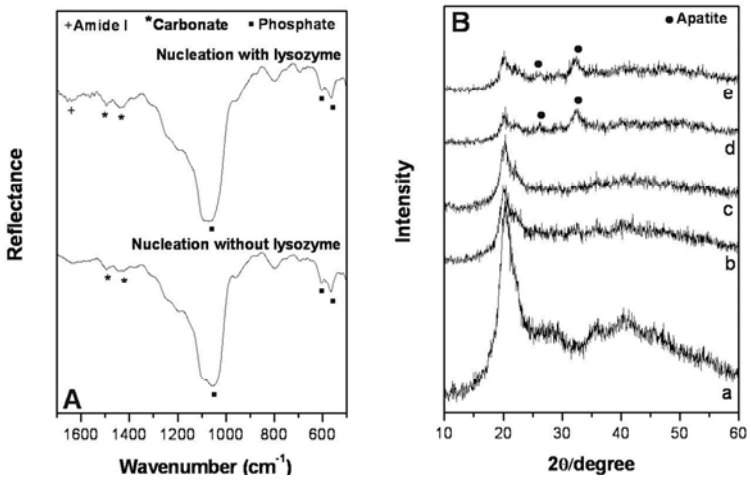


Figure 2. FTIR spectra of CaP coatings, with and without incorporated lysozyme at nucleation stage (A) and TF-XRD spectra (B) of uncoated chitosan scaffolds (a); CaP coated chitosan scaffolds at nucleation stage (b) and after 7 days of growth (d); CaP coated chitosan with incorporated lysozyme at nucleation stage (c) and after 7 days of growth (e).

3.2. Degradation studies

The degradation behavior of the chitosan scaffolds developed (uncoated chitosan scaffolds, CaP coated chitosan scaffolds with and without incorporated lysozyme) was investigated by incubation in buffer solutions for different periods of time. To simulate *in vivo* conditions and the ability of *in situ* pore formation, two different pHs were tested: pH 7.4 to simulate normal physiological conditions; and pH 5 to simulate inflammatory response.

On analysis of the weight loss profile at pH 7.4 (Figure 3A), all scaffolds presented gradual weight loss as a function of degradation time. The lowest weight loss was observed for uncoated chitosan scaffolds, with almost 4% after 60 days. The corresponding SEM images show an increase in the surface roughness as a function of immersion time (Figures 4D, 4G and 4J). These observations are in accordance with weight loss results (Figure 3A). The CaP coated chitosan scaffolds presented a significant weight loss of 7.6 ± 0.2% after 60 days (Figure 3A).

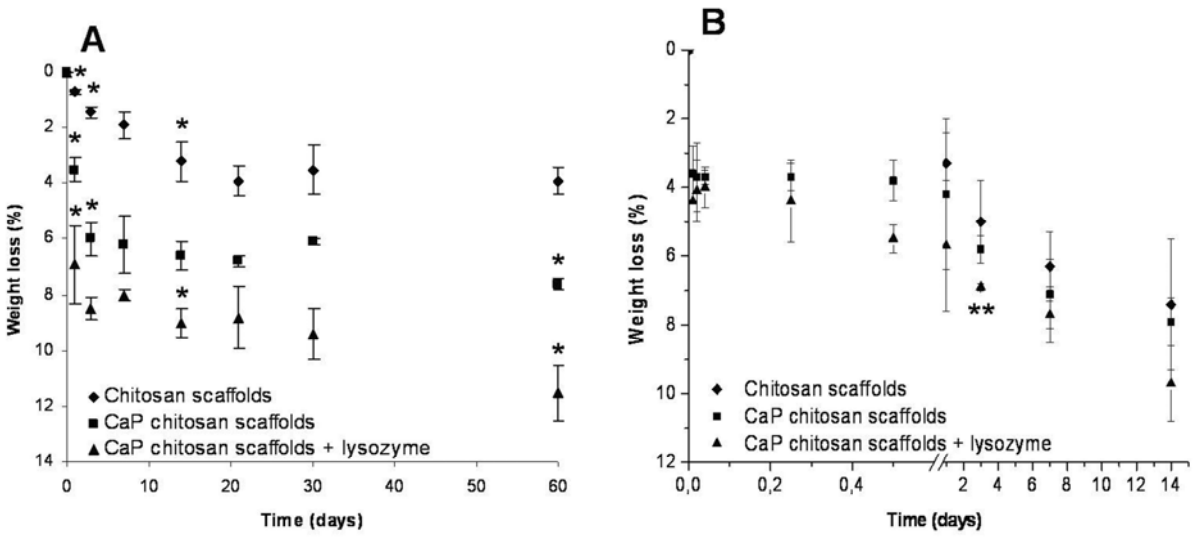


Figure 3. Weight loss profile of uncoated chitosan scaffolds, CaP coated chitosan scaffolds, CaP coated chitosan scaffolds with incorporated lysozyme as a function of immersion time at pH 7.4 (A) and pH 5 (B). (*) indicates a significant difference between time points for each condition. At pH 7.4 for each time point all difference between conditions is significant. (**) indicates a significant difference between conditions at the same time point. The weight loss at pH 5 for chitosan scaffolds is significantly different when compared with pH 7.4.

SEM images show several changes in the CaP coatings morphology after only 3 days of immersion at pH 7.4, suggesting that the coatings may be gradually dissolved with time

(Figures 4E, 4H and 4K). CaP coated chitosan scaffolds with incorporated lysozyme presented the highest weight loss as compared with the other two conditions (uncoated chitosan and CaP coated chitosan scaffolds), presenting a significant weight loss of approximately 9% after 14 days, which slightly increases to 11.5 ± 1.0 % upon 60 days of immersion (Figure 3A). Analysing SEM images (Figures 4C, 4F, 4I and 4L), some differences between the coatings in Tris-HCl pH 7.4 were observed as a function of immersion time. However, these differences are not pronounced when compared with CaP coatings in the absence of lysozyme. Lysozyme seems to promote the degradation of chitosan scaffolds surfaces, as it is possible to observe the highest weight loss when lysozyme is present. These findings are corroborated by the results of enzyme activity that showed that the enzyme present on the coatings was still active after 30 days (Figure 6A). Nevertheless, immersion periods at pH 7.4 up to 30 days induced roughness in the surface of uncoated chitosan scaffolds (Figures 4D, 4 G and 4J), and changes of the CaP coating morphology (in the case of CaP coated chitosan scaffolds with and without incorporated lysozyme). However, all scaffolds were coated with a CaP layer, meaning that the coatings are quite stable at normal physiological pH.

The results of degradation studies performed at pH 5 are shown in Figure 3B. The same trend was observed for the weight loss results at pH 7.4. Coated scaffolds with incorporated lysozyme exhibited a faster degradation rate, when compared with the other two conditions (uncoated chitosan and CaP coated chitosan scaffolds) (Figure 3B). This indicates the role of this enzyme on the hydrolysis of chitosan. These results are confirmed by the results of enzyme activity at pH 5, which show that lysozyme is active at that pH (Figure 6B). Independent of the pH, the presence of lysozyme seems to control the degradation rate of the scaffolds.

Analysing the SEM images of uncoated chitosan scaffolds after 14 days of degradation at pH 5, it is possible to observe increased degradation with immersion time (Figures 5A, 5D, 5G, 5J and 5M). After only 3 days, evident changes are observed on the surface of uncoated chitosan scaffolds (Figure 6D). This appears to be related with high susceptibility of chitosan at acidic pH. In Figures 5E, 5H, 5K and 5N, the images of CaP coated chitosan scaffolds after different times at pH 5 are presented. After 1 hour almost all CaP layer was dissolved (data not shown), and it was non-existent after 1 day of degradation (Figure 5E). SEM images evidence the formation of pores after only 1 day, but the formation of interconnected pores is not clearly visible (Figures 5E, 5H, 5K and 5N).

The most interesting results were obtained for CaP coated scaffolds with incorporated lysozyme (Figures 5F, 5I, 5L and 5O). The degradation effect of lysozyme on chitosan is

clearly visible from the emergence of a highly porous structure with time (Figures 5F, 5I, 5L and 5O). After 1 hour, it is possible to observe a CaP layer on the surface of scaffolds (data not shown). However, after 1 day, as previously described, the dissolution of the coatings and pore formation as a function of degradation time was observed. In this case, the formation of pores is clearly visible after 7 days with a structure having interconnected pores (Figures 5L and 5L1). After 14 days, the scaffolds exhibit pores with diameter of approximately 50-300 μm (Figure 5O1). This pore formation is corroborated by the weight loss results. The CaP coated chitosan scaffolds with incorporated lysozyme presented the highest weight loss. In addition, lysozyme activity measurements at pH 5 showed that this enzyme is active.

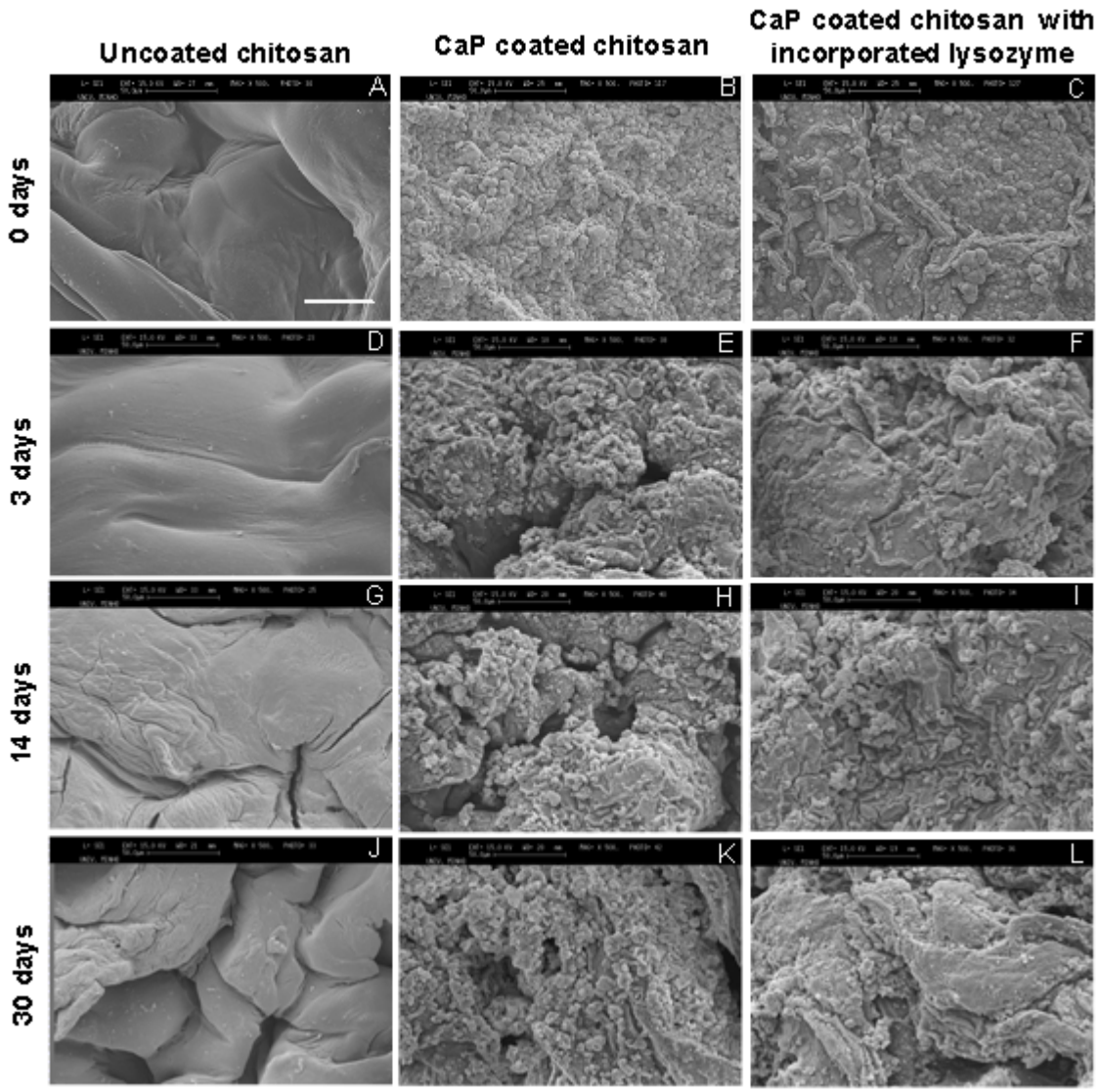


Figure 4. SEM images of chitosan scaffolds, CaP chitosan scaffolds and CaP chitosan scaffolds with incorporated lysozyme before and after degradation at pH 7.4 up to 30 days. Scale bar is 50 μm and applies to all images.

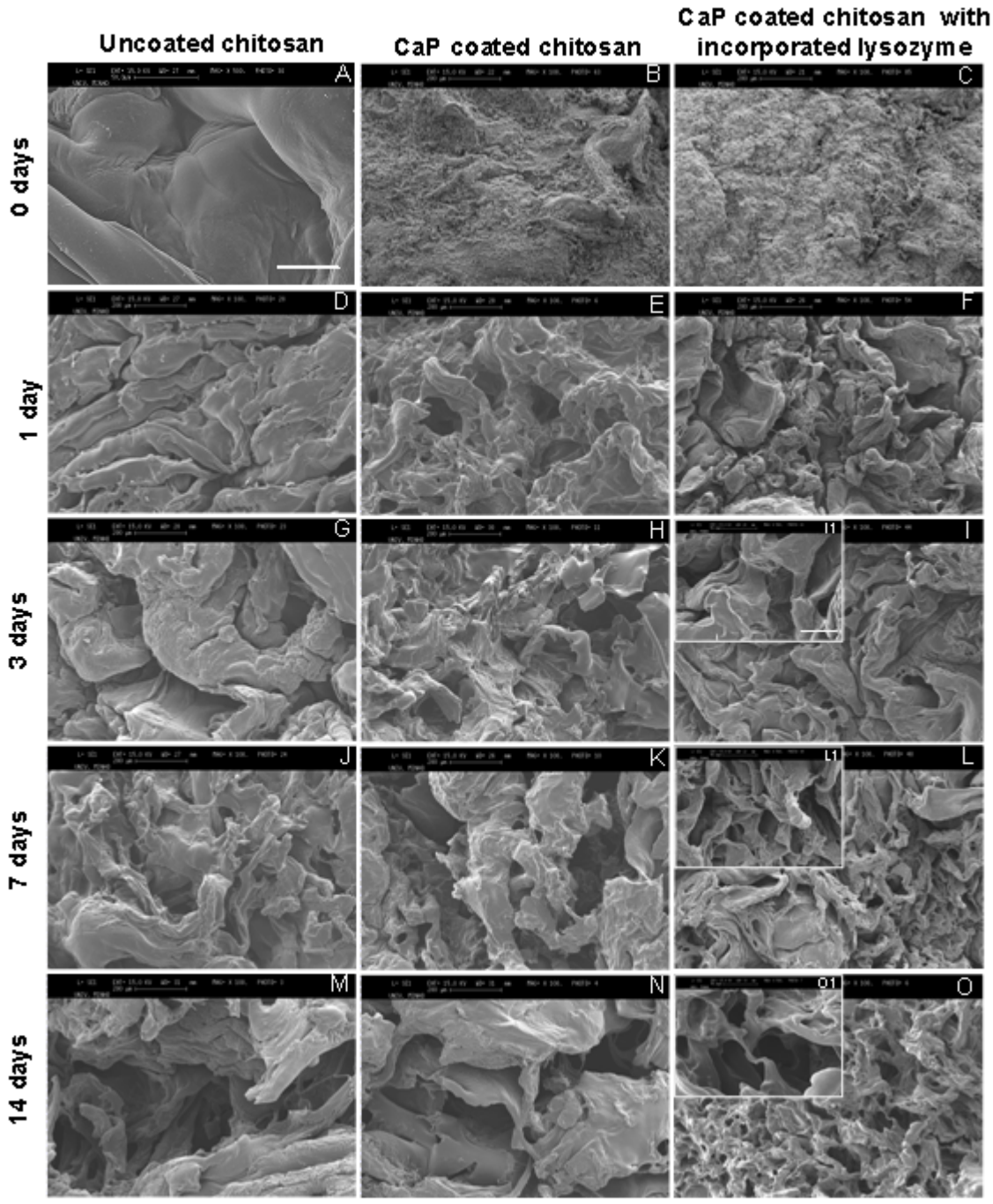


Figure 5. SEM images of chitosan scaffolds, CaP chitosan scaffolds and CaP chitosan scaffolds with incorporated lysozyme before and after degradation at pH 5 up to 14 days. The scale bar is 200 μm for all images except for images I1, L1, O1 (50 μm).

The incorporation of lysozyme into CaP coatings, grown on the surface of chitosan scaffolds may be used as a strategy to control their degradation rate better. Both degradation studies (pH 7.4 and pH 5) show that the presence of lysozyme enhanced the degradation of chitosan scaffolds. The pH of the degradation media has a remarkable influence on CaP coatings. At pH 7.4, all scaffolds remained coated up to 60 days. However, at pH 5, after 1 day, the dissolution of the coatings and formation of pores was observed mostly when due to the presence of lysozyme. These results show that lysozyme has an important role in the degradation of chitosan scaffolds. CaP coated chitosan scaffolds with incorporated lysozyme presented the highest values of weight loss at both pH 7.4 and pH 5. At pH 7.4, no effect of lysozyme on the scaffold morphology was evident. Nevertheless, it enhanced the formation of a porous structure with interconnected pores at pH 5.

3.3. Lysozyme activity in solution and released from the coatings

Evaluation of the activity of the lysozyme released from the coatings (Figure 6A) revealed that the enzyme was able to hydrolyze the peptidoglycan of the bacteria cell walls (as detected by the decrease in optical density with time). The results of this study (Figure 6A) showed that the enzyme remained active after 30 days of immersion in buffer solution (pH 7.4).

Changes in the pH of the environment can alter or inhibit enzyme activity. In order to confirm that lysozyme is active at both pH 5 and pH 7.4, known lysozyme concentrations were used to construct a calibration curve. OD slopes were determined for different lysozyme concentrations (Figure 6B) and an increase in enzymatic activity as a function of increasing lysozyme concentration was observed. Lysozyme is active at pH 5 and pH 7.4. The OD slope for the first 5 minutes in the graph was also calculated (Figure 6A) to determine lysozyme activity released from the coatings. The activity of lysozyme released from the coatings was 0.0375 U (1U corresponds to the amount of enzyme which decreases the absorbance at 450 nm per minute at pH 7.4, 37ºC using a suspension of *Micrococcus lysodeikticus* as substrate).

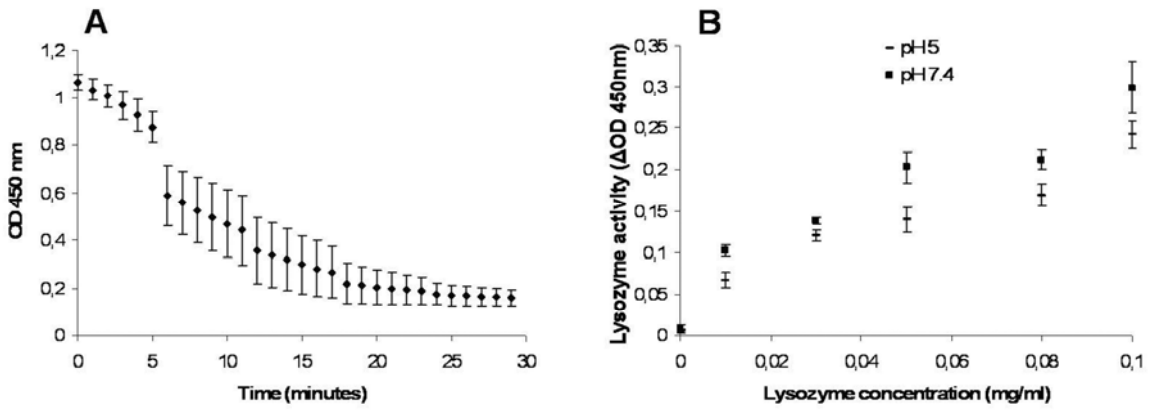


Figure 6. Lysozyme activity (measured as a decrease in the optical density of a *Micrococcus lysodeikticus* bacteria suspension) released from CaP coatings after immersion in buffer (pH 7.4) for 30 days (A) and lysozyme activity at pH 5 and 7.4 as a function of lysozyme concentration (B).

4. CONCLUSIONS

In this work, lysozyme was successfully incorporated into CaP coatings produced on the surface of chitosan scaffolds, using a biomimetic technique. Degradation studies at pH 7.4 to simulate normal physiological conditions showed that the morphology of uncoated scaffolds and CaP coatings changed. However, the formation of pores as a function of immersion time was not observed. Moreover, CaP coatings are very stable at pH 7.4 and, after 30 days, all scaffolds remained covered with a CaP layer. At pH 5, to simulate an *in vivo* inflammatory response, a porous structure was formed when lysozyme was incorporated into the CaP coatings. The degradation effect of lysozyme on chitosan at pH 5 is clearly visible from the appearance of pores. In addition, at high magnifications, SEM images suggest that these pores are interconnected. It was also shown that lysozyme incorporated into the coatings was active after 30 days of immersion in buffer solution (pH 7.4). This approach is very promising, as the presence of lysozyme incorporated into the coatings will allow chitosan scaffolds with gradual *in vivo* pore-forming ability and antibacterial properties that can simultaneously exhibit osteoconductive properties via the presence of CaP coating to be obtained.

ACKNOWLEDGEMENTS

This work was supported by the European NoE EXPERTISSUES (NMP3-CT-2004-500283), the European STREP HIPPOCRATES (NMP3-CT-2003-505758), the Portuguese Foundation for Science and Technology (FCT) through POCTI and/or FEDER programmes.

REFERENCES

1. Martins AM, Santos MI, Azevedo HS, Malafaya PB, Reis RL. Natural origin scaffolds with in situ pore forming capability for bone tissue engineering applications. Acta Biomater 2008;4(6):1637-45.
2. Chatelet C, Damour O, Domard A. Influence of the degree of acetylation on some biological properties of chitosan films. Biomaterials 2001;22(3):261-8.
3. Klokkevold PR, Vandemark L, Kenney EB, Bernard GW. Osteogenesis enhanced by chitosan (poly-N-acetyl glucosaminoglycan) in vitro. J Periodontol 1996;67(11):1170-5.
4. Varum KM, Myhr MM, Hjerde RJ, Smidsrod O. In vitro degradation rates of partially N-acetylated chitosans in human serum. Carbohydr Res 1997;299(1-2):99-101.
5. Tomihata K, Ikada Y. In vitro and in vivo degradation of films of chitin and its deacetylated derivatives. Biomaterials 1997;18(7):567-75.
6. Hankiewi.J, Swiercze.E. Lysozyme in Human Body-Fluids. Clinica Chimica Acta 1974;57(3):205-209.
7. Porstmann B, Jung K, Schmechta H, Evers U, Pergande M, Porstmann T, Kramm HJ, Krause H. Measurement of lysozyme in human body fluids: comparison of various enzyme immunoassay techniques and their diagnostic application. Clin Biochem 1989;22(5):349-55.
8. Proctor VA, Cunningham FE. The chemistry of lysozyme and its use as a food preservative and a pharmaceutical. Crit Rev Food Sci Nutr 1988;26(4):359-95.
9. Torsteinsdottir I, Hakansson L, Hallgren R, Gudbjornsson B, Arvidson NG, Venge P. Serum lysozyme: a potential marker of monocyte/macrophage activity in rheumatoid arthritis. Rheumatology (Oxford) 1999;38(12):1249-54.
10. Habibovic P, Li J, van der Valk CM, Meijer G, Layrolle P, van Blitterswijk CA, de Groot K. Biological performance of uncoated and octacalcium phosphate-coated Ti6Al4V. Biomaterials 2005;26(1):23-36.
11. Liu Y, de Groot K, Hunziker EB. BMP-2 liberated from biomimetic implant coatings induces and sustains direct ossification in an ectopic rat model. Bone 2005;36(5):745-57.
12. Habobovic P, de Groot K. Osteoinductive biomaterials - properties and relevance in bone repair. Journal of Tissue Engineering and Regenerative Medicine 2007;1(1):25-32.
13. Abe Y, Kokubo T, Yamamuro T. Apatite Coating on Ceramics, Metals and Polymers Utilizing a Biological Process. Journal of Materials Science-Materials in Medicine 1990;1(4):233-238.
14. Reis RL, Cunha AM, Fernandes MH, Correia RN. Treatments to induce the nucleation and growth of apatite-like layers on polymeric surfaces and foams. J Mater Sci Mater Med 1997;8(12):897-905.
15. Oliveira AL, Elvira C, Reis RL, Vazquez B, San Roman J. Surface modification tailors the characteristics of biomimetic coatings nucleated on starch-based polymers. J Mater Sci Mater Med 1999;10(12):827-35.
16. Tuzlakoglu K, Reis RL. Formation of bone-like apatite layer on chitosan fiber mesh scaffolds by a biomimetic spraying process. J Mater Sci Mater Med 2007;18(7):1279-1286.

17. Ohtsuki C, Kamitakahara M, Miyazaki T. Coating bone-like apatite onto organic substrates using solutions mimicking body fluid. Journal of Tissue Engineering and Regenerative Medicine 2007;1(1):33-38.
18. Campbell AA. Bioceramics for implant coatings. Materials Today 2003;6(11):26-30.
19. Leonor IB, Azevedo HS, Alves CM, Reis RL. Effects of the incorporation of proteins and active enzymes on biomimetic calcium-phosphate coatings. Bioceramics 15 2003;240-2:97-100.
20. Liu Y, Hunziker EB, Randall NX, de Groot K, Layrolle P. Proteins incorporated into biomimetically prepared calcium phosphate coatings modulate their mechanical strength and dissolution rate. Biomaterials 2003;24(1):65-70.
21. Liu Y, Hunziker EB, Layrolle P, De Bruijn JD, De Groot K. Bone morphogenetic protein 2 incorporated into biomimetic coatings retains its biological activity. Tissue Eng 2004;10(1-2):101-8.
22. Azevedo HS, Leonor IB, Alves CM, Reis RL. Incorporation of proteins and enzymes at different stages of the preparation of calcium phosphate coatings on a degradable substrate by a biomimetic methodology. Materials Science & Engineering C-Biomimetic and Supramolecular Systems 2005;25(2):169-179.
23. Atala A. Engineering tissues, organs and cells. Journal of Tissue Engineering and Regenerative Medicine 2007;1(2):83-96.
24. Tuzlakoglu K, Alves CM, Mano JF, Reis RL. Production and characterization of chitosan fibers and 3-D fiber mesh scaffolds for tissue engineering applications. Macromol Biosci 2004;4(8):811-9.
25. Xie J, Riley C, Kumar M, Chittur K. FTIR/ATR study of protein adsorption and brushite transformation to hydroxyapatite. Biomaterials 2002;23(17):3609-16.
26. Mann S. Biomineralization. Principles and Concepts in Bioinorganic Materials Chemistry. Oxford: Oxford University Press; 2001.

CHAPTER VII

Natural Stimulus Responsive Scaffolds/Cells for Bone Tissue Engineering: Influence of Lysozyme upon Scaffold Degradation and Osteogenic Differentiation of Cultured Marrow Stromal Cells Induced by CaP Coatings

CHAPTER VII

Natural Stimulus Responsive Scaffolds/Cells for Bone Tissue Engineering: Influence of Lysozyme upon Scaffold Degradation and Osteogenic Differentiation of Cultured Marrow Stromal Cells Induced by CaP Coatings[1]

ABSTRACT

This work proposes the use of non-porous, "smart" and stimulus responsive chitosan-based scaffolds for bone tissue engineering applications. The overall vision is to use biodegradable scaffolds based on chitosan and starch that present properties that will be regulated by bone regeneration, with the capability of gradual *in situ* pore formation. Biomimetic calcium phosphate (CaP) coatings were used as a strategy to incorporate lysozyme at the surface of chitosan-based materials with the main objective of controlling and tailoring their degradation profile as a function of immersion time. In order to confirm the concept, degradation tests with a lysozyme concentration similar to that incorporated into CaP chitosan-based scaffolds was used to study the degradation of the scaffolds and the formation of pores as a function of immersion time. Degradation studies with lysozyme (1.5 g/L) showed the formation of pores, indicating an increase of porosity (~5% - 55% up to 21 days) resulting in porous three-dimensional (3D) structures with interconnected pores. Additional studies investigated the influence of a CaP biomimetic coating on osteogenic differentiation of rat marrow stromal cells (MSCs) and showed enhanced differentiation of rat MSCs seeded on the CaP coated chitosan-based scaffolds with lysozyme incorporated. At all culture times, CaP coated chitosan-based scaffolds with incorporated lysozyme demonstrated greater osteoblastic differentiation of MSCs, bone matrix production, and mineralization as demonstrated by calcium deposition measurements, compared with controls (uncoated scaffolds). The ability of these CaP coated chitosan-based scaffolds with incorporated lysozyme to create an interconnected pore network *in situ* coupled with the demonstrated positive effect of these scaffolds upon osteoblastic differentiation of MSCs and

[1] This chapter is based on the following publication:

A.M. Martins, Q.P. Pham, P.B. Malafaya, R.M. Raphael, F.K. Kasper, R.L. Reis, and A.G. Mikos. Natural Stimulus Responsive Scaffolds/Cells for Bone Tissue Engineering: Influence of Lysozyme upon Scaffold Degradation and Osteogenic Differentiation of Cultured Marrow Stromal Cells Induced by CaP Coatings. Tissue Engineering: Part A, in press, DOI: 10.1089=ten.tea.2008.0023 (2009).

mineralized matrix production illustrate the strong potential of these scaffolds for application in bone tissue engineering strategies.

1. INTRODUCTION

Tissue engineering strategies include two general categories: (1) the use of acellular matrices (artificial scaffolds or decellularized tissues), which depend upon the natural ability of the body to regenerate for proper orientation and direction of new tissue growth, and (2) the use of scaffolds with cells (1, 2). The typical strategy involves the use of a porous scaffold, which serves as a transplantation vehicle for cultured cells and a template to guide tissue regeneration, thereby playing an important role in transforming the cell seeded scaffold into a new tissue. To allow a high density of colonizing cells and to promote neovascularization when implanted *in vivo*, the scaffolds should have high porosity, large surface area, mechanical properties and pore sizes appropriate for the application, and a highly interconnected pore structure (1). In addition, biocompatibility and biodegradability are also required properties. Bone regeneration is a complex series of events involving proliferation and differentiation of mesenchymal stem cells into osteoblasts, bone matrix production and mineralization (3).

As extensively described in the literature, scaffold porosity is inversely related to the mechanical properties of the scaffold, thus it is necessary to balance the mechanical needs of the particular tissue that is going to be replaced and the scaffold porosity sufficient to allow tissue growth (4, 5). Therefore, this work proposes the use of non-porous scaffolds composed of an *in vivo* responsive material that will be regulated by bone regeneration, with gradual *in situ* pore formation and consequent scaffold resorption (6). This novel approach includes the use of “smart” and stimulus responsive scaffolds that might be “intelligent” enough to control their degradation profile as a function of implantation time and to induce osteogenic differentiation of MSCs.

Chitosan has been considered to be a promising material for tissue engineering applications (7-9). It is a linear copolymer of N-acetyl-D-glucosamine and D-glucosamine, derived from the deacetylation of chitin. The deacetylation degree measures the percentage of glucosamine units in the polymer chain and influences its physicochemical properties such as solubility, crystallinity, swelling behaviour and biological properties (10), such as osteogenesis enhancement (11-13). The N-acetylglucosamine present in chitosan is also responsible for nitric oxide production by rat peritoneal exudate macrophages (14) at reasonable levels in terms of inflammatory response but very effective in terms of wound

tissue repair (15). It has been also demonstrated that chitosan is degraded in vitro and in vivo by lysozyme (15-17), an enzyme ubiquitous in the human body. Moreover, hydrolytic actions of lysozyme are able to activate macrophages and to promote collagen deposition. The biocompatibility of chitosan might be attributed to its structural similarity to glycosaminoglycan, which is a major component of the extracellular matrix (ECM) of bone and cartilage (12).

Starch was used as a component of the scaffolds presented in this study as a sacrifice material that will be easily degraded by several enzymes occurring in the human body (6). Several in vitro and in vivo studies have shown that starch-based biomaterials are biocompatible (18-20) and biodegradable (6, 21, 22). The main enzymes involved in starch degradation are α-amylases, β-amylases, α-glucosidases, glucoamylases, and other debranching enzymes (pullulanase and isoamylase) (23, 24). The enzymatic degradation products of starch hydrolysis are mainly glucose, maltose and dextrin (24).

Chitosan and starch scaffolds typically do not present adequate bone bonding, osteoconductive or osteoinductive properties for bone tissue engineering applications. One possible solution is to apply on the surface of 3D structures a calcium phosphate (CaP) biomimetic coating with a composition similar to the major inorganic component of bone, hydroxyapatite (HA). In addition, biomimetic CaP coatings have been considered as potential carriers of bioactive proteins without compromising their activity, as they are generated under physiological conditions (pH 7.4, 37ºC) (22, 25-28). It has been shown that different proteins can be directly integrated into the structure of CaP coatings without compromising their activity, and their release is mainly controlled by the dissolution mechanism of the coating (22, 25-27). In this sense, biomimetic coatings were used to tailor the material surface properties or to directly enhance cell adhesion, proliferation and osteogenic differentiation. Moreover, CaP coatings are used as a means to functionalize biomaterials with biological affinity and protein adsorption properties, as previously mentioned (28). The incorporation of different enzymes into CaP coatings, prepared on the surface of scaffolds by means of a biomimetic coating technique seems to be a very interesting strategy to control their degradation rate. In this work, lysozyme was incorporated into the coatings with the aim of developing a self-regulating degradable material with a capacity for gradual in situ pore formation. In addition, this system can simultaneously exhibit osteoinductive and osteoconductive properties in the sense that it can act as a carrier system for the controlled release of multiple biologically active proteins. In the past decade, a large number of publications showed osteoinduction by calcium phosphate coatings in several animal models (29, 30). Recent research has shown that the biological performance of osteoinductive

biomaterials, namely on new bone growth orthotopically, is significantly better than non-osteoinductive biomaterials (30).

The present study reports the use of CaP coated chitosan-based scaffolds with incorporated lysozyme. This study was designed to answer the following questions: How does lysozyme influence the formation of pores in chitosan scaffolds, using a similar concentration to the one incorporated into CaP coatings? 2) Does this concentration of lysozyme allow the formation of interconnected pores? 3) Are CaP coated chitosan-based scaffolds able to enhance osteogenic differentiation of rat MSCs compared with uncoated (without CaP coating) scaffolds?

2. MATERIALS AND METHODS

2.1. Materials

In this work, degradable scaffolds based on chitosan and corn starch were developed. Two different compositions were prepared using a precipitation method (7): chitosan (Ch) and chitosan/starch scaffolds (CS). Briefly, chitosan was dissolved in acetic acid 1% (v/v) to obtain a 5% (w/v) solution. Then, using the same procedure, another formulation was prepared with the following ratio: 60/40 chitosan/starch. The chitosan and chitosan/starch solutions were cast into moulds and frozen (-18ºC) overnight (6). They were then immersed in a precipitation solution (25% (v) NaOH 1M and 75% (v) Na_2SO_4 0.5M) overnight, adapted from (7). After precipitation, the samples were washed several times with distilled water to remove excess salt from the precipitation solution. After this procedure, two other formulations were prepared based on biomimetic coating methodology (31, 32), consisting of an impregnation of the materials with bioactive glass called Bioglass® (45S5) supplied by NovaMin Technology (Alachua, Florida, USA) followed by an immersion in a simulated body fluid (SBF, 37ºC, pH 7.4), presenting ionic concentrations similar to human blood plasma. Briefly, chitosan (Ch) and chitosan/starch (CS) scaffolds were immersed in a wet bed of bioglass for 6 hours in a rotator. After that, the scaffolds where immersed in simulated body fluid (1.0 SBF) solution with lysozyme (1 g/L) for 7 days at 37ºC (nucleation stage). This stage allows for the formation of CaP nuclei. After the nucleation stage, all samples were washed with distilled water and immersed in a concentrated simulated body fluid solution (1.5 SBF) for 7 days at 37ºC in order to enhance CaP nuclei growth. Two different samples were obtained after the biomimetic coating technique: CaP chitosan scaffolds with incorporated lysozyme (CaP/Ch + lysozyme) and CaP chitosan/starch scaffolds with incorporated lysozyme (CaP/CS + lysozyme) (33).

2.2. Degradation studies

Degradation studies were performed in triplicate by incubating the chitosan scaffolds (Ch) in phosphate buffered saline (PBS) solution (pH 7.4) with lysozyme (1.5 g/L), a concentration similar to the ones incorporated into CaP biomimetic coatings, at 37ºC up to 21 days. Lysozyme solution was changed every 7 days. At the end of the degradation period, the samples were removed, washed with distilled water and dried in a graded series of ethanol for later calculation of weight loss. The porosity, pore interconnectivity, pore size and three-dimensional structures of dry chitosan scaffolds were analysed before and after degradation by micro-computed tomography (μ -CT).

2.3. Micro-Computed Tomography (μ-CT)

The scaffolds were analysed using micro-Computed Tomography (μ-CT) before and after degradation with lysozyme for the different periods of immersion (0, 3, 14 and 21 days). μ-CT was carried out using a Skyscan 1072 (Skyscan, Kontich, Belgium) (pixel size resolution of 6.59 μm), with X-ray source settings of 40 keV and 250 μA. The data sets were acquired over a rotation range of 180° (0.45° rotation step) and reconstructed with software (NRecon v1.4.3, SkyScan). Representative data sets were segmented with a dynamic threshold of 40-255 and were used for morphometric analysis (CT Analyser, v1.5.1.5, SkyScan) and to build the 3D models (ANT 3D creator, v2.4, SkyScan). The morphometric analysis included porosity, pore interconnectivity, mean pore size and mean fiber thickness. 3D virtual models of representative regions in the bulk of the scaffolds were created, visualized and registered using both image processing software packages to access the morphological changes after degradation (CT Analyser and ANT 3D creator). The interconnectivity was quantified as the accessible void fraction over a range of minimum connection sizes using an analysis software tool (CT Analyser, v1.5.1.5, SkyScan). A 3D shrink-wrap process was performed to shrink the outside boundary of the volume of interest (VOI) in a scaffold through any openings whose size was equal to or larger than ~50 μm. Any pore size below this value was considered to be a closed pore, based upon reported minimum pore interconnection sizes for bone tissue ingrowth (34). Interconnectivity was calculated as follows (35):

$$\text{Interconnectivity} = (V_t - V_{sw})/(V_t - V_m) \times 100\%$$

where V_t is the total volume of the VOI, V_{sw} is the VOI volume after 3D shrink-wrap processing, and V_m is the volume of scaffold material.

The wall thickness was defined as the pore wall thickness and was quantified with μ-CT analysis based upon structural indices using a software tool (CT Analyser, v1.5.1.5, SkyScan). Specifically, quantitative analysis of the pore wall thickness was retrieved from the 3D analysis using structure thickness (St.Th) parameters.

2.4. MSCs isolation

Rat marrow stromal cells (MSCs) were obtained from femurs and tibias of 41-44 days old male Wistar rats (Charles River Laboratories, USA) using the method described by Maniatoupoulos *et al.* (36). The harvested cells were cultured until confluence in a humidified atmosphere with 5% CO_2 at 37ºC. Non-adherent cells were removed after 1 and 3 days. Upon reaching confluence, the cells were trypsinized, centrifuged, and resuspended in a known amount of medium and 10% dimethyl sulfoxide (DMSO) to obtain a final concentration of $3x10^6$ cells/ml. This cell suspension was then aliquoted into cryotubes for storage in liquid nitrogen (~1 ml/cryotube).

2.5. Cell seeding

Chitosan-based scaffolds with 6 mm diameter and thickness of 0.8-1.0 mm were press fit into 6 mm diameter cassettes and covered with complete osteogenic medium [α-MEM supplemented with 10% fetal bovine serum (FBS) from Cambrex/BioWhittaker (Walkersville, MD), 50 μg/ml gentamicin, 100 μg/ml ampicilin, 10 mM fungizone, 50 μg/ml L-ascorbic acid, 0.01 M β-glycerophosphate, and 10^{-8} M dexamethasone] overnight. After 1 day, each scaffold was seeded with 280,000 cells contained in 100 μl of complete osteogenic media in accordance with previous studies (37, 38). Three hours after cell seeding, 10 ml of complete osteogenic media was added to each well of a 6-well plate. After 24 hours of attachment, the scaffolds were placed in new 6-well plates for 8, 16 and 21 days with complete osteogenic medium. Media were changed every 3 days. Each group consisted of *n* = 6 samples.

At the end of each culture period, samples were removed from the cassettes and rinsed with phosphate buffered saline solution. Three samples from each group were stored at -20ºC in ddH_2O until analyses were performed. One of the remaining 3 samples was immersed in PBS with calcein-AM for 45 minutes for observation under confocal microscopy, and the other two samples were fixed with 2.5% glutaraldehyde for FTIR analysis and for observation under SEM.

2.6. DNA analysis

Measurement of the cell number in chitosan-based scaffolds was assessed from cell lysates using the Picogreen dsDNA Quantification Kit according to the instructions of the manufacturer (Molecular Probes). All standards and samples were prepared in triplicate. The fluorescence at 545 nm was read on a plate reader (FLx800, Bio-Tek Instruments Inc., Winooski, Vermont) to determine DNA concentrations per scaffold. The cellularity of each scaffold was calculated by correlation with the DNA concentrations measured from a known number of marrow stromal cells.

2.7. Alkaline phosphatase activity measurements

Alkaline phosphatase activity assays were performed on cell lysates using an established protocol (37). All reagents were purchased from Sigma (St. Louis, MO). All samples were prepared in triplicate and compared against *p*-nitrophenol standards. The reaction was stopped by adding 100 μl of 0.3 N NaOH. Absorbance was read at 405 nm on a plate reader (PowerWave x340; Bio-Tek Inc., Winooski, Vermont) to determine the alkaline phosphatase activity per scaffold.

2.8. Calcium deposition measurement

Calcium deposition measurements were made in triplicate. CaP coated chitosan-based scaffolds with incorporated lysozyme without cells at the end of each time period were used as controls to determine the calcium content of the coating. Then, these values were subtracted from the calcium content obtained by CaP coated chitosan-based scaffolds with incorporated lysozyme cultured with cells to normalize the data. Calcium deposition was evaluated using a calcium assay from Diagnostic Chemicals Limited. After ALP and DNA assays were completed, a volume of 1N acetic acid equal to the remaining volume was added to each well (for a final concentration of 0.5 N), and the plate was placed on an orbital shaker overnight. A volume of 300 μl of calcium assay reagent was added to 20 μl of sample solution in 96-well plates. All samples were assessed in triplicate. To generate a standard curve, serial dilutions of $CaCl_2$ were prepared (0-50 μg/ml). Absorbance was read at 650 nm with a spectrophotometer plate reader (PowerWave x340; Bio-Tek Inc., Winooski, Vermont). The calcium deposition in each scaffold is reported as μg Ca^{2+}.

2.9. Microscopy analysis

After each time period, chitosan-based scaffolds were removed from the cassettes, washed with PBS and stained with calcein-AM (Molecular Probes) according to the manufacturer's instructions. After 45 minutes immersion in PBS with calcein-AM, images were recorded using a laser scanning confocal microscope with a 10x APO objective (Zeiss LSM 510 Axiovert, Carl Zeiss, Germany). Samples for scanning electron microscopy (SEM) were washed twice in PBS and fixed with 2.5% glutaraldehyde for 30 minutes. Then, the scaffolds were washed with PBS and dehydrated in a graded series of ethanol, and dried after immersion in hexamethyldisilazane.

2.10. Fourier transformed infrared spectroscopy with attenuated total reflectance (FTIR-ATR)

Chitosan-based scaffolds before (control samples) and after 16 days of culture were analysed by FTIR-ATR. The scaffolds were fixed in 2.5% glutaraldehyde, dehydrated in a graded series of ethanol and dried at room temperature. All spectra were recorded using 64 scans and 4 cm^{-1} in a FTIR spectrophotometer (IR Prestige-21, Fourier Transformer infrared spectrophotometer, Shimadzu).

2.11. Statistics

Results of DNA, ALP, and calcium assays are expressed as mean ± standard deviation with n=3 for each group. Statistically significant differences were determined using Student's t-test multiple comparison procedure at a confidence interval of 95% ($p < 0.05$).

3. RESULTS AND DISCUSSION

3.1. Degradation studies

The degradation of chitosan in the human body has been reported to be carried out by lysozyme (16, 17). Previous studies have identified the optimal concentration of lysozyme for the degradation of chitosan-based scaffolds *in vitro* to be 1.5 g/L (33). Accordingly, a lysozyme concentration of 1.5 g/L was used in the present study for optimal degradation of the chitosan-based scaffolds, as well as to approximate the concentration of similar enzymes previously incorporated into biomimetic CaP coatings (22) and the concentration of lysozyme

incorporated into the CaP coatings in the present study (37, 38). As observed in Figure 1, chitosan scaffolds were degraded gradually as a function of immersion time in lysozyme solution (1.5 g/L). The weight loss (%) after 3, 7, 14 and 21 days was: 11.6 ± 0.5, 14.9 ± 0.4, 15.6 ± 0.4 and 18.2 ± 1.1, respectively (Figure 1). This gradual weight loss is confirmed by images obtained by μ-CT, where an almost non-porous structure before degradation was observed (Figure 2A) with a significant increase in porosity after different time periods, being obvious after 14 days (Figure 2D) and 21 days (Figure 2E). These results demonstrate the ability of lysozyme to induce degradation and subsequent formation of pores into chitosan scaffolds.

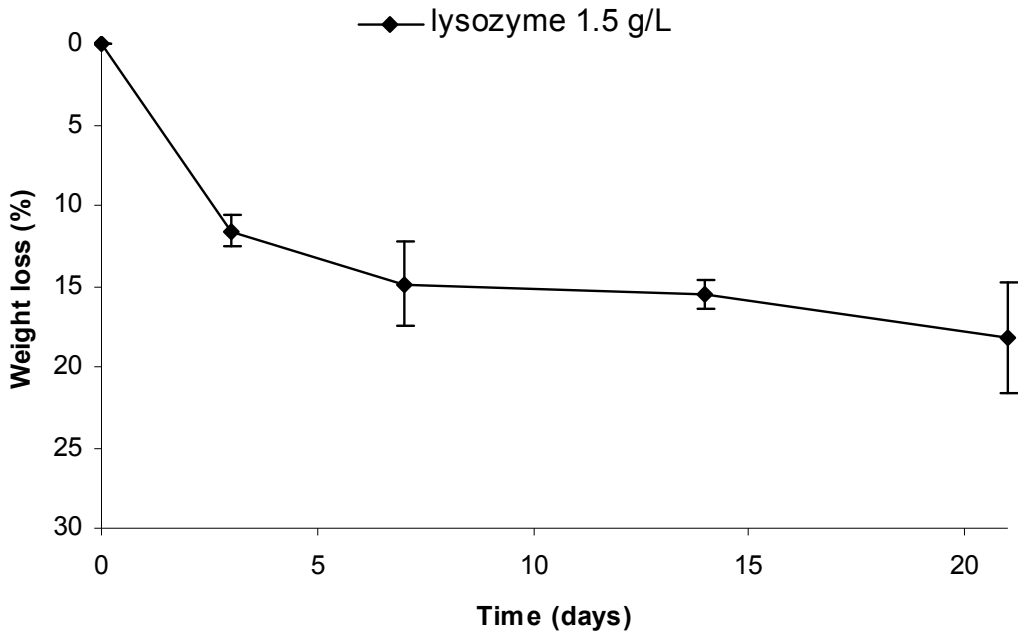


Figure 1. Weight loss of chitosan (Ch) scaffolds after 21 days of immersion in PBS with lysozyme (1.5 g/L) solution.

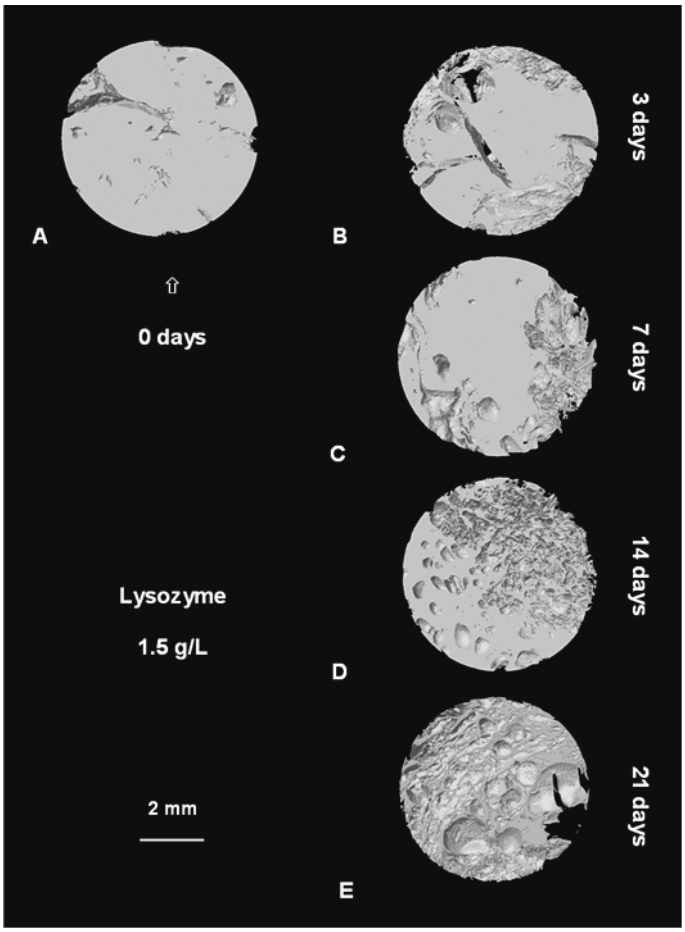


Figure 2. Images of chitosan (Ch) scaffolds obtained by μ-CT: before degradation (A), after 3 days (B), 7 days (C), 14 days (D), and 21 days (E) of degradation with lysozyme (1.5 g/L). Lysozyme solution induced degradation and enhanced subsequent formation of pores in chitosan scaffolds as a function of immersion time.

Upon analysing the images of chitosan (Ch) scaffolds obtained by μ-CT, it is possible to see the increase of porosity as a function of immersion time (Figure 2). The control scaffolds (before degradation) presented ~5% porosity. According to Figure 3A lysozyme enhanced the porosity of the scaffolds as a function of degradation time. After different time points, lysozyme had a significant effect on chitosan scaffolds, inducing the formation of a porous structure (Figure 2 and Figure 3A). Furthermore, the interconnectivity of chitosan scaffolds increased significantly after 21 days (Figure 3B). Moreover, the effect of lysozyme was also detected in pore size and wall thickness results (Figures 4A and 4B), where a significant increase in size of pores (Figure 4A) and a significant decrease of wall thickness (Figure 4B) was evident compared with control scaffolds (before degradation). These results were expected since after different periods of degradation with lysozyme the formation of pores was observed, evidencing a significant increase of porosity as a function of

degradation time ~ 5% - 55% (Figure 3A) up to 21 days, resulting in porous 3D structures with interconnected pores (~78%).

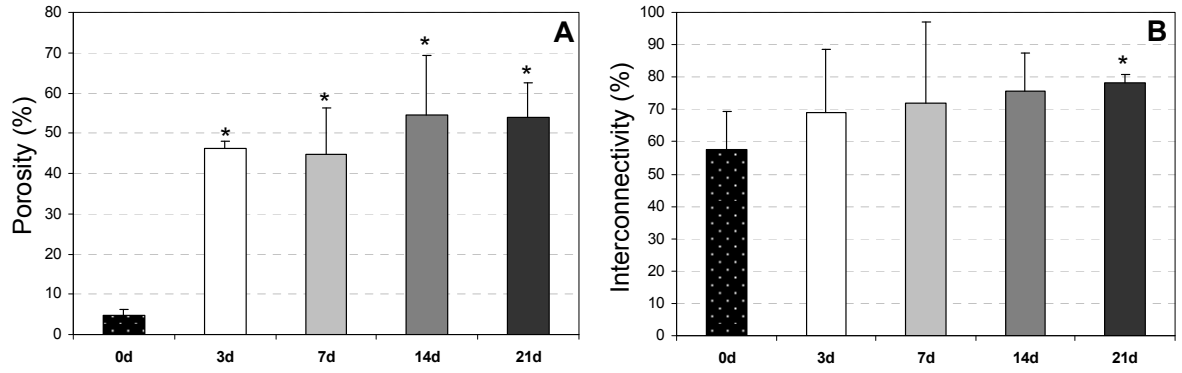


Figure 3. Porosity (A) and interconnectivity (B) of chitosan scaffolds as a function of immersion time with lysozyme (1.5 g/L). Results are expressed as means ± standard deviation with n = 3 for each bar. (*) indicates a significant difference (p < 0.05) as a function of time compared with control samples. Immersion of chitosan scaffolds in lysozyme solution increased the porosity and pore interconnectivity of the scaffolds with time.

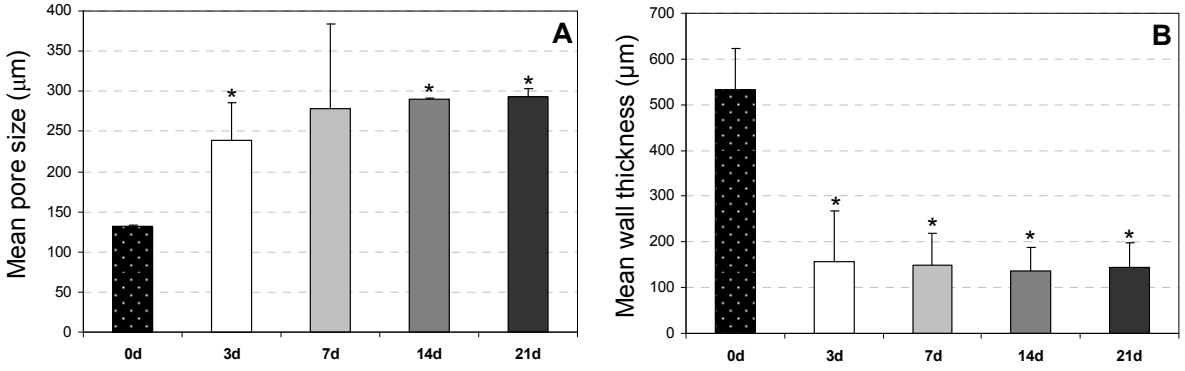


Figure 4. Pore size (A) and wall thickness (B) of chitosan scaffolds as a function of immersion time with lysozyme (1.5 g/L). Results are expressed as means ± standard deviation with n = 3 for each bar. (*) indicates a significant difference (p < 0.05) as a function of time compared with control samples. Immersion of chitosan scaffolds in lysozyme solution increased the mean pore size and decreased the mean wall thickness of the scaffolds with time.

3.2. Assays

Confocal microscopy images after 8 days show that rat marrow stromal cells were able to adhere to all scaffold formulations and maintain their viability. Cells covered the surface of all scaffolds, and no differences can be observed among groups (Figure 5).

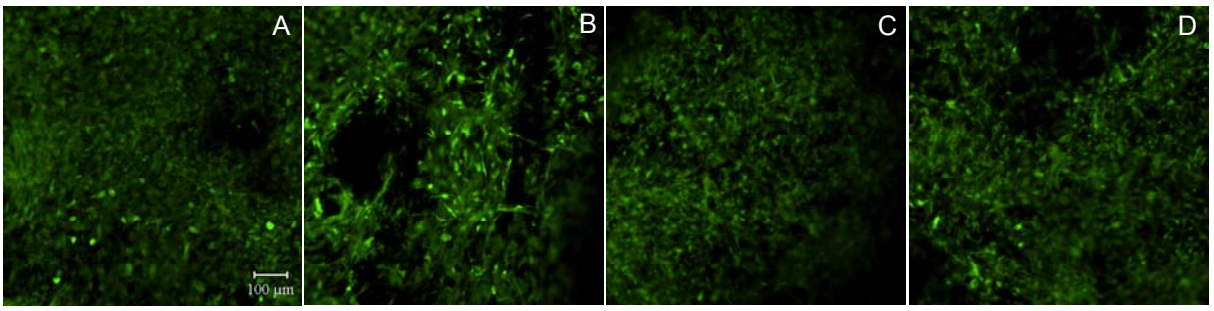


Figure 5. Laser scanning confocal microscope images of cells stained with calcein-AM at the top surface of scaffolds after 8 days: (A) chitosan (Ch); (B) CaP coated chitosan scaffolds with incorporated lysozyme; (C) chitosan/starch (CS) and (D) CaP coated chitosan/starch scaffolds with incorporated lysozyme. All images obtained 45 minutes after incubation with calcein-AM using a 10X APO objective. The scale bar is 100 µm and applies to all images. Rat MSCs adhered to all scaffold formulations and maintained viability after 8 days of culture, with no differences observed among the groups.

Scaffold cellularity is presented in Figure 6. It should be noted that for cases in which cells were completely entrapped within extracellular matrix produced during culture, such that the DNA therein could not be fully liberated for inclusion in the lysate for assessment of cellularity, then the measured results may reflect an underestimation of the actual number of cells on/within the scaffold, especially at later time points. However, an increase in cell number indicating cell proliferation was observed between day 16 and day 21 for all groups. The number of cells after 8 days was lower than was expected, except for CaP coated chitosan/starch with incorporated lysozyme. This can be related to the small surface area of scaffolds where cells were seeded and explained by a lack of initial porosity in these scaffolds. However after 21 days, a significant increase was observed in the number of cells for CaP coated chitosan scaffolds with incorporated lysozyme which corresponds to the increase in porosity as a function of time, as was shown in the degradation results (Figure 1). During the time of culture with MSCs, it was expected that lysozyme would be able to degrade CaP coated chitosan-based scaffolds, inducing the formation of pores by lysozyme and allowing the penetration and colonization of cells into the scaffolds, as shown in Figure 7B after 21 days.

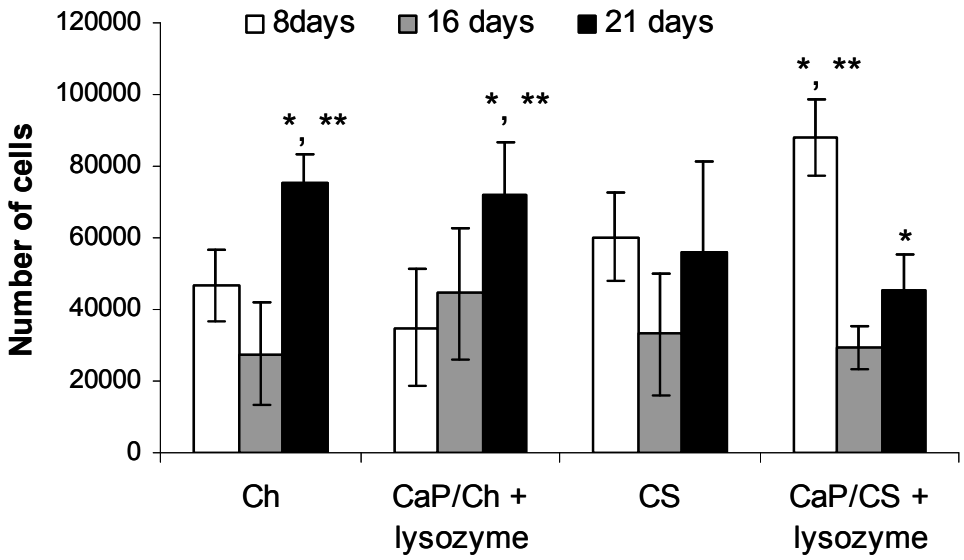


Figure 6. Cellularity of chitosan-based scaffolds seeded with MSCs after 8, 16 and 21 days. Results are expressed as means ± standard deviation with *n*=3 for each bar. (*) indicates a significant difference ($p < 0.05$) between conditions at the same time point. (**) indicates a significant difference ($p < 0.05$) between different time periods for each condition. Ch, chitosan scaffolds; CaP/Ch+ lysozyme, CaP-coated chitosan scaffolds with incorporated lysozyme; CS, chitosan/ starch scaffolds; CaP/CS + lysozyme, CaP-coated chitosan/starch scaffolds with incorporated lysozyme.

The use of biomimetic coating methodology in this study allowed the incorporation of lysozyme that will be able to degrade chitosan-based scaffolds. It is expected that CaP coatings will enhance the osteoconductive properties of the resulting materials. The SEM images after 8 days show cells attached to scaffold surfaces, however after 16 and 21 days all surfaces were completely colonized by the cells, and after 21 days mineralized matrix was observed on CaP coated chitosan-based scaffolds (Figure 7A), clearly visible at high magnifications for scaffolds with incorporated lysozyme (Figure 7B). These results corroborate the calcium content measurements, where calcium was detected after 16 and 21 days (Figure 9). Additionally, small pores were observed in the dense layer for CaP/CS + lysozyme at high magnifications after 8 and 21 days. These pores seem to be induced by the action of lysozyme present in CaP coatings (Figure 7B).

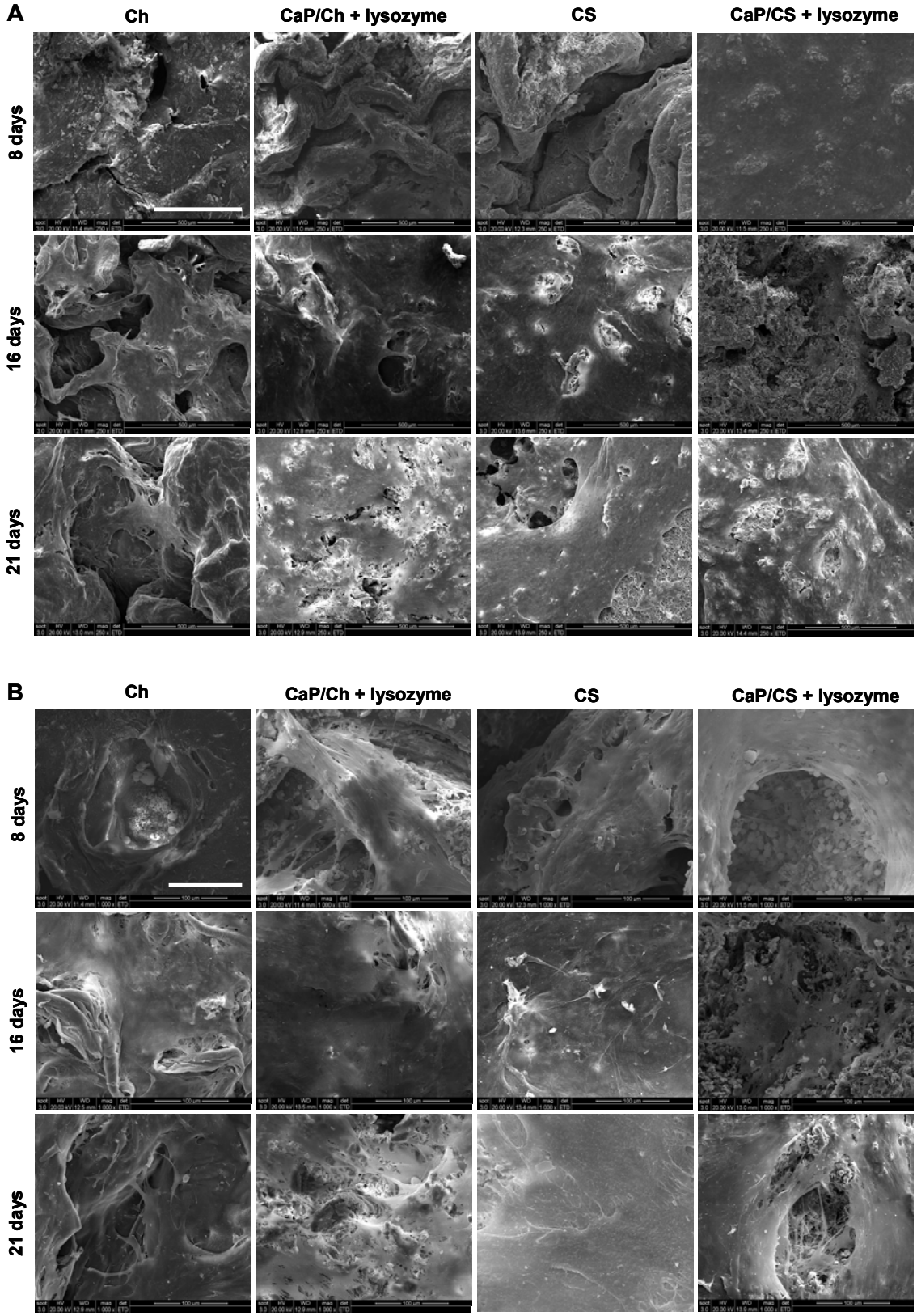


Figure 7. (A) SEM images of the surfaces of cultured chitosan-based scaffolds after 8, 16 and 21 days. The scale bar is 500 μm and applies to all images. (B) SEM images of the surfaces of cultured chitosan-based scaffolds after 8, 16 and 21 days. The scale bar is 100 μm and applies to all images.

Alkaline phosphatase is an enzyme expressed by cells and is an early marker of osteoblastic differentiation in MSCs (39). CaP/CS + lysozyme and uncoated scaffolds (Ch and CS) reached their maximum measured ALP activity on day 8 and 16, respectively (Figure 8), reflecting the early osteogenic differentiation stage of the MSCs. The highest value of ALP activity for CaP/Ch + lysozyme was obtained at day 21, however the difference between the 16th and 21st days was not statistically significant.

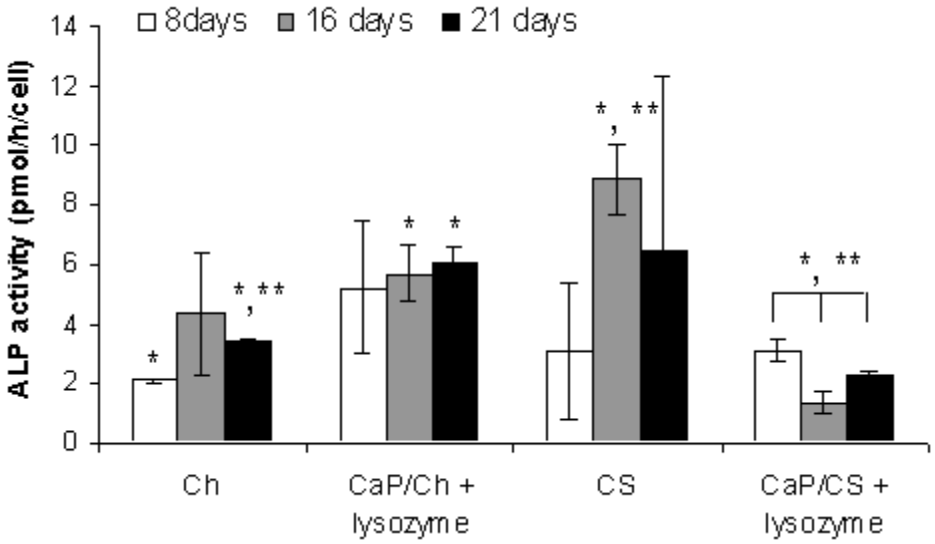


Figure 8. Alkaline phosphatase (ALP) activity of chitosan-based scaffolds seeded with MSCs after 8, 16 and 21 days. Results are expressed as means ± standard deviation with *n*=3 for each bar. (*) indicates a significant difference ($p < 0.05$) between conditions at the same time point. (**) indicates a significant difference ($p < 0.05$) between 8, 16 and 21 days for each condition. Ch, chitosan scaffolds; CaP/Ch+ lysozyme, CaP coated chitosan scaffolds with incorporated lysozyme; CS, chitosan/ starch scaffolds; CaP/CS + lysozyme, CaP coated chitosan/starch scaffolds with incorporated lysozyme.

Calcium deposition is an indicator of the level of mineral deposition, which is a marker of the full maturation of osteoblastic cells. No calcified extracellular matrix deposition was observed at day 8 (Figure 9). After 16 days calcium deposition was detected for CaP coated chitosan-based scaffolds with incorporated lysozyme. At the end of the 3rd week, the calcium measurements indicated the deposition of significant amounts of mineralized matrix for all scaffolds, with a significant increase for CaP coated chitosan-based scaffolds with incorporated lysozyme (Figure 9). The amount of calcium detected on CaP coated scaffolds was higher for both time points of CaP/Ch + lysozyme, however when comparing cellularity (Figure 6), it is apparent that the number of cells was also higher, indicating that the lower

number of cells present in CaP/CS + lysozyme also were able to produce mineralized extracellular matrix. Nevertheless, when comparing the number of cells present in these two scaffolds with the calcium content, both scaffolds had a similar effect on the cells. Indeed, comparison of cellularity results (Figure 6) and ALP activity results (Figure 8) reveals that the maximum ALP activity occurred at either day 16 or 21 for all groups except the CaP/CS + lysozyme group. As ALP activity is an early marker of osteoblastic differentiation of cells, and as cellular differentiation and proliferation are inversely proportional, it follows that a minimum in cellularity at day 16 may reasonably correspond with a peak in ALP activity at day 16. Further, the presence of mineralized matrix, as measured by calcium content of constructs, increased with time for all groups, indicating the osteogenic differentiation of cells in all groups, although this effect was most pronounced in the CaP coated scaffolds with incorporated lysozyme.

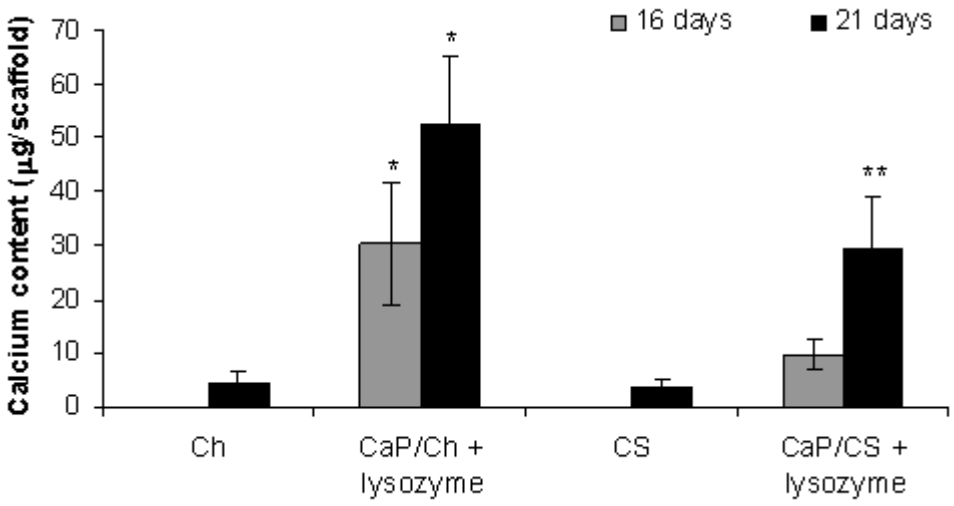
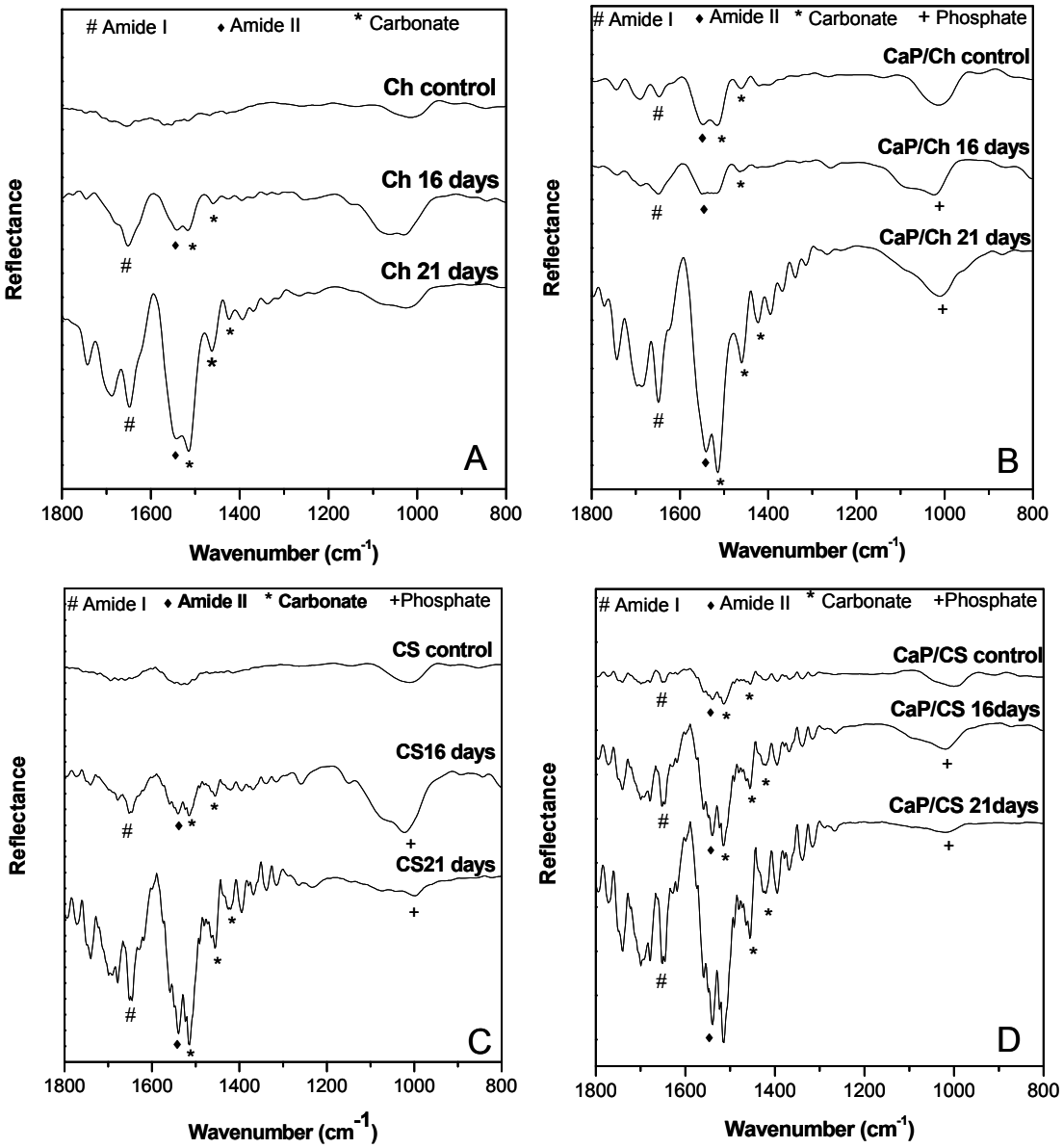


Figure 9. Calcium content in chitosan-based scaffolds after day 16 and day 21 culture periods. Results are expressed as means ± standard deviation with *n*=3 for each bar. (*) indicates a significant difference ($p < 0.05$) between conditions at the same time point. (**) indicates a significant difference between day 16 and day 21 for each condition. Ch, chitosan scaffolds; CaP/Ch+ lysozyme, CaP coated chitosan scaffolds with incorporated lysozyme; CS, chitosan/ starch scaffolds; CaP/CS + lysozyme, CaP coated chitosan/starch scaffolds with incorporated lysozyme.

3.3. Fourier transformed infrared spectroscopy with attenuated total reflectance (FTIR-ATR)

Analysing FTIR-ATR spectra of controls (without cells) of chitosan (Ch) and chitosan/starch (CS) scaffolds, the characteristic bands of chitosan (1150–890 cm^{-1}) were detected (Figures 10A and 10C). After 16 and 21 days of culture (Figures 10A and 10C), these spectra showed the presence of amide bands: 1650 cm^{-1} (amide I) and 1542 cm^{-1} (amide II), which can be related to protein matrix formation. Carbonate groups at 1500-1418 cm^{-1} were also detected (Figures 10A and 10B). These carbonate groups are related to carbonate apatite, one of the calcium phosphates present in bone tissue, suggesting the presence of mineralized extracellular matrix. In Figures 10B and 10D are presented the spectra of CaP/Ch with incorporated lysozyme and CaP/CS with incorporated lysozyme scaffolds. In FTIR-ATR spectra of the CaP coated chitosan-based scaffolds when lysozyme was incorporated, the presence of amide I and amide II in uncultured scaffolds (controls) was detected (Figures 10B and 10D). The amide I band represents the stretching vibrations of C=O bonds in the backbone of the protein (40). Furthermore, the amide II band arises from the combination of C-N stretching and N-H bending vibrations of the protein backbone (40). These bands obtained in the case of the control samples could indicate the adsorption of lysozyme on the surface of chitosan and chitosan/starch scaffolds. However, an increase of intensity of these bands was observed as a function of culture time (Figures 10B and 10D). As previously mentioned, these might indicate a protein matrix formation. In the spectra of control scaffolds (Figures 10B and 10D), carbonate bands (1500-1418 cm^{-1}) were also detected, which are associated with CaP coating on the surface of the scaffolds. In addition, these bands became more intense with culture time, suggesting the formation of mineralized extracellular matrix. However, phosphate bands (1190-976 cm^{-1}) were not clearly detected, which was likely related to overlapping with the polysaccharide ring band of chitosan (1150-890 cm^{-1}).

FTIR-ATR results confirm the calcium measurements results, clearly suggesting protein matrix formation and the presence of mineralized extracellular matrix. Furthermore, these results suggest that the mineral formed by rat marrow stromal cells cultured for 16 and 21 days is carbonate apatite mineral similar to the major mineral component of bone.



Figures 10. FTIR-ATR of chitosan (A), CaP/Ch + lysozyme (B), chitosan/starch (C) and CaP/CS + lysozyme scaffolds (D) before and after 16 and 21 days of culture with rat MSCs. Increases in amide, carbonate, and phosphate bands indicate increased deposition of mineralized ECM with time.

4. CONCLUSIONS

The degradation studies performed with lysozyme using similar concentration to those incorporated into CaP coatings showed the formation of pores as a function of immersion time, indicating an increase of porosity ~5% - 55% up to 21 days. Lysozyme had a significant effect on chitosan scaffolds resulting in porous 3D structures with interconnected pores (~78%). On the basis of these studies it was concluded that CaP biomimetic coatings

with incorporated lysozyme enhance osteogenic differentiation of rat marrow stromal cells. Therefore, the use of CaP biomimetic coating strategy with incorporated lysozyme on the surface of chitosan-based scaffolds provides an improved environment for rat marrow stromal cell differentiation along the osteogenic lineage when compared with uncoated scaffolds, as was shown by calcium deposition measurements and FTIR-ATR results, indicating the production of mineralized extracellular matrix. The demonstrated ability of these novel surface coated scaffolds to form an interconnected pore structure *in situ* coupled with the positive effect of these scaffolds on the osteoblastic differentiation of MSCs and mineralized matrix production clearly illustrate the strong potential of these scaffolds for application in bone tissue engineering strategies.

ACKNOWLEDGEMENTS

The authors would like to acknowledge Dr. Serena Danti. This work was supported by the European NoE EXPERTISSUES (NMP3-CT-2004-500283), the European STREP HIPPOCRATES (NMP3-CT-2003-505758), the Portuguese Foundation for Science and Technology (FCT) through POCTI and/or FEDER programmes. This work was also supported by a grant from the National Institute of Health (R01 DE15164) (AGM) and a Bioengineering Research Partnership with the Baylor College of Medicine through the National Institute of Biomedical Imaging and Bioengineering (NIH Grant No. 5 R01 EB005173-02). FKK is supported by a training fellowship from the Keck Center Nanobiology Training Program of the Gulf Coast Consortia (NIH Grant Nº 5 T90 DK070121-03).

REFERENCES

1. Langer, R., and Vacanti, J.P. Tissue engineering. Science 260, 920, 1993.

2. Atala, A. Engineering tissues, organs and cells. Journal of Tissue Engineering and Regenerative Medicine 1, 83, 2007.

3. Bruder, S.P., and Fox, B.S. Tissue engineering of bone. Cell based strategies. Clin Orthop Relat Res, S68, 1999.

4. Salgado, A.J., Coutinho, O.P., and Reis, R.L. Bone Tissue Engineering: State of the Art and Future Trends. Macromol Biosci 4, 743, 2004.

5. Hutmacher, D.W., Schantz, J.T., Lam, C.X.F., Tam, K.C., and Lim, T.C. State of the art and future directions of scaffold-based bone engineering from a biomaterials perspective. Journal of Tissue Engineering and Regenerative Medicine 1, 245, 2007.

6. Martins, A.M., Santos, M.I., Azevedo, H.S., Malafaya, P.B., and Reis, R.L. Natural origin scaffolds with in situ pore forming capability for bone tissue engineering applications. Acta Biomater, 2008.

7. Tuzlakoglu, K., Alves, C.M., Mano, J.F., and Reis, R.L. Production and characterization of chitosan fibers and 3-D fiber mesh scaffolds for tissue engineering applications. Macromol Biosci 4, 811, 2004.

8. Malafaya, P.B., Pedro, A.J., Peterbauer, A., Gabriel, C., Redl, H., and Reis, R.L. Chitosan particles agglomerated scaffolds for cartilage and osteochondral tissue engineering approaches with adipose tissue derived stem cells. J Mater Sci Mater Med 16, 1077, 2005.

9. Oliveira, J.M., Rodrigues, M.T., Silva, S.S., Malafaya, P.B., Gomes, M.E., Viegas, C.A., Dias, I.R., Azevedo, J.T., Mano, J.F., and Reis, R.L. Novel hydroxyapatite/chitosan bilayered scaffold for osteochondral tissue-engineering applications: Scaffold design and its performance when seeded with goat bone marrow stromal cells. Biomaterials 27, 6123, 2006.

10. Chatelet, C., Damour, O., and Domard, A. Influence of the degree of acetylation on some biological properties of chitosan films. Biomaterials 22, 261, 2001.

11. Klokkevold, P.R., Vandemark, L., Kenney, E.B., and Bernard, G.W. Osteogenesis enhanced by chitosan (poly-N-acetyl glucosaminoglycan) in vitro. J Periodontol 67, 1170, 1996.

12. Lahiji, A., Sohrabi, A., Hungerford, D.S., and Frondoza, C.G. Chitosan supports the expression of extracellular matrix proteins in human osteoblasts and chondrocytes. J Biomed Mater Res 51, 586, 2000.

13. Pound, J.C., Green, D.W., Chaudhuri, J.B., Mann, S., Roach, H.I., and Oreffo, R.O. Strategies to promote chondrogenesis and osteogenesis from human bone marrow cells and articular chondrocytes encapsulated in polysaccharide templates. Tissue Eng 12, 2789, 2006.

14. Peluso, G., Petillo, O., Ranieri, M., Santin, M., Ambrosio, L., Calabro, D., Avallone, B., and Balsamo, G. Chitosan-mediated stimulation of macrophage function. Biomaterials 15, 1215, 1994.

15. Muzzarelli, R.A. Human enzymatic activities related to the therapeutic administration of chitin derivatives. Cell Mol Life Sci 53, 131, 1997.

16. Varum, K.M., Myhr, M.M., Hjerde, R.J., and Smidsrod, O. In vitro degradation rates of partially N-acetylated chitosans in human serum. Carbohydr Res 299, 99, 1997.

17. Tomihata, K., and Ikada, Y. In vitro and in vivo degradation of films of chitin and its deacetylated derivatives. Biomaterials 18, 567, 1997.

18. Mendes, S.C., Reis, R.L., Bovell, Y.P., Cunha, A.M., van Blitterswijk, C.A., and de Bruijn, J.D. Biocompatibility testing of novel starch-based materials with potential application in orthopaedic surgery: a preliminary study. Biomaterials 22, 2057, 2001.

19. Marques, A.P., Reis, R.L., and Hunt, J.A. The biocompatibility of novel starch-based polymers and composites: in vitro studies. Biomaterials 23, 1471, 2002.

20. Salgado, A.J., Coutinho, O.P., Reis, R.L., and Davies, J.E. In vivo response to starch-based scaffolds designed for bone tissue engineering applications. J Biomed Mater Res A 80, 983, 2007.

21. Azevedo, H.S., Gama, F.M., and Reis, R.L. In vitro assessment of the enzymatic degradation of several starch based biomaterials. Biomacromolecules 4, 1703, 2003.

22. Azevedo, H.S., Leonor, I.B., Alves, C.M., and Reis, R.L. Incorporation of proteins and enzymes at different stages of the preparation of calcium phosphate coatings on a degradable substrate by a biomimetic methodology. Mat Sci Eng C-Bio S 25, 169, 2005.

23. Reis, R.L., and Cunha, A.M. Starch and starch based thermosplastic. In: Jurgen, K.H., Buschow, R., Cahn, W., Flemings, M.C., Ilschner, B., Kramer, E.J., and Mahajan, S., eds. Encyclopedia of Marerials Science and Technology. Amsterdam: Pergamon-Elsevier Science, 2001, pp. 8810-8816.

24. Azevedo, H.S., and Reis, R.L. Understanding the enzymatic degradation of biodegradable polymers and strategies to control their degradation rate. In: Reis, R.L., and Roman, J.S., eds. Biodegradable systems in tissue engineering and regenerative medicine: CRC Press, 2005, pp. 177-201.

25. Liu, Y., Hunziker, E.B., Randall, N.X., de Groot, K., and Layrolle, P. Proteins incorporated into biomimetically prepared calcium phosphate coatings modulate their mechanical strength and dissolution rate. Biomaterials 24, 65, 2003.

26. Liu, Y., Hunziker, E.B., Layrolle, P., De Bruijn, J.D., and De Groot, K. Bone morphogenetic protein 2 incorporated into biomimetic coatings retains its biological activity. Tissue Eng 10, 101, 2004.

27. Azevedo, H.S., Leonor, I.B., and Reis, R.L. Incorporation of proteins with different isoelectric points into biomimetic Ca-P coatings: a new approach to produce hybrid coatings with tailored properties. Key Eng Mat 309-311, 755, 2006.

28. Ohtsuki, C., Kamitakahara, M., and Miyazaki, T. Coating bone-like apatite onto organic substrates using solutions mimicking body fluid. Journal of Tissue Engineering and Regenerative Medicine 1, 33, 2007.

29. Barrere, F., van der Valk, C.M., Meijer, G., Dalmeijer, R.A., de Groot, K., and Layrolle, P. Osteointegration of biomimetic apatite coating applied onto dense and porous metal implants in femurs of goats. J Biomed Mater Res B Appl Biomater 67, 655, 2003.

30. Habobovic, P., and de Groot, K. Osteoinductive biomaterials - properties and relevance in bone repair. Journal of Tissue Engineering and Regenerative Medicine 1, 25, 2007.

31. Abe, Y., Kokubo, T., and Yamamuro, T. Apatite Coating on Ceramics, Metals and Polymers Utilizing a Biological Process. J Mater Sci-Mater M 1, 233, 1990.

32. Reis, R.L., Cunha, A.M., Fernandes, M.H., and Correia, R.N. Treatments to induce the nucleation and growth of apatite-like layers on polymeric surfaces and foams. J Mater Sci Mater Med 8, 897, 1997.

33. Martins, A.M., Salgado, A.J., Azevedo, H.S., Leonor, I.B., and Reis, R.L. Lysozyme incorporation in biomimetic coated chitosan scaffolds: Development and behaviour in contact with osteoblastic-like cells. Tissue Engineering 12, 1018, 2006.

34. Lu, J.X., Flautre, B., Anselme, K., Hardouin, P., Gallur, A., Descamps, M., and Thierry, B. Role of interconnections in porous bioceramics on bone recolonization in vitro and in vivo. J Mater Sci Mater Med 10, 111, 1999.

35. Shi, X., Sitharaman, B., Pham, Q.P., Liang, F., Wu, K., Edward Billups, W., Wilson, L.J., and Mikos, A.G. Fabrication of porous ultra-short single-walled carbon nanotube nanocomposite scaffolds for bone tissue engineering. Biomaterials 28, 4078, 2007.

36. Maniatopoulos, C., Sodek, J., and Melcher, A.H. Bone formation in vitro by stromal cells obtained from bone marrow of young adult rats. Cell Tissue Res 254, 317, 1988.

37. Datta, N., Holtorf, H.L., Sikavitsas, V.I., Jansen, J.A., and Mikos, A.G. Effect of bone extracellular matrix synthesized in vitro on the osteoblastic differentiation of marrow stromal cells. Biomaterials 26, 971, 2005.

38. Holtorf, H.L., Jansen, J.A., and Mikos, A.G. Ectopic bone formation in rat marrow stromal cell/titanium fiber mesh scaffold constructs: effect of initial cell phenotype. Biomaterials 26, 6208, 2005.

39. Toquet, J., Rohanizadeh, R., Guicheux, J., Couillaud, S., Passuti, N., Daculsi, G., and Heymann, D. Osteogenic potential in vitro of human bone marrow cells cultured on macroporous biphasic calcium phosphate ceramic. J Biomed Mater Res 44, 98, 1999.

40. Xie, J., Riley, C., Kumar, M., and Chittur, K. FTIR/ATR study of protein adsorption and brushite transformation to hydroxyapatite. Biomaterials 23, 3609, 2002.

CHAPTER VIII

In Vivo Responsive Self-Regulated Degradation System with *In Situ* Pore Formation Ability: A Novel Strategy for Bone Tissue Engineering

CHAPTER VIII

In Vivo Responsive Self-Regulated Degradation System with *In Situ* Pore Formation Ability: A Novel Strategy for Bone Tissue Engineering[1]

ABSTRACT

Previously, we have studied the *in vitro* application of a self-regulating degradable material with gradual *in situ* pore formation ability. For the aim of those studies, lysozyme was incorporated into biomimetic calcium phosphate (CaP) coatings at the surface of chitosan-based scaffolds in order to control the scaffold degradation and subsequent pore formation. With the goal of validating the concept *in vivo,* a rat subcutaneous model was used to investigate the degradation of the scaffolds and the *in situ* pore formation. Chitosan or chitosan/starch scaffolds were studied with or without a CaP coating in the presence or absence of lysozyme for a total of 6 experimental groups. Twenty four scaffolds per group were implanted, and eight scaffolds were retrieved at each of three time points (3, 6 and 12 weeks). Harvested samples were analyzed for weight loss, micro-computed tomography, and histological analysis. All scaffolds showed pronounced weight loss and pore formation as a function of time. Nevertheless, the highest weight loss at week 12 was 29.8 ± 1.5% for CaP chitosan/starch scaffolds with lysozyme incorporated. All experimental groups showed a significant increase in porosity after 12 weeks. At all time points no adverse tissue reaction was observed, and as degradation increased, histological analysis showed cellular ingrowth throughout the implants. Using this innovative methodology, the ability to gradually generate pores *in situ* was clearly demonstrated *in vivo*.

[1] This chapter is based on the following publication:

A.M. Martins, F.K. Kasper, A.G. Mikos, J.D. Kretlow, A.R. Costa-Pinto, P.B. Malafaya, N.M. Neves, C.M. Alves, R.L. Reis. *In vivo* responsive self-regulated degradation system with *in situ* pore formation ability: a novel strategy for bone tissue engineering, submitted.

1. INTRODUCTION

The evaluation of a bone tissue engineering constructs in a subcutaneous model *in vivo* is often the first step following *in vitro* characterization. In previous studies we proposed the use of non-porous, stimulus responsive chitosan-based scaffolds with self-regulated degradation for bone tissue engineering applications [1, 2]. Additional studies [3] investigated the influence of a CaP biomimetic coating on the osteogenic differentiation of rat bone marrow stromal cells (MSCs) and showed enhanced differentiation of rat MSCs seeded on the CaP coated chitosan-based scaffolds with lysozyme incorporated to aid degradation. When compared with cells seeded onto control (uncoated) scaffolds, cells seeded onto CaP coated chitosan-based scaffolds with incorporated lysozyme demonstrated at all culture times greater osteogenic differentiation, bone matrix production and mineralization as demonstrated by calcium deposition measurements [3].

This approach is based on the use of a material that exhibits both self-regulated degradation and gradual *in situ* pore formation ability [1, 2]. It has been demonstrated that lysozyme, an enzyme ubiquitous in the human body [4, 5], degrades chitosan *in vitro* and *in vivo* [6, 7]. Lysozyme can attack cell wall polysaccharides of different bacterial species, especially Gram positive species, leading to rupture of the cell wall and subsequent death of the microorganism [8, 9]. The anti-inflammatory action of lysozyme is based on the neutralization of acidic substances released in the inflammatory process [10]. Previously, using a biomimetic technique, the surface of the scaffolds was coated with a calcium phosphate with a composition similar to the major inorganic component of bone, hydroxyapatite (HA) [2, 3, 11]. The main advantage of the biomimetic method [12-14] is the use of physiological conditions (pH 7.4 at 37ºC) that simulate the manner that apatite is formed in bone [15]. Moreover, this technique allows the incorporation of proteins and bioactive agents into CaP coatings without compromising their activity [2, 16, 17]. Chitosan and starch by themselves or in combination do not have adequate bone bonding, osteoconductive or osteoinductive properties for bone tissue engineering applications, and CaP coating may give raise to such key properties.

The incorporation of lysozyme into CaP coatings prepared at the surface of chitosan-based scaffolds using a biomimetic methodology was employed to control and tailor the scaffolds' degradation rate and subsequent formation of pores [2, 3, 11]. *In vitro,* these scaffolds gradually exhibit *in situ* pore formation [2]. Based on previous work [1, 2], it is hypothesized that following implantation of the scaffold, an acute inflammatory response will occur with a subsequent pH decrease, and neutrophils and monocyte-derived macrophages will be recruited. Different enzymes, such as lysozyme, and other reactive species will be

released in high levels from these cells, inducing degradation of the scaffolds *in situ* with subsequent pore formation. To prove the concept of *in situ* pore formation *in vitro*, previous studies simulating the inflammatory response were performed, and the formation of pores was clearly visible when CaP chitosan scaffolds with incorporated lysozyme were used [2]. Highly porous structures were formed as a function of degradation time, with pore diameters ranging from 50-300 μm, suggesting that the pores were fully interconnected [2]. This size of pores greater than 150 μm encourages the ingrowth of mineralized bone [18].

The combination of chitosan with other biodegradable materials has already shown to be effective for bone-related applications [19-21].

The inclusion of starch in chitosan matrices constitutes an interesting approach towards obtain scaffolds with enhanced degradation rates since starch is acting as a sacrifice material [1]. Furthermore, starch is enzymatically hydrolysed by α-amylase, an enzyme present in blood serum. Starch is a natural polymer that presents excellent characteristics for biomaterials applications, such as low toxicity [22, 23]. Several *in vitro* and *in vivo* studies have shown that scaffolds produced from starch-based biomaterials are biocompatible in specific applications [24-26] and biodegradable in different conditions [1, 3, 27, 28].

In order to prove the concept of *in situ* pore formation within chitosan-based scaffolds *in vivo*, a rat subcutaneous implantation model was employed. It was hypothesized that using this innovative methodology, the scaffolds, which at the time of implantation exhibit very promising mechanical properties due to the absence of macroporosity [1], will exhibit *in situ* pore formation facilitated by enzymes present in the body (namely the α-amylase and lysozyme). This study was designed to investigate the following specific aims: (i) assess the degradation of the scaffolds *in vivo*, (ii) characterize the *in situ* formation of pores, and (iii) assess *in vivo* the concept of *in situ* pore-formation.

2. MATERIALS AND METHODS

2.1. Materials

Degradable scaffolds based on chitosan and corn starch were used. Two different compositions were prepared using a precipitation method: chitosan (CH) and chitosan/starch scaffolds (CS) [1]. Briefly, chitosan was dissolved in 1% (v/v) acetic acid to obtain a 5% (w/v) solution. Then, using the same procedure, another formulation was prepared with the following ratio: 60/40 chitosan/starch. The chitosan and chitosan/starch solutions were cast

into moulds and frozen (-20 ºC) overnight [1]. They were then immersed in a precipitation solution (25% (v) NaOH 1M and 75% (v) Na_2SO_4 0.5M) [1, 29] and washed several times with distilled water. After this procedure, four other formulations were prepared based on previously used biomimetic coating techniques [2, 3, 11] consisting of an impregnation of the materials with bioactive glass called Bioglass® (45S5; NOVABONE Alachua, Florida, USA) followed by an immersion in a 1× simulated body fluid (SBF, 37ºC, pH 7.4), which has ionic concentrations similar to those of the human blood plasma. Briefly, chitosan (CH) and chitosan/starch (CS) scaffolds were immersed in a wet bed of bioglass for 6 hours on an orbital rotator. After that, the scaffolds where immersed in 1× SBF with and without lysozyme (1 g/L) for 7 days at 37ºC (nucleation stage). This stage allows for the formation of CaP nuclei. After the nucleation stage, all samples were washed with distilled water and immersed in 1.5× SBF for 7 days at 37ºC in order to enhance CaP nuclei growth (growth stage). Four different samples were obtained using the biomimetic coating technique: CaP chitosan scaffolds (CaPCH), CaP chitosan/starch scaffolds (CaPCS), CaP chitosan scaffolds with incorporated lysozyme (CaPCH + lysozyme) and CaP chitosan/starch scaffolds with incorporated lysozyme (CaPCS + lysozyme) [2, 3, 11]. All chemical reagents were purchased from Sigma (St. Louis, MO, USA) unless otherwise specified.

2.2. Implant preparation

In this study 5 mm diameter and approximately 1.5 mm thick scaffolds were used. All scaffolds were sterilized with ethylene oxide gas for 14 h prior to implantationin conditions described elsewhere [30, 31]. One day before subcutaneous implantation surgery, the implants were prewetted with phosphate buffered saline (PBS) solution in 24-well plates overnight under sterile conditions.

2.3. Subcutaneous implantation

All animal manipulations were approved by Rice University's Institutional Animal Care and Use Committee. Twenty four male Wistar rats 41-44 days old (Charles River Laboratories, USA) were used for subcutaneous implantation of acellular scaffolds. Three implantation periods were used: 3, 6 and 12 weeks. Anesthesia was induced with a 4% isoflurane/oxygen mixture, and maintained with 2% isoflurane during surgical manipulation. The rats were monitored to ensure that an appropriate surgical plane of anesthesia was maintained. The fur on the dorsum of the rat was clipped closely prior to surgery. Then, the

animals were placed in a ventral position, the clipped dorsum was disinfected with povidone-iodine and six small longitudinal incisions were made as described in Figure 1. A pocket was bluntly dissected at each incision, and one scaffold was placed in each pocket. One implant from each experimental group was implanted in twenty four rats (six implants per rat). A total of 8 scaffolds per experimental group per time point were implanted. Previous studies reported successful implantation of 6 materials in rat dorsal subcutaneous pockets using Wistar rats of similar or lower size [32-35]. The incisions were closed with simple interrupted 5-0 Vicryl sutures. Each animal received an intraperitoneal injection of sterile saline to aid post-operative recovery (1 ml/100 g/hour of anesthesia) and a subcutaneous injection of buprenorphine (0.025 mg/kg) both before and 8-12 hours after surgery for analgesia. On the following day, two additional doses of subcutaneous buprenorphine (0.025 mg/kg) were injected for continued post-operative analgesia (i.e., at 20-24 and 32-36 hours post-op). Care was taken to give all subcutaneous injections caudal to the implantation sites. Animals were housed individually with water and food given *ad libitum*. At each time point, animals were anesthetized by isoflurane inhalation and euthanized with carbon dioxide asphyxiation. The implants were retrieved after a bilateral thoracotomy was performed to ensure death.

2.4. Preparation of samples for weight loss and micro-computed tomography (μ-CT) analysis

After each implantation time, three scaffolds from each group were decellularized prior to weight loss measurement and micro-computed tomography analysis. Briefly, the scaffolds were immersed in double-distilled water (ddH_2O) and placed in a 24-well plate at -20 ºC. After that, scaffolds underwent three freeze/thaw cycles in liquid nitrogen and in a 37 ºC water bath, respectively, to disrupt attached cells and remove cellular debris [36]. After this process scaffolds were air-dried in a laminar flow hood.

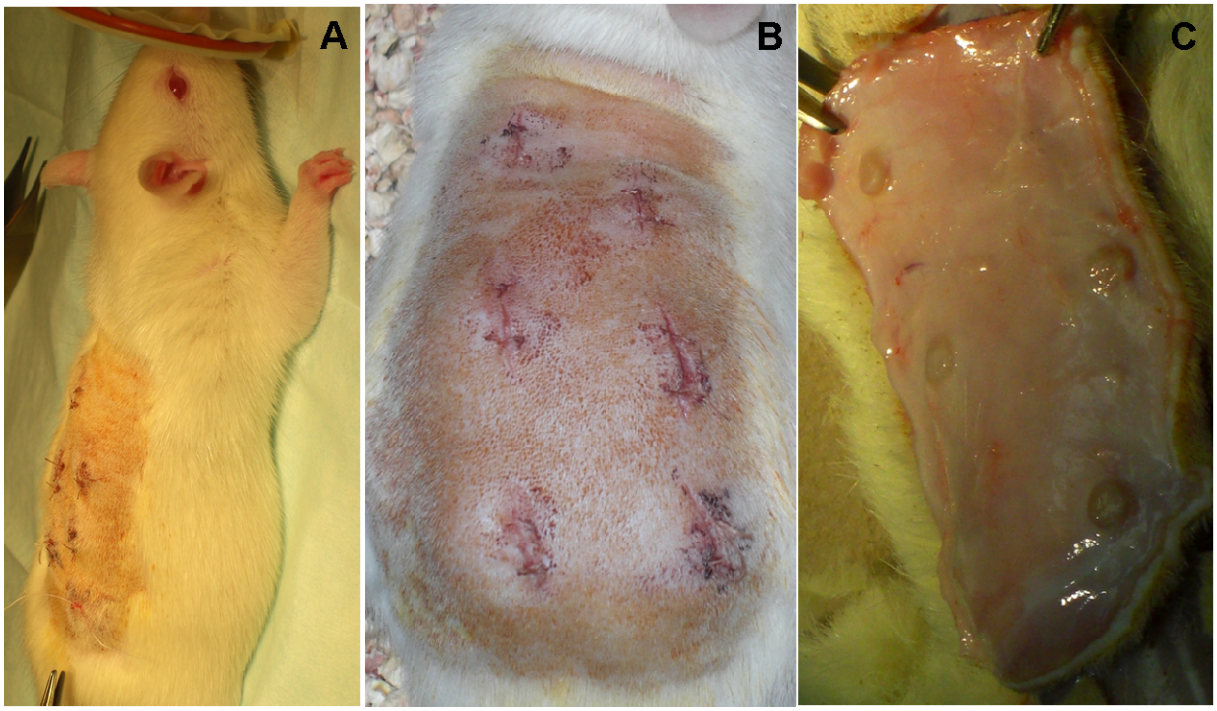


Figure 1. Aspect of the rat dorsum with 6 longitudinal incisions (A) immediately after subcutaneous implantation surgery and (B) after 5 days post-surgery. (C) Harvested scaffolds after 6 weeks with no signs of infection.

2.5. Weight loss measurements

All samples were weighed before subcutaneous implantation (initial weight). After 3, 6 and 12 weeks of implantation three decellularized samples of each condition were dried and weighed to determine the final weight and calculate the weight loss (1).

$$(1)\ \text{Weight loss (\%)} = \frac{\text{Initial weight} - \text{Final weight}}{\text{Initial weight}}$$

2.6. Micro-computed tomography (μ-CT) analysis

Retrieved implants used for weight loss measurements were also used for μ-CT analysis. Three samples from each group were used as controls (i.e., non-implanted specimens). μ-CT was carried out with a high-resolution μ-CT scanner (Skyscan 1072, Skyscan, Kontich, Belgium) using a pixel size of 5.27 μm and integration time of 1.7 ms. The X-ray source was set at 70 keV of energy and 142 μA of current. Approximately 400

projections were acquired over a rotation range of 180° with a rotation step of 0.45°. Data sets were reconstructed using standardized cone-beam reconstruction software (NRecon v1.4.3, SkyScan). The output format for each sample was 400 serial 1024x1024 bitmap images. Representative data sets were segmented into binary images using a dynamic threshold of 40-255 for polymer and 130-255 for CaP coating (grey values). These representative data sets were used for morphometric 3D analysis (CT Analyser, v1.5.1.5, SkyScan) and to build 3D models (ANT 3D creator, v2.4, SkyScan). The morphometric analysis included porosity and pore interconnectivity. 3D virtual models of representative regions in the bulk of the scaffolds were created, visualized and registered using image processing software (CT Analyser and ANT 3D creator).

2.7. Histology

After euthanasia, the implants were retrieved along with the surrounding tissue and processed for histology. Five specimens from each group per time point were fixed in 10% neutral buffered formalin and then dehydrated in a graded series of ethanol, immersed in infiltration solutions, embedded in Technovit glycol methacrylate (kit 8100, Heraeus Kulzer, EBSciences, CO, USA) and subsequently polymerized. Three specimens from each group per time period were cut to obtain longitudinal sections and two specimens were cut to obtain transverse sections of 7 μm thickness using a modified microtome equipped with a tungsten blade (Leica RM 2155).

Sections were stained with hematoxylin and eosin (H&E) to evaluate the *in vivo* degradation, pore formation and cellular infiltration through the implants. For visualization of the CaP coating, additional sections were exposed to 5% silver nitrate solution under UV for 25 min and counterstained with 0.5% safranin O solution. All images were obtained using an Olympus BX61 Motorized System Microscope and attached video camera (Olympus DP70). Histological sections from all time points were scored by the authors (AMM, ARP and CMA) blinded for group conditions and implantation time, and consensus was reached on the final score. The cellular ingrowth within the implants and the degradation of each sample was qualitatively scored based on dissolution, cracks, and fragmentation on a scale modified from De Jong, as shown in Table 1 [37].

Table 1. Histological grading scale for the degradation and cellular growth within the implants (Adapted from De Jong *et al.* [33]).

Scoring category	Response	Score
Cellular growth within implant	Abundance presence of cells and fibrous tissue around all fragments	4
	Marked presence of cells and/or formation of fibrous tissue around most fragments	3
	Moderate presence of cells in cracks of implant and/or formation of fibrous tissue around fragments of implant	2
	Minimal presence of cells within cracks of the implant (some cells present with or without connective tissue formation)	1
Degradation	Abundant degradation of implant with (almost) complete fragmentation	4
	Marked degradation of implant with presence of several fragments	3
	Moderate degradation of implant with cracks in implant and/or some fragments	2
	Minimal degradation of implant, some minor dissolution on edges, cracks in implant and/or small fragment present	1

2.8. Statistics

Results of weight loss and μ-CT analysis are expressed as means ± standard deviation with n=3 for each group. Results of histological scoring are expressed as means ± standard deviation with n=5 for each group. Single factor analysis of variance (ANOVA) was used to determine statistical significance within a data set. If ANOVA detected a significant difference within the data set, Tukey's honestly significantly different (HSD) multiple comparison test was used to determine significant differences between groups and conditions. All tests were conducted with a confident interval of 95% ($p < 0.05$).

3. RESULTS AND DISCUSSION

3.1. Weight loss measurements

Lysozyme, an enzyme ubiquitous in the human body [5, 38], has been reported to be responsible for the *in vivo* degradation of chitosan [6, 39]. As observed in Figure 2, all groups degraded gradually as a function of implantation time. Statistically significant weight loss ($p < 0.05$) was observed for chitosan/starch scaffolds with and without CaP coating and both in the presence and in absence of lysozyme after 12 weeks of implantation. The highest weight loss after 12 weeks was 29.8 ± 1.5% for CaP chitosan/starch scaffolds with lysozyme incorporated (Figure 2). It is expected that for longer implantation times, the degradation and the *in situ* formation of pores will be greater that the obtained in the herein presented studies performed up to 12 weeks. Comparing all groups at the same time point, chitosan scaffolds had the lowest weight loss overall, but this was, as expected, slightly increased when lysozyme was present. Chitosan/starch scaffolds with and without CaP and in the presence or absence of lyzozyme demonstrated significantly greater weight loss than chitosan scaffolds for all time points (Figure 2).

Previous studies investigated the degradation of chitosan scaffolds with and without CaP coating and in the presence and absence of lysozyme at pH 5 to simulate the inflammatory response [2]. The weight loss *in vitro* was not as pronounced as that observed *in vivo.* Similar to the *in vivo* experiments described herein, *in vitro* CaP coated chitosan scaffolds with incorporated lysozyme had the highest weight loss [2]. However, the complete dissolution of the CaP coatings was not observed *in vivo*, although it was *in vitro* at pH 5, possibly indicating that the inflammatory response following implantation *in vivo* does not achieve such a low pH or does not sustain this low pH for as long as the previously performed *in vitro* study [2].

This study also examined the effect of the addition of starch into the chitosan phase compared with chitosan scaffolds alone. The presence of starch in addition to chitosan seems to accelerate the degradation of scaffolds compared to that of chitosan alone (Figure 2). Starch is degraded by α-amylase, an enzyme also present in the human body namely in the human blood [40]. Starch granules with 5-10 μm dimensions were homogeneously distributed throughout the chitosan matrix enhancing hydrolysis by enzymes existing *in vivo*, namely lysozyme and α-amylase [1]. The pore size and distribution in the scaffold are controlled by the location of the “sacrifice” phase (starch), the degradation of which increases the microporosity by the release of starch granules (small dots visible at high magnifications

in Figure 5 for chitosan/starch scaffolds). These results are in agreement with the weigh loss data (Figure 2).

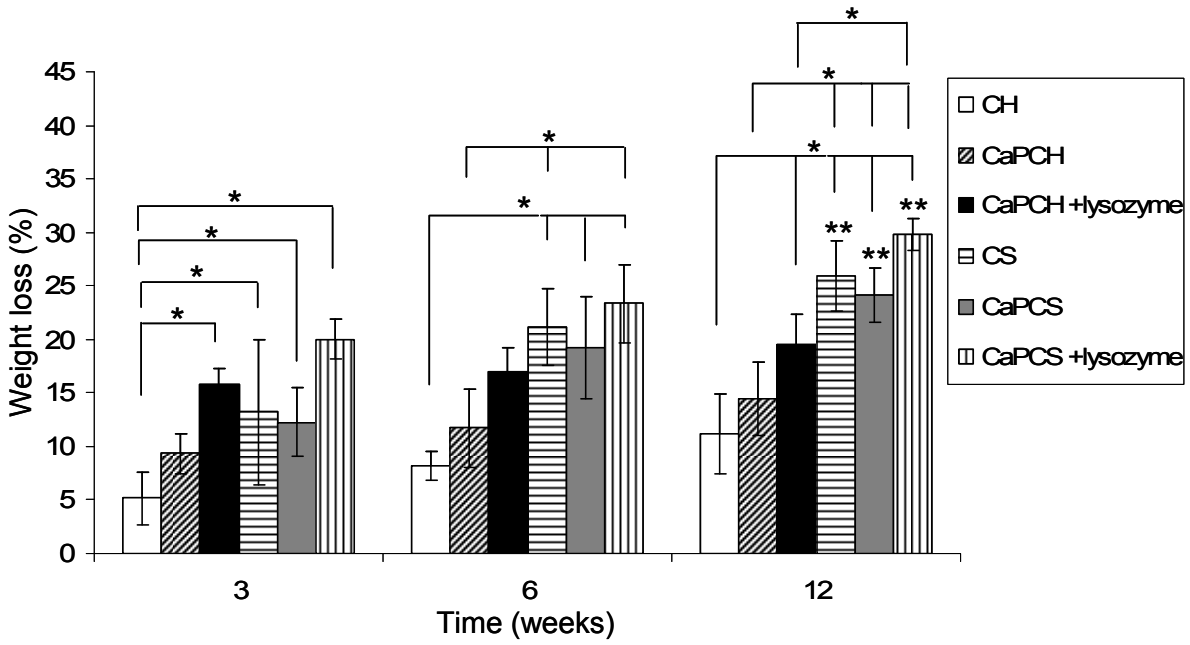


Figure 2. Weight loss profile of different groups after subcutaneous implantation for up to 12 weeks. Results are expressed as means ± standard deviation with n = 3 for each bar. (*) indicates a significant difference ($p < 0.05$) between groups at the same time point. (**) indicates a significant difference ($p < 0.05$) between the same condition at different time points.

3.2. µ-CT analysis

The µ-CT analysis performed on all experimental groups showed an increase in scaffold porosity as a function of implantation time (Figure 3). After 3 weeks post-implantation, degradation was observed in 3D images for chitosan-based formulations compared with controls (Figure 3). After 6 weeks, results indicated increased degradation for all the materials. The trend towards an accelerated increase in porosity/degradation was observed for all conditions up to week 12. Nevertheless, analysis of the 3D images did not indicate a remarkable effect for the presence of lysozyme in chitosan scaffolds, but there did appear to be enhanced degradation after 6 and 12 weeks when lysozyme was incorporated in CaP chitosan/starch scaffolds (Figure 3). Furthermore, the CaP coating (dark grey) was observed in 3D images at all time points for CaP coated scaffolds, indicating the aforementioned lack of coating degradation as was seen *in vitro* (Figure 3).

According to Figure 4A no significant differences in porosity were found between groups at the same time point with the exception of CaP chitosan/starch scaffolds with incorporated lysozyme after 6 weeks of implantation. This condition (CaPCS + lysozyme) presented significant higher porosity (p<0.05) compared with chitosan/starch scaffolds (CS) (43% ± 7 and 27% ± 4, respectively). Lysozyme seems to positively enhance porosity after 6 weeks of implantation, corroborating the weight loss results (Figure 2). After 3 weeks, no significant differences were found for all studied groups when compared with the porosity of the control (non-implanted) samples. However, after 6 weeks of implantation, porosity significantly increased for chitosan (CH), chitosan/starch (CS) and CaP chitosan/starch scaffolds with incorporated lysozyme (CaPCS + lysozyme) (Figure 4A). The same trend was observed after 12 weeks of implantation, showing significantly higher porosity for all scaffolds compared to that of control samples. These results indicate that all groups have the ability to form pores *in situ* as a function of implantation time. All groups presented a significantly increasing porosity over time ranging at least from 22% (chitosan/starch scaffolds with an initial porosity of 10 ± 8% increased after 12 weeks to 32 ± 10%) up to 32% observed for CaPCS+lysozyme with 9 ± 5% prosity before implantation and 43 ± 7% after 6 weeks. The degradation and consequently the porosity is expected to be greater for longer implantation times. Furthermore, results suggested that lysozyme positively affected pore formation by enhancing porosity in the case of chitosan/starch scaffolds.

The interconnectivity of chitosan (CH) scaffolds significantly increased with increased implantation time when compared to the interconnectivity of control samples (Figure 4B). No significant differences in interconnectivity were observed between groups at the same time point. After 12 weeks all groups demonstrated an increase in interconnectivity with the exception of chitosan/starch scaffolds and CaPCS + lysozyme. Lysozyme seems to have no effect on interconnectivity; however, interconnectivity increased for all groups over time with a range of values from 24-31% and 43-79%, before and after 12 weeks implantation, respectively.

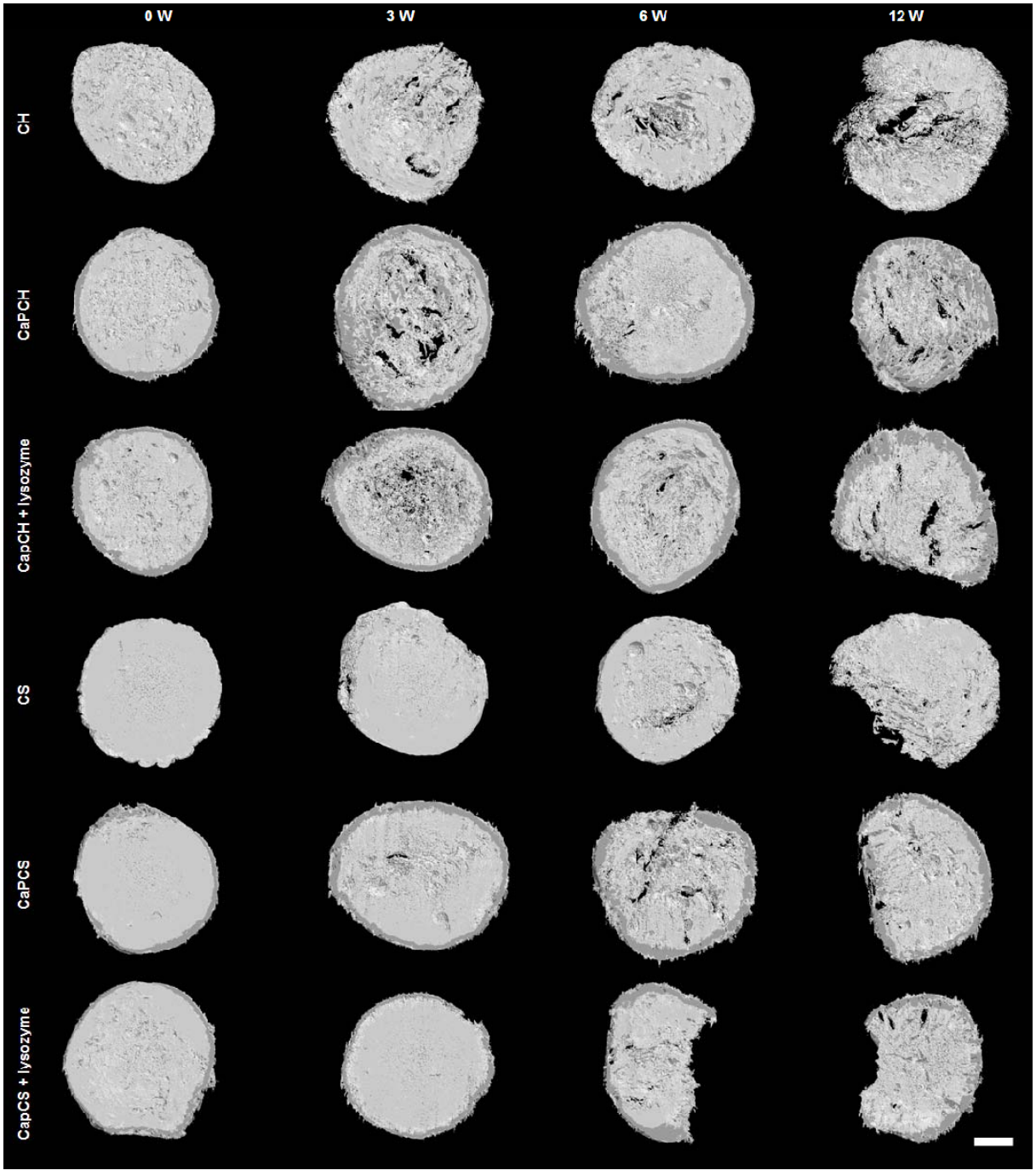


Figure 3. Images of chitosan-based scaffolds obtained by μ-CT: before implantation (control) and after 3, 6 and 12 weeks of subcutaneous implantation. The scale bar is 1 mm and applies to all images.

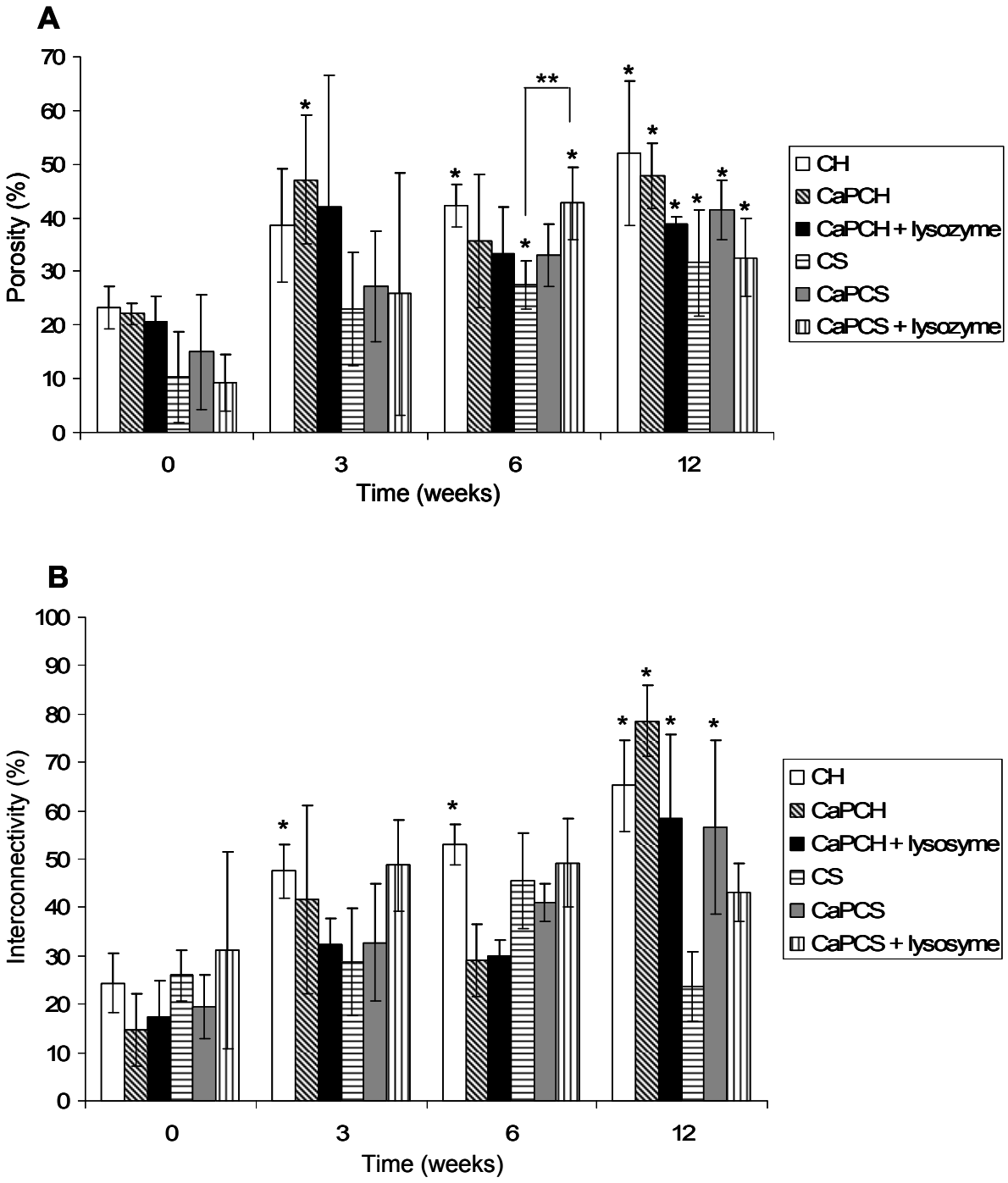


Figure 4. Porosity (A) and interconnectivity (B) of chitosan-based scaffolds as a function of implantation time. Results are expressed as means ± standard deviation with n = 3 for each bar. (*) indicates a significant difference ($p < 0.05$) between groups at different time points compared with controls (0 days). (**) indicates a significant difference ($p < 0.05$) between different groups at the same time point.

3.3. Microscopic analysis

At retrieval of the implants, no macroscopic signs of infection were seen at the surgical sites (Figure 1C). Furthermore, no adverse tissue reactions (toxic effects) were observed with light microscopy. Specimens for microscopy were retrieved at 3, 6 and 12 weeks post-implantation. Polymer and CaP coating degradation and cellular ingrowth within the implants were assessed using histological techniques. Remaining scaffolds were easily identified after H&E staining, as chitosan and chitosan/starch stained red, and cells stained blue and pink. In Figure 5, CaP coatings are not easily identified (appear in dark blue/black) but in order to specifically stain calcium, several sections were stained with von Kossa (Figure 7). For all scaffold formulations, even at the earliest implantation time, the formation of pores and the infiltration of cells throughout the scaffolds (clearly visible at high magnifications) were evident (Figure 5). Degradation of scaffolds within the initially almost non-porous network of chitosan or chitosan/starch is evident through the presence of circular or irregular structures (pores) filled with cells (Figure 5). Furthermore, as a function of implantation time, scaffolds have changed their shape and size, meaning that the scaffolds have been degraded and subsequently resorbed (Figure 5). The infiltration of cells as a function of time is clearly visible (Figure 6A), and occurred mainly when lysozyme was present. The progression of *in vivo* degradation was also evident by the formation of pores (Figure 5). The increased scoring of degradation, especially when lysozyme was present, corroborated these data (Figure 6B). The degradation of scaffolds did not elicit a severe inflammatory response. For the success of a bone tissue engineering implant, the scaffold must have a rate of degradation that corresponds to the rate of new bone ingrowth. This strategy seems to be very useful since the ideal scaffold should have appropriate mechanical properties for the site of implantation. It was previously demonstrated that in both dry and wet states these CaP coated chitosan scaffolds have appropriate mechanical properties for bone applications [1].

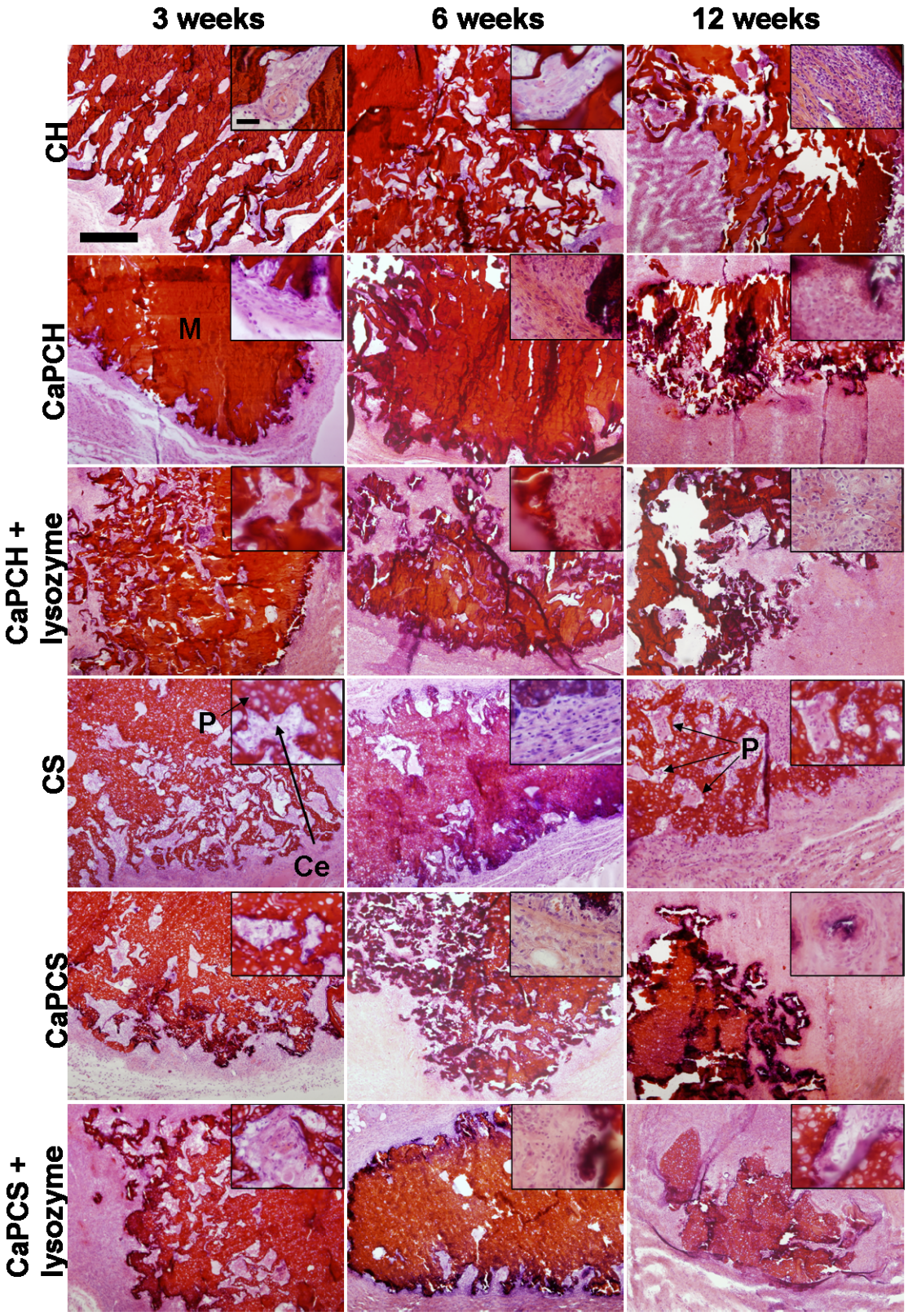


Figure 5. Representative histological sections of scaffolds implanted subcutaneously stained with hematoxylin and eosin after 3, 6 and 12 weeks. The images are presented at 4x and 40x magnification. The scale bars represent 500 μm and apply to all images. Chitosan-based scaffolds (M) appear in red. Pores (P) appear filled by cells (Ce) in pink or blue.

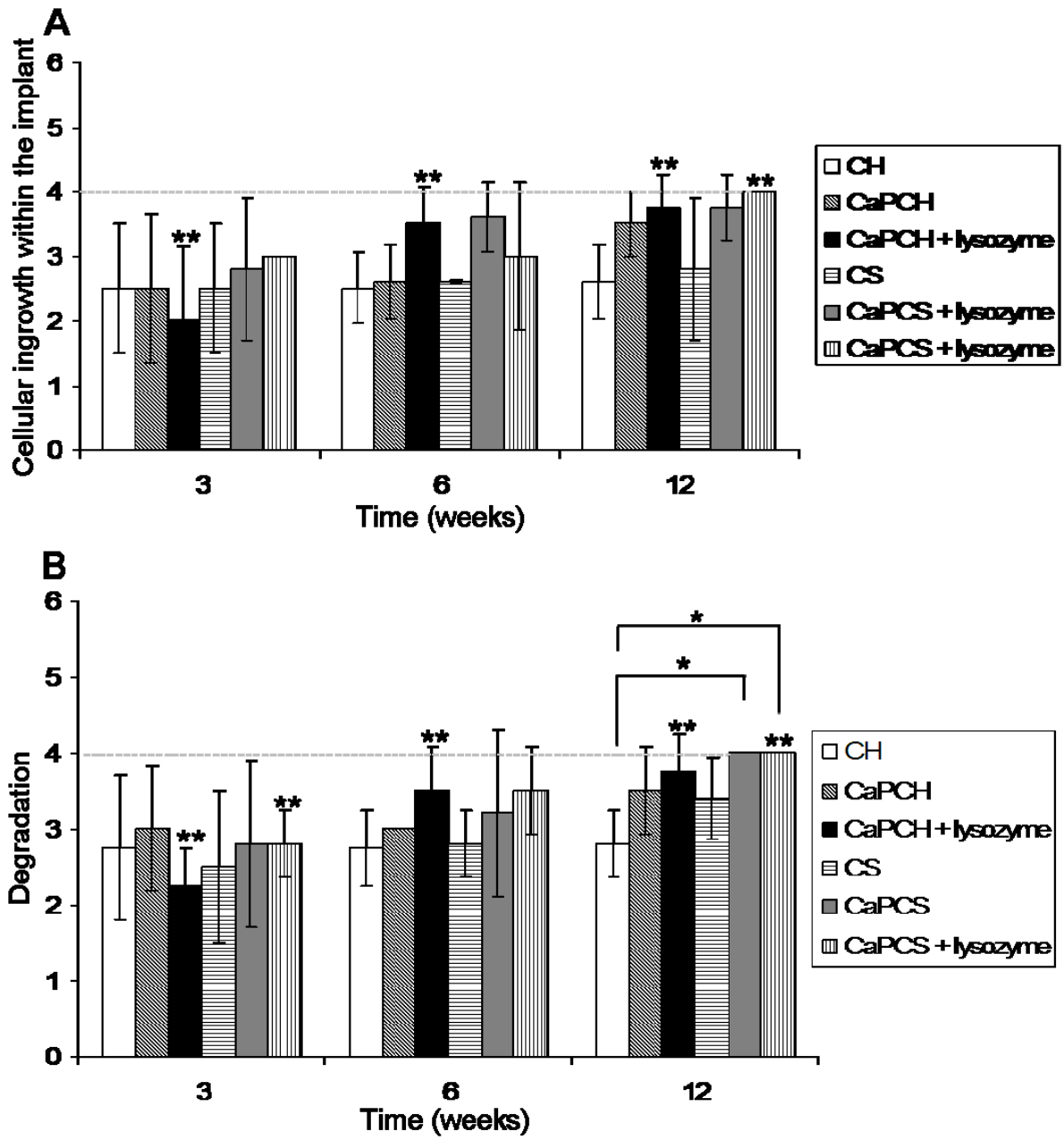


Figure 6. Results of histological scoring of: (A) cellular growth within the implants and (B) degradation after 3, 6 and 12 weeks of subcutaneous implantation. Data are presented as means ± standard deviation for n = 4–5. (*) indicates a significant difference ($p < 0.05$) between group conditions at the same time point. (**) indicates a significant difference ($p < 0.05$) between the same condition at different time points.

During resorption, the degradation products of CaP coatings (calcium and phosphate ions) are naturally metabolized and do not induce abnormal calcium and phosphate levels in urine, serum, or organs [41, 42]. The dissolution of CaP coatings depends on the particle size, crystallographic features, density and the nature of the solution used to make the

coating (composition, pH and temperature) [42, 43]. Highly soluble and poorly crystalline coatings might accelerate the dissolution process and consecutively favor osteoconduction [44]. These CaP coatings are partially amorphous and quite stable at pH 7.4 [2]. Figure 7 shows von Kossa stained sections with CaP coating that remained on or within the implants. The material is stained in grey, cells in pink and CaP coating in black. All sections, with the exception of the controls (without CaP coatings), have black regions around or within the implants, meaning that the CaP coating did not dissolve completely. Signs of degradation of CaP coating were evident in Figure 7 but some CaP coating remained on the implants. These results are corroborated by 3D images obtained with μ-CT (Figure 3). Complete loss of the coatings was not observed (Figure 7), as illustrated in 3D images obtained by μ-CT (Figure 3). Furthermore, we can state that *in vivo* the pH did not seem to decrease to 5 because these biomimetic CaP coatings are soluble at pH 5 or below as it was demonstrated previously [2]. Or, perhaps the pH did drop below 5 but not for a sufficiently long period of time to dissolve the coatings. Von Kossa stained sections also support the H&E results and histological scoring showing pronounced implant degradation as a function of implantation time and infiltration of cells throughout the implants (Figures 6 and 7).

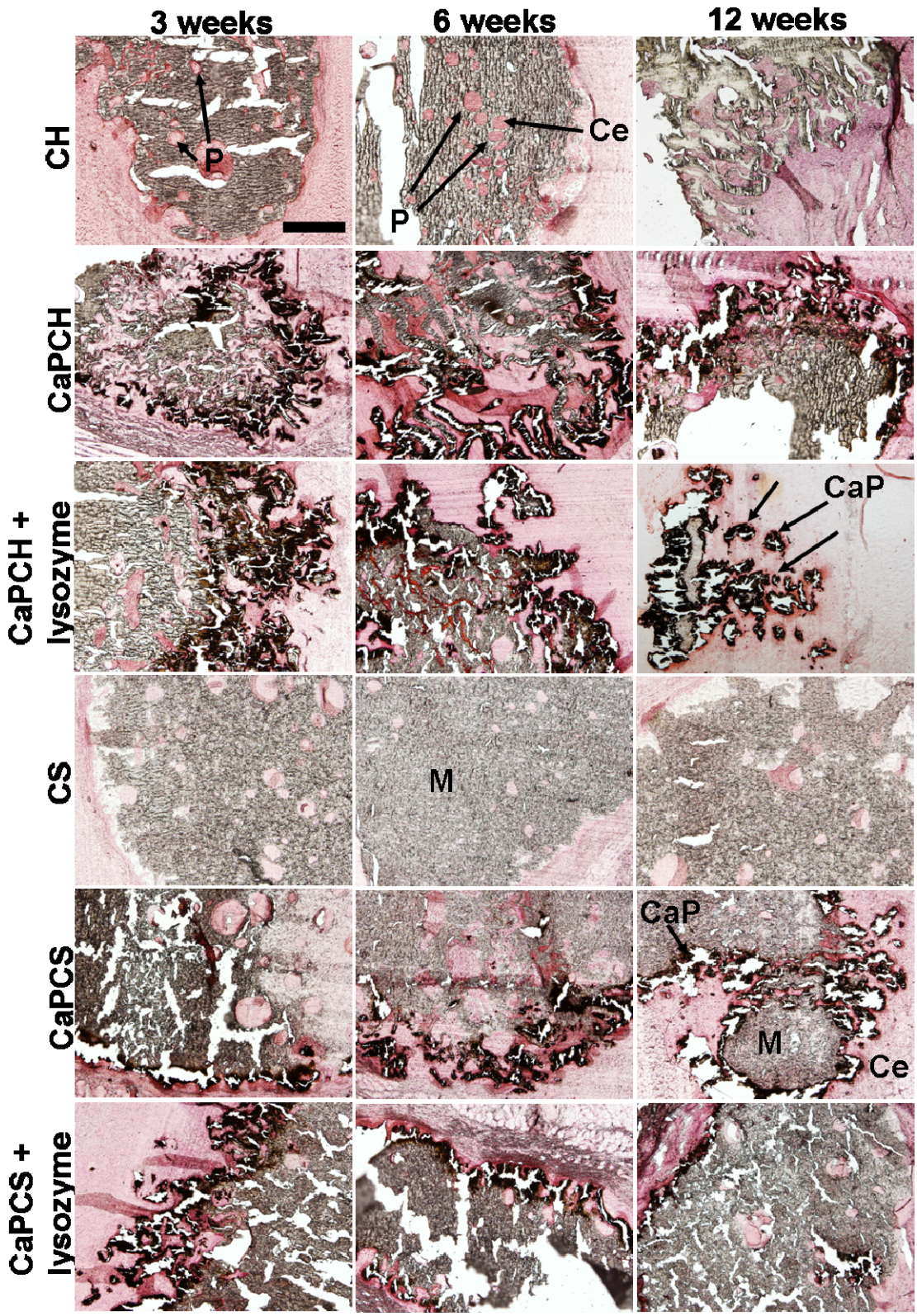


Figure 7. Representative light microscope images of chitosan-based sections stained with von Kossa after 3, 6 and 12 weeks of subcutaneous implantation. The images are presented at 4x magnification. The scale bar is 500 μm and applies to all images. Chitosan-based scaffolds (M) are stained in gray. Pores (P) are filled with cells (Ce) and appear in pink. CaP coatings (CaP) appear in black.

4. CONCLUSIONS

In vivo degradation of all specimens was clearly demonstrated by weight loss measurements, porosity increase, and images of H&E stained sections where there were visible pores completely filled with cells. Porosity significantly increased after 12 weeks of implantation, ranging from 22% up to 32% for all conditions. This strategy, using biodegradable naturally occurring polymers such as chitosan and starch, seems to maintain structural support throughout the implantation period tested, with the formation of pores *in situ* allowing for the penetration of cells into the implants. The gradual *in situ* pore forming ability of chitosan-based scaffolds was clearly demonstrated *in vivo*. Furthermore, this approach is very promising since incorporated lysozyme has antibacterial properties and CaP coated chitosan-based scaffolds can simultaneously exhibit osteoconductive properties. While further *in vivo* characterization within an orthotopic site is needed, these findings indicate that *in situ* pore-forming CaP coated chitosan-based materials have potential for future use in bone tissue engineering applications.

ACKNOWLEDGEMENTS

The authors would like to acknowledge Goreti Pinto, Luís Martins and Deolinda Teixeira (Life and Health Sciences Research Institute – University of Minho, Portugal) for excellent technical assistance on histological sectioning and microscopy analysis; the Portuguese Foundation for Science and Technology (FCT) for the Postdoctoral Grant to Catarina M. Alves (SFRH/BPD/26763/2006) and Doctoral Grant to Ana R. Costa-Pinto (SFRH/BD/24735/2005). This work was supported by the European NoE EXPERTISSUES (NMP3-CT-2004-500283). JDK acknowledges support from the Baylor College of Medicine Medical Scientist Training Program (NIH T32 GM07330), Rice Institute of Biosciences and Bioengineering's Biotechnology Training Grant (NIH T32 GM008362), and is currently supported by a training fellowship from the Keck Center Nanobiology Training Program of the Gulf Coast Consortia (NIH Grant No. 5 T90 DK070121-04)

REFERENCES

1. Martins AM, Santos MI, Azevedo HS, Malafaya PB, Reis RL. Natural origin scaffolds with in situ pore forming capability for bone tissue engineering applications. Acta Biomater 2008 Nov;4(6):1637-1645.

2. Martins AM, Pereira RC, Leonor IB, Azevedo HS, Reis RL. Chitosan scaffolds incorporating lysozyme into CaP coatings produced by a biomimetic route: a novel concept for tissue engineering combining a self-regulated degradation system with in situ pore formation. Acta Biomater 2009;in press.

3. Martins AM, Pham QP, Malafaya PB, Raphael RM, Kasper FK, Reis RL, et al. Natural Stimulus Responsive Scaffolds/Cells for Bone Tissue Engineering: Influence of Lysozyme upon Scaffold Degradation and Osteogenic Differentiation of Cultured Marrow Stromal Cells Induced by CaP Coatings. Tissue Eng Part A 2009 Jan 20;in press.

4. Hankiewi.J, Swiercze.E. Lysozyme in Human Body-Fluids. Clin Chim Acta 1974;57(3):205-209.

5. Porstmann B, Jung K, Schmechta H, Evers U, Pergande M, Porstmann T, et al. Measurement of lysozyme in human body fluids: comparison of various enzyme immunoassay techniques and their diagnostic application. Clin Biochem 1989 Oct;22(5):349-355.

6. Tomihata K, Ikada Y. In vitro and in vivo degradation of films of chitin and its deacetylated derivatives. Biomaterials 1997 Apr;18(7):567-575.

7. Varum KM, Myhr MM, Hjerde RJ, Smidsrod O. In vitro degradation rates of partially N-acetylated chitosans in human serum. Carbohydr Res 1997 Mar 26;299(1-2):99-101.

8. Proctor VA, Cunningham FE. The chemistry of lysozyme and its use as a food preservative and a pharmaceutical. Critical reviews in food science and nutrition 1988;26(4):359-395.

9. Torsteinsdottir I, Hakansson L, Hallgren R, Gudbjornsson B, Arvidson NG, Venge P. Serum lysozyme: a potential marker of monocyte/macrophage activity in rheumatoid arthritis. Rheumatology (Oxford, England) 1999 Dec;38(12):1249-1254.

10. Ogundele MO. A novel anti-inflammatory activity of lysozyme: modulation of serum complement activation. Mediators of inflammation 1998;7(5):363-365.

11. Martins AM, Salgado AJ, Azevedo HS, Leonor IB, Reis RL. Lysozyme incorporation in biomimetic coated chitosan scaffolds: Development and behaviour in contact with osteoblastic-like cells. Tissue engineering 2006 Apr;12(4):1018-1019.

12. Reis RL, Cunha AM, Fernandes MH, Correia RN. Treatments to induce the nucleation and growth of apatite-like layers on polymeric surfaces and foams. Journal of materials science 1997 Dec;8(12):897-905.

13. Oliveira AL, Elvira C, Reis RL, Vazquez B, San Roman J. Surface modification tailors the characteristics of biomimetic coatings nucleated on starch-based polymers. Journal of materials science 1999 Dec;10(12):827-835.

14. Oliveira AL, Malafaya PB, Reis RL. Sodium silicate gel as a precursor for the in vitro nucleation and growth of a bone-like apatite coating in compact and porous polymeric structures. Biomaterials 2003 Jul;24(15):2575-2584.

15. Habibovic P, de Groot K. Osteoinductive biomaterials--properties and relevance in bone repair. J Tissue Eng Regen Med 2007 Jan-Feb;1(1):25-32.

16. Liu Y, Hunziker EB, Layrolle P, De Bruijn JD, De Groot K. Bone morphogenetic protein 2 incorporated into biomimetic coatings retains its biological activity. Tissue engineering 2004 Jan-Feb;10(1-2):101-108.

17. Azevedo HS, Leonor IB, Alves CM, Reis RL. Incorporation of proteins and enzymes at different stages of the preparation of calcium phosphate coatings on a degradable substrate by a biomimetic methodology. Materials Science & Engineering C-Biomimetic and Supramolecular Systems 2005 Apr 28;25(2):169-179.

18. Petite H, Viateau V, Bensaid W, Meunier A, de Pollak C, Bourguignon M, et al. Tissue-engineered bone regeneration. Nat Biotechnol 2000 Sep;18(9):959-963.

19. Oliveira JM, Rodrigues MT, Silva SS, Malafaya PB, Gomes ME, Viegas CA, et al. Novel hydroxyapatite/chitosan bilayered scaffold for osteochondral tissue-engineering applications: Scaffold design and its performance when seeded with goat bone marrow stromal cells. Biomaterials 2006 Dec;27(36):6123-6137.

20. Malafaya PB, Santos TC, van Griensven M, Reis RL. Morphology, mechanical characterization and in vivo neo-vascularization of chitosan particle aggregated scaffolds architectures. Biomaterials 2008 Oct;29(29):3914-3926.

21. Costa-Pinto AR, Salgado AJ, Correlo VM, Sol P, Bhattacharya M, Charbord P, et al. Adhesion, proliferation, and osteogenic differentiation of a mouse mesenchymal stem cell line (BMC9) seeded on novel melt-based chitosan/polyester 3D porous scaffolds. Tissue Eng Part A 2008 Jun;14(6):1049-1057.

22. Gomes ME, Reis RL, Cunha AM, Blitterswijk CA, de Bruijn JD. Cytocompatibility and response of osteoblastic-like cells to starch-based polymers: effect of several additives and processing conditions. Biomaterials 2001 Jul;22(13):1911-1917.

23. Salgado AJ, Coutinho OP, Reis RL. Novel starch-based scaffolds for bone tissue engineering: cytotoxicity, cell culture, and protein expression. Tissue engineering 2004 Mar-Apr;10(3-4):465-474.

24. Mendes SC, Reis RL, Bovell YP, Cunha AM, van Blitterswijk CA, de Bruijn JD. Biocompatibility testing of novel starch-based materials with potential application in orthopaedic surgery: a preliminary study. Biomaterials 2001 Jul;22(14):2057-2064.

25. Marques AP, Reis RL, Hunt JA. The biocompatibility of novel starch-based polymers and composites: in vitro studies. Biomaterials 2002 Mar;23(6):1471-1478.

26. Salgado AJ, Coutinho OP, Reis RL, Davies JE. In vivo response to starch-based scaffolds designed for bone tissue engineering applications. Journal of biomedical materials research 2007 Mar 15;80(4):983-989.

27. Azevedo HS, Gama FM, Reis RL. In vitro assessment of the enzymatic degradation of several starch based biomaterials. Biomacromolecules 2003 Nov-Dec;4(6):1703-1712.

28. Gomes ME, Azevedo HS, Moreira AR, Ella V, Kellomaki M, Reis RL. Starch-poly(epsilon-caprolactone) and starch-poly(lactic acid) fibre-mesh scaffolds for bone tissue engineering applications: structure, mechanical properties and degradation behaviour. J Tissue Eng Regen Med 2008 Jul;2(5):243-252.

29. Tuzlakoglu K, Alves CM, Mano JF, Reis RL. Production and characterization of chitosan fibers and 3-D fiber mesh scaffolds for tissue engineering applications. Macromol Biosci 2004 Aug 9;4(8):811-819.

30. Pham QP, Kasper FK, Mistry AS, Sharma U, Yasko AW, Jansen JA, et al. Analysis of the osteoinductive capacity and angiogenicity of an in vitro generated extracellular matrix. Journal of biomedical materials research 2009 Feb;88(2):295-303.

31. Young S, Patel ZS, Kretlow JD, Murphy MB, Mountziaris PM, Baggett LS, et al. Dose Effect of Dual Delivery of Vascular Endothelial Growth Factor and Bone Morphogenetic Protein-2 on Bone Regeneration in a Rat Critical-Size Defect Model. Tissue Eng Part A 2009 Feb 24.

32. Yoshikawa T, Ohgushi H, Akahane M, Tamai S, Ichijima K. Analysis of gene expression in osteogenic cultured marrow/hydroxyapatite construct implanted at ectopic sites: a comparison with the osteogenic ability of cancellous bone. J Biomed Mater Res 1998 Sep 15;41(4):568-573.

33. Nishikawa M, Myoui A, Ohgushi H, Ikeuchi M, Tamai N, Yoshikawa H. Bone tissue engineering using novel interconnected porous hydroxyapatite ceramics combined with marrow mesenchymal cells: quantitative and three-dimensional image analysis. Cell transplantation 2004;13(4):367-376.

34. Uemura T, Dong J, Wang Y, Kojima H, Saito T, Iejima D, et al. Transplantation of cultured bone cells using combinations of scaffolds and culture techniques. Biomaterials 2003 Jun;24(13):2277-2286.

35. Oliveira JM, Kotokuki N, Tadokoro M, Hirose M, Mano JF, Reis RL, et al. Ex Vivo Culturing of Rat Bone Marrow Stromal Cells with Dexamethasone-loaded Carboxymethylchitosan/Poly(amidoamine) Dendrimer Nanoparticles Enhances Ectopic Bone Formation on Tissue Engineered Constructs. submitted 2008.

36. Datta N, Holtorf HL, Sikavitsas VI, Jansen JA, Mikos AG. Effect of bone extracellular matrix synthesized in vitro on the osteoblastic differentiation of marrow stromal cells. Biomaterials 2005 Mar;26(9):971-977.

37. De Jong WH, Eelco Bergsma J, Robinson JE, Bos RR. Tissue response to partially in vitro predegraded poly-L-lactide implants. Biomaterials 2005 May;26(14):1781-1791.

38. Hankiewicz J, Swierczek E. Lysozyme in human body fluids. Clin Chim Acta 1974 Dec 17;57(3):205-209.

39. Lim SM, Song DK, Oh SH, Lee-Yoon DS, Bae EH, Lee JH. In vitro and in vivo degradation behavior of acetylated chitosan porous beads. J Biomater Sci Polym Ed 2008;19(4):453-466.

40. Junge W, Troge B, Klein G, Poppe W, Gerber M. Evaluation of a new assay for pancreatic amylase: performance characteristics and estimation of reference intervals. Clin Biochem 1989 Apr;22(2):109-114.

41. den Hollander W, Patka P, Klein CP, Heidendal GA. Macroporous calcium phosphate ceramics for bone substitution: a tracer study on biodegradation with 45Ca tracer. Biomaterials 1991 Aug;12(6):569-573.

42. Barrere F, van Blitterswijk CA, de Groot K. Bone regeneration: molecular and cellular interactions with calcium phosphate ceramics. Int J Nanomedicine 2006;1(3):317-332.

43. Leeuwenburgh SC, Wolke JG, Siebers MC, Schoonman J, Jansen JA. In vitro and in vivo reactivity of porous, electrosprayed calcium phosphate coatings. Biomaterials 2006 Jun;27(18):3368-3378.

44. Goyenvalle E, Aguado E, Nguyen JM, Passuti N, Le Guehennec L, Layrolle P, et al. Osteointegration of femoral stem prostheses with a bilayered calcium phosphate coating. Biomaterials 2006 Mar;27(7):1119-1128.

SECTION 5

CHAPTER IX

GENERAL CONCLUSIONS AND FINAL REMARKS

CHAPTER IX

GENERAL CONCLUSIONS AND FINAL REMARKS

The main aims of the developed studies reported in this thesis were the successful use of natural based scaffolds by means of applying two main bone tissue engineering strategies. The experimental work presented in this thesis is divided in two main parts: 1) The first strategy involves the culture of cells onto natural-based scaffolds with osteogenic media supplemented with several enzymes that mimic the physiological concentrations, under static cultures and flow perfusion conditions (Section 3); 2) The second strategy describes the development and applications of naturally derived scaffolds, based on chitosan and starch, and validation of in situ pore forming concept *in vitro* and *in vivo* (Section 4).

In the first part of this thesis (Section 3), we have used SPCL fiber mesh scaffolds known to be degraded by enzymes present in the human blood serum, namely α-amylase and lipase. Culture of rat marrow stromal cells (MSCs) on flow perfusion conditions enhances differentiation of marrow stromal cells with subsequent formation of a bone-like extracellular matrix. This work intended to mimic the *in vitro* and *in vivo* degradation of the starch/poly(ε-caprolactone) (SPCL) fiber meshes using enzymes responsible for their degradation at the same concentrations as those found in human serum. Besides characterizing the susceptibility of SPCL fiber meshes to enzymatic degradation, this study aimed also to investigate the osteogenic differentiation of MSCs and subsequent formation of extracellular matrix (ECM) under static and flow perfusion conditions in the presence of hydrolytic enzymes (lipase and/or α-amylase). The degradation studies performed in static and dynamic conditions demonstrated the effect of lipase and α-amylase on degradation of SPCL fiber mesh scaffolds, showing that after 30 days these enzymes did not have a negative effect on SPCL fiber integrity. Lipase had a positive effect on the porosity and size of pores when dynamic conditions were used. Porosity and pore size were also enhanced by α-amylase. When SPCL fiber meshes were cultured with osteogenic media supplemented with several enzymes in static and flow perfusion conditions, the following was concluded:

- culture media supplemented with α-amylase or lipase revealed that these enzymes promoted the proliferation MSCs on SPCL when cultured under static conditions
- cuture media supplemented with lipase and with both α-amylase and lipase enzymes enhanced the proliferation MSCs when cultured on SPCL on flow perfusion bioreactors

- lipase had a superior effect in the osteogenic differentiation of MSCs and on the mineralization of the extracellular matrix when added to osteogenic culture medium as compared with the results obtained without enzymes or with α-amylase or both enzymes together under static and flow perfusion conditions.
- flow perfusion culture dramatically improved the distribution of ECM through the cultured scaffolds and mineralized matrix production.

These results demonstrated that supplementation of culture media with lipase holds great potential for the generation of bone tissue engineering constructs from MSCs seeded onto SPCL fiber mesh scaffolds under static or flow perfusion conditions. Lipase enhanced the osteoblastic differentiation of the seeded MSCs and promoted matrix mineralization without deleteriously affecting the structural integrity of the meshes over 16 days of culture.

In Section 4, the second part of experimental results of this thesis, we have proposed novel responsive scaffolds based on chitosan and starch with an *in situ* pore forming ability. The results of the compressive tests showed that these materials exhibited mechanical properties that fall in the normal ranges of strength and modulus for trabecular bone. Degradation studies using α-amylase and lysozyme with similar concentrations to those found in human serum were selected in order to simulate the physiological conditions and subsequently assess pore formation. It was demonstrated that these scaffolds were susceptible to these enzymes and were able to degrade and to induce the formation of pores using enzymatic physiological concentrations. Biocompatibility studies showed that the extracts of the scaffolds were non cytotoxic.

Since the formation of pores in the presence of lysozyme in conditions similar to those found in human blood serum was only moderate compared to those obtained with α-amylase or with the two enzymes together (α-amylase and lysozyme), an alternative approach was selected to improve these results. The alternative was to incorporate lysozyme at high concentrations in CaP coatings prepared at the surface of these materials. Our hypothesis proposed that a biomimetic CaP coating would further enhance the *in vivo* performance of using a CaP coating since these materials, which *per se* are not osteoinductive and osteoconductive. Degradation studies at pH 7.4, to simulate normal physiological conditions, showed that in these conditions, CaP coatings are very stable as the materials remained covered with a CaP layer. At pH 5, to simulate an *in vivo* inflammatory response, a porous structure was formed when lysozyme was incorporated into the CaP coatings. The degradation effect of lysozyme on chitosan scaffolds at pH 5 was clearly visible by the appearance of pores.

Degradation studies performed with lysozyme using similar concentration to those incorporated into CaP coatings showed the formation of pores as a function of immersion time, indicating an increase of porosity from 5% to 55%. Lysozyme had a significant catalytic effect on chitosan scaffolds resulting in porous 3D structures with interconnected pores (~78%). On the basis of these studies it was concluded that CaP biomimetic coatings with incorporated lysozyme enhance osteogenic differentiation of rat marrow stromal cells. Therefore, the use of a CaP biomimetic coating strategy with incorporated lysozyme on the surface of chitosan-based scaffolds is able to provide an improved environment for rat MSCs differentiation along the osteogenic lineage when compared with uncoated scaffolds.

Finally, to validate the *in situ* pore forming concept *in vivo* chitosan-based scaffolds with or without CaP coating and in the presence and absence of lysozyme, a rat subcutaneous model was used. *In vivo* degradation of all scaffolds was clearly demonstrated by weight loss measurements, porosity increase, and images of H&E stained sections where were visible pores completely filled out with cells. Porosity significantly increased after 12 weeks ranging from 22% up to 34%. It is expected that for longer implantation times, the degradation and the *in situ* formation of pores will be greater than the obtained in the herein presented studies performed up to 12 weeks. These findings indicate the potential that CaP coated chitosan-based materials can have in bone tissue engineering applications and further motivates future *in vivo* studies using an orthotopic model.

As final remarks, it can be stated that the work developed and included in this thesis provided interesting results on different types of natural based scaffolds and targeted two different bone tissue engineering strategies. In the first strategy we tried to simulate physiologic enzymatic conditions, since the ideal scaffold for bone tissue engineering should be biodegradable and bioresorbable while being able to support the growth of new bone. Static culture conditions and flow perfusion bioreactor cultures were successfully used in combination with enzymes such as α-amylase and/or lipase on the osteogenic differentiation of rat bone marrow stromal cells.

Lastly, we have proposed the use of a self-regulating degrading material with gradual *in situ* pore formation ability *in vitro* and *in vivo.* The success of this approach is mainly dictated by the presence of lysozyme incorporated into the coatings that will grant chitosan scaffolds with a gradual *in vivo* pore forming ability and antibacterial activity, while the presence of the CaP coating can simultaneously enable osteoconductive properties to the scaffolds. The demonstrated ability of these novel surface coated scaffolds to form an interconnected pore structure *in situ* coupled with their positive effect on the osteoblastic differentiation of MSCs

and mineralized matrix production clearly illustrate the strong potential of these scaffolds for application in bone tissue engineering strategies. These “smart” and responsive scaffolds, with *in situ* pore forming capability and interesting mechanical properties, seem to be advantageous when compared with other presently available conventional materials.